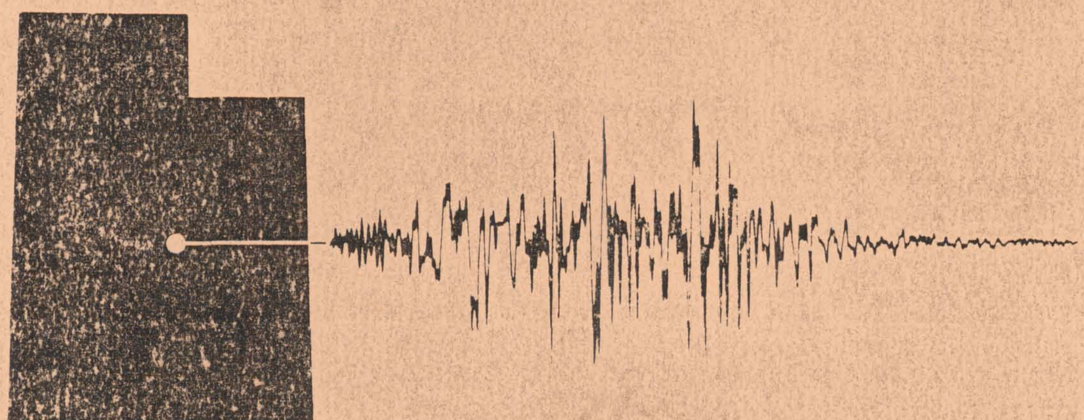

# Seismotectonic Study

## for Joes Valley, Scofield, and Huntington North Dams, Emery County and Scofield Projects, Utah

U. S. DEPARTMENT OF THE INTERIOR
BUREAU OF RECLAMATION
ENGINEERING AND RESEARCH CENTER
SEISMOTECTONIC SECTION
DENVER, COLORADO

# SEISMOTECTONIC STUDY FOR JOES VALLEY, SCOFIELD AND HUNTINGTON NORTH DAMS, EMERY COUNTY AND SCOFIELD PROJECTS, UTAH

Seismotectonic Report No. 86-7

by

Lucy L. Foley
Richard A. Martin, Jr.
J. Timothy Sullivan

Seismotectonic Section
Geologic Services Branch
Division of Geology
Engineering and Research Center
U.S. Bureau of Reclamation
Denver, Colorado

1986

Prepared by:

Lucy L. Foley
Geologist

2/3/87
Date

Richard A. Martin, Jr.
Seisomologist

2-3-87
Date

J. Timothy Sullivan
Geologist

2/3/87
Date

Technical approval by:

Dean A. Ostenaa
Head, Seismotectoic Section

2/10/87
Date

Reviewed by:

Robert B. MacDonald
Chief, Geologic Services Branch

2-10-87
Date

Approved by:

Steve D. Markwell, Chief
Division of Geology

2/13/87
Date

# CONTENTS

CONTENTS - CONTINUED

CONTENTS - CONTINUED

CONTENTS - CONTINUED

LIST OF FIGURES

## LIST OF FIGURES - CONTINUED

## PLATES



## TABLES

## SUMMARY


This report presents the results of a seismotectonic study conducted for Joes Valley, Scofield, and Huntington North Dams located in central Utah. The conclusions of this report are based on data collected from a program of detailed geologic mapping, trenching of suspected late Quaternary (<150 ka) faults, relative age dating of Quaternary deposits, and collection and analysis of microseismic information. The principal seismic hazards of potential significance to the subject structures are the possible occurrence of large magnitude (M>7) earthquakes on faults <1 km from Joes Valley Dam, <1.5 km from Scofield Dam and <30 km from Huntington North Dam.

Joes Valley and Scofield Dams are located on the Wasatch Plateau, a 5 000 $km^2$ area of nearly flat-lying Mesozoic and lower Tertiary sedimentary rocks in central Utah. Huntington North Dam is located in Castle Valley about 8 km east of the eastern escarpment of the plateau. The Wasatch Plateau is in a complex north-south trending transition zone 50 to 100 km wide between the Colorado Plateau to the east and the Basin and Range to the west and is transected by numerous north and northeast-trending normal faults. The two most prominent of these structures, and the most significant to the three dams, are the Joes Valley and Pleasant Valley fault zones. The Joes Valley fault zone approaches within 0.12 km of Joes Valley Dam and underlies the reservoir. The Pleasant Valley fault zone is within 1.3 km of Scofield Dam and also underlies the reservoir. Huntington North Dam is located 16 km east of the southern end of the Pleasant Valley fault zone and 28 km east of the Joes Valley fault zone. Post-Eocene normal displacement in the Joes Valley fault zone ranges from 300 to 900 m with the greatest displacement occurring adjacent to Joes Valley Dam. In the Pleasant Valley fault zone the normal displacement of the Paleocene-Eocene rocks ranges from less than 100 m to about 400 m in the graben adjacent to Scofield Dam.

The Wasatch Plateau is situated within the ISB (Intermountain seismic belt), a north-trending zone of diffuse but locally intense seismicity that extends for over 1300 km from southern Utah to northern Montana. Earthquakes as large as M 7.5 have occurred within the ISB in historic times including the 1959 Hebgen Lake, Montana and 1984 Borah Peak, Idaho earthquakes of surface wave magnitudes 7.5 and 7.3, respectively. Within Utah, earthquakes as large as M 6.6 have occurred since settlement began in 1847. The Hebgen Lake and Borah Peak earthquakes have been used to develop a model for large magnitude earthquakes in the ISB. This earthquake model, which applies to extensional stress environments, involves predominantly dip-slip motion, originating at depths of 10-15 km on moderate to high angle planar faults (45°-60°) with accompanying surface displacements of 1-4 m. The faults in this model are typically more than 20 km long and have had repeated late Quaternary (<150 ka) surface displacement.

The preferred model of contemporary tectonics for the Wasatch Plateau is one involving large scarp-forming earthquakes occurring on moderate- to steeply-dipping normal faults. This model is based on seismicity data and geologic evidence acquired in this study, and a review of seismic reflection data. Four major fault zones on the Wasatch Plateau exhibit characteristics associated with late Quaternary surface faulting: Joes Valley, Pleasant Valley, Snow Lake, and Gooseberry fault zones. Faults bounding the northern Joes Valley graben in the vicinity of Joes Valley Dam and the Pleasant Valley graben in the vicinity of Scofield Dam are the predominant sources of potential seismic hazards to the three dams being considered and are the main focus of this study.

The northern Joes Valley graben, part of the Joes Valley fault zone, is the only structure containing direct evidence, in the form of scarps in upper Quaternary deposits, for recurrent late Quaternary surface displacement. Six backhoe trenches were excavated across scarps on three faults in the Joes Valley graben: the East and West Joes Valley faults and the Middle Mountain fault. Stratigraphic data from these trenches, in addition to scarp heights measured in upper Quaternary deposits, are used to estimate apparent vertical surface displacement in single faulting events of less than 1 m to more than 5 m, and average recurrence intervals for these events of about 10 to 20 kyrs on the two graben-bounding faults and a major intragraben fault.

Evidence for Quaternary surface displacement in the Pleasant Valley fault zone is more difficult to assess than in the Joes Valley fault zone because of the limited extent of deposits of Quaternary age. Several faults exhibit geomorphic characteristics that are similar to the Quaternary faults in Joes Valley. The faults closest to Scofield Dam with these characteristics and which therefore are inferred to be seismogenic are the East and West Pleasant Valley faults, 1.3 and 4.0 km west of the dam, respectively. Because these faults share geomorphic characteristics with faults in the northern Joes Valley fault zone, and because of a lack of evidence to the contrary, we infer a similar displacement history.

MCE's (Maximum credible earthquakes) for the Joes Valley and Pleasant Valley fault zones are based on a comparison of the estimated length of surface rupture and the amount of single event vertical displacement for these faults with similar data for large-magnitude historical earthquakes in the Basin and Range and the ISB. Seismologic evidence indicates that these historical earthquakes occur at the base of the seismogenic zone with focal depths of 10-15 km. Based on these comparisons, the Joes Valley fault zone, 0.12 km west of Joes Valley Dam, is assigned an MCE of $M_S$ 7.5. On the same basis, the Pleasant Valley fault zone, 1.3 km west of Scofield Dam, is assigned an MCE of $M_S$ 7.0. These MCE's also apply to Huntington North Dam with epicentral distances of 28 km to the Joes Valley fault zone and 35 km to the portion of the Pleasant Valley fault zone inferred to have had late Quaternary surface displacement. In addition to assigning MCE's to specific geologic structures, a random earthquake, capable of occurring anywhere throughout the Utah portion of the ISB, must be considered in this hazard analysis. The MCE for this random earthquake is $M_L$ 6 to 6.5.

Potential hazards to Joes Valley Dam associated with the MCE's on the Joes Valley faults include slope instability in the vicinity of the dam and surface faulting in the reservoir with resultant seiches on the water surface. Hazards to Scofield Dam associated with MCE's on the Pleasant Valley faults include surface faulting in the reservoir and associated waves on the water surface as well as a potential for slope instability in the right abutment which should be studied further. Huntington North Dam has no faults underlying the reservoir so surface faulting does not pose a hazard. Unconsolidated sediments in the foundations of Scofield and Huntington North Dams should be studied for liquefaction potential under seismic loading associated with the MCE's.

## 1.0 Introduction

This report includes both regional and site specific seismotectonic studies conducted for the following USBR dams:(1) Joes Valley Dam, Emery County Project, Utah, (2) Scofield Dam, Scofield Project, Utah, and (3) Huntington North Dam, Emery County Project, Utah.

### 1.1 Purpose and scope of study

The seismotectonic study for Joes Valley, Scofield and Huntington North Dams was undertaken for the purpose of providing information on the seismic hazard to these structures for MDA (Modification Decision Analysis). The study encompasses the central and northern Wasatch Plateau which covers an area of approximately 5 000 km2 in central Utah. MCE's (Maximum credible earthquakes) and recurrence estimates for earthquakes on specific fault zones are presented.

The scope of the work for the seismotectonic study for Joes Valley, Scofield and Huntington North Dams consisted of a review of previous geologic investigations conducted in the region, analysis of stereo pairs of black and white and color aerial photographs covering the northern Wasatch Plateau, selected regional and site-specific geologic mapping, photolineament studies, profiling of fault scarps in Quaternary deposits, and excavation of trenches across selected scarps and soil pits on representative geomorphic surfaces for relative age dating. These field investigations were carried out during the summers of 1983 and 1984.

Stereo pairs of color aerial photographs at a scale of 1:15 000 (U.S. Department of Agriculture, 1976) and black and white aerial photographs at scales of 1:63 000 (USGS, 1976, VEFL series) and 1:80 000 (U.S. Geological Survey,1975, VDXT series) covering the northern Wasatch Plateau, were examined. Photolineaments observed on these photographs were mapped on mylar overlays and were further examined in the field to determine their origin. Lineaments considered to be fault generated after field inspection were compiled on topographic base maps.

Profiles were measured on fault scarps in order to obtain data on scarp height, maximum slope angle, and vertical displacement following the methods of Bucknam and Anderson (1979). The small number and short length of scarps suitable for measurement limited the amount of data recoverable and restricted their use to accurate height estimates. These measurements are included on plate 2.

Field reconnaissance was conducted in those areas determined by the aerial photograph study to have either evidence for Quaternary faulting or deposits that could elucidate the Quaternary history of the Wasatch Plateau. A geologic map of the northern Joes Valley fault zone (plate 2) shows the relationship between faults and Quaternary deposits. Detailed brunton and tape maps were surveyed at two sites where fault scarps cut deposits of different ages. In the Pleasant Valley fault zone geologic field mapping was conducted to clarify structural relationships at the northern end of the fault zone. In the Snow Lake area, field studies consisted of mapping stratigraphic units within the upper Flagstaff Formation to measure the displacement, and locating Quaternary deposits which bore some relationship to the faulting. In Gooseberry graben, a geologic map at a scale of 1:24 000 (Oberhansley, 1980) was already available so field reconnaissance consisted of checking photolineaments for evidence of Quaternary displacement and looking for fault scarps in areas where Quaternary deposits were mapped as overlying faults.

Subsurface investigations included the excavation by backhoe of 6 trenches and 20 soil pits at selected sites in the Joes Valley fault zone to study the details of the history of fault movement and to provide relative age dating criteria for Quaternary deposits. An extensive study of soils in the Joes Valley area was conducted in an attempt to develop relative age dating criteria for Quaternary deposits related, directly or indirectly, to faulting. The results are presented in Appendix A.

In the summer of 1984, a multi-institutional 6-week microearthquake monitoring program was conducted on the eastern Wasatch Plateau in the vicinity of Joes Valley, East Mountain, and Gentry Mountain. The objectives of this monitoring relative to the seismotectonic study were to: 1) determine the state of stress in the crust beneath Joes Valley, 2) map the depth distribution of earthquakes in the eastern Wasatch Plateau, and 3) determine the relationship between ongoing seismicity and geologic structure, in particular the Joes Valley faults. The results of this microearthquake study are discussed in section 8.0.

## 1.2 Joes Valley Dam

Joes Valley Dam is a zoned earthfill structure 58 m high and 229 m long constructed in 1966 across the east-flowing Seely Creek approximately 24 km west of Castledale, Utah. The reservoir capacity is 7.7 x $10^7$ $m^3$. Joes Valley Dam is 120 m downstream (east) from the northern Joes Valley graben, a major structural feature on the Wasatch Plateau, and the reservoir is within the graben.

## 1.3 Scofield Dam

Scofield Dam is a homogeneous earthfill structure located on a tributary of the Price River, about 35 km northwest of Price, Utah. The dam, which was completed in 1946, has a structural height of 38 m and a crest length of 175 m at an elevation of 2327 m. The reservoir has a capacity of 6.7 x $10^7$ $m^3$. Scofield Dam is 1.2 km downstream (east) from Pleasant Valley graben, a major structural feature on the northeast Wasatch Plateau.

## 1.4 Huntington North Dam

Huntington North Dam consists of a dam in two sections and a dike composed of zoned earthfill embankment materials which total about 1.8 km in length with a maximum height of 20 m. The dam is located off

Huntington Creek in the Castle Valley, 2 km northeast of the town of Huntington, Utah. The reservoir impounded by Huntington North Dam has a capacity of 6.7 x $10^6$ $m^3$ at an elevation of 1780 m.

## 1.5 Acknowledgments

We would like to thank the Upper Colorado Region, in particular the Uinta Basin Construction Office, for the logistical support required for the excavation, shoring, and restoration of the several trenches and soil pits that were essential to this study. This work was accomplished in a timely and safe manner in remote areas where access was difficult at best. The Land Acquisitions Branch in Salt Lake City was very helpful in acquiring permission to make these excavations on privately owned land. Personnel of the U.S. Forest Service office in Ferron, in particular Bill Dye and John Niebergoll, were instrumental in helping us acquire permission for excavations in the Manti-La Sal National Forest and allowed us to stay at Forest Service facilities in Joes Valley. Irving Witkind of the USGS (U.S. Geological Survey) provided us with unpublished data and discussion of the regional structure as well as logistical support and advice for our field work. Chuck Pillmore (USGS) authorized our use of the PG-2 photogrammetric plotter. Ed Baltzer and Carol Krinsky provided extensive field and office technical assistance and Bill Manley assisted in the office. Alan Nelson reviewed the Quaternary geology section.

Our appreciation is extended to F. Royse and L. Standlee of Chevron Oil Company, Denver, for allowing us to review their seismic reflection data across the Wasatch Plateau and for their helpful discussions regarding the interpretation of these data. We also thank CGG of Denver for allowing us to review their proprietory reflection data at no cost. We would especially like to thank W. J. Arabasz of the UU (University of Utah) for his major contribution towards the planning and execution of the 1984 Eastern Wasatch Plateau Experiment and for the subsequent data analysis and interpretation he performed together with D. J. Williams. I. G. Wong of WCC (Woodward-Clyde Consultants) was also a co-investigator in the field experiment and his input and support is greatly appreciated. Other individuals providing significant contributions to the data collection include J. C. Pechmann, D. C. Martin, E. McPherson, T. L. Olson, J. F. Peindo, K. A. Poulson, and J. K. Whipp of the UU, and J. Humphreys and J. A. Adams of WCC. C. K. Wood, R. LaForge, and R. A. Hansen of the E&R Center also contributed to the microearthquake data collection. M. Foster of the Regional Office provided helicopter support for the installation of the portable microearthquake array.

## 2.0 Tectonic Setting

Joes Valley and Scofield Dams are located on the Wasatch Plateau, a 5000 $km^2$ area of flat-lying Cretaceous through Eocene sedimentary rocks that is part of a structural and physiographic transition zone between the Basin and Range and Colorado Plateau physiographic and tectonic provinces (figure 2.1). The Wasatch Plateau is bounded on the west by the Sanpete-Sevier Valley and on the east by an erosional escarpment that forms the western edge of the San Rafael Swell, a Laramide anticlinal upwarp on the Colorado Plateau (figure 2.1). Huntington North Dam is located 8 km east of this escarpment in the Castle Valley.

The stratigraphic sequence in the San Rafael Swell and underlying the Cretaceous rocks of the Wasatch Plateau consists of Paleozoic and Mesozoic marine and nonmarine sedimentary rocks that thicken westward to the western margin of the North American craton. During the late Jurassic to Eocene Sevier orogeny, major west to east thrusting occurred across the margin of the craton on imbricate low-angle faults (Armstrong, 1968; Standlee, 1982). In central Utah, the leading edge of this system of thrust sheets was originally thought to be the Mount Nebo thrust (Baker and others, 1949), 25 km west of the Wasatch Plateau, but recent interpretations of seismic reflection data suggest that thrust faults extend farther east, below the Wasatch Plateau and Castle Valley (Standlee, 1982; Arabasz, 1986; Appendix D, this report).

Folds and monoclinal flexures on the Colorado Plateau resulted from the Cretaceous-Eocene Laramide orogeny and relative stability has prevailed on this crustal block since the early Tertiary (Davis, 1978). Middle and late Cenozoic predominantly east-west extensional deformation has occurrred in the Basin and Range and the BR-CP (Basin and Range-Colorado Plateau) transition zone. The system of north-trending normal faults on the Wasatch Plateau that is the main focus of this study appears to be the easternmost expression of this extensional deformation.

In this section, the general geologic characteristics, tectonic history and historic seismicity of the Basin and Range and BR-CP transition zone are summarized.

### 2.1 Basin and Range

The middle and late Cenozoic evolution of the western Cordillera, east of the Sierra Nevada, has been dominated by extensional deformation as evidenced by physiography, late Cenozoic fault patterns, and surface faulting associated with both prehistoric and historic earthquakes. The Basin and Range physiographic province, as defined by Fenneman (1931) and including surrounding transition areas with similar geological and geophysical characteristics, occupies an area of more than $10^6$ $km^2$

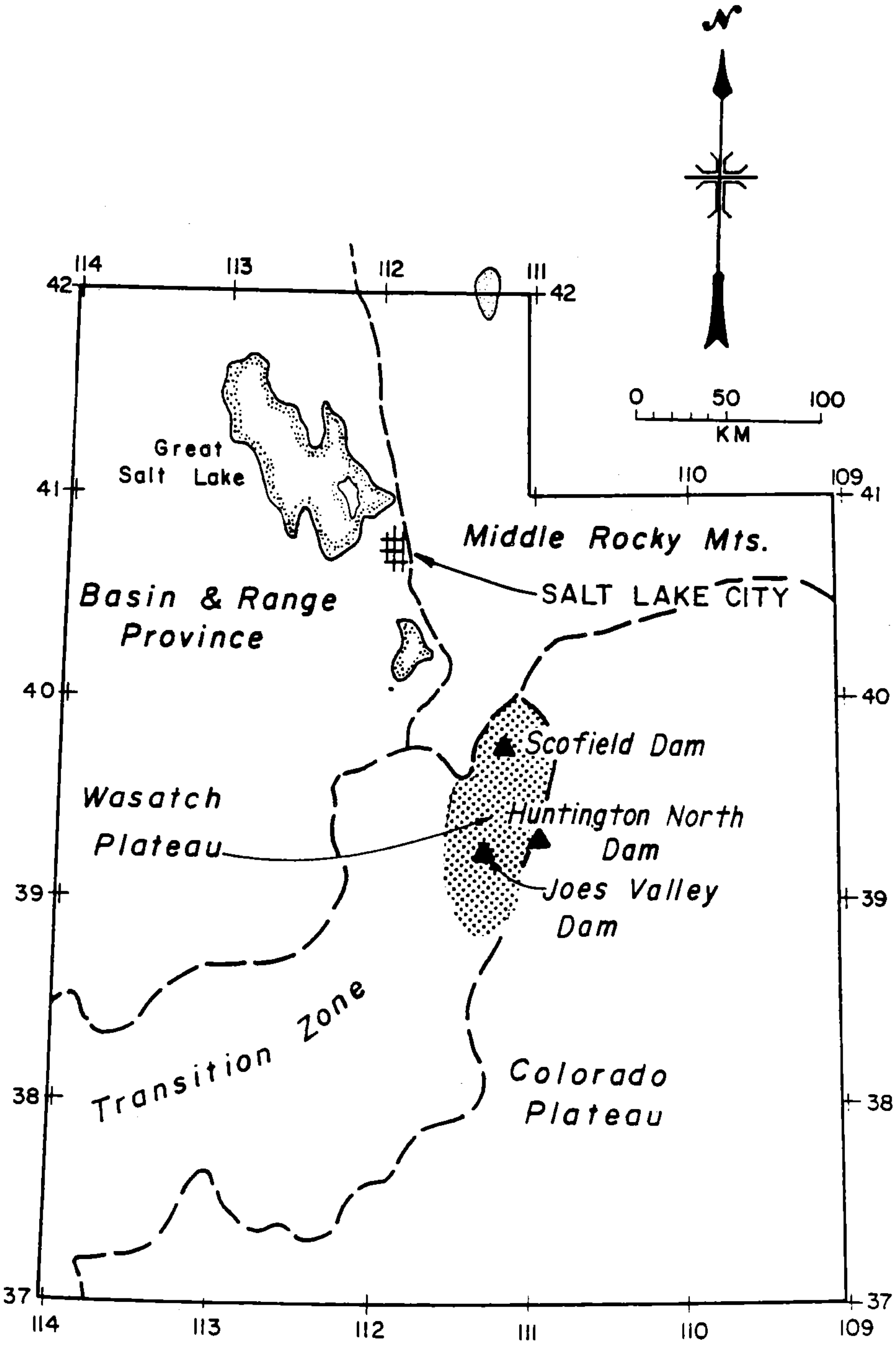


Figure 2.1: Location of the Wasatch Plateau and Joes Valley, Scofield, and Huntington North Dams in relation to the Basin and Range and the Colorado Plateau. The Wasatch Plateau (stippled) is located in the transition zone between these two major physiographic provinces of Utah (from Stokes, 1977; Arabasz and Julander, 1986).

(Eaton,1982). The Basin and Range province consists of a series of generally north-trending linear mountain blocks, typically 15-20 km wide, separated by structural basins of similar width. The ranges consist of tilted and faulted Tertiary volcanic rocks and older igneous and sedimentary rocks bounded by normal faults on one or both margins. The intervening valleys are filled for the most part by late Tertiary sediments. The resulting structural relief of individual range-basin pairs is estimated to vary from 2 to 5 km (Stewart,1978). The relative scarcity of sedimentary basin fill deposits older than 17-18 Ma and the occurrence of numerous sheetlike ash flow tuffs of early Neogene age (20-25 Ma) deposited across areas of low relief (Christiansen and McKee, 1978) indicate that "Basin and Range faulting" dates from about 17 Ma.

The Basin and Range province exhibits characteristics that are similar to those of continental rift zones in which crustal extension is the fundamental mechanism of deformation. Recent papers by Stewart (1978), Eaton (1982), Zoback and others (1981), and Zoback (1983) discuss a basin-range topography of linear valleys and ranges bounded by late Cenozoic normal faults as one characteristic that distinguishes this region from surrounding areas. Others include: high heat flow, thin lithosphere, the occurrence of low seismic velocities in the underlying upper mantle, a history of long-lived episodic magmatism, and a pronounced crustal low velocity layer at depths of 8.5-13.0 km (Keller and others, 1975).

Average elevations of closed basins in the eastern Basin and Range vary from 1200-1500 m and the basins are separated by tilted range blocks about 30 km apart. These basins typically contain thicknesses of 900-1500 m of late Cenozoic basin fill and are bounded by normal faults on one or both sides with estimated displacements of 2-5 km (Stewart, 1978).

Two general models of Basin and Range faulting have been proposed for the western United States. The first is a listric fault model, based on both the mapped geometry of normal faults developed in extensional terrains during the middle Cenozoic and exposed in range blocks elevated in the late Cenozoic, and on the interpretation of numerous seismic reflection profiles. In this model normal faults flatten with depth and sole into a subhorizontal detachment at depths of 5-17 km (e.g. Anderson, 1971; Proffet, 1971; Effimoff and Pinezich, 1981). The second model considers normal faults to be planar, dipping 45°- 60° and extending to mid-crustal depths of 12-15 km. This model is based on geodetic measurements of subsidence associated with the Borah Peak earthquake (Stein and Barrientos, 1985) and seismologic analysis of large magnitude earthquakes in the Great Basin and the ISB (Intermountain seismic belt) (Doser, 1984). These faults root in a mid crustal zone of intrusion or plastic flow (Eaton, 1982; Stewart, 1971; 1978) or at the brittle-ductile transition (Smith and Bruhn, 1984).

Interpretations of seismic reflection profiles (MacDonald, 1976; Allmendinger and others, 1983) indicate the presence of a low-angle, west-dipping detachment in the Sevier desert in south-central Utah that appears to root in the lower crust (Wernicke, 1981; Anderson and others, 1983). For example, on the east side of Cricket Mountain, one of these high-angle planar normal faults, characteristic of the second model, has a minimum of 187 m of late Cenozoic vertical displacement as well as evidence for Holocene displacement (Crone and Harding, 1984). This Holocene displacement is interpreted to be a response to movement on the low-angle detachment. Crone and Harding (1984) further suggest that if low-angle normal faults can store and release strain energy, then the most intense ground shaking associated with a large magnitude earthquake may be located several kilometers from the site of the surface rupture (Anderson and others, 1983). This interpretation is difficult to reconcile, however, with recent theories of earthquake nucleation (Das and Scholz, 1983).

## 2.2 Basin and Range-Colorado Plateau transition zone

The BR-CP transition zone is a region defined by geologic structure and crustal thickness, and delineated by contemporary seismicity (discussed in section 2.4). It spans a distance of about 100 km between the eastern margin of the Basin and Range province and the Colorado Plateau (figure 2.1). As a result of profound, generally east-west oriented extension in western North America, crustal thickness varies from 15-20 km in the Basin and Range to 40 km in the Colorado Plateau (Keller and others, 1979). Earthquake focal mechanisms indicate a change from east-west extension in the Basin and Range to compression in the Colorado Plateau (Zoback and Zoback, 1980). Recent studies have defined more accurately the location of this change in the direction and magnitude of least principal stresses both on the Wasatch Plateau (McKee and Arabasz, 1982; Arabasz and Julander, 1986; also see section 8 of this report) and in the Uinta Basin (Martin and others, 1986). Recent hydrofracture studies at two locations near the central Wasatch Front have also shown that the region is characterized by northeast-southwest least principal stresses and potentially active normal fault slip conditions along northwest striking planes of discontinuity. (Haimson, 1981; 1984; Haimson and Lee, 1985; Zoback and others, 1981).

This transition zone is also manifested in regional topography. In contrast to the closed basins in the Basin and Range, the transition zone in central Utah consists of a high (2 400-3 000 m elevation) upland surface, the Wasatch Plateau, that is disrupted by narrow north-trending graben (plate 1) with floors at elevations of 1 800-2 400 m. The Wasatch fault, the Sevier-Sanpete Valley, and the Wasatch Plateau, three major features within the transition zone that are pertinent to this study, are discussed in the following sections.

### 2.2.1 Wasatch fault

The Wasatch fault (figure 2.1) is a major, late Quaternary, range-bounding normal fault that marks the abrupt physiographic boundary between the Basin and Range and Colorado Plateau provinces in north-central Utah. The fault extends for 370 km north from Gunnison, Utah to Malad City, Idaho. The fault trace is mapped near the base of the triangular facets that form the west face of the Wasatch Mountains. Along almost its entire length, vegetation lineaments and scarps in lacustrine sediments of Lake Bonneville, moraines and Holocene alluvial and colluvial deposits indicate the occurrence of late Quaternary surface displacements (Cluff and others, 1974; Swan and others, 1979; 1980; 1981a; 1981b).

Schwartz and Coppersmith (1984) recognize six major, independently behaving segments of the Wasatch fault based on variability in timing of individual events, changes in scarp morphology, and fault geometry. They suggest that only large earthquakes occur on the fault, all of a similar or characteristic size associated with average surface displacements of about 2 m. Schwartz and Coppersmith (1984) present the following conclusions based on the interpretation of trenches excavated on four of the six inferred segments of the Wasatch fault: (1) maximum stratigraphic displacement of Lake Bonneville sediments is more than 11 m, (2) the Holocene and late Pleistocene slip rate on the fault is 0.56 - 1.46 mm/yr, (3) the recurrence interval of surface displacements at the localities trenched is 1700-2700 years, and (4) the average displacement per event is 1.6-2.6 m.

Smith and Bruhn (1984) suggest that prexisting structure partly controls the position of segment boundaries of the Wasatch fault by demonstrating a coincidence of some segment boundaries with the location of lateral and sidewall ramps in Sevier age thrust faults. They also present cross sections, based on seismic reflection profiles, depicting subsurface dips of the Wasatch fault that are less than the 60°-80° dips of the surface scarps. On the southern segments of the fault, south of the town of Nephi, both the late Quaternary slip rate and the range-front relief associated with the Wasatch fault diminish as the fault dies out at Gunnison, Utah (Schwartz and Coppersmith, 1984).

The lack of spatial correlation of earthquake epicenters with the mapped trace of late Cenozoic faults, particularly the Wasatch fault, has been a notable feature of the ISB in Utah since the initiation of earthquake monitoring. For the southern part of the Wasatch fault, based on local microseismic monitoring, McKee and Arabasz (1982) conclude that the lack of correlation of epicenters with the Wasatch fault is not simply due to poor epicentral resolution, but may be related to the orientation and behavior of the fault at depth (see section 8.1). They support this conclusion by presenting a "sanitized" section across the Wasatch fault based on proprietary seismic reflection profiles which depicts the fault as shallowing in dip in the subsurface and becoming subhorizontal at a depth of 6-7 km (McKee and Arabasz, 1982, p.143).

### 2.2.2 Sevier-Sanpete Valley

The Sevier-Sanpete Valley is between the Wasatch fault and the Wasatch Plateau in the BR-CP transition zone. The origin of this valley, as well as the Wasatch monocline along its eastern margin and the folds in Mesozoic and Cenozoic rocks within and adjacent to the Sevier-Sanpete Valley, has long been a subject of controversy. Stokes (1952; 1956) was the first to suggest salt movement as a mechanism to form these folds and compared this region with the Paradox Basin of eastern Utah where salt-cored folds are exposed. Recently, Witkind (1982), Witkind and Sprinkel (1982), and Witkind and Page (1984) have further elaborated on this hypothesis in interpreting the complex structures at the surface as resulting from the episodic development and subsequent erosion and collapse of salt diapirs in the Jurassic Arapien Shale, implying that the related folds and faults do not persist at depth below this horizon. Witkind (1982) postulates at least three episodes of diapiric movement: (1) late Cretaceous, (2) Paleocene to Oligocene, and (3) Oligocene to Pliocene or Pleistocene.

As in the Idaho-Wyoming thrust belt to the north (Royse and others, 1975; Dixon, 1982), geophysical data generated for oil and gas exploration, locally detailed surface mapping, and seismologic investigations suggest that the folds and faults in central Utah result from a complex interaction between older thrust faults and younger normal faults. Standlee (1982) discusses the role of Sevier-age thrust faulting in accomodating late Cenozoic extension in the region and presents cross sections based on seismic reflection profiles and drill holes that depict blind thrusts and normal faults joining or being truncated by these reactivated thrusts. Royse (1983) suggests that the Wasatch monocline results from extension above a west-facing ramp on an underlying thrust fault. Both of these interpretations suggest that normal faults in the region have limited depth. Microseismic data, however, indicate the presence of hypocenters to depths of about 15 km. In addition, these data produce a diffuse pattern of earthquakes which lacks spatial association with mapped faults, and a predominance of normal focal mechanisms with moderate to steep dips (Mckee and Arabasz, 1982; Arabasz and Julander, 1986).

Anderson and Barnhard (1984) point out that the chaotic pattern of Cenozoic normal faults in the transition zone is similar to that found in areas underlain by low-angle detachment faults. Based on compilations of the rake angles measured on exposed fault planes they also suggest that Cenozoic strike-slip faulting has played a significant role in the structural development of the region. This interpretation is consistent with focal mechanisms that suggest strike-slip faulting at depth (Mckee and Arabasz, 1982). Miocene and Pliocene age basin-fill deposits in Sevier and Sanpete valleys and late Quaternary fault scarps in Sevier Valley indicate that deformation has continued in the region in the late Cenozoic (Anderson and Bucknam, 1979).

### 2.2.3 Wasatch Plateau

The Wasatch Plateau, located on the eastern margin of the BR-CP transition zone (figure 2.1), is an upland plateau reaching elevations of over 3 000 m, capped by nearly flat-lying lower Tertiary sedimentary rocks. It is bounded by the Wasatch monocline where the sedimentary rocks of the Wasatch Plateau dip west below the Sevier-Sanpete Valley and by a high erosional escarpment separating it from the Castle Valley to the east. The plateau is disrupted by numerous north and northeast-trending en echelon normal faults that bound narrow steep-sided symmetric grabens with tens to hundreds of meters of topographic relief. Joes Valley and Scofield Dams and Reservoirs are located in the two most prominent of these structures - the Joes Valley and Pleasant Valley grabens, respectively (plate 1).

2.2.3.1 Stratigraphy and structure

The stratigraphy of the Mesozoic and Cenozoic rocks which comprise the Wasatch Plateau was defined and later revised by E.M. Spieker and his students, and their works form the basis for all subsequent studies. Following the detailed work by Clark (1928) of Mesozoic rocks in the Book Cliffs which are adjacent to the Wasatch Plateau on the northeast, Spieker and Reeside (1925) provided the first general description of the Cretaceous and Tertiary rocks of the plateau. Subsequently, Spieker and Baker (1928) described the geology of the coal fields in the southern part of the region. In 1931, Spieker published a landmark study in which he presented the first detailed descriptions of the stratigraphy and structure of the eastern Wasatch Plateau and included geologic maps of the area that remain useful today. He later revised the late Mesozoic and early Cenozoic geologic history of the region based on new stratigraphic and paleontologic data (Spieker, 1946, 1949). Detailed mapping has since been carried out in selected areas of the plateau, mainly to address questions related to oil and gas exploration (Walton, 1954) or coal investigations (Hayes and Sanchez, 1979; Sanchez and Hayes, 1979; Ellis, 1981a; 1981b; Ellis and Frank, 1981; Sanchez and Brown, 1983).

A generalized stratigraphic section for the Wasatch Plateau is presented in figure 2.2. The oldest exposed rocks of the plateau, found along the southeast margin, are marine shale and sandstone members of the Cretaceous Mancos Formation. Separating the Mancos from the Blackhawk Formation is the Star Point Sandstone, a prominent cliff-former exposed on the eastern escarpment of the plateau. In the central and northern plateau, where Joes Valley and Scofield Dams are located, the stratigraphic section consists of a thick section of Cretaceous rocks of the Mesaverde Group including Blackhawk Formation sandstones, siltstones and coal beds, the prominent cliff-forming Castlegate Sandstone, and the Price River Sandstone (figure 2.3). The Cretaceous-Tertiary North Horn Formation, the predominant bedrock unit on the surface of the plateau, is the source of numerous landslides due to its easily erodible and unstable nature (Godfrey, 1978). A distinctive layer of gray, resistant Eocene non-marine Flagstaff Limestone caps the Wasatch Plateau.

The sedimentary beds of the Wasatch Plateau are gently folded and dip northward at the northern edge, and west, corresponding to the attitude of the San Rafael Swell, in the central portion. On the west side of the plateau, the Wasatch monocline plunges into the Sanpete-Sevier Valley.

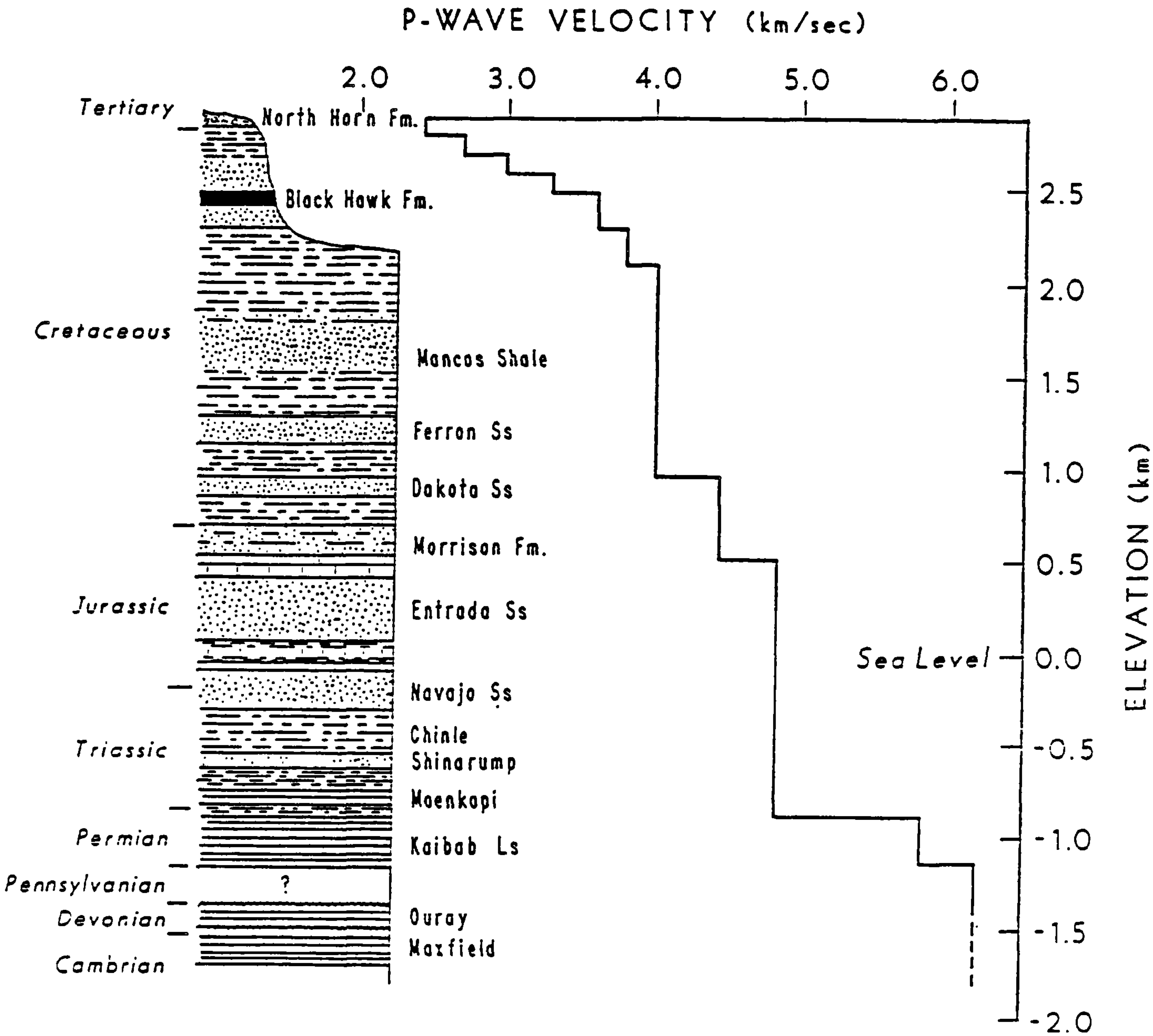


Figure 2.2: Generalized stratigraphic section and p-wave velocity model of the Wasatch Plateau region (from Arabasz and Williams, 1986).

| SYSTEM | SERIES | FORMATION | SYMBOL | LITHOLOGY | THICKNESS IN FEET (METERS) | DESCRIPTION |
|---|---|---|---|---|---|---|
| QUATERNARY | | Unconsolidated deposits | Qal Qc Qf Qls Qm | | 0-66+ (0-20+) | alluvium, colluvium, alluvial fans, landslide deposits, and moraines |
| | | | | | 460+ (140+) | limestone, white, with minor light colored shale, channel sandstone, gypsum and chert |
| TERTIARY | Paleocene | Flagstaff Limestone | Tfb Tfa | | 385 (117) | shale and limestone, dark blue-gray, thin-bedded |
| | | North Horn Formation | TKnd | | 427 (130) | sandstone, conglomeratic sandstone, light gray, olive gray or pale pink, medium to coarse-grained, locally has variegated shales and mudstones |
| | | | TKnc | | 377 (115) | limestone, micritic gray brown to tan and fossiliferous in lower part, sandstone, light gray, gray-orange pink or pale orange, mostly fine-grained, and calcareous |
| UPPER-CRETACEOUS | | | TKnb | | 371 (113) | sandstone, dark yellow orange weathering, medium to thick-bedded, and fine-grained, weathers to angular blocks |
| | | | TKna | | 410 (125) | sandstone, gray to yellow gray, fine- to medium-grained interbedded with conglomerate and gray limestone |
| | | Price River Formation | Kpu | | 295 (90) | sandstone, yellow to yellow-brown, fine- to medium-grained, generally thin-bedded and poorly cemented, slope forming, with an occasional ledge-forming thick bedded sandstone |
| | | | Kpl | | 394 (120) | sandstone, yellow to yellow brown, fine- to medium-grained, medium to thick bedded, well cemented, crossbedded, ledge-forming with some shaly interbeds |
| | | Castlegate Sandstone | Kc | | 328 (100) | sandstone, yellow to dark yellowish orange weathering, fine- to medium-grained, calcareous, forms prominent cliffs |
| | | Blackhawk Formation | Kb | | 525 (160) | interbedded sandstone, muddy sandstone, siltstone, shale, shaly sandstone, shaly to thickbedded, contains coal-beds in the unexposed subsurface (not shown), generally slope forming |

Figure 2.3 Stratigraphy of the central Wasatch Plateau in the vicinity of Joes Valley Dam (from Kitzmiller, 1982).

The most prominent structures on the plateau are the north-trending normal faults that displace the Flagstaff Limestone and underlying units by tens to hundreds of meters. Four of these structures are discussed in detail in this report: the Joes Valley, Pleasant Valley, Snow Lake and Gooseberry fault zones (plate 1). Evidence for Quaternary displacement on these faults has been observed by several previous investigators (Spieker and Billings, 1940; Kucera, 1954; Witkind and others, 1978; 1982; Anderson and Miller, 1979; Kitzmiller, 1982). Bucknam (U.S. Geological Survey, 1976), in a memorandum to the USBR (U.S. Bureau of Reclamation), refers to fault scarps in Quaternary deposits which underlie Joes Valley Reservoir.

The origin of the long linear grabens on the Wasatch Plateau cannot be resolved with presently available geologic and seismologic data. Because of limited data and differing interpretations of the geologic structure underlying the plateau, three distinct models have been developed to explain the existence of the surface geologic structure: the first model, a reactivated thrust fault model, is based on work in the overthrust belt to the west (Royse and others, 1975; Dixon, 1982; Standlee, 1982) and interprets the Wasatch Plateau normal faults to be shallow listric faults that join a west-dipping detachment surface or a reactivated thrust fault; the second model assumes that the faults are related to the collapse of salt diapirs similar to that proposed for the origin of the Sanpete-Sevier Valley; and the third model, based on seismologic data discussed in section 2.4, defines the faults to be moderate- to steeply-dipping planar normal faults that extend to seismogenic depths.

The reactivated thrust fault model is illustrated in figure 2.4, a hypothetical east-west cross section that disects the Wasatch Plateau in the vicinity of Joes Valley Dam. A key assumption of this model is the termination of the high-angle portion of the Joes Valley faults above both the Navajo Sandstone and an inferred low-angle detachment that is believed to extend east across the plateau into Castle Valley. In this model, Joes Valley graben formed as a result of "thin-skinned" horizontal extension of the upper 3-5 km of crust above the low-angle detachment (Standlee, 1982; Royse, 1983). This detachment intersects and/or merges with the Ancient Ephraim fault, a major normal fault bounding the western Wasatch Plateau. The formation of the Joes Valley graben may have resulted from a process involving gravity backsliding on the low-angle detachment in response to extensional stresses dominating to the west or subsurface displacement on the Ancient Ephraim fault.

The second model involves the interpretation of the normal faults as having resulted from the mobilization of salt beds including the repeated development and collapse of salt diapirs and is based on the model proposed for the Sanpete-Sevier Valley to the west (see section 2.2.2). In this model, up to 300 m of surface displacement is assumed to have been accomodated at depth by mobilization of the salt beds of the Jurassic Arapien Shale. The Arapien Shale lies above the Navajo Sandstone, therefore, in this model the graben-bounding faults die out before they reach the Navajo Sandstone.

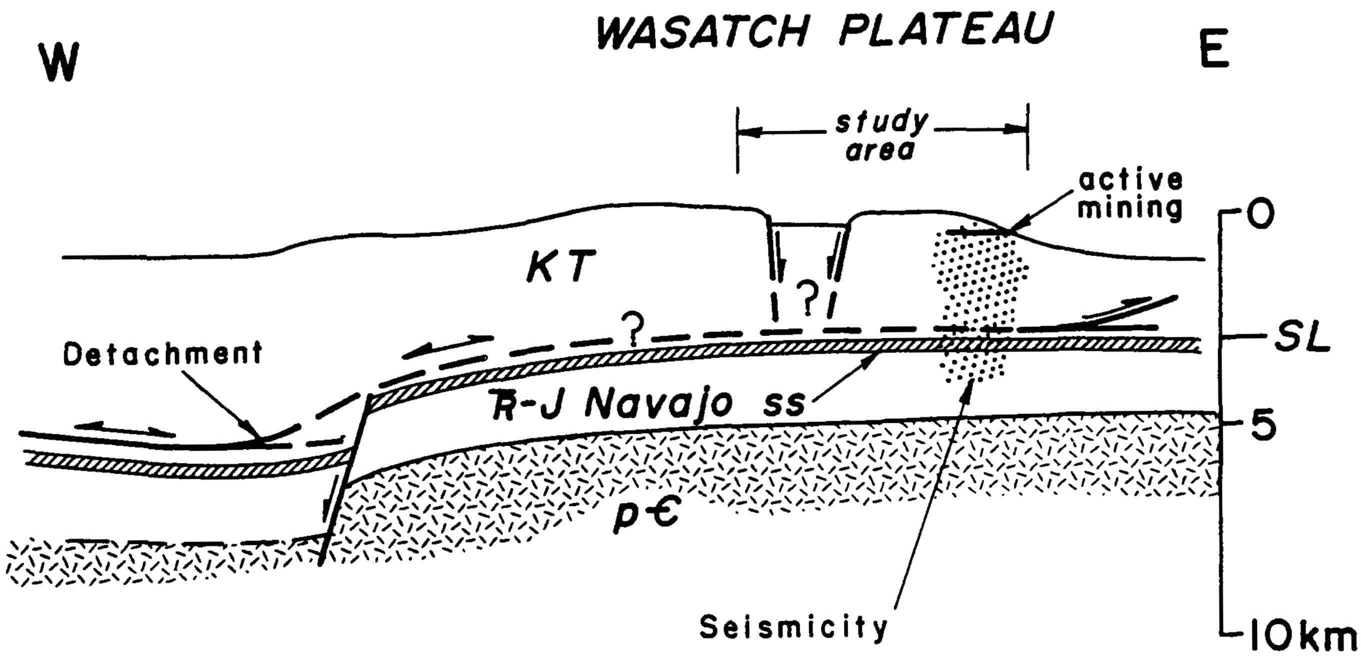


Figure 2.4: Schematic geologic cross section illustrating hypothetical interpretation of "thin-skinned" horizontal extension in the Wasatch Plateau (from Arabasz, 1986).

The third model is based on seismologic data associated with large-magnitude scarp-forming earthquakes occurring in the ISB and assumes the Wasatch Plateau faults to be moderate- to high-angle planar normal faults that extend to mid-crustal, seismogenic depths cutting the inferred low angle detachment. This model is discussed in more detail in section 2.4.

#### 2.2.3.2 Quaternary geology

The first description of the Quaternary geology of the Wasatch Plateau was published by Spieker and Billings (1940). In this paper they presented evidence for Pleistocene glaciation on the plateau. Kucera (1954), a student of Spieker's, studied the geology of the Joes Valley area and provided more detailed descriptions of Pleistocene moraines and outwash deposits as well as debris flows, landslides, and alluvial fans. More recently, Kitzmiller (1982) mapped the Joes Valley quadrangle. Oberhansley (1980) mapped the Fairview Lakes quadrangle which covers part of the Gooseberry graben and contains moraines correlated to the Pinedale glaciation in the Rocky Mountains. Detailed mapping and age dating of Quaternary deposits in the northern part the Joes Valley graben were conducted as part of the present study in order to evaluate the history of surface faulting and are summarized in Appendix A.

## 2.3 Historic seismicity

The historic record of earthquake occurrence in Utah dates back to about 1847 when Morman settlers first moved to the Salt Lake City area. Regional-scale instrumental coverage, however, did not exist in Utah until a nine-station statewide network was installed in 1962. Major instrumentation of Utah, and especially the Wasatch Front, took place in 1974 with the installation of a telemetered network of high-gain seismograph stations, thereby increasing the number of operating stations in Utah to 31. The distribution of the 58 operational seismograph stations within or near the border of Utah as of December 1985 is shown in figure 2.5. In the next section a general discussion of the occurrence of earthquakes for the past 130+ years in Utah and adjoining areas on a regional scale is presented. This will be followed by a more detailed discussion of the historic seismicity local to the study area.

### 2.3.1 Regional seismicity - the Intermountain seismic belt

Approximately 8 to 10 years after the installation of the statewide network in Utah in 1962, a noticable pattern of earthquake epicenters emerged from what was the apparently random distribution of seismicity in central and northern Utah. A sufficient set of well located earthquakes existed by 1972 to define a northsouth trending zone of diffuse, but locally intense, seismicity at least 100 km wide, roughly centered on the Wasatch fault (Smith and Sbar, 1974). This zone of intraplate seismicity is formally referred to as the ISB (Intermountain seismic belt), and has subsequently been shown to extend for over 1300 km, from the Arizona-Nevada border, through Utah, Idaho and Wyoming, and into Montana (Arabasz and others, 1979).

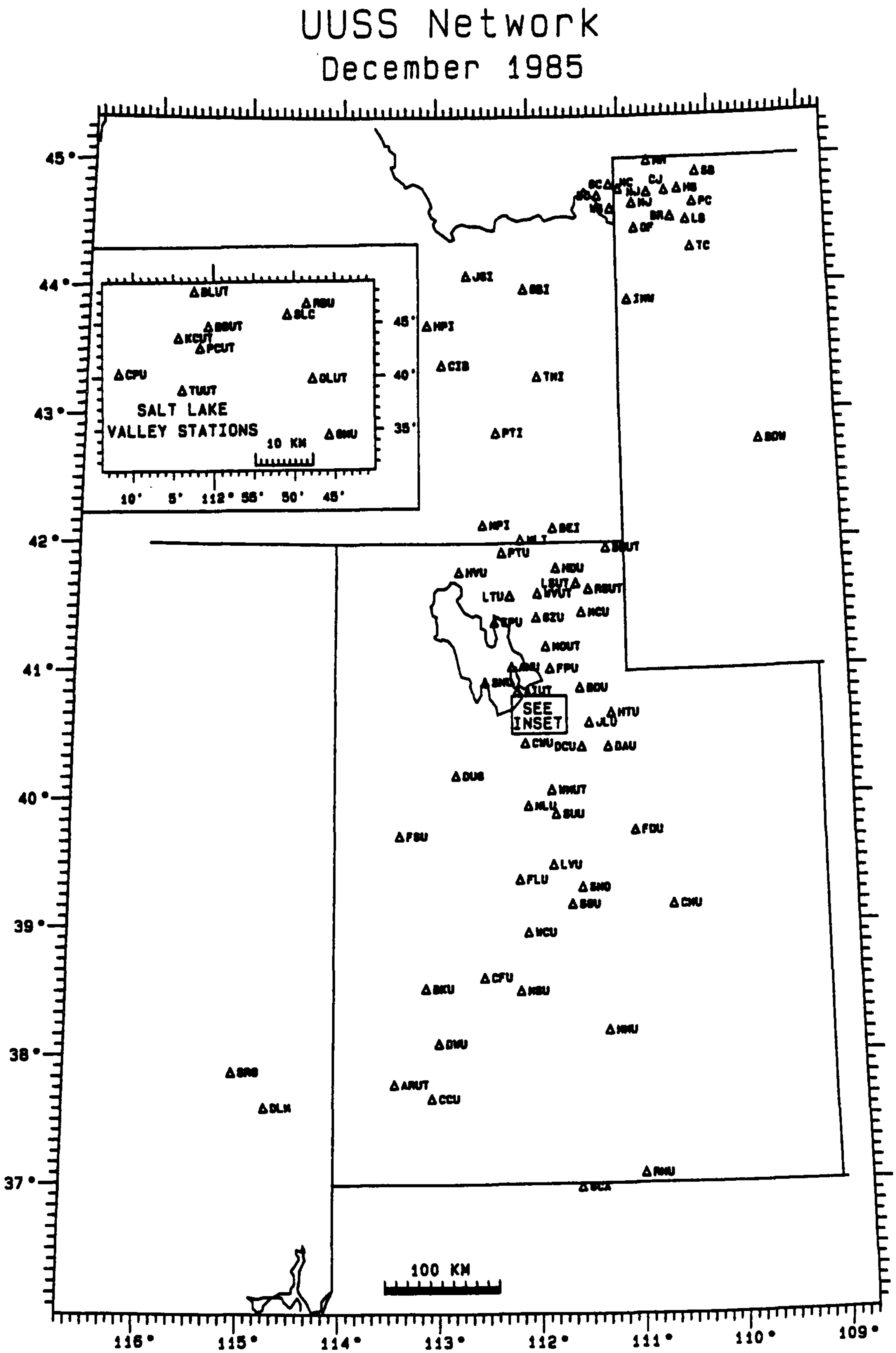


Figure 2.5: University of Utah Seismograph Network as of December 1985.

Detailed observations of earthquakes occurring within the ISB suggest a complicated relationship between contemporary tectonic processes and regional seismicity patterns. Contemporary seismicity has been related to a complex interaction among subplates of the North American plate (Atwater, 1970; Suppe and others, 1975; Smith, 1977; 1978), and has also been related to the migration of the Yellowstone hot spot (Smith and others, 1985). The resulting regional stress field is superposed on Laramide thrust faults, which further modifies an already intricate deformation process.

The correlation of contemporary seismicity with geologic structure in the ISB has been for the most part ambiguous. Targeting potential sources of moderate- to large-magnitude earthquakes using seismologic versus geologic data often leads to conflicting interpretations, since data from these two avenues of study are frequently not complimentary. For example, locations of recurrent sources of large-magnitude (greater than 7.0) earthquakes are typically indicated from geologic field studies since evidence of displacement will generally be preserved in the Quaternary record. However, studies of contemporary seismicity have not demonstrated that epicenters of small- and moderate-magnitude earthquakes, which generally do not produce surface rupture, are concentrated near late Quaternary faults. Furthermore, the occurrence of events such as the 1975 Pocatello Valley earthquake in southeastern Idaho (magnitude 6.0), where seismologic evidence indicates that faulting cuts across preexisting late Quaternary faults, suggests that the probable locations of moderate-magnitude earthquakes (up to 6.5) may not be indicated in the surficial geology (Arabasz and Smith, 1981; Arabasz and others, 1981).

Although the association between hypocenters and geologic structure has not been well defined, earthquakes occurring throughout the ISB have been shown to have many similar properties. Commonly observed features of earthquake occurrence within the ISB have been described by Smith and Sbar (1974), Smith (1978), and Arabasz and Smith (1979), and will be reviewed briefly. Among these features are: (1) diffuse seismicity which shows only general correlation with locations exhibiting late Quaternary surface faulting; (2) apparent lack of correlation between small- to moderate-magnitude earthquakes and surficial faults or other geologic structures; (3) shallow focal depths (less than 15 to 20 km); (4) sporadic occurrence of earthquakes both spatially and temporally; and (5) a persistent pattern of normal faulting indicating predominatly east-west extension.

Earthquakes occur in the ISB at relatively low rates when compared to plate margins. Low strain rates ($10^8$ to $10^9$ per year) are indicated from moment release calculations using contemporary seismicity (Doser, 1980; Greensfelder and others, 1980), and from examination of the distribution of late Quaternary faulting (Wallace, 1981). None the less, the ISB is considered to have one of the highest levels of earthquake risk in the contiguous United States outside California and Nevada (Arabasz and Smith, 1979). Normal faulting predominates, though strike-slip focal mechanisms have been observed.

Historic seismicity and the late Quaternary geologic record both indicate that moderate- and large-magnitude earthquakes occur infrequently; since the 1880's (Coffman and others, 1982; NOAA, 1985) there have been only two events with magnitude greater than 7 and roughly twenty events with magnitude greater than 6 within the entire ISB. Return periods of large-magnitude earthquakes (7 or greater) for active faults, as determined from the late Quaternary geologic record, are typically on the order of 1 000 to 10 000 years or greater (Arabasz and Smith, 1981; Wallace, 1981; Doser and Smith, 1983). Magnitude 6 plus events are more common, and since about 1870 (the earliest date for reliable records throughout the entire ISB) have occurred at an average rate of roughly once every 5 years (Coffman and others, 1982; NOAA, 1985).

On August 18, 1959, a sequence of earthquakes shook the area around Hebgen Lake, Montana, causing in excess of 11 million dollars in damage and the loss of 28 lives. On October 28, 1983, a large earthquake occurred in central Idaho, near Challis, which resulted in 2 deaths and a property loss of over 12 million dollars. These are the largest documented earthquakes in the historic catalog for the ISB.

The Hebgen Lake earthquake was originally assigned a magnitude (approximately $M_L$, Toucher, 1962) of 7.1, but recent analyses of the data suggest more likely magnitude values of $M_L$ 7.7 (Bolt, 1984), $M_L$ 7.6, $m_b$ 7.0, and $M_s$ 7.2 (Doser, 1984). The Borah Peak event has been assigned magnitudes of $M_L$ 7.2 (Bolt, 1984), $m_b$ 6.9, and $M_s$ 7.3 (National Earthquake Information Service, 1983). The seismic moment of the Hebgen Lake earthquake was estimated at $1.0 \times 10^{27}$ dyne-cm by Doser (1984). The moment for the Borah Peak earthquake was estimated at about $3 \times 10^{26}$ dyne-cm by Doser and Smith (1985), which is in good agreement with the value of $3.12 \times 10^{26}$ dyne-cm found by Ekstrom and Dziewonski (1985). These values are very close to the geodetically determined moment of $4.0 \times 10^{26}$ dyne-cm determined by Stein and Barrientos (1984). Stress drops for the Hebgen Lake and Borah Peak events were estimated at 115 and 24 bars, respectively (Doser, 1984; Doser and Smith, 1985).

Geodetic and seismological evidence strongly suggests that the Hebgen Lake and Borah Peak events occurred on normal faults dipping 45° to 60°. Rupture propagated unilaterally from one end of the fault, and nucleation of rupture occurred at about the 15 km-depth for both events. Doser (1984) determined a fault dip of 45° to 60° for the Hebgen Lake earthquake from a reanalysis of seismic records. Waveform modeling indicated a focal depth of 15 km, near the base of the seismogenic zone, with rupture propagating upwards to the surface and along the length of the fault zone. Many varied observations of the Borah Peak earthquake indicate that slip occurred on a 45 to 60° dipping planar normal fault (e.g., Barrientos and others, 1985; Smith and others, 1984; Stein and Barrientos, 1985; Ekstrom and Dziewonski, 1985). The main shock hypocenter had a depth of 14 to 16 km, and rupture propagated unilaterally along the fault. Barrientos and others (1985) modeled observed vertical deformation associated with the earthquake and suggested that moment release was concentrated in the depth range of 8 to 12 km.

Near-field acceleration data are not available for either the Hebgen Lake or Borah Peak earthquakes, however the Borah Peak event was recorded by strong motion instruments located at INEL (Idaho National Engineering Laboratory) some 100 km southeast of the main shock. These data were presented by Jackson (1985) and Jackson and Boatwright (1985). Peak horizontal accelerations recorded at two free-field sites were 0.04 and 0.08 g. Duration of the record segment where peak horizontal accelerations exceeded 0.02 g was 10 to 15 s, and the acceleration amplitude spectra were peaked in the frequency band of 5 to 15 Hz. Extrapolation of aftershock data recorded both at INEL and in the epicentral area suggested an upper limit of 0.8 g for near-field ground acceleration of the main shock.

The Hebgen Lake and Borah Peak earthquakes produced extensive surface rupture, with maximum recorded displacements of 6.7 and 2.7 m, respectively (Myers and Hamilton, 1964; Crone and Machette, 1984). The Hebgen - Red Canyon fault system showed an average surface displacement of about 2 m over a length of about 30 km (Myers and Hamilton, 1964). Crone and Machette (1984) measured an average surface displacement of 0.8 m along the 34 km rupture at Borah Peak. Both events occurred on faults exhibiting multiple late Quaternary displacements (Myers and Hamilton, 1964; Malde, 1971; Hait and Scott, 1978; Pierce, 1985).

Eight of the magnitude 6+ ISB historical earthquakes have occurred in Utah, including the 1936 M 6.6 Hansel Valley event, the only earthquake in Utah to have been accompanied by documented surface rupture during historic times (Shenon, 1936). Table 2.1 lists the pertinent data for the 15 historic Utah earthquakes that have magnitudes greater than or equal to 5.5. Figure 2.6 shows the epicentral distribution of all earthquakes greater than or equal to magnitude 4.0 in the Utah region together with zones of major faulting, and the locations of Joes Valley, Scofield, and Huntington North Dams.

Table 2.1 - Largest earthquakes in the Utah region, 1850 - 1986*

| local date | Lat. ( N.) | Long. ( W.) | Io | Magnitude ML | Location |
|---|---|---|---|---|---|
| 1884 Nov. 10 | 42.0 | 11.3 | 8 | (6) | Bear Lake Valley |
| 1887 Dec. 05 | 37.1 | 112.5 | 7 | (5-1/2) | Kanab |
| 1900 Aug. 01 | 40.0 | 112.1 | 7 | (5-1/2) | Eureka |
| 1901 Nov. 13 | 38.3 | 112.1 | 9 | (6-1/2+) | Richfield |
| 1902 Nov. 17 | 37.4 | 113.5 | 8 | (6) | Pine Valley |
| 1909 Oct. 05 | 41.8 | 112.7 | 8 | (6) | Hansel Valley |
| 1910 May 22 | 40.8 | 111.9 | 7 | (5-1/2) | Salt Lake City |
| 1914 May 13 | 41.2 | 112.0 | 7 | (5-1/2) | Ogden |
| 1921 Sep. 29 | 38.7 | 112.2 | 8 | (6) | Elsinore |
| 1921 Oct. 01 | 38.7 | 112.2 | 8 | (6) | Elsinore |
| 1934 Mar. 12 | 41.7 | 112.8 | 9 | 6.6 | Hansel Valley (Kosmo) |
| 1959 Jul. 21 | 37.0 | 112.5 | 6 | 5.5+ | Utah-Arizona border (Kanab) |
| 1962 Aug. 30 | 42.0 | 111.7 | 7 | 5.7 | Cache Valley (Logan) |
| 1966 Aug. 16 | 37.5 | 114.2 | 6 | 5.6 | Nevada-Utah border |
| 1975 Mar. 27 | 42.1 | 112.5 | 8 | 6.0 | Idaho-Utah border (Pocatello Valley) |

* Modified from Arabasz and Smith, 1979. Table includes earthquakes of Maximum Modified Mercalli intensity (Io) of VII or greater, or Richter magnitude 5.5 or greater. Magnitudes in parentheses are estimated from Io. Aftershocks excluded.

### 2.3.2 Local seismicity

In Utah, including the region of the subject dams, the ISB is characterized by: (1) a general predominance of normal faulting, with maximum earthquake magnitudes about 7-1/2 to 7-3/4; (2) moderate background seismic flux, which is lower by a factor of 4-6 than that along the western North American plate boundary; (3) diffuse seismicity with weak correlation with major active faults and with focal depths almost exclusively shallower than 15-20 km; (4) relatively long (>1000 yr) average recurrence intervals for surface faulting; and (5) a historical paucity of large (M 7) surface faulting earthquakes, despite abundant late Quaternary and Holocene fault scarps (Arabasz and Julander, 1986).

The distribution of seismicity across the BR-CP transition zone in the region of the dams for the period October 1, 1974 to December 31, 1981, as recorded by the University of Utah's telemetered seismic network, is shown in figures 2.7 and 2.8. These data clearly demonstrate the diffuse nature of earthquake occurrence within the transition zone as well as the intense clustering of seismicity associated with active areas of coal mining in the East Mountain area and east of Scofield Dam. There is a general lack of correlation with mapped faults across the transition zone, although an apparent clustering of seismicity is noted in the vicinity of the northern Joes Valley fault zone.

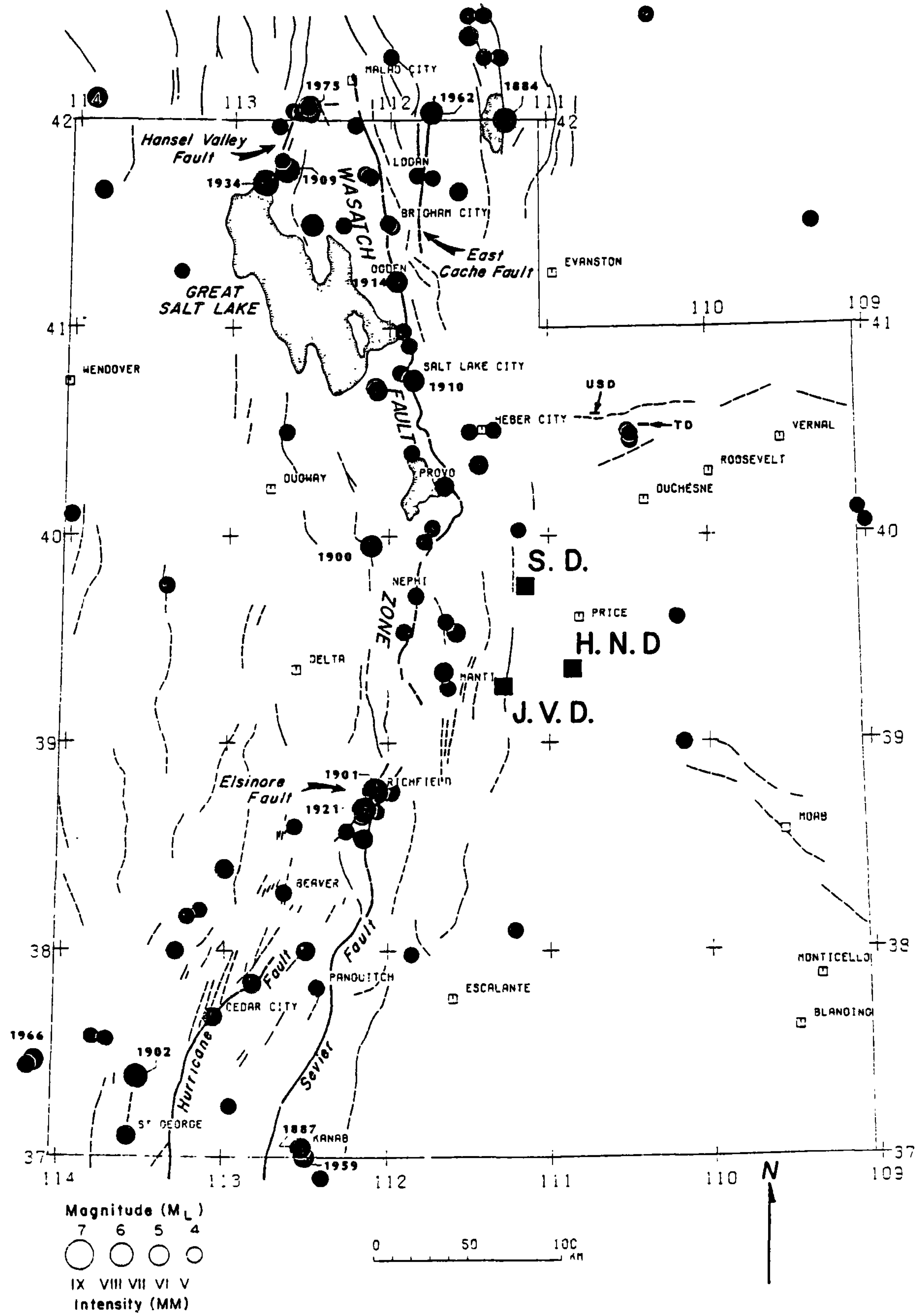


Figure 2.6: Epicenter map of the largest historical earthquakes in the Utah region, 1850-1985. For coincident epicenters, only the largest event is shown. Earthquakes of magnitude 5.5 or greater are dated by year. Cenozoic faults shown for reference. The locations of Joes Valley, Scofield, and Huntington North Dams are indicated by squares and identified by JVD, SD, and HND, respectively (modified from Arabasz and Smith, 1979).

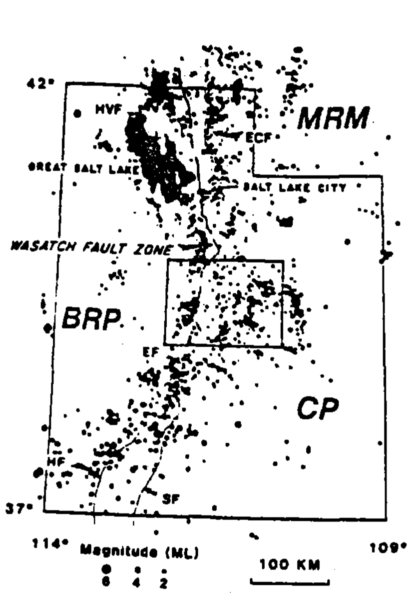


Index map of the Utah region showing the Intermountain seismic belt and the setting of the area of this study (rectangle). Seismicity is for the period July 1962-June 1978, based on University of Utah data (Arabasz et al. 1979). BRP indicates Basin and Range province. CP—Colorado Plateau. MRM—Middle Rocky Mts., HVF—Hansel Valley fault. ECF—East Cache fault. EF—Elsinore fault. HF—Hurricane fault. SF—Sevier fault.

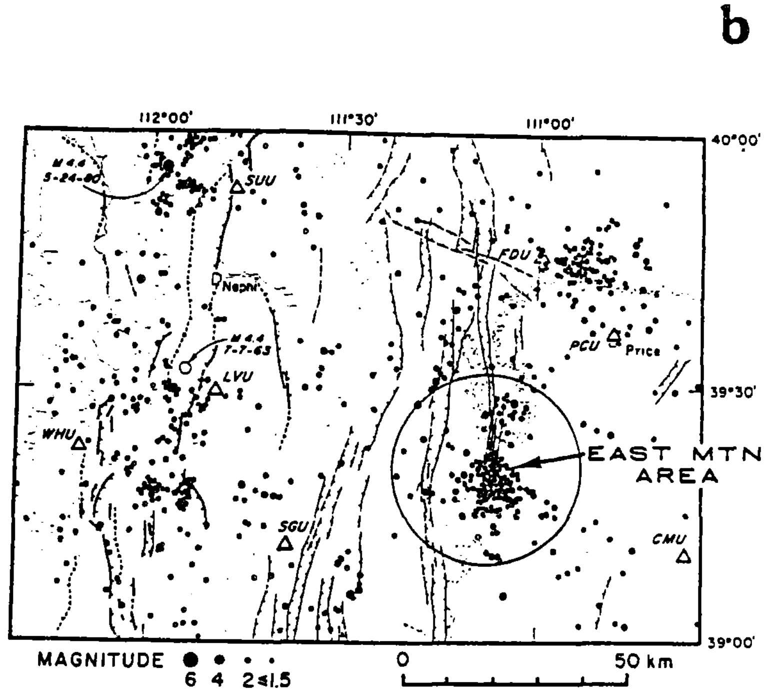


—Seismicity map of study area for the period: October 1, 1974-December 31, 1981, based on network monitoring by the University of Utah.

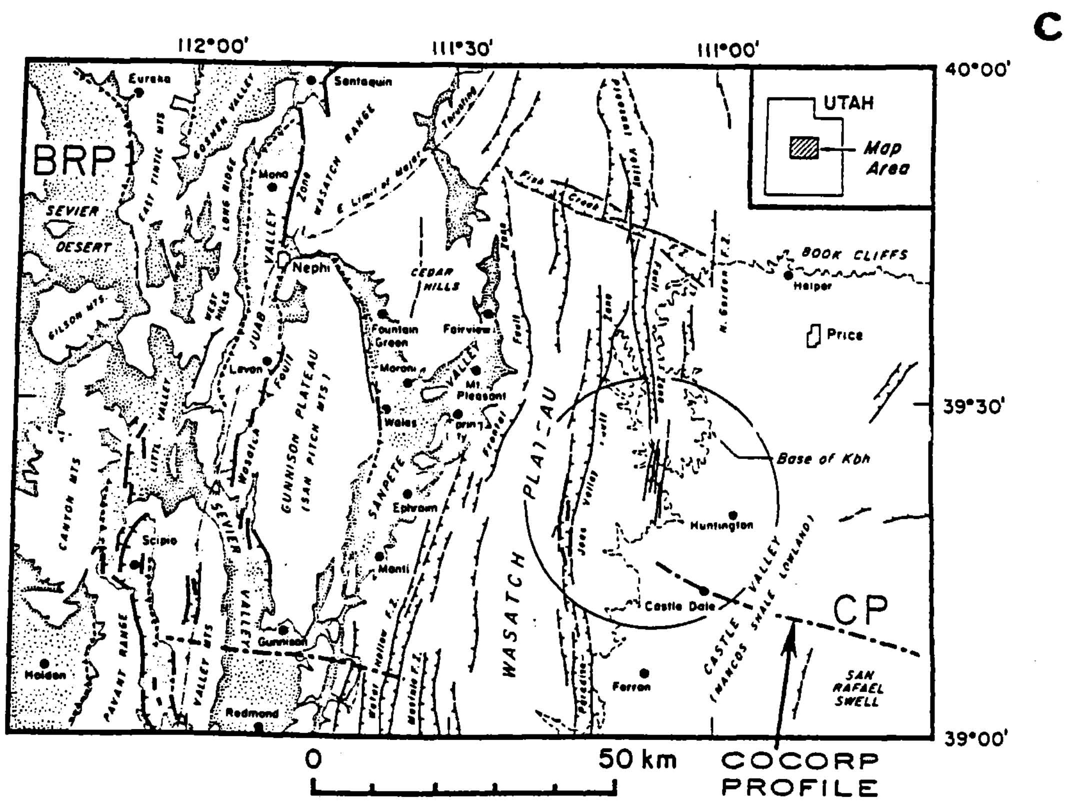


—Geologic sketch map of central Utah study area. Valleys floored with Quarternary alluvium shown by stippled pattern. Cenozoic normal faults shown by heavy lines, hachures on downthrown side; short dashes indicate concealed faults; broad pattern, late Quaternary fault scarps; BRP—Basin and Range province, CP—Colorado Plateau. Outcrop trace of Cretaceous Blackhawk Formation (Kbh) roughly defines erosional eastern boundary of Wasatch Plateau. Geology adapted from Stokes (1963), Witkind et al (1978), Bucknam and Anderson (1979), Doelling (1972), Burchfiel and Hickcox (1972).

Figure 2.7: Seismicity and generalized geology of the Central Utah Study Area of Mckee and Arabasz, 1982.

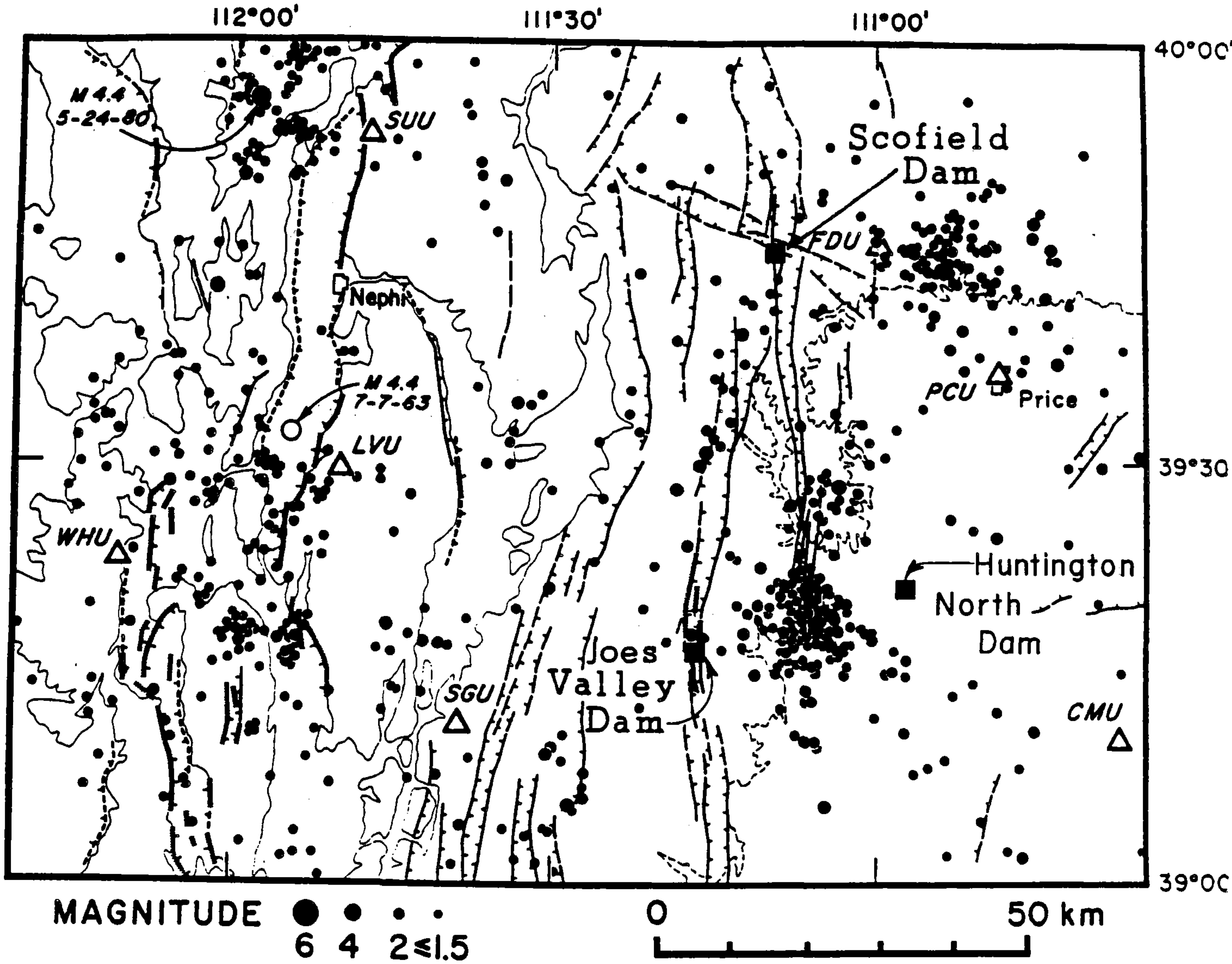


Figure 2.8: Enlarged view of figure 2.7b showing locations (squares) of Joes Valley, Scofield, and Huntington North Dams together with instrumental seismicity for the period October 1, 1974 to December 31, 1981.

A somewhat different picture of the seismicity relative to the setting of the subject dams is shown in figure 2.9, and includes: (1) all earthquakes of magnitude 2.0 or greater recorded by the University of Utah for the period October 1, 1974, to June 30, 1984; (2) all earthquakes of magnitude 4.0 or greater since 1962; and (3) all earthquakes of magnitude 5.0 or greater since 1850 (Arabasz and Julander, 1986). This figure demonstrates the diffuse nature of earthquake occurrence, but with intense clustering that predominately reflects accumulated background seismicity rather than isolated temporal sequences. Extensive efforts at refining the precision of the epicenters has verified the scattered regional pattern (Wecshler, 1979). Most earthquake epicenters in figure 2.9 have accuracies of ±3 km, however, errors of ±10 km cannot be ruled out, especially near the fringes of the main seismic belt. At the scale of figure 2.9, these data give a fairly accurate depiction in map view of the distribution of seismicity, but are inadequate for resolving the association of seismicity with geologic structure. This is primarily due to large errors in the focal depth of these earthquakes, which is expected when the distance to the nearest seismograph station is greater than the focal depth. More than three-fourths of the 2000+ earthquakes shown in figure 2.9 were located with the distance to the closest station exceeding 15 km.

Figure 2.9 indicates that earthquakes in the magnitude 5 range have occurred within 40-50 km of the dams. Since the beginning of instrumental monitoring in 1962, the largest shock to have occurred within 100 km of the dams was the magnitude 4.4 Juab Valley earthquake of July 7, 1963. Within 25 km of Joes Valley and Huntington North Dams, the largest shock since 1962 was a M 3.2 earthquake on February 9, 1977. Within 25 km of Scofield Dam, the largest shock was one of magnitude 2.6 on March 18, 1977.

## 2.4 Tectonic models for the ISB

### 2.4.1 Moderate-magnitude earthquake model

Since 1870 there have been fifteen earthquakes reported in the ISB with magnitudes in the range of approximately 6 to 6-3/4 (Coffman and others, 1982; NOAA, 1985). This figure does not include foreshocks or aftershocks. Earthquakes in this magnitude range, which are referred to as moderate-magnitude events, typically produce no surface displacement and do not appear to be related to active late Quaternary faults. For the purpose of hazard analysis, the occurrence of these events is interpreted to be a process quite distinct from the large-magnitude earthquakes discussed in the next section.

Precise magnitude determination of the earlier events is difficult, particularly for those occurring before 1930, since these magnitudes may have been based on maximum intensity reports in the epicentral region, or on the size of the felt area. Comparison with recent earthquakes in the ISB for which instrumental magnitudes are available suggests that an earthquake of magnitude 6 or greater produces a maximum Modified Mercalli Intensity of VII or more, and is felt over an area on the order

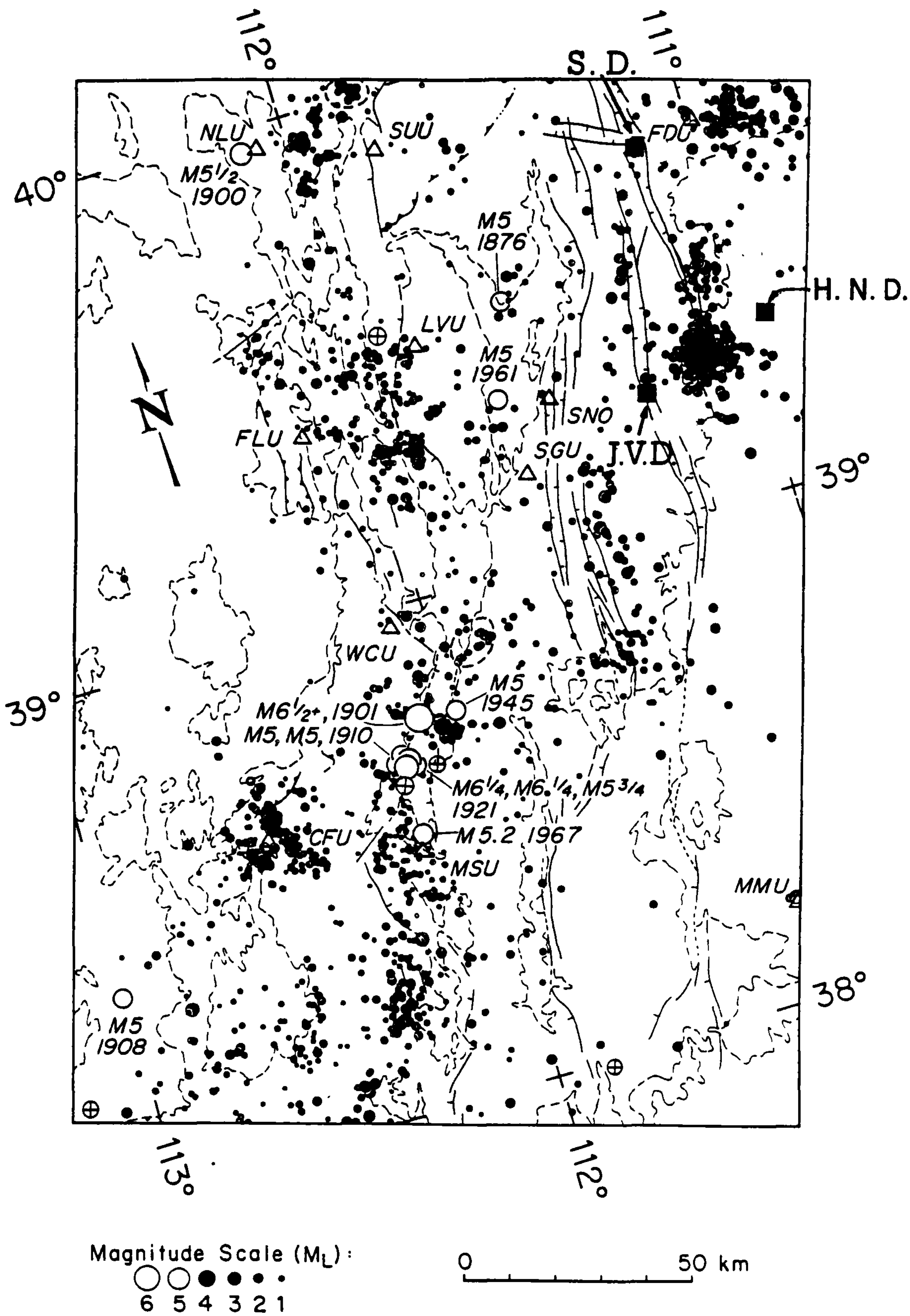


Figure 2.9: Seismicity map of the central Utah region based on University of Utah data (see text for explanation). Joes Valley, Scofield, and Huntington North Dams are indicated by squares and identified by JVD, SD, and HND, respectively (modified from Arabasz and Julander, 1986).

of 10 000 km$^2$. Uncertainty in the magnitude determination for events not recorded instrumentally makes it possible that three or more of the assumed 15 magnitude 6 to 6-3/4 earthquakes were actually in the magnitude 5-1/2 to 6 range. Regardless of the ambiguity in some of the magnitude determinations, detection of moderate-magnitude earthquakes has probably been uniform since at least 1870 because of the large felt areas associated with these events.

Surface rupture resulting from moderate-magnitude earthquakes has rarely been observed. Of the fifteen magnitude 6 to 6-3/4 earthquakes documented in the ISB, only the magnitude 6.6 1934 Hansel Valley, Idaho, earthquake has been associated with surface rupture (Shenon, 1936) on a late Quaternary fault (McCalpin and others, in press). This event produced 0.5 m maximum surface displacement on en echelon scarps in mostly unconsolidated sediments along a discontinuous 10 km-long zone. Pardee (1926) reported that the 1925 magnitude 6.7 Clarkston, Montana, earthquake produced only isolated surface cracks of up to 0.6 m related to local subsidence, but no observable scarp with surface displacement.

Within the ISB there is evidence for the existence of a threshold magnitude for the occurrence of surface rupture. This magnitude apparently lies in the 6-1/2 to 6-3/4 range, and likely varies somewhat with location. Doser (1984) has noted that surface rupture has not been observed for magnitude 6 to 6-1/2 earthquakes in the ISB, and suggests that magnitude 6-3/4 is the threshold for surface rupture. This was based on the observation that no surface rupture was recorded for the 1975 $M_L$ 6.1 Yellowstone, Wyoming, 1975 $M_L$ 6.0 Pocatello Valley, Idaho, and the 1947 M? 6.3 Virginia City, Montana, earthquakes. Though the magnitude determinations for the Hansel Valley and Clarkston earthquakes are somewhat uncertain, they appear to have been near the threshold magnitude. Recent trenching studies by McCalpin and others (in press) indicate that the Hansel Valley event is at the low end of the large-magnitude earthquake range, which suggests that for Utah the threshold for surface faulting is M 6-1/2.

Locations of moderate-magnitude earthquakes suggest that these earthquakes occur without correlation to late Quaternary faults. Evidence from the Pocatello Valley earthquake indicates that the earthquake ruptured on a fault that cuts across a major late Quaternary fault in the area (Bache and others, 1980; Arabasz and others, 1981).

Because only one (Hansel Valley) of the moderate-magnitude earthquakes studied produced surface rupture or showed evidence of occurring on late Quaternary faults, the likelihood that potential sites of moderate-magnitude earthquakes in the ISB can be reasonably predicted from Quaternary geology appears to be low. Although detailed geologic field studies of the 15 magnitude 6 to 6-3/4 earthquakes observed in the ISB have not in general been conducted, the available literature suggests that the specific locations of these events could easily have been overlooked (Arabasz and Smith, 1981). Potential sites of future earthquakes in the magnitude 6 to 6-3/4 range might therefore remain unidentified if based on geologic data alone. Without further advances in earthquake prediction, enabling use of contemporary seismicity data, it may only be possible to assume that these events will occur on "blind" structures.

### 2.4.2 Large-magnitude/characteristic earthquake model

Observed displacements from the Hebgen Lake and Borah Peak events (see section 2.3.1) were similar to paleoseismic single-event surface displacements measured on late Quaternary normal faults elsewhere in the ISB and Basin and Range. For example, Schwartz and Coppersmith (1984) measured single-event surface displacements exposed in trenches across several segments of the Wasatch fault zone. They found that displacements ranged between 1.6 to 2.6 m, with an average displacement per event of 2 m. This suggests that the Hebgen Lake and Borah Peak earthquakes are representative of large-magnitude surface-faulting events elsewhere in the ISB.

Further examination of the paleoseismic record of the Wasatch fault suggests a model for large-magnitude earthquake occurrence on recurrently active faults. Although Schwartz and Coppersmith (1984) were not able to rule out single-event displacements of less than 0.5 m, they felt that displacements of between 0.5 and 1.6 m, had they been present, would have been observed. These observations led them to suggest that the characteristic earthquake model, where individual faults and fault segments tend to generate only earthquakes having magnitudes and displacements in a narrow range about the maximum, was applicable to the Wasatch and other faults.

The characteristic earthquake model of faulting is in marked contrast to the typical log-linear relationship between earthquake frequency versus magnitude (Gutenberg and Richter, 1954) widely observed for seismically active regions. The model was initially developed by Allen (1968) from observations of seismicity along the San Andreas fault, and may also describe faulting in other tectonic environments. In a detailed study of both seismicity data and late Quaternary displacement on strike-slip and reverse faults in Japan, Wesnousky and others (1983) concluded that the characteristic earthquake model better describes the behavior of individual faults than does the Gutenberg-Richter relationship.

Sufficient data do not yet exist to conclusively demonstrate the applicability of the characteristic earthquake model to late Quaternary faults throughout the ISB, however it is presently the most favored model. Thus, it is assumed that earthquakes that occur on late Quaternary normal faults in the ISB will be of a size which is in a narrow range about the maximum for the particular fault. For a suite of faults, or for the region around a fault, a Gutenberg-Richter type relation is still assumed to be valid. The characteristic sizes of the Hebgen Lake and Borah Peak earthquakes are therefore taken to provide estimates of earthquake parameters which can be applied to other normal faults in the ISB.

Evidence that the Hebgen Lake and Borah Peak earthquakes are representative of maximum magnitude earthquakes which occur on late Quaternary normal faults in the ISB has been reviewed. Furthermore, earthquake occurrence on recurrently active normal faults appears to be limited to characteristic surface-rupturing events that produce displacements greater than 0.5 m. Quoting Doser (1984), a model for large earthquakes (magnitude 7 - 7.5) in the ISB which "would predict a fault rupture length of 20 to 30 km, an average surface displacement of 1 to 4 m, a paucity of foreshocks, displacement along major fault systems showing repeated movements in Quaternary-Holocene times, and unilateral rupture nucleating at a depth that is at or near the base of the seismogenic zone" should be considered potentially applicable throughout the ISB. Ground motion parameters for such earthquakes are expected to be similar to those observed for the Hebgen Lake and Borah Peak events.

### 2.4.3 Application to the eastern Wasatch Plateau

The historic record of earthquake occurrence on the Wasatch Plateau demonstrates that the moderate-magnitude earthquake model is applicable to this region of the ISB. It is not so clear, however, whether the large-magnitude/characteristic earthquake model applies to fault systems of the Joes Valley and Pleasant Valley variety. The primary hesitancy in applying this model to the long (120 km), linear, graben-bounding faults of the eastern Wasatch Plateau is related to the general lack of data and resulting ambiguity in the interpretation of the underlying subsurface geology (discussed in section 2.2.3.1). In addition, there is generally no measurable displacement across the graben, the faults have vertical or near-vertical dips at the surface and in the shallow subsurface (as defined on seismic reflection sections), and the basins are relatively narrow as compared to other late Quaternary basins in the ISB and Basin and Range.

If the graben bounding faults are listric, as they are assumed to be in the reactivated thrust fault model, then the large-magnitude earthquake model probably does not apply to the Wasatch Plateau. This is because it has yet to be demonstrated that sufficient seismic strain energy can be stored in the shallow crust across low-angle faults to cause large-magnitude (M 7+) earthquakes (Arabasz, 1986). The listric fault model suggests, therefore, that the Joes Valley faults, and presumably other similiar faults on the Wasatch Plateau, are not associated with the occurrence of large-magnitude scarp forming earthquakes, and may be due entirely to non-seismic related processes. One possible process might include gravity backsliding on the low-angle detachment in response to extensional stresses dominating to the west or subsurface displacement on the Ancient Ephraim fault.

For the large-magnitude earthquake model to apply to the Wasatch Plateau faults, some as yet undefined rupture pathway must exist to connect the surface with seismogenic depths where large-magnitude earthquakes are known to nucleate. The preferred ISB type rupture pathway involves a 45° to 60° uniformly-dipping planar fault that extends from the surface down to depths of 12-15 km. An alternative rupture pathway might include the Ancient Ephraim fault from the earthquake focus up to where this fault intersects the low-angle detachment. At this intersection the pathway may follow the detachment east to the Joes Valley faults. The major difference between these two types of rupture pathways relative to the determination of expected ground motions involves the location of the earthquake focus and the corresponding hypocentral distance to the surface scarps. Clearly the model involving the Ancient Ephraim fault requires a greater hypocentral distance and a correspondingly lower level of expected ground shaking at Joes Valley Dam, for example, than the model involving a planar high-angle fault.

The main issue regarding the origin of the scarps in Joes Valley involves whether or not these faults formed in response to recurrent large-magnitude earthquakes. The available data on the subsurface geometry of the Wasatch Plateau faults is equivocal, therefore, the possibility that the Joes Valley faults and other similiar faults extend to seismogenic depths cannot be precluded. Because resolution of this issue would have a significant impact on the conclusions of this hazard study, a large percentage of the geologic, and all of the seismologic field invesigations discussed in the following sections were conducted with the objective of determining the relationship between earthquakes and faulting in Joes Valley.

## 3.0 Site geology

### 3.1 Joes Valley Dam

Joes Valley Dam is a zoned earthfill embankment 58 m high and 229 m long, located in Straight Canyon, a narrow gorge 300 m deep incised by the east-flowing Seely Creek into the Cretaceous sedimentary rocks of the eastern Wasatch Plateau. Seely Creek parallels the axis of a gently west-plunging syncline which causes the beds to dip slightly toward the channel. The foundation of the dam is composed of sandstone and shale with occasional coal seams within the Blackhawk Formation which are overlain by up to about 10 m of alluvium and colluvium. About 10 meters of loose, landslide-prone colluvium and talus cover the dam abutments, and alluvium in the channel of Seely Creek is about 3 m thick (USBR, 1962; 1980).

Joes Valley Dam is situated 120 m east of the East Joes Valley fault (plate 1) and the reservoir, which has a maximum volume of 8.2 x $10^7$ $m^3$, is in the central and deepest part of the Joes Valley graben. No faults were observed in the dam foundation during construction (USBR, 1962), and none are visible in the walls of the canyon east of the East Joes Valley fault. Several discontinuous west-facing scarps and lineaments occur in Quaternary deposits within and surrounding the reservoir.

### 3.2 Scofield Dam

Scofield Dam is a homogeneous earthfill structure completed in 1946, 38 m high and 175 m long, located on a tributary of the Price River in a canyon about 400 m deep incised into the nearly flat-lying upper Cretaceous Blackhawk, Castlegate and Price River Formations. The dam is founded in alternating beds of sandstone and shale of the Blackhawk Formation which are overlain by 21 m of alluvium in the Price River channel.

Scofield Dam is located 1.2 km east of the Pleasant Valley fault zone (plate 3) and the reservoir, which has a maximum volume of 9.6 x $10^7$ $m^3$, occupies the central part of the Pleasant Valley graben. No faults were found in the dam foundation although faults with small (<5 m) displacement and variable orientation are visible in outcrops of Blackhawk Formation in the vicinity of the dam.

### 3.3 Huntington North Dam

Huntington North Dam is an earthfill embankment 20 m high located 800 m north of Huntington Creek near the town of Huntington in the Castle Valley (plate 1). The reservoir has a capacity of 6.7 x $10^6$ $m^3$. The Castle Valley is on the Colorado Plateau, between the eroded eastern escarpment of the Wasatch Plateau and the west flank of the San Rafael swell, a large domelike structure in the Mesozoic sediments of the northern Colorado Plateau. The dam consists of two sections and a dike constructed between eroded pediment remnants in the Bluegate Shale Member of the Mancos Formation. The foundation of Huntington North Dam consists of shale unconformably overlain by about 3 m of very gravelly alluvium. The gently west-dipping shale beds are weathered to a depth of about 10 m. The closest Cenozoic faults to Huntington North Dam are within the Pleasant Valley fault zone, 16 km to the west, and the Joes Valley fault zone, 28 km to the west. Photolineaments reported in the vicinity of the dam (USBR, 1983b) were examined on aerial photographs and in the field and proved to be the result of erosion by Huntington Creek and are therefore not fault-related.

## 4.0 The Joes Valley fault zone

The Joes Valley fault zone consists of parallel, en echelon and occasionally overlapping, north to northeast-trending faults which extend for 120 km on the east side of the Wasatch Plateau. This fault system contains two major structures: a southern graben bounded by the northeast-trending Muddy and Paradise faults and a northern graben bounded by the north and northeast-trending East and West Joes Valley faults (plate 1). These structures overlap in the vicinity of Ferron Canyon where the displacement of the Cretaceous and Tertiary rocks is taken up by several small parallel faults over a 5 km wide zone. The southern and northern grabens have distinct geomorphic characteristics which may reflect differences in the amount of total displacement and the most recent displacement on the bounding faults. The northern Joes Valley graben contains a sequence of Quaternary deposits that are displaced by faults and exhibit pronounced scarps. Because of the potential for establishing a chronology of late Quaternary (<150 ka) faulting, and because of the proximity of this structure to Joes Valley Dam, the northern Joes Valley graben was chosen as the main focus for detailed geologic mapping and trenching studies. The general characteristics of the Joes Valley fault zone are described in the following sections beginning with the southern graben and proceeding to the northern graben, accompanied by discussions of the detailed geologic work conducted in the northern Joes Valley graben.

### 4.1 Southern Joes Valley fault zone

The southern Joes Valley graben extends from the area south of Quitchupah Creek to the vicinity of Ferron Canyon, a distance of about 35 km (plate 1). From its southern terminus where it trends northeast, the southern Joes Valley graben curves to the north eventually trending due north in the vicinity of Ferron Canyon. This graben is close to the east edge of the Wasatch Plateau where the older part of the stratigraphic section is exposed both within the graben and in the deeply incised canyons that cross it. The section consists of the following flat-lying Cretaceous formations: from top to bottom, the Starpoint Sandstone, a prominent cliff-former bed, the Masuk Shale, Emery Sandstone, and Bluepoint Shale, the last three being members of the Mancos Formation.

The southern Joes Valley graben is included on the geologic map and detailed stratigraphic and structural descriptions contained in Spieker's (1931) study of the Wasatch Plateau coal fields. More recently, the geology of the Joes Valley fault system south of Joes Valley Reservoir has been mapped at a larger scale on several 7.5 minute quadrangles by Hayes and Sanchez (1979), Sanchez and Hayes (1979), Ellis (1981a, 1981b), Ellis and Frank (1981), and Sanchez and Brown (1983).

The southern Joes Valley graben is bounded by the Muddy fault on the west and the Paradise fault on the east with numerous smaller faults occurring within the graben (fig. 4.1), and is distinguished from the northern graben by less total displacement in the Cretaceous-Tertiary section, less overall topographic definition of the faults, and apparent

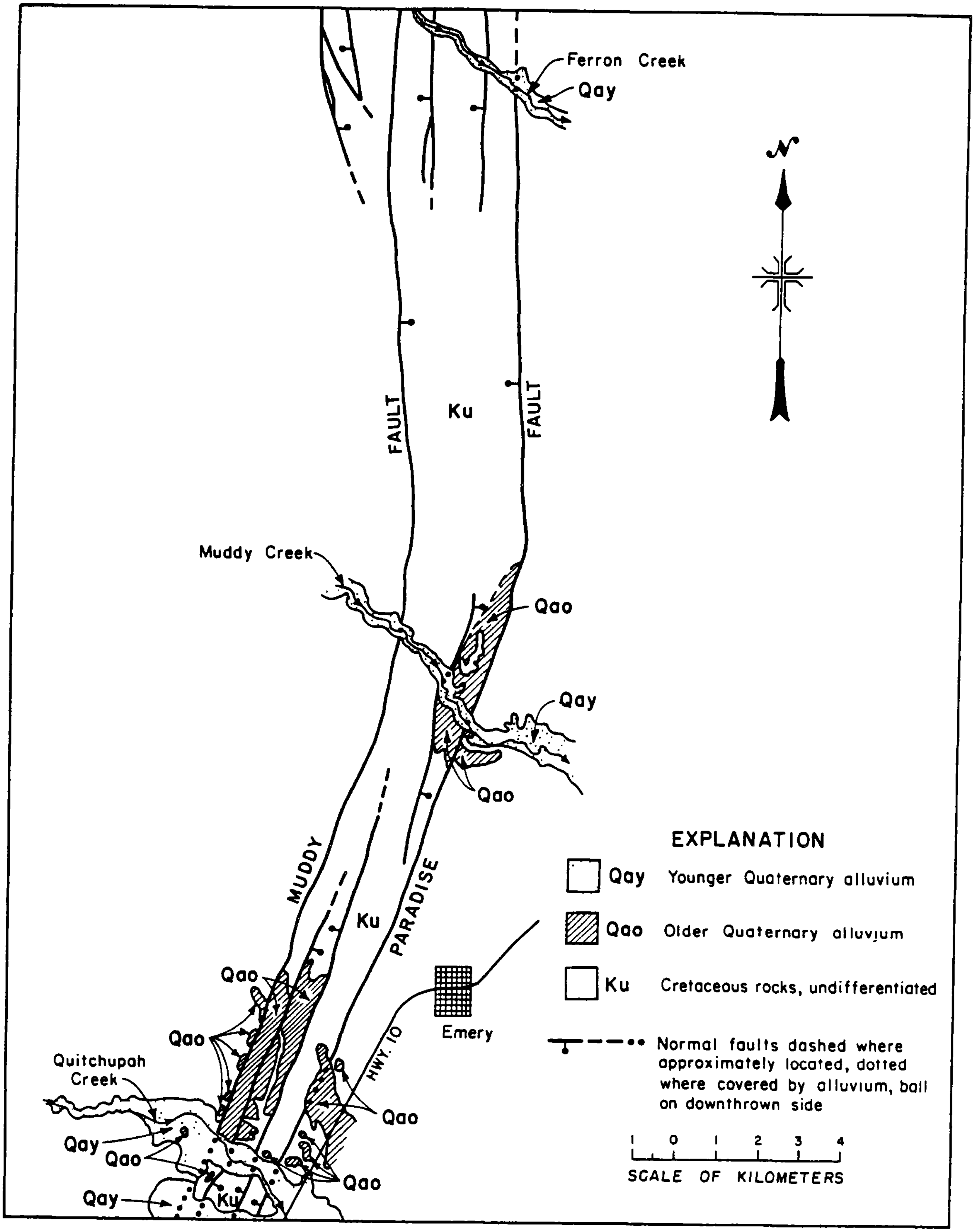


Figure 4.1: Major faults in the southern Joes Valley fault zone. Modified from Hayes and Sanchez (1979), Sanchez and Brown (1983), and Sanchez and Hayes (1979).

lower Quaternary activity rates. Our work in the southern graben consisted of a study of the geologic maps and literature available for the area and a review of aerial photographs (USDA, 1976, scale 1:15,800). The result of these analyses indicated that there was little evidence for late Quaternary displacement in this part of the graben. Therefore our field effort was limited to field reconnaissance in those few localities where there is evidence on pre-existing maps and in the literature and/or on aerial photographs for fault scarps in Quaternary deposits. The following discussion of the southern Joes Valley graben focuses on the geomorphic characteristics of the two bounding faults, the Muddy fault and the Paradise fault, and the presence or absence of evidence for Quaternary displacement, either in the form of geomorphic characteristics such as sinuosity (Bull and McFadden, 1977) and degree of incision or erosion of the graben-bounding scarps, or more directly by the presence of fault scarps in Quaternary deposits.

### 4.1.1 Muddy fault

The Muddy fault, the west-bounding fault of the southern Joes Valley graben, extends for 35 km from the vicinity of Quitchupah Creek in the south to Ferron Canyon in the north (fig. 4.1) where it terminates in the North Horn Formation (Sanchez and Hayes, 1979). South of Quitchupah Creek, at the southern terminus of the graben, the Muddy fault exhibits no topographic relief. On the geologic map of the Emery West 7.5 minute quadrangle (Hayes and Sanchez, 1979) it is mapped on the basis of a fault contact between Emery Sandstone and Bluegate Shale exposed in a bedrock knob surrounded by Quaternary alluvium about 1 km south of Quitchupah Creek. The total displacement in the bedrock at this locality is about 200 m, the thickness of the Emery Sandstone.

Two Quaternary deposits are distinguished in this area on published geologic maps: older gravels (Qao on fig. 4.1) on high bedrock surfaces and pediments, and younger alluvium (Qay on fig 4.1) in fans and along modern stream courses. The older gravels occur on eastward-sloping pediments, as small erosional remnants of former surfaces that have been truncated by the faults, and as a <50 m thick basin fill within the graben. The older gravels are capped by a 50 cm thick cap of strongly indurated pedogenic calcrete (stage IV-V) that is similar to deposits elsewhere in the western U.S. that are of early and middle Pleistocene age (0.15 to 2.0 Ma) (Harden and others, 1985; Machette, 1985). Comparison of the degree of carbonate cementation on the Qao surface (referred to from here on as the "older gravels") with soil development on similar deposits in the northern Joes Valley graben where a detailed soils study was performed (discussed in Appendix A) suggests that, even allowing for climatic differences, the gravels in the Quitchupah and Muddy Creek areas are at least as old as mid-Pleistocene (>150 ka) and possibly as old as Pliocene (2 to 6 Ma) in age.

Quitchupah Creek has incised a channel more than 70 m deep, the height of the present canyon walls, into the Emery Sandstone and the underlying

Bluegate Shale. The creek flows perpendicular to the trend of the graben and has incised it by at least 50 m exposing the Masuk Shale beneath 40 m of older gravels. The younger alluvium (Qay) in the channel of Quitchupah Creek includes the modern floodplain. The geomorphic position of the younger alluvium and its undissected nature suggest that it is latest Pleistocene and/or Holocene in age (<30 ka).

North of Quitchupah Creek for a distance of 4.5 km is a small graben bounded by the Muddy fault on the west and an intragraben fault on the east. A 30 m high scarp on the Muddy fault exposes the older gravels and the underlying Bluegate Shale on the footwall. The hanging wall contains older gravel overlying Masuk Shale (Hayes and Sanchez, 1979). Total displacement in the bedrock at this location is approximately 450 m while displacement of the older gravel (> 150 ka) appears to be about 30 m. The gravel-filled portion of this graben extends for a distance of 4.5 km to the north of Quitchupah Creek and its east-bounding fault terminates in the Blackhawk Formation 8 km to the north. This 8 km long graben appears to be the only location at the southernmost end of the Joes Valley fault zone with Quaternary displacement.

Between the north end of this graben and Muddy Creek, a distance of 8 km, the Muddy fault is an eroded escarpment with little topographic expression along the contact between the Masuk Shale on the footwall and the Blackhawk Formation rocks on the hanging wall.

The greatest displacement on the Muddy fault, 550 m, is near the central part of the fault, 5 km north of Muddy Creek, where a lineament is evident along the contact between the Flagstaff Limestone on the downthrown side and the Price River Formation on the upthrown side. Since the limestone is more resistant to erosion, the topography is reversed with the surface of the downthrown block several meters higher than the surface of the upthrown block. The amount of erosion that must have occurred since the last movement of the Muddy fault suggests that, although there is an obvious lineament in the bedrock, this segment of the fault has not had significant Quaternary displacement. North of this point the Muddy fault continues as an eroded escarpment in the Cretaceous rocks until Ferron Creek. Immediately to the north of Ferron Creek, the Muddy fault terminates in the North Horn Formation in a zone where the displacement in the graben is taken up by several parallel faults (plate 1). A pair of down-to-the-east normal faults, possibly an extension of the Muddy fault, begins 100 m to the west of the termination of the Muddy fault. This pair of faults extends for several kilometers to the north, bounding the Dragon Ridge horst on the east (plate 2) with a total displacement of 100 m in the Flagstaff Formation (Ellis, 1981b).

In summary, evidence for late Quaternary (<150 ka) displacement on the Muddy fault is confined to one short segment north of Quitchupah Creek where basin fill deposits estimated to be at least mid-Pleistocene (150-730 ka) in age are displaced about 30 m.

4.1.2 Paradise fault

The Paradise fault forms the eastern boundary of the southern Joes Valley fault zone from Quitchupah Creek in the south to 7 km north of Ferron Canyon (plate 1), a total distance of 35 km. The Paradise fault is similar to the Muddy fault in that it exhibits scarps in the older gravels discussed in the previous section, topographically reversed scarps in soft shales on the upthrown side of the fault, and similar amounts of displacement in the bedrock.

At the southern end of the fault zone, in the vicinity of Quitchupah Creek, the total displacement on the Paradise fault is approximately 200 m measured in the flat-lying Bluegate Shale. The Paradise fault at this locality is overlain by the older gravels (Hayes and Sanchez, 1979) that do not appear to be displaced (fig. 4.1).

Evidence for Quaternary displacement on the Paradise fault is limited to a narrow (150 m-wide) 6 km-long graben on the east side of the fault zone at Muddy Creek. The footwall of the Paradise fault contains Emery Sandstone overlain by erosional remnants of Masuk Shale and older Quaternary gravels. Total displacement on the Paradise fault at this locality is 500 to 650 m. The graben contains a basin fill about 30 m thick of the older gravels overlying sandstone of the Blackhawk Formation. The displacement of the gravels across the Paradise fault is approximately 30 m. On the west, this graben is bounded by an intagraben fault with Masuk Shale overlain by Star Point and Blackhawk Formations on the footwall. The total vertical displacement within the fault zone, based on stratigraphy, is 500-650 m at this point with no net displacement across it. On the east side this displacement is produced on a single fault, the Paradise fault, while on the west side of the fault zone, displacement on the Muddy fault is 350-550 m and on an intragraben fault is 250-300 m.

This graben continues north of Muddy Creek for 4 km: the Paradise fault is a near vertical escarpment in the Emery Sandstone for 1 km and then becomes an obvious lineament for 3 km where the Masuk Shale is preserved in fault contact with the older gravels that fill the graben. The Masuk Shale, which is more easily erodible than the strongly indurated gravels, is slightly lower topographically in spite of its being on the upthrown block of the Paradise fault. This reversed topographic expression is an indication of the antiquity of the last surface rupture on the fault and supports the argument that activity on the Paradise fault ceased prior to the late Pleistocene proposed on the basis of the inferred age (>150 ka) of the older gravels. The total length of the gravel-filled graben is 5 km.

From the northern end of this graben to Ferron Canyon, a distance of 10 km, the Paradise fault is expressed as an eroded escarpment in the Blackhawk Formation with a total displacement of about 450 m.

North of Ferron Canyon, the Paradise fault parallels the southern end of the East Joes Valley fault and delineates the east side of a 6 km long narrow graben floored with Price River Sandstones. The Paradise fault eventually dies out in the Price River Formation north of this graben (Ellis, 1981a).

#### 4.1.3 Southern Joes Valley fault zone: summary

The portion of the Joes Valley fault zone that lies south of Ferron Canyon is composed of numerous narrow graben bounded by the Muddy, Paradise and several unnamed intragraben faults. Total displacement in the bedrock ranges from 100 m at the northern and southern extremities to 650 m near the middle with no net displacement across the fault zone. Late Quaternary surface displacement in the southern part of the Joes Valley fault zone is restricted to two small graben: one on the west side, north of Quitchupah Creek, that is bounded on the west by the Muddy fault and the second graben, at Muddy Creek, that is bounded by the Paradise fault on the east. Alluvial gravels inferred to be at least mid-Pleistocene (>150 ka) in age, within and adjacent to these graben, are displaced approximately 30 m. Undisplaced alluvium inferred to be latest Pleistocene and Holocene (<30 ka) in age fills channels incised perpendicular to these grabens. These data indicate that surface displacement on the major bounding faults in the southern graben ceased at least by the late Pleistocene and that the post-mid-Pleistocene displacement was approximately 30 m. The highly segmented nature of the faults in the southern part of the fault zone contrasts with the longer fault lengths in the northern portion.

### 4.2 Northern Joes Valley fault zone

The northern part of the Joes Valley fault zone extends from the vicinity of Ferron Canyon to Electric Lake, a distance of about 50 km (plate 2). This part of the fault zone is generally characterized by greater total stratigraphic throw, the presence of two graben-bounding faults that are longer and more linear, and geomorphic features suggestive of higher Quaternary activity rates than the faults in the southern part of the fault zone. The principal faults in the northern fault zone are the East Joes Valley fault, the West Joes Valley fault, and the Middle Mountain fault. Discussion of the northern part of the fault zone will focus on the geomorphic characteristics of these faults.

### 4.3 East Joes Valley fault

The East Joes Valley fault is the major graben-bounding fault on the east side of the main northern Joes Valley graben and is the closest fault to Joes Valley Dam (120 m west of the dam). It extends from 4 km south of Ferron Creek (Ellis, 1981a) to the vicinity of Electric Lake, a distance of about 50 km, and forms a steep, topographic escarpment in the Blackhawk, Castlegate, and Price River Sandstones.

The East Joes Valley fault is divided into three segments, the Ferron, Straight Canyon, and Miller Flat segments (plate 1) based on the presence or absence of evidence for late Quaternary displacement. Since direct evidence for late Quaternary displacement, in the form of scarps in late Quaternary deposits, is found at only one locality along the East Joes Valley fault, other forms of evidence, such as the degree of incision, straightness or sinuosity of the bedrock fault scarp, and amount of total post-Eocene displacement have been used to distinguish the segments.

### 4.3.1 Ferron segment

The Ferron segment of the East Joes Valley fault is 5 km long, extending from 4 km south to 1 km north of Ferron Canyon (plate 1). In this area the fault juxtaposes the Blackhawk Formation against the Price River Formation with a total displacement of approximately 100 m. The topographic relief across the fault ranges from 0 to 60 m. Quaternary deposits in this graben are sparse and thin, consisting of a veneer of colluvium a few meters thick on top of the bedrock. At its southern end the fault bifurcates and borders a small graben. Ferron Creek has incised a southeast-oriented canyon 750 m deep oblique to the north-south faults of the Joes Valley graben. The low topographic relief of the fault scarp, the relatively small total displacement, and the amount of incision on this segment contrast with the main Straight Canyon segment to the north (discussed below) and suggest that the Ferron segment has had less Quaternary displacement.

### 4.3.2 Straight Canyon segment

The Straight Canyon segment, characterized by a steep linear escarpment in the Blackhawk, Castlegate and Price River Formations, extends 42 km from the vicinity of Ferron Canyon in the south to Miller Flat Creek in the north (plate 1). The more erodible North Horn rocks form a slope above the Price River Sandstones and are capped by the resistant cliff-forming Flagstaff Limestone. The total topographic relief along this section of the fault ranges from 750 m at Joes Valley Reservoir to 500 m between Upper Joes Valley and Scad Valley. The stratigraphic dispacement is also at a maximum at Joes Valley Reservoir (900 m estimated by Kucera, 1954) and diminishes to the north and south.

South of the reservoir, the Straight Canyon segment is covered by landslide deposits similar to deposits on the west side of the reservoir inferred to be late Pleistocene (150-10 ka) in age (see Appendix A). Small alluvial fans occur at the mouths of gullies incised into these landslides. No fault scarps are evident in the landslide deposits, however the preservation of small scarps is unlikely in deposits as unstable as these. Therefore post-landslide displacement on this part of the Straight Canyon segment cannot be precluded.

A west-facing scarp in Quaternary deposits is 120 m west of Joes Valley Dam and 100 m west of the bedrock escarpment of the East Joes Valley fault (figure 4.2). This scarp is presently beneath the reservoir, but has been identified on pre-reservoir aerial photographs (DRX-28K-1952, 1:20 000 scale). The scarp is of undetermined height and forms the abrupt upstream end of what appears to be a small remnant of a debris flow related to the late Pleistocene Seely Creek debris flow

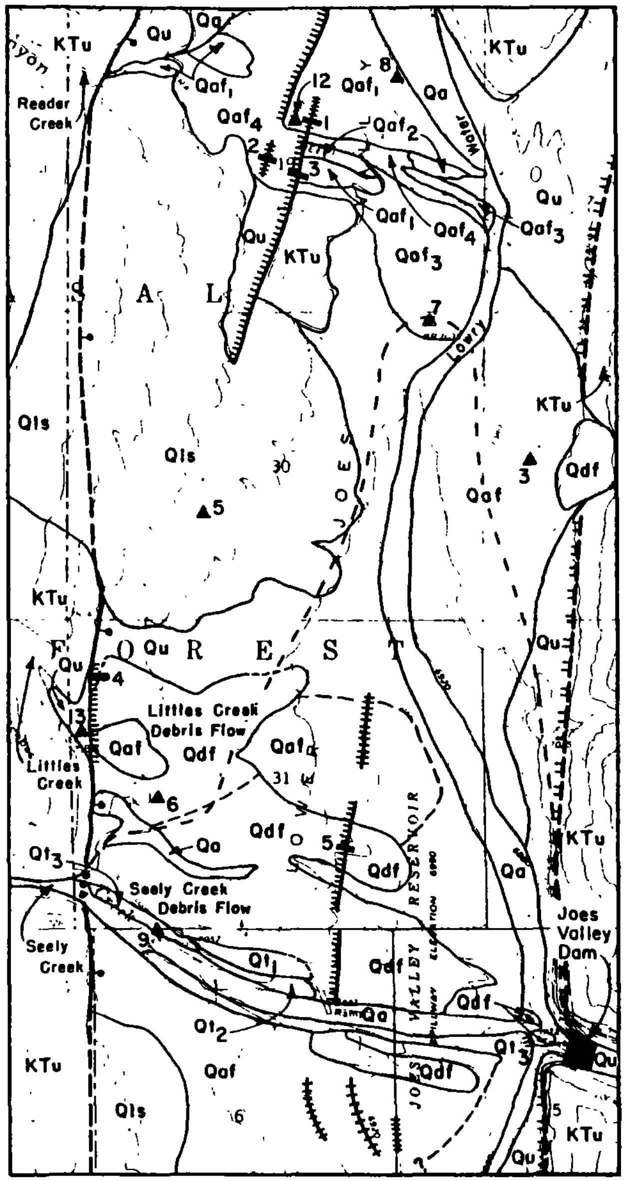


# EXPLANATION

**QUATERNARY DEPOSITS**

- Qu — Alluvium and colluvium, undifferentiated
- Qa — Alluvium on modern flood plains of major drainages
- Qaf — Alluvial fan
- Qdf — Debris flow
- Qls — Landslide deposits

**QUATERNARY LANDFORMS**

Terraces at Seely Creek:

- $Qt_3$ — Alluvial terrace, 7 m above Seely Creek
- $Qt_2$ — Alluvial terrace, 12 m above Seely Creek
- $Qt_1$ — Alluvial terrace, 24 m above Seely Creek

Alluvial fan remnants at Reeder Creek:

- $Qaf_4$ — Alluvial fan remnant, 6 m above Lowry Water
- $Qaf_3$ — Alluvial fan remnant, 12 m above Lowry Water
- $Qaf_2$ — Alluvial fan remnant, 15 m above Lowry Water
- $Qaf_1$ — Alluvial fan remnant, 24 m above Lowry Water

**BEDROCK**

- KTu — Cretaceous and Tertiary rocks, undifferentiated
- Photolineament
- Fault scarp
- Trench
- Soil pit
- Normal fault associated with fault scarps in late Quaternary deposits, ball on downthrown side, dashed where approximately located
- Normal fault inferred to be late Quaternary, but not directly associated with scarps in late Quaternary deposits, hachures on downthrown side

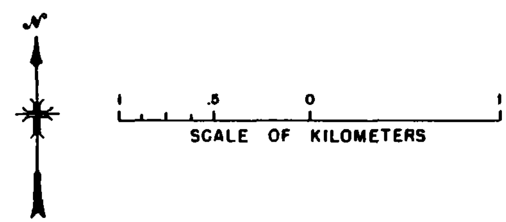


Figure 4.2: Quaternary geology in the vicinity of Joes Valley Dam and Reservoir (see plate 2 for location). Topographic base map is a portion of the U.S. Geological Survey Joes Valley 7.5 minute quadrangle.

(Appendix A). The length of the scarp is limited to the length of the deposit which is about 65 m from south to north. The scarp could be erosional in origin, but a tectonic origin cannot be ruled out. This debris flow remnant is surrounded by younger (Holocene) alluvium which shows no evidence of scarps or lineaments. The only evidence for a continuation of this scarp is the linear trend of the creek called Lowry Water to the north of the scarp (U.S. Geological Survey, 1976).

North of Joes Valley Dam, a series of alluvial fans head at the bedrock escarpment. A late Pleistocene alluvial fan that heads at the East Joes Valley fault 2 km north of the dam (figure 4.2) and a smaller, lower, probably Holocene, fan contain no visible lineaments or scarps. The lack of scarps is not definitive evidence for lack of recent displacement since the fans do not cross the main escarpment. There is no evidence of displacement of the fan surface although there is a 10 m high vertical scarp in the Castlegate Sandstone immediately east of the head of the fan. The scarp has been eroded approximately 20 m east of the main escarpment. The amount of retreat of the scarp face belies the initial impression that the scarp formed recently. The Straight Canyon segment is covered by colluvium and alluvium (Qu on plate 2) between Joes Valley Reservoir and Upper Joes Valley.

Upper Joes Valley is a closed basin which is being filled with sediment from the gullies draining the 650 m high escarpment on the east, and the Middle Mountain and Bald Ridge horst blocks on the west. The Straight Canyon segment is extremely linear with small, well-defined, active alluvial fans heading at the base of the eastern escarpment. Although no evidence for fault scarps in these alluvial fans was found either on aerial photographs or upon field inspection, the fans appear to be sufficiently active that such evidence would probably not be preserved for long. The active alluviation on these fans and their lack of incision suggest that the rate of base level change due to tectonic lowering of the basin is greater than the rate of downcutting on the escarpment (Peterson, 1979).

Bald Ridge, a block of flat-lying to slightly (<15°) south-dipping North Horn rocks capped by a thin layer of Flagstaff Limestone, separates the East Joes Valley fault from the Middle Mountain fault at the north end of Upper Joes Valley. These two down-to-the-west normal faults merge at Scad Valley (plate 2).

Scad Valley is a structural valley between the East Joes Valley fault on the east and Bald Mountain on the west. The west side of Scad Valley appears to be fault-bounded since a down-to-the-east fault scarp in Quaternary gravels is found to the north, in the vicinity of Miller Flat Creek. At the south end of Scad Valley is a NNE-trending scarp that is visible on a colluvium-covered bedrock slope on the northwest flank of Bald Ridge. The scarp continues as a double scarp across an alluvial fan (location of trench 6, discussed in section 4.3.4) and as a photolineament farther north on the main colluvium-covered escarpment on the east side of the graben almost as far as Miller Flat Creek, a distance of about 7 km.

The displaced alluvial fan appears to be a composite of at least two fans of different ages with an older, higher surface preserved on the northern half and a slightly (about 1 m) lower surface to the south (fig. 4.3). Two parallel fault scarps are present on the older alluvial fan surface, and only one scarp occurs on the younger surface, suggesting that erosion of the former scarp preceded deposition of the younger alluvial fan. Three profiles were measured across these scarps (figure 4.4). The apparent total vertical displacement across the scarps on the older fan surface (profiles 1 and 2) ranges from 5.7 to 6.3 m, increasing to the north. The southernmost profile (#3) is on the younger fan where apparent vertical displacement was estimated to be 2.8 m. Trench 6 is located at the site of profile #3.

Whether the Scad Valley scarp is related to displacement on the Middle Mountain fault or the East Joes Valley fault is ambiguous because they appear to merge at Scad Valley (plate 2). Therefore, the evaluation of Quaternary faulting on the East Joes Valley fault is not based solely on data from this locality but also from data collected from trenches on the West Joes Valley and Middle Mountain faults.

At Miller Flat Creek the escarpment is more eroded and incised than to the south. However, a small graben provides indirect evidence suggesting Quaternary displacement on the East Joes Valley fault at Miller Flat Creek. The fault bounding the west side of the graben, the East Bald Mountain fault, has formed a 3-5 m high 2.5 km long scarp in upper Pleistocene outwash gravels. This fault is inferred to continue south along the east side of Bald Mountain although no scarps are evident.

In summary, the 42 km long Straight Canyon segment between Ferron Canyon and Miller Flat Creek exhibits geomorphic characteristics such as linearity and steepness of the bedrock fault scarp that suggest the occurrence of late Quaternary displacement. Direct evidence for Quaternary displacement on this fault segment that is also accessible to exploratory trenching, is found at one locality, Scad Valley, where the Middle Mountain fault merges with the East Joes Valley fault and scarps are evident in hillslope colluvium and alluvial fan deposits for a distance of 6.5 km. The results of exploratory trenching on these scarps demonstrate recurrent late Pleistocene activity on this segment of the fault. Scarps in debris flow deposits beneath Joes Valley Reservoir provide further evidence to suggest Quaternary displacement on this fault segment.

### 4.3.3 Miller Flat segment

The third and northernmost segment of the East Joes Valley fault consists of a zone approximately 8 km long north of Miller Flat Creek (plate 2) where the displacement diminishes to less than 100 m in the Blackhawk Formation and is taken up by several parallel and branching faults instead of a single graben-bounding fault as it is to the south. No fault scarps are evident in Quaternary deposits and the bedrock scarp is an eroded hillslope less steep than the segment to the south. At its

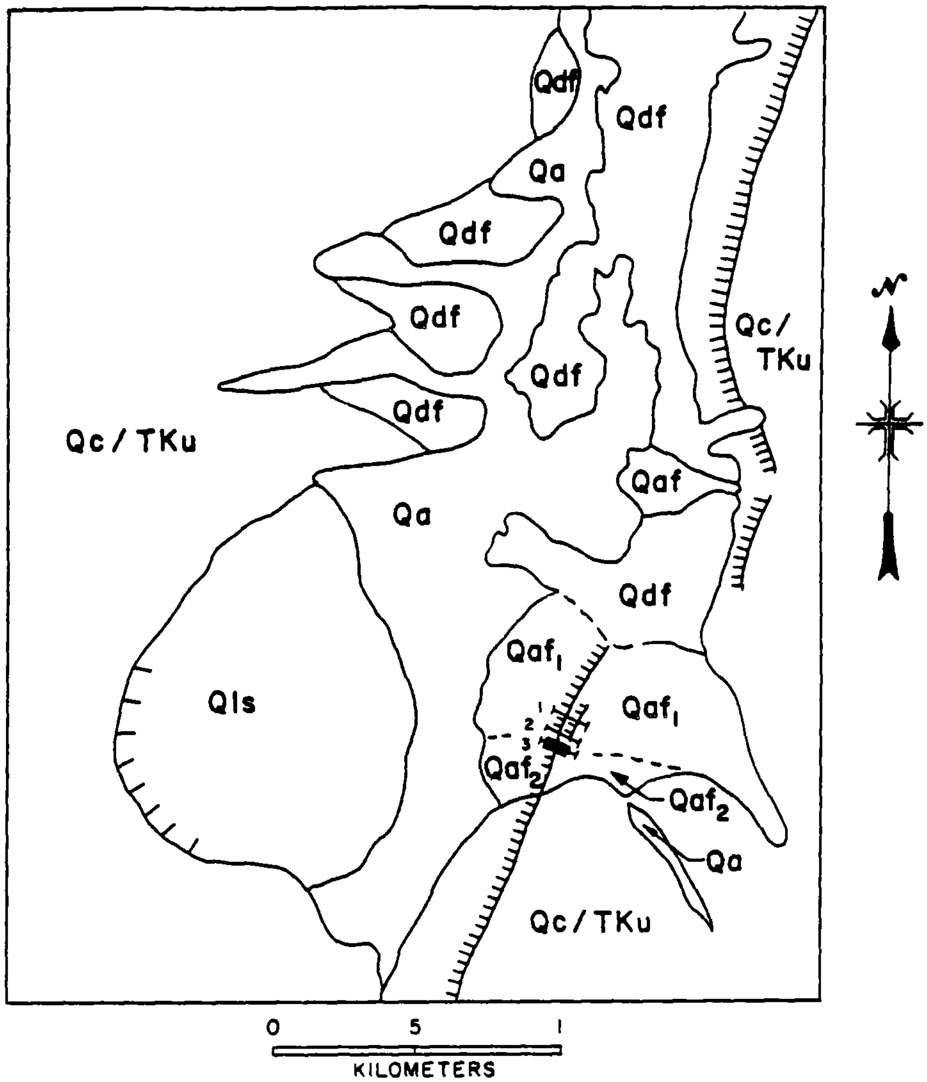


## EXPLANATION

- **Qa** Alluvial fill in Scad Valley
- **Qaf** Alluvial fan
- **Qdf** Debris flow deposits
- **Qls** Landslide deposits
- **Qc/TKu** Colluvium overlying Tertiary and Cretaceous rocks, undifferentiated
- **$Qaf_2$** Younger alluvial fan deposits
- **$Qaf_1$** Older alluvial fan deposits
- ▬ Location of trench 6
- 2 ├──┤ Location of scarp profile
- Fault scarp
- Landslide headscarp
- ——--- Geologic contact, dashed where approximately located

Figure 4.3: Quaternary deposits in Scad Valley (see plate 2 for location) and location of trench 6.

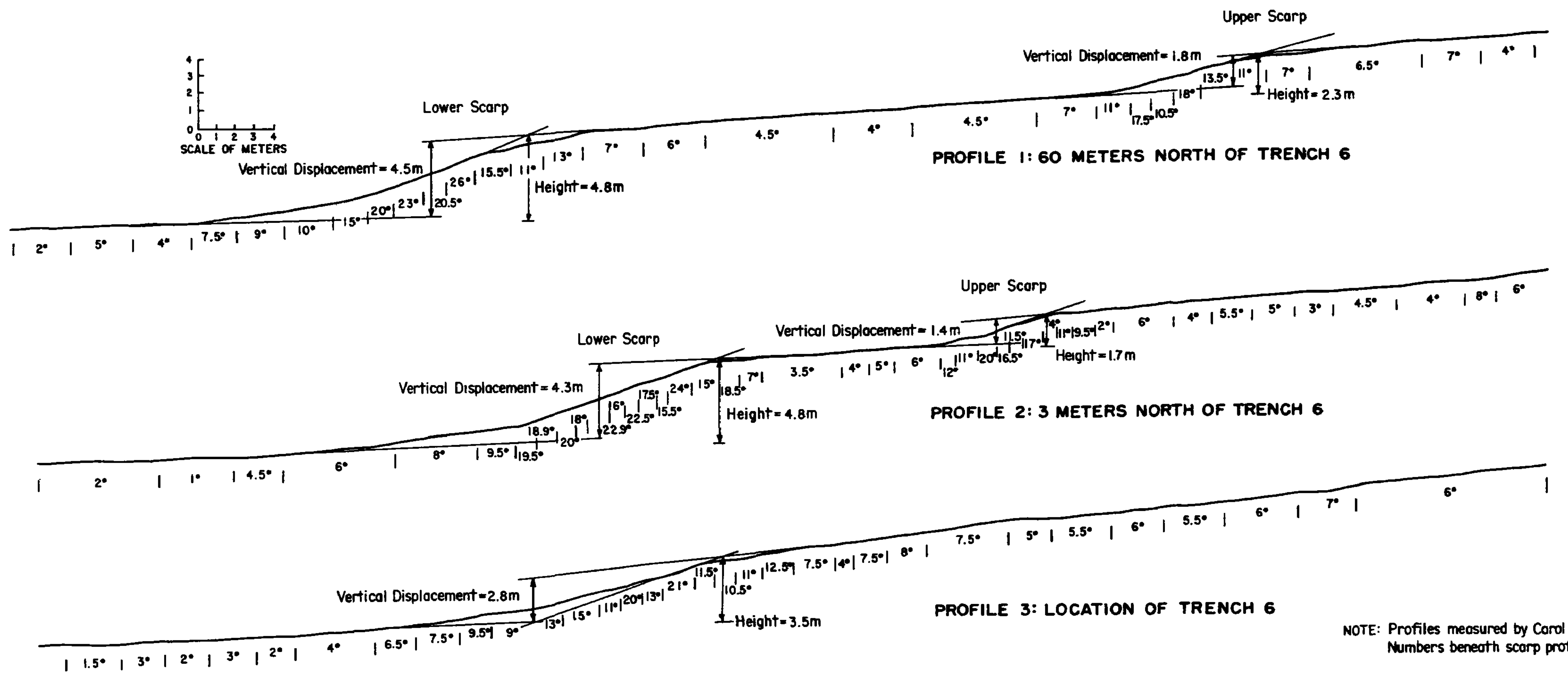


NOTE: Profiles measured by Carol Krinsky and Ed Baltzer.
Numbers beneath scarp profiles are average slope angles.

JOES VALLEY DAM
SEISMOTECTONIC STUDY

PROFILES ON

SCAD VALLEY SCARP

FIGURE 4.4

northern extremity there is no geomorphic evidence to suggest the continuation of the East Joes Valley fault. Our field investigation yielded no evidence for the fault in exposures perpendicular to its strike on the south shore of Electric Lake, although it has been mapped within the Blackhawk Formation north of Electric Lake (Witkind and others, 1978; 1982).

4.3.4 Trench on the East Joes Valley/Middle Mountain fault

Trench 6 was located on the southeast side of Scad Valley, where a northeast trending scarp transects an alluvial fan. This fan appears on the surface as a composite of two fans (fig. 4.3) and the trench was sited near the northern edge of the younger fan where it merges laterally with the older fan. The scarp profile measured at the trench site (profile 3, fig. 4.4) contains a single scarp in the position of the lower scarp on the older fan surface to the north with an estimated vertical displacement of 2.8 m. The trench shows that at this location the older fan deposits are buried by approximately 1 m of sandy colluvium deposited by the younger fan. The stratigraphy exposed in trench 6 includes alluvial fan deposits consisting of debris flows, alluvium and colluvium containing two buried soils (fig. 4.5). Our interpretation of the stratigraphic evidence is that the deposits have been faulted and subsequently buried by the younger sandy colluvium. Four faults are exposed in trench 6 (designated F1..F4 on fig. 4.5). Two of these are visible in the trench wall and two are inferred from the apparent displacement of stratigraphic units. In addition, we identified several zones of unstratified (and in some locations open work) loose gravel with no apparent displacement of strata across them. These zones are designated L1..L3 on figure 4.5. Following is a summary of the stratigraphic evidence followed by an interpretation of the faulting history at this locality.

The oldest stratigraphic unit in the trench (unit 1) is a gravelly silty clay, interpreted to be a debris flow, which is distinctive because it contains shells of Oreohelix ch. strigosa. This unit is exposed in the trench wall between stations 33 and 34. Similar shell-bearing deposits were found at station 31, at a depth of 3.5 m below the ground surface and at station 37 at a depth of 4-4.5 m. After these deep excavations were made the trench was filled in to a shallower depth for safety reasons. Samples of the shells in unit 1 at each of the three locations were analyzed for amino acid racemization. The results of these analyses, presented in Appendix C and on figure 4.5, indicate that the three samples are within the age range of 150-300 ka.

The next younger strata are best exposed in the eastern part of the trench between stations 0 and 30 where unit 1 is overlain by layers of debris flow and alluvial deposits (units 2 and 3). Unit 2 is identified in several places at the base of the trench by its sandier texture compared with the overlying strata. The upper contact of unit 2 is difficult to recognize in some areas of the trench and is queried on the trench log. Unit 4 (4A,4B,4C,4D,4E) consists of several layers of gravel, sand, and sandy clay that record a period of significant alluviation on the fan surface. Unit 4A, exposed east of station 27, is a

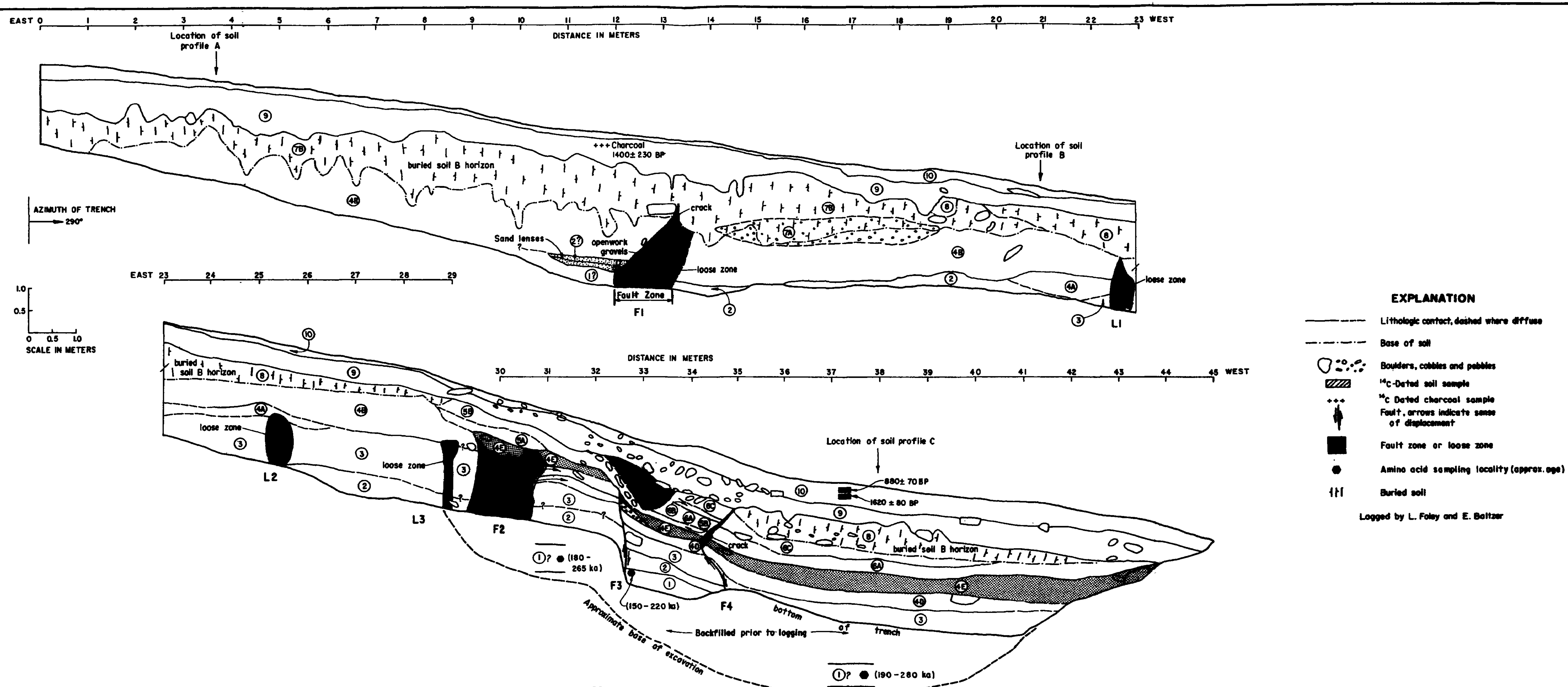


## DESCRIPTION OF TRENCH UNITS

(1) Debris flow: Light olive brown (2.5Y 5/4,m) gravelly silty clay, massive, poorly sorted, contains shells of Oreohelix cf. strigosa.

(2) Debris flow: Yellowish brown (10YR 5/4,m) gravelly sandy clay, massive, poorly sorted.

(3) Alluvium: Brownish yellow (10YR 6/5,m) very gravelly silty sand, moderately well bedded, moderately well sorted.

(4A) Alluvium: Brownish yellow (10YR 6/5,m) very gravelly sand, massive, moderately well sorted.

(4B) Debris flow: Very pale brown (10YR 7/4,d) very gravelly clayey silt, massive, poorly sorted, stage II carbonate is part of buried soil in unit 5A.

(4C) Alluvium: Light yellowish brown (10YR 6/4,m) very gravelly silty sand, massive, moderately well sorted, stage II carbonate.

(4D) Debris flow: Yellowish brown (10YR 7/4,d) gravelly silty sand, massive, poorly sorted, stage II carbonate.

(4E) Alluvium: Light yellowish brown (10YR 6/4,m) very gravelly silty sand, massive, moderately well sorted, stage II carbonate.

(5A) Colluvium: Light yellowish brown (10YR 6/4,d) very gravelly sand, massive, moderately well sorted, stage I+ carbonate.

(5B) Colluvium: Yellowish brown (10YR 5/4,d) very gravelly silty sand, massive, moderately well sorted, stage I+ carbonate.

(6A) Alluvium: Light yellowish brown (10YR 6/4,m) very gravelly sandy clay, massive, moderately well sorted, stage I+ carbonate.

(6B) Alluvium: Very pale brown (10YR 7/3,d) very gravelly sand, moderately well bedded, moderately well sorted, stage I+ carbonate.

(6C) Alluvium: Yellowish brown (10YR 5/4,m) very gravelly silty sand, massive, moderately to poorly sorted.

(7A) Debris flow, buried soil: Dark yellowish brown (10YR 4/4,m) very pebbly clay, massive, moderately well sorted, buried argillic soil horizon is in the upper half of this unit.

(7B) Debris flow, buried soil: Strong brown (7.5YR 5/6,d) gravelly clay, buried argillic soil horizon formed in debris flow deposits, moderate medium prismatic structure, poorly sorted.

(8) Colluvium: Brownish yellow (10YR 6/6,d) and strong brown (7.5YR 5/8,d) gravelly silty clay and gravelly silty sand, massive, poorly sorted, buried soil B horizon on upthrown side of lower scarp at Stn. 20-29 and downthrown side at Stn. 35-43.

(9) Colluvium: Very pale brown (10YR 7/4,d) very gravelly silty sand, massive, unsorted, contains B horizon of modern soil.

(10) Loessial colluvium: Dark brown (7.5YR 3/3,m) silty clay, massive, well sorted, A horizon of modern soil.

JOES VALLEY DAM
SEISMOTECTONIC STUDY

LOG OF TRENCH 6

FIGURE 4.5

lens of gravelly alluvium underlying finer grained sediments (4B) inferred to be a debris flow. West of F2, unit 4 contains three distinct strata designated 4C,4D, and 4E, inferred to be distal facies of unit 4B. These strata are distinct enough to correlate across F3 and F4 allowing displacement to be measured.

Units 5A and 5B are inferred to be colluvium deposited across the small scarps following the displacement of the underlying beds on F2 and F3. Unit 6 (6A, 6B, 6C) consists of stratified gravelly sand, clay and silty sand, and attests to continued alluviation at the distal end of the fan and at the base of the slope after displacement on F3.

Unit 7, a debris flow that covers unit 4 in the eastern half of the trench, is subdivided into units 7A and 7B. Unit 7A, a channel fill within the larger debris flow, contains a higher proportion of coarse pebbles and is slightly more sorted than unit 7B. Unit 7B is a massive poorly sorted gravelly clay containing a reddish brown (7.5YR) argillic B horizon 30-60 cm thick with thick clay films. This soil obscures its lower contact with unit 4B, and the upper part of unit 7A. The degree of profile development is comparable to soils as old or older than 130 ka (see discussion of soil relative ages in Appendix A) indicating that the surface of unit 7 was exposed for at least this length of time. Unit 7 was not recognized west of station 19.

Unit 8 is a sandy colluvium probably deposited as slopewash across the fan surface and later remobilized and mixed by downslope creep and bioturbation because it is unstratified and contains cobbles and krotovinas. A moderately well-developed, predominantly brownish yellow (10YR), argillic horizon, thinner than the soil in unit 7B, is present in unit 8 (see Appendix A). Unit 8 was not found between stations 29 and 35, although it was recognized west of F4.

Unit 9 is a distinctive layer of very gravelly silty sand resulting from alluvial deposition on the younger fan surface and subsequent downslope movement. A radiocarbon date of 1400±230 yrs BP was obtained from a small piece of charcoal within unit 9 at station 12 (Appendix B). Whether this charcoal is in situ or brought in later by a burrowing animal is not certain, although no evidence for a krotovina was found near the charcoal. Because of the uncertainty of its provenance, the date is considered a minimum age for unit 9.

The youngest deposit exposed in the trench is loose gravelly active slope colluvium in unit 10. The modern soil on this younger fan surface is forming in units 10 (A horizon) and 9 (B horizon). Two radiocarbon dates were obtained from the organic clay fraction of the A horizon (unit 10) at station 37. These two dates of 1620±80 and 880±70 yrs BP (Appendix B) suggest that this soil has been forming for approximately one to two millenia. Both the charcoal and the soil $^{14}C$ dates indicate a much more rapid rate of soil development in Scad Valley than in the area around Joes Valley Reservoir, where dates from the modern A horizon are in the 6 ka range. This accelerated soil development could be attributed to the coarser texture of the parent material combined with greater effective precipitation at this elevation (Appendix A) and is consistent with soil development observed in other profiles in this northernmost part of the Joes Valley graben.

The stratigraphic evidence in trench 6 is used to interpret surface displacement in the form of faulting and monoclinal folding in at least four discrete events. Zones of loose gravel (L2, L3, and F2 on fig. 4.5) record the earliest event that disturbed units 1, 2 and 3. These loose zones were subsequently buried by unit 4.

Unit 4 can be traced across the entire trench and has been displaced at three locations. These displacements may have resulted from the same event or from three separate events that preceded the deposition of units 5A and 5B. A zone of loose unstratified gravel (F1) is inferred to be a fault zone because it occurs at the location where the trench intersects a projection of a fault scarp on the older fan surface. The surface expression of this older fan and fault scarp terminates about 3 m north of the trench where the older fan appears to have been first eroded and then buried by younger fan materials equivalent to units 9 and 10 in the trench. In the trench there is no evident displacement of the base of unit 7B across this fault zone. The amount of displacement is about 1.5-2 m on the scarp to the north, as measured on two scarp profiles (fig. 4.4). The debris flow in unit 4B and the underlying unit 2 are unstratified, so displacement cannot be determined.

A second fault zone, F2, is represented by a zone of loose gravel about 1.4 m wide. The contact between units 2 and 3 does not appear to be displaced, although the overlying contact (between units 3 and 4) is displaced about 40 cm. This apparent stratigraphic anomaly is a result of the diffuse nature of the contact between units 2 and 3, making it difficult to locate accurately on the trench log.

The third location with evidence for post-unit 4/pre-unit 5 surface displacement is at F3 where units 4C, 4D, and 4E are are displaced along a near vertical fault plane. The 4D/4E contact, a readily distinguishable marker, has a net vertical displacement of about 1 m across F3. Unit 4C was not recognized on the downthrown side of this fault probably because it is thin and may have lensed out at this point.

The third surface displacement event postdates deposition of unit 7 since it is not recognized in the trench to the west of station 21, where the lower scarp begins, where unit 7 is unconformably overlain by unit 8. Unit 7 appears to have been displaced by faulting or monoclinal folding and then eroded from the scarp or slope and the downthrown block. The irregular surface of unit 7 supports this interpretation. Whether this post unit 7 event is the same or a separate one from the event that displaced unit 4 is not clear from the evidence in the trench.

The fourth and most recent surface displacement occurred after deposition of unit 8 and formation of a soil profile within it. Unit 8 is missing between stations 29-35 and has an apparent vertical displacement of approximately 2.5 m down to the west. Most of this displacement must have occurred by folding since the underlying beds (for example, unit 6A) have been displaced less than 2.5 m.

In summary, the four surface displacement events inferred from the trench stratigraphy are: (1) post units 1, 2 and 3 and before deposition of unit 4 on F1, (2) after deposition of unit 4 and prior to deposition of unit 5 with evidence for displacement in three locations: F2, F3, and F4, (3) after deposition of unit 7 and development of a thick soil profile within it and prior to deposition of unit 8, probably as folding along the lower scarp, west of station 16, and (4) the most recent event that displaced unit 8 as monoclinal folding between stations 29-35 and minor faulting on F4.

The total apparent vertical displacement of the top of unit 3 across the entire fault zone (F1..F4) is about 3 m. The unit 3/unit 4 contact is displaced about 0.6 m across F2, 1.1 m across F3, and 0.7 m across F4, for a total of 2.4 m. The discrepency between the totals illustrates the problem of accurately projecting the surfaces of the strata, the variability introduced by facies and thickness changes in the sediments, and the displacement that is the result of folding instead of faulting. Projecting the top of unit 8 from its position at station 21 along a slope similar to the present fan surface, the difference in height between this slope and the surface of unit 8 at station 37 is an approximate measurement of the vertical displacement of unit 8 across the fault zone. This measurement of 2.5 m of displacement has occurred on the lower scarp since deposition of unit 8 and formation of the soil within it. This displacement seems to have produced a monoclinal fold rather than a scarp with a small amount of vertical displacement on F4. Prior events produced less than a meter of displacement in total. If the fault at Scad Valley has behaved consistently, then the last 2.5 m of displacement is more likely the result of several small events over a long time than the result of one large event.

The timing of these faulting events can be approximated from the chronological data derived from trench 6. The maximum age of the deposits (unit 1) and therefore the observed displacements is 150-300 ka, and probably about 250 ka. The earliest displacement produced loose zones in unit 3. The next displacement of unknown amount at this location but about 1.5-2.0 m on the scarp present to the north, predates a soil (unit 7B) that is interpreted to be older than 130 ka. This soil, as well as stratified alluvial deposits that stratigraphically underlie it, were displaced about 0.5 m in the third faulting event and subsequently covered by a soil (unit 8) interpreted to be no younger than 14-30 ka. Unit 8 was in turn displaced about 2.5 m in the fourth faulting event and later buried by colluvium that is 1.5 kyrs old. Although this 2.5 m of displacement is most likely the result of several small events, the possibility that one major event produced this displacement cannot be ruled out.

In summary, we interpret the stratigraphy exposed in trench 6 to be the result of at least 4 faulting events with a total vertical displacement of about 3 m. Data from scarp profiles measured on well defined scarps to the north indicate that the displacement is greater there than at the trench site. Estimates of the length of recurrence intervals for surface faulting events on the Scad Valley scarp are discussed in section 4.7.

### 4.3.5 East Joes Valley fault: summary

The East Joes Valley fault is expressed on the surface as a linear escarpment approximately 50 km long along the east side of the northern Joes Valley graben. The fault can be subdivided into three segments based on the amount of total stratigraphic displacement, the degree of topographic expression, and the occurrence of scarps in upper Quaternary deposits. The three segments of the East Joes Valley fault are, from south to north, (1) the 5 km long Ferron segment, (2) the 42 km long Straight Canyon segment between Ferron Canyon and Miller Flat Creek, and (3) the 8 km long Miller Flat segment at the northern end of the fault where displacement and topographic expression are minimal. The Straight Canyon segment, where total displacement in the bedrock is greatest, is the only one of the three segments that is inferred to have significant late Quaternary displacement. The evidence for late Quaternary displacement includes geomorphic criteria such as linearity and steepness of the bedrock scarp and the presence of fault scarps in Quaternary deposits. Joes Valley Dam is located adjacent to the Straight Canyon segment and the reservoir covers a portion of it.

## 4.4 The West Joes Valley fault

The west-bounding fault of the northern Joes Valley graben extends from about 5 km south of Ferron Canyon, where it parallels the Muddy fault, to Spring Creek at the northern end of the graben, with an overall length of about 60 km (plate 1). The West Joes Valley fault is similar to the parallel east-bounding fault in that displacement in the bedrock is greatest near the center of the fault diminishing to the north and south, and evidence for Quaternary displacement is restricted to this central portion. The West Joes Valley fault is divided into the Dugway Hollow, Seely, and Huntington segments.

### 4.4.1 Dugway Hollow segment

At its southern end, the West Joes Valley fault bounds a small, 7.5 km long, graben with about 150 m of displacement in the Price River Formation (Ellis, 1981b). The topographic relief across the fault is approximately 100 m. This graben is similar to the small graben at the southern end of the East Joes Valley fault (section 4.3.1) in that the total displacement is relatively small, it is deeply incised by Ferron Creek, the scarp has low topographic relief, and Quaternary deposits are scarce both on the scarp face and in the graben. These characteristics suggest that the Dugway Hollow segment, like the Ferron segment to the east, has not had significant surface displacement in the Quaternary.

### 4.4.2 Seely segment

The Seely segment is composed of two en echelon sections (plate 2) that are characterized by the presence of scarps in Quaternary deposits of similar age. The southern part of the Seely segment extends 32 km from Ferron Canyon in the south to Browns Canyon in the north. The fault in this area is characterized by a steep linear escarpment along the west side of the graben with topographic relief that is roughly equal to the total amount of late Cenozoic displacement. The greatest displacement occurs in the central part of the fault, near Joes Valley Reservoir, and diminishes to the north and south.

The bedrock escarpment in this area is incised by numerous east-flowing drainages which head at the crest of the Wasatch Plateau. The canyons associated with these drainages have been subjected to glacial erosion and mass wasting processes which have resulted in the extensive accumulation of landslide, debris flow, and morainal deposits at the mouths of these canyons. The presence of these deposits on the trace of the fault allows for a more accurate assessment of the amount of late Quaternary faulting than on the East Joes Valley fault.

The southern part of the Seely segment is crossed by four major drainages (plate 2): Seely, Littles, Reeder, and Black Creeks, and three of these drainages (Littles, Reeder, and Black) contain evidence for scarps in upper Quaternary deposits.

Seely Creek is a major east-flowing stream that has maintained a course directly across the graben, incising the footwalls of the bounding faults by about 300 m. A large upper Pleistocene debris flow (Qdf on fig. 4.2) issued from Seely Creek and was deposited in a fan-shaped configuration in Joes Valley, on the north side of the present drainage. To the south of Seely Creek are alluvial fan deposits and colluvium. Three terraces inset into these deposits extend from the mouth of Seely Creek, at the West Joes Valley fault, 2.5 km east to the main south-flowing drainage in the graben, Lowry Water. The presence of these terraces (Qt1, Qt2, Qt3, on fig. 4.2) indicates progressive lowering of base level during the late Pleistocene and Holocene. Whether this base level lowering is the result of tectonic, climatic, or other factors is unclear. Whatever the cause, the presence of the terraces indicates that the rate of incision has been greater than the rate of base level lowering (Peterson, 1979) during this period. The soil profile developed on Qt3, as well as its geomorphic position relative to the large debris flows inferred to be late Pleistocene in age, and its position 7 m above Seely Creek suggest a Holocene age (see discussion in Appendix A).

Littles Creek crosses the West Joes Valley fault 0.9 km north of Seely Creek in a canyon 100-150 m deep incised into the bedrock escarpment (plate 2). A debris flow from Littles Canyon is visible on aerial photographs as a large fan that crosses the fault (fig. 4.2). The southern boundary of this deposit is difficult to distinguish from the Seely Creek debris flow since they appear to interfinger. Three terraces in alluvium and debris flow materials, 15 m (Qt1), 5 m (Qt2), and 2 m (Qt3) above the present creek level are present at the mouth of Littles Canyon (fig. 4.6). A 450 m long scarp parallels the West Joes Valley fault in the two higher terraces, while the lowest terrace is not displaced. The scarp is 8 to 12 m high in Qt1 and 6 m high in Qt2. These differences in scarp height suggest at least two surface faulting events since deposition of Qt1. Trench 4 was excavated near the northern end of the scarp where it is approximately 8 m high. The stratigraphy exposed in trench 4 is discussed in section 4.4.4.

Reeder Canyon is 3.5 km north of Littles Canyon (plate 2). No east facing scarps are evident in the alluvium at the mouth of Reeder Canyon, probably because the narrow width of the canyon mouth does not allow for the deposition of alluvium. However, in the area to the east of the mouth of Reeder Canyon, within the graben, is a succession of four terraces in debris flow and alluvial fan deposits that originated from Reeder Canyon (fig. 4.2). West-facing scarps associated with the Middle Mountain intragraben fault (discussed in section 4.5) are present in these fans.

At the mouth of Black Canyon, 5.3 km north of Reeder Canyon (plate 2), is a series of four alluvial terraces, the two oldest of which (Qt1 and Qt2) have been cut by a fault scarp associated with the West Joes Valley fault. A detailed map of this locality is presented in figure 4.7 along with the measured heights of the fault scarps. The Quaternary history of this canyon can be reconstucted from geomorphic relationships inferred from aerial photographs.

The oldest Quaternary deposit at this locality is an end moraine that extends down to a minimum elevation of 2440 m, immediately west of the mouth of Black Canyon (plate 2). Similarities in elevation and surface morphology suggest that the moraine resulted from the same glacial advance identified farther north in the graben which is correlated with the Pinedale glaciation in the Rocky Mountains that occurred between 14 and 30 ka (Appendix A). A large debris flow (Qdf on fig. 4.7 and plate 2), probably derived from morainal material, flowed from the mouth of Black Canyon and was deposited in the graben, to the south of the canyon mouth. Subsequent displacement of this deposit on the West Joes Valley fault has produced a 12 m high east-facing scarp in the 20 m terrace (Qt1). Displacement on the Middle Mountain fault has resulted in the formation of three small (<4 m) west-facing scarps in the debris flow deposit in the graben. Because the moraine, the high terrace (Qt1) and the east (upthrown) side of the debris flow all fall on a projection of the same sloping surface when measured on a Kern PG-2 photogrammetric plotter, they may have been originally (prior to faulting and erosion) a continuous deposit with the debris flow being slightly younger than the moraine.

The Qt1 terrace at Black Canyon is inferred to be the same age as the highest terrace at Littles Canyon (>23 ka). The relative degree of soil profile development on the surfaces of the three oldest Black Canyon terraces (Appendix A) indicates that the next two lower terraces (Qt2 and Qt3) are probably equivalent to latest Pinedale (11-14 ka). The

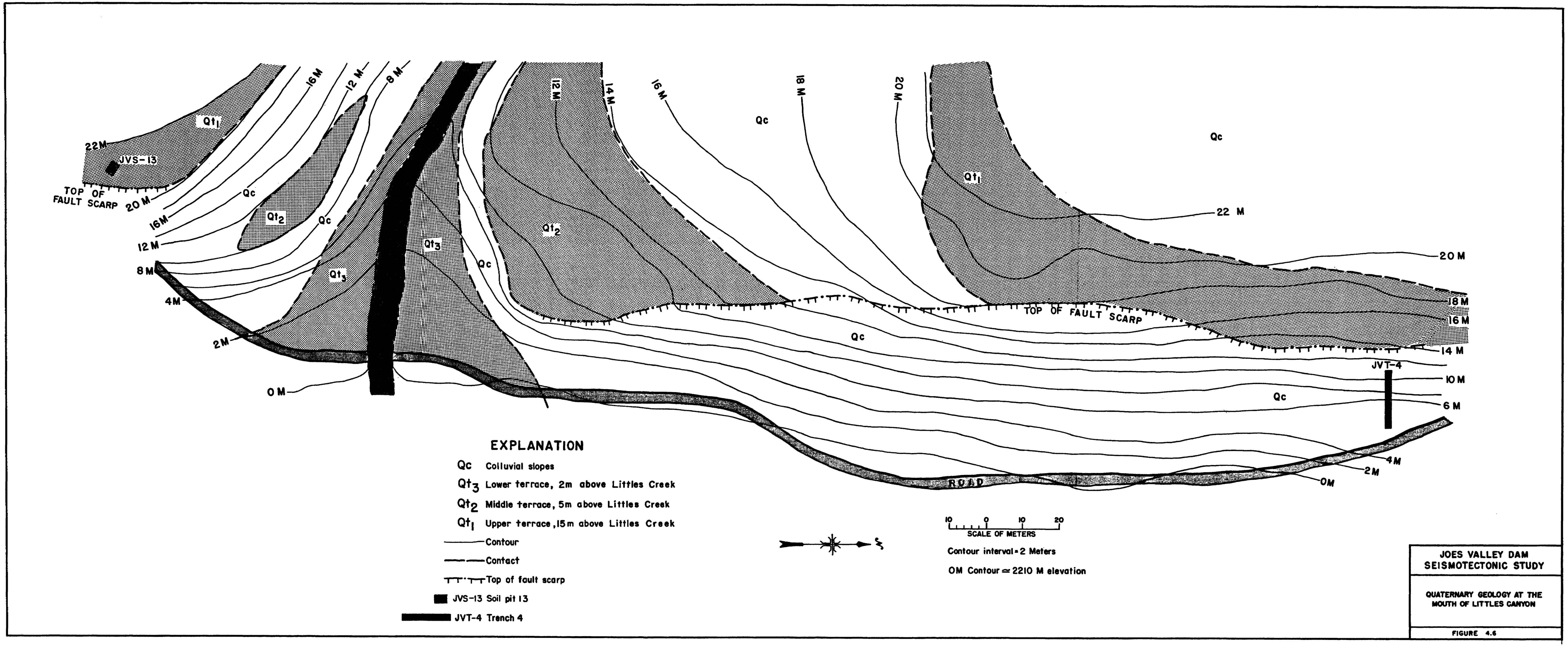

Qt1
22M
JVS-13
TOP OF FAULT SCARP
20 M
16M
12 M
8 M
4M
2M
0 M
16 M
12 M
8 M
Qc
Qt2
Qc
Qt3
Qt3
Qc
12 M
14 M
16 M
18 M
20 M
Qc
Qt2
Qt1
Qc
22 M
20 M
18 M
16 M
14 M
TOP OF FAULT SCARP
Qc
JVT-4
10 M
Qc
6 M
4 M
2 M
0 M
ROAD
EXPLANATION
Qc Colluvial slopes
Qt3 Lower terrace, 2m above Littles Creek
Qt2 Middle terrace, 5m above Littles Creek
Qt1 Upper terrace, 15m above Littles Creek
Contour
Contact
Top of fault scarp
JVS-13 Soil pit 13
JVT-4 Trench 4
10 0 10 20
SCALE OF METERS
Contour interval = 2 Meters
OM Contour ≃ 2210 M elevation
JOES VALLEY DAM
SEISMOTECTONIC STUDY
QUATERNARY GEOLOGY AT THE MOUTH OF LITTLES CANYON
FIGURE 4.6

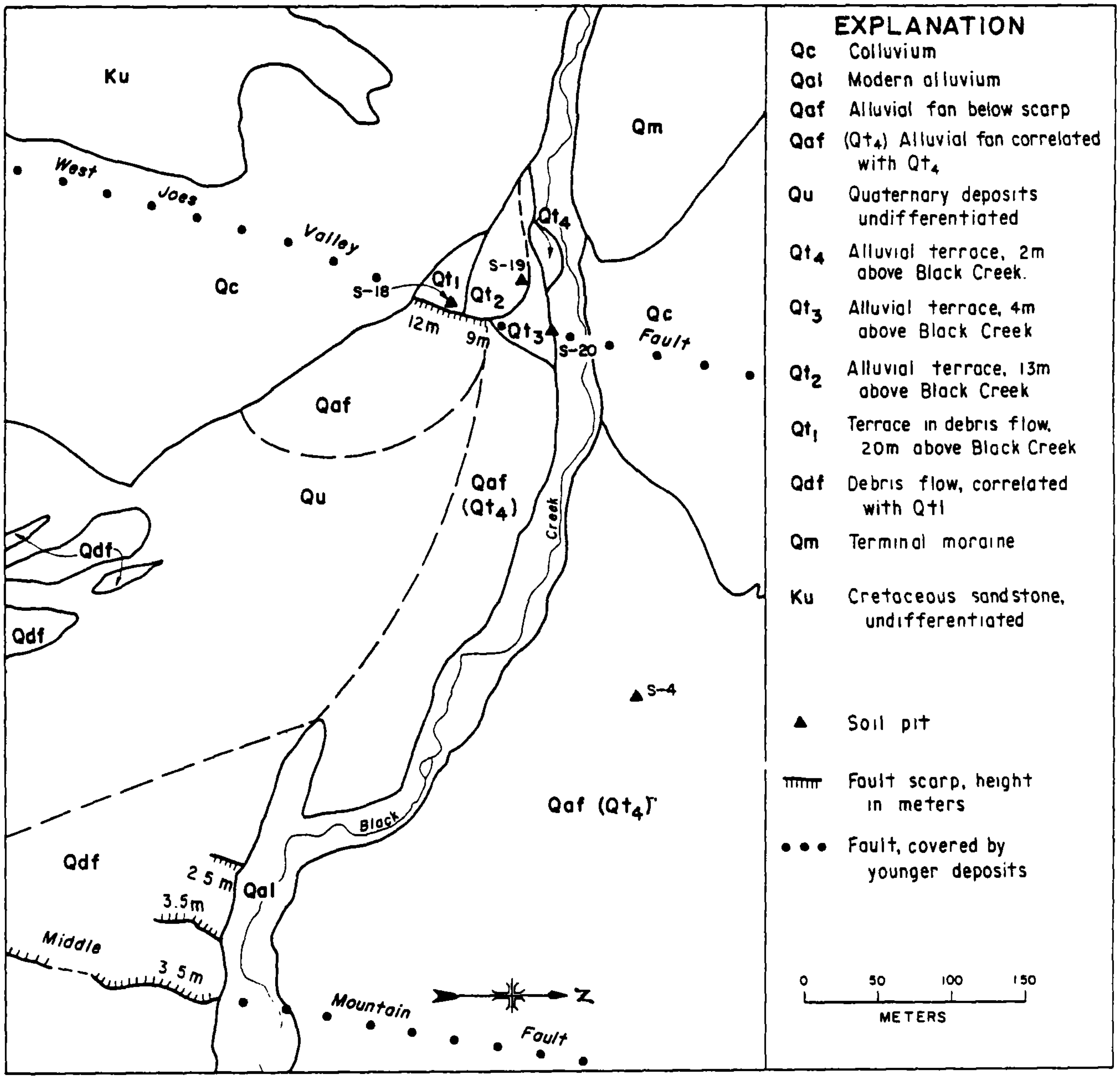


Figure 4.7: Quaternary deposits at the Black Canyon locality (see plate 2 for location).

fourth terrace, a small remnant 2 m above the modern floodplain, is inferrred to be Holocene (<10 ka). The following table lists the scarp heights and the height of each terrace above the creek as well as the age of the deposit on which the terrace is cut estimated from geomorphic and soils criteria.

Table 4.1: Scarp height and age estimates for the terraces at the mouth of Black Canyon (see Fig. 4.7)

| Terrace | Height above creek (m) | Scarp height (m) | Incision (m)[1] | Age of deposit |
|---|---|---|---|---|
| Qt1 | 20 | 12 | 8 | 23-30 ka |
| Qt2 | 13 | 9 | 4 | 11-14 ka |
| Qt3 | 4 | 0 | 4 | 11-14 ka |
| Qt4 | 2 | 0 | 2 | < 10 ka |

1 Amount of incision by Black Creek measured by subtracting scarp height from height above creek.

At least two scarp-forming events with a total scarp height of about 12 m prior to formation of Qt3 (11-24 ka) are apparent from table 4.1. In contrast to the evidence at Littles Canyon, at Black Canyon the second event appears to have had greater displacement than the earlier one. The chronology of these events, one displacing a Pinedale age (Qt1) terrace and a later one occurring sometime between deposition of two latest Pinedale (Qt2 and Qt3) terraces generally corresponds with the stratigraphic interpretation from trench 4 (section 4.4.4).

This part of the Seely segment continues for another 8 km to Browns Canyon. North of the mouth of Browns Canyon undisplaced glacial deposits and younger alluvium/colluvium (Qu on plate 2) overlie the projection of the fault. At Browns Canyon the bedrock scarp takes an en echelon step 1.5 km to the west. Although the portion of the fault between Browns and Staker Canyons is covered at both ends by undisplaced glacial deposits, scarps about 12-14 m high are present in moraines at the mouths of Bennetts, Seeley, and Jordan Canyons (plate 2). The irregular nature of the moraine surfaces and the presence of deep gullies parallel to the scarps in some locations make accurate scarp height measurements difficult to obtain. The moraines in which the scarps are located (Qm3) are correlated to the latest Pinedale (11-14 ka) glacial advance in the Rocky Mountains based on soils data, geomorphic characteristics, and position relative to other end moraines (see Appendix A).

Because these scarps are all in deposits of the same age, the number of events that has occurred cannot be estimated. However, the scarp heights imply that more than one episode of surface displacement has occurred since the latest Pinedale advance at this northern end of the Seely segment.

### 4.4.3 Huntington segment

The northernmost segment of the West Joes Valley fault is poorly defined topographically, but seems to extend at least 4 km between Staker and Lake Canyons (plate 2). Three terminal moraines, at the mouths of Staker, Rolfson, and Lake canyons, overlie this segment of the West Joes Valley fault with no evidence of having been displaced. Therefore, this fault segment has not had surface displacement since at least 11 ka. The trace of the fault is defined by an eroded escarpment 200 m high in the North Horn Formation west of the projection of the Seely segment to the south. Total stratigraphic displacement on the West Joes Valley fault has diminished to under 500 m at this point, and north of Lake Canyon the fault terminates in the Blackhawk Formation (Witkind and others, 1978).

### 4.4.4 Trench on the West Joes Valley fault

Trench 4 is located near the northern end of a 450 m long scarp in the highest (Qtl) of three terraces at the mouth of Littles canyon (fig. 4.6). The terrace is composed of debris flow and alluvial deposits from Littles Creek. The surface of the terrace is covered by colluvium from the steep slope above it on the escarpment along the West Joes Valley fault. The trench exposed Price River Sandstone overlain by these debris flow, alluvial and colluvial deposits (fig. 4.8). Following is a description of the deposits in the trench and an interpretation of the faulting history at the Littles Creek locality based on the stratigraphic relationships observed in the trench and the position of the fault scarp relative to the three terraces.

At the base of the trench is fractured sandstone bedrock (unit 1) that is overlain by debris flow deposits (unit 2). On top of unit 2 are alluvial deposits consisting of finely laminated sand and pebbly sand (units 3A, 3B, and 4). Units 5, 6, and 7 are inferred to be derived from the older alluvial and debris flow deposits. Units 8A and 8B, poorly sorted gravelly clay, are from a younger debris flow. Charcoal from unit 8B yielded a $^{14}C$ date of 23,140 ± 350 yrs BP (Appendix B). Unit 9 is a younger debris flow, similar to unit 8, and unit 10 is an organic-rich colluvium. Unit 11 is loose active colluvium containing the A horizon of the modern soil.

At least two surface faulting events are inferred from the stratigraphic relationships in trench 4. The fault zone is located where a zone of shearing overlies a near-vertical face in the sandstone bedrock at stations 8-10. Units 1 through 4 appear to have been displaced initially by at least 5.5 m, the difference in height between the top of unit 4

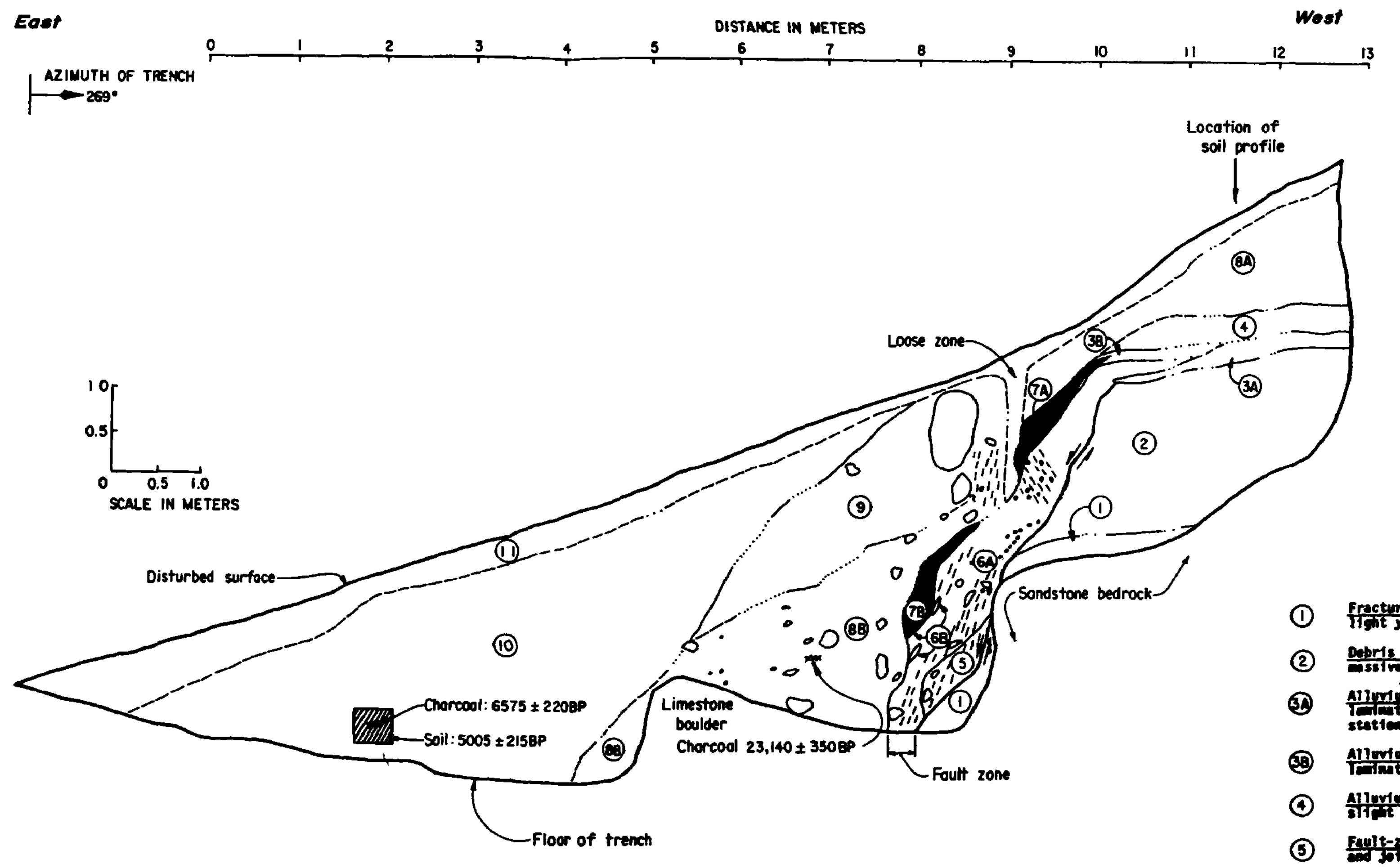


## EXPLANATION

- Lithologic contact, dashed where diffuse, dotted where concealed by shoring
- Boulders, cobbles and pebbles
- Vertical shears and joints in fault zone
- Charcoal samples for $^{14}C$ dating
- Soil sample for $^{14}C$ dating
- Fault, arrows indicate sense of displacement

Logged by L. Foley, E. Baltzer, and C. Krinsky

## DESCRIPTION OF TRENCH UNITS

(1) Fractured sandstone bedrock: Yellow (2.5Y 7/6,m) sandstone with light yellowish brown (10YR 6/4,m) clay filling vertical joints.

(2) Debris flow: Very pale brown (10YR 7/3,d) gravelly silty clay, massive, very poorly sorted.

(3A) Alluvium: Pale brown (10YR 6/3,d) silt and sand, medium horizontal laminations in places, very well sorted, laminations deformed between stations 10 and 11 to dip 20° E.

(3B) Alluvium: Very pale brown (10YR 8/3,d) very fine sand, fine horizontal laminations, very well sorted.

(4) Alluvium: Very pale brown (10YR 7/3,d) very pebbly sand, very slight imbrication, moderately well sorted.

(5) Fault-zone: Brown (10YR 5/3,m) gravelly clay, vertical micro-shears and joints, very poorly sorted.

(6A) Fault-zone: Yellowish brown (10YR 5/4,m) gravelly sandy clay, vertical and near vertical micro-shears and joints, very poorly sorted.

(6B) Fault-zone: Light yellowish brown (10YR 6/4,m) very fine sand, in thin (<2cm) lenses which parallel shears in 6A.

(7A) Faulted alluvium: Very pale brown (10YR 7/3,d) gravelly clay with lenses of fine sand.

(7B) Fault-zone: Very pale brown (10YR 7/3,d) gravelly silty sand, few vertical joints, poorly sorted.

(8A) Debris flow: Pale brown (10YR 6/3,d) very gravelly clay, massive, very poorly sorted, stage I carbonate.

(8B) Debris flow: Very pale brown (10YR 7/3.5, d) very gravelly clay, massive, very poorly sorted.

(9) Debris flow: Pale brown (10YR 6/3, d) very gravelly clay, massive, very poorly sorted, stage I carbonate.

(10) Slope colluvium: Grayish brown (10YR 5/2, d) gravelly clay, loose, very poorly sorted.

(11) Slope colluvium: Light grayish brown (2.5Y 5/2,d) gravelly silty clay, loose, very poorly sorted.

JOES VALLEY DAM
SEISMOTECTONIC STUDY

LOG OF TRENCH 4

FIGURE 4.8

and the base of the trench (subtracting later displacement). The corresponding beds were not exposed on the hanging wall, so 5.5 m is a minimum estimate of the vertical displacement. Unit 3A, a thin bed of laminated silt and sand, is fractured and dips toward the fault (east) in the area within 75 cm of the fault. The overlying beds, units 3B and 4, appear to be draped over the fault and to be continuous with units 6 and 7. Unit 7A contains lenses of fine sand that are similar to sandy strata within 3A. These stratigraphic relationships could have occurred if the sediments on the alluvial terrace were in a saturated condition at the time of displacement and flowed over the scarp, covering the free face. Unit 8, dated at about 23 ka, is a debris flow that was deposited after the underlying deposits were faulted. The age of unit 8 provides a minimum age for the high terrace (Qtl) and the earlier displacement on the scarp at this locality. A maximum age for the terrace is derived from geomorphic relationships and soils data discussed in Appendix A, and is about 30 ka.

The most recent faulting event displaced units 7, 8, and 9 by about 0.5 m (the difference in height between 7A and 7B and the tops of 8A and 8B), and resulted in vertical joints and shears in the clay-rich sediments within the fault zone. The remnants of unit 9 were probably removed subsequently from the upthrown side of the scarp since they are not evident in the trench, or they may have been incorporated into the colluvium in unit 10. This colluvium does not appear to be displaced by the fault since no younger colluvium overlies it as would be expected if the scarp had been steepened suddenly. Radiocarbon dates were obtained from the soil organic fraction and from charcoal found in the trench wall within unit 10. These dates, 5005±215 yrs BP and 6575±220 yrs BP (Appendix B), respectively, provide a minimum age for the last surface faulting event recorded in the trench.

In summary, we infer at least two surface-faulting events on the Littles Canyon scarp from the stratigraphy in trench 4: the earlier displacement of 5.5 m occurred prior to 23 ka and a more recent event with displacement of about 0.5 m occurred between 23 ka and 6.5 ka. Displacement appears to have been greater to the south along the scarp. Evidence from Black Canyon (table 4.1) would suggest that the most recent event on this part of the Seely segment occurred between 11 and 14 ka. The length of the recurrence interval of surface faulting events on this fault is discussed in section 4.7.

#### 4.4.5 West Joes Valley fault: summary

The 60 km long west-bounding fault of the northern Joes Valley graben is divided into three segments based on the amount of total stratigraphic displacement in the bedrock, the degree of topographic expression of this displacement, and the presence or absence of fault scarps in upper Quaternary deposits. The three segments of the West Joes Valley fault are the 7.5 km long Dugway Hollow segment at the southern end, the Seely segment with a total length of 42 km, and the Huntington segment that is approximately 4 km long at the northern end of the fault.

Evidence for Quaternary surface displacement on the West Joes Valley fault is found only on the central (Seely) segment that is composed of two en echelon sections. Fault scarps in upper Quaternary deposits are present at five localities along the fault. Determinations of the age of these scarps are based on $^{14}C$ dates from trench 4 and relative age dating of the deposits (Appendix A) in which the scarps are found. Scarps ranging in height from 8 to 12 m are present in deposits of latest Pleistocene age at the mouths of Littles and Black Canyons. Data from trench 4 on the Littles Canyon scarp indicate that at least two events have occurred on this part of the fault with a total displacement of about 8 to 12 m: the earlier displacement (one or more events) between 23 and 30 ka and a later event prior to 6.5 ka and and possibly between 11 and 14 ka. Measurements of scarp and terrace heights at the Black Canyon locality indicate two events with similar timing to those at Littles Canyon. Along the section of the fault between Browns and Lake Canyons, scarps possibly as high as 12-14 m are present at three localities (Bennets, Seeley, and Jordan Canyons) in moraines attributed to the latest Pinedale glacial advance, about 11 to 14 ka. Therefore, at each of five localities on the West Joes Valley fault there is evidence for approximately 12 m of displacement in deposits that range in age between 11 and 30 ka.

## 4.5 Intragraben faults

The part of Joes Valley graben that is north of Joes Valley Reservoir contains scarps in upper Quaternary deposits between the two major graben-bounding faults. Some of these scarps occur along intragraben horst blocks, such as the Middle Mountain and Bald Mountain faults, while others, for example the scarps in the reservoir, do not bear a clear spatial relationship to bedrock faults (plate 2). Previous workers in the area (Kucera, 1954; Witkind and others, 1978; 1982a; Kitzmiller, 1982) have mapped several additional intragraben faults. For this study we have included on plate 2 only those faults with clear evidence for surface displacement in Quaternary deposits.

### 4.5.1 Middle Mountain fault

The Middle Mountain fault, which bounds the Middle Mountain horst block on the west (plate 2), is the longest intragraben fault with evidence for Quaternary surface displacement. The trace of this fault is composed of many NNE trending en echelon, down-to-the-west scarps and photolineaments extending from just south of Reeder Creek to Scad Valley, a distance of 25 km. Recurrent late Pleistocene surface rupture is demonstrated by the presence of higher scarps in progressively older upper Pleistocene alluvial deposits and their absence in younger Holocene alluvial fans (plate 2 and fig. 4.2). Data from three trenches excavated across traces of the Middle Mountain fault suggest that two surface faulting events have occurred in the late Quaternary.

The northern end of the Middle Mountain fault appears to merge with the East Joes Valley fault at Scad Valley and at its southern end, the surface expression of the Middle Mountain fault disappears into a large landslide deposit (plate 2). The southern end of the fault is on strike with the West Joes Valley fault which has an opposite sense of displacement. Possibly the fault continues in an en echelon pattern to include the scarps located beneath the reservoir to the southeast.

Several north-trending, west-facing scarps and photolineaments are present on the western edge of Joes Valley Reservoir, in the center of the graben. These scarps could be associated either with the fault on the west side of Dragon Ridge horst block to the south (plate 2), or with the Middle Mountain fault to the NNW. No evidence for Quaternary displacement is found on the Dragon Ridge fault.

### 4.5.2 Trenches on the Middle Mountain fault

Three trenches were excavated on the Middle Mountain fault in the area east of the mouth of Reeder Canyon where two parallel en echelon scarps and photolineaments occur in the three oldest of a sequence of four upper Pleistocene alluvial fans (fig. 4.2). A fourth trench was excavated across one of the reservoir scarps that may be a southern extension of the Middle Mountain fault.

#### 4.5.2.1 Trench 1

Trench 1 is located on a relatively large eroded remnant of the highest alluvial fan, af1 (fig. 4.2), whose apex is at the mouth of Reeder Creek, on the west side of Joes Valley graben. Several smaller remnants of this fan are surrounded by younger and topographically lower alluvium. A west-facing 1.6 km-long scarp from 0 m (photolineament) to 1.7 m-high cuts the surface of af1. At the site of trench 1 there is no apparent displacement of the ground surface but there is a linear depression on the fan surface. The trench was located here because of the possibility for finding datable organic material in the depression. However, none was found in trench 1.

The stratigraphy in trench 1 (fig. 4.9) is interpreted to consist of debris flow deposits, colluvium, slopewash, alluvial fan gravels and loess, all of which have been faulted and finally covered by another layer of loess. The oldest unit (units 1A,1B) in the trench is composed of poorly sorted gravelly clay interpreted as the product of debris flows emanating from Reeder Canyon to the west that form the core of the oldest alluvial fan remnant (af1) at this locality. Unit 1 is covered by very gravelly alluvium (unit 2) also attributed to deposition on the af1 surface. Unit 5 (5A, 5B, 5C, 5D), massive brown clay, is inferred to be loess that accumulated in a depression on the uphill side of a west-facing scarp. Because no loess deposits were found elsewhere in the study area on surfaces of comparable age it appears that the loess only accumulated in protected positions such as this one. Stage I carbonate and slight color changes within unit 5 indicate that loess deposition was slow enough or periodic enough to allow soil formation to occur. A thin debris flow of sandy clay (unit 6), probably derived from a mixture of alluvial fan gravels and loess from higher on the fan surface to the west, overlies unit 5 and is in turn overlain by loess in units 7 and 8.

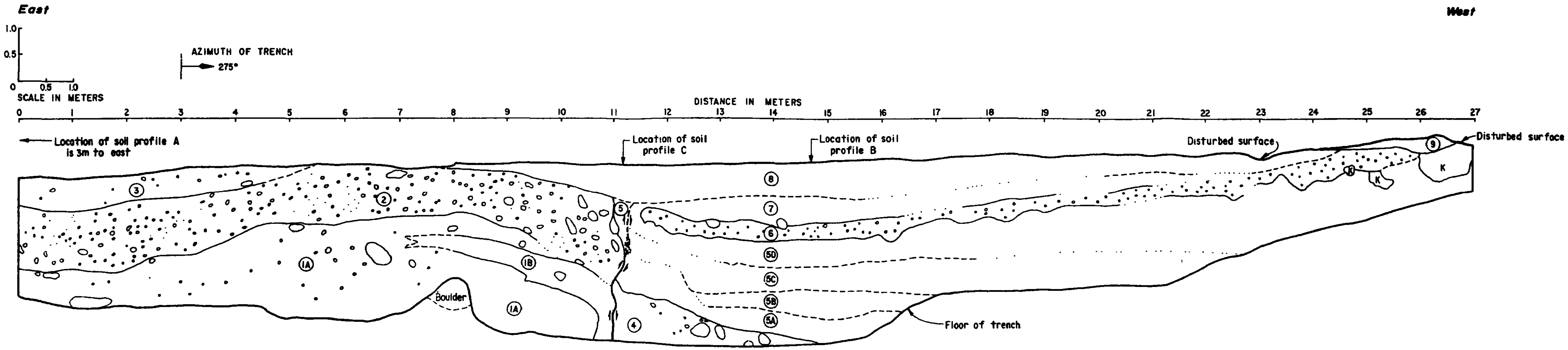


## DESCRIPTION OF TRENCH UNITS

(1A) Debris flow: Light yellowish brown (10YR 6/4,d) very gravelly clay, massive, unsorted.

(1B) Debris flow: Dark gray (10YR 4/1,d) very gravelly clay, massive, unsorted.

(2) Alluvium. Very pale brown (10YR 8/3,d), very gravelly sandy silt, moderately sorted, poorly imbricated, stage I+ carbonate.

(3) Slopewash: Very pale brown (10YR 7/5,d) clayey sand, massive, poorly sorted, stage I+ carbonate.

(4) Alluvium: Brownish yellow (10YR 6/6,m), very gravelly clayey sand, massive, poorly sorted.

(5A) Loess: Strong brown (7.5YR 4/6,m) clay, massive, well sorted, stage I+ carbonate, common vertical seams of $CaCO_3$.

(5B) Loess: Strong brown (7.5YR 4/6,m) clay, massive, well sorted.

(5C) Loess: Strong brown (7.5YR 5/6,m) clay, massive, well sorted.

(5D) Loess: Brown (7.5YR 5/4,m) silty clay, massive, well sorted, stage I carbonate.

(6) Debris flow: Light gray (10YR 7/2,d) sandy clay, massive, very poorly sorted.

(7) Slope colluvium: Very pale brown (10YR 8/4,d) sandy silt, massive, moderately sorted, soil Bk horizon.

(8) Loess: Brown (7.5YR 5/4 to 10YR 5/3,d) clay, soil A and B horizons, blocky and prismatic structure, very well sorted.

(9) Slope colluvium: Brown (10YR 5/3,d) sandy clay, massive, poorly sorted.

## EXPLANATION

Lithologic contact, dashed where diffuse, dotted where concealed by shoring

Boulders, cobbles, pebbles

Vertical shears and joints in fault zone

Fault, arrows indicate sense of displacement

(K) Krotavina

Logged by L. Foley and E. Baltzer

JOE S VALLEY DAM SEISMOTECTONIC STUDY

LOG OF TRENCH I

FIGURE 4.9

The soil on this youngest loess blanket has a well developed argillic horizon and stage I-II carbonate and is interpreted to be of latest Pleistocene age (11-30 ka) (Appendix A).

Two surface-faulting events are inferred from the stratigraphic evidence in the trench. The feature interpreted to be a fault is the vertical contact between units 1 and 2 and units 4,5,6,7 at station 11. The first event displaced units 1 and 2 and created a west-facing scarp at station 11. The determination of the amount of displacement that occurred depends on the interpretation of the origin of unit 4, which is similar to unit 2 in appearance. If unit 4 were colluvium derived from a free-face in unit 2 gravels, then the top of the downthrown block would not be exposed in the trench and the displacement in this event could be more than 3 m. If unit 4 were the top of the downthrown block of unit 2, then the displacement would be as little as 1.5 m. However, the eroded condition of the top of unit 2, apparent on the trench log between stations 8 and 11 suggests that at least part of unit 4 is colluvium derived from it and that the displacement in the first event was more likely about 2 m.

Loess comprising units 5A,5B,5C,5D and a debris flow (unit 6) were subsequently deposited against the scarp. Enough relief must have persisted at the scarp face to prevent the terminus of the debris flow from crossing the fault trace. The second event on the fault is inferred from the presence of microshears in the unit 5 loess at station 11. The amount of displacement in the second event can be measured on the trench log as the difference in height between the top of unit 4 at the fault and the point where the fault penetrates the loess above. This relatively minor amount of displacement, approximately 0.5 m, is consistent with the lack of evidence for a scarp having formed in this second event. Another interpretation of the trench, based on the greater degree of warping of the loess layers in unit 5 relative to the younger debris flow in unit 6, would be that several very small surface faulting events occurred after the first comparatively large event.

In summary, trench 1 contains evidence for at least two surface faulting events on the Middle Mountain fault, that displaced the oldest alluvial fan at the mouth of Reeder Creek. The apparent vertical displacement in the first event documented in the trench is at least 1.5 m and possibly greater than 3 m. The second surface-faulting event produced microshears in loess and displaced the top of unit 4 with apparent vertical displacement of approximately 0.5 m.

#### 4.5.2.2 Trench 3

Trench 3 is located 0.3 km south of trench 1 on a small eroded remnant of the oldest alluvial fan (af1) from Reeder Canyon (fig. 4.2). The trench is on a 1.7 m high north-trending scarp on trend with the lineament where trench 1 is located. Our intepretation of the stratigraphy exposed in the walls of trench 3 is generally that alluvium, colluvium, and debris- and mudflows have been displaced by two surface-faulting events on the Middle Mountain fault.

The oldest deposits in the trench (units 1A,1B,2,3), exposed between stations 0-11 (fig. 4.10), consist of very gravelly alluvium and debris flow sediments, similar to those in trench 1, that were deposited on the af1 surface. The next stratigraphically younger deposits are located at the base of the trench at station 12-13. Unit 4 is inferred to be alluvium and unit 5 a debris flow, both originating from higher on the original fan surface to the west. Continuing deposition by mud- and debris-flows is indicated by the presence of units 7 through 13. From observation of aerial photographs, these flows appear to be derived from and therefore younger than the large landslide 240 m southwest of the trench (fig. 4.2). Unit 12 contains a buried soil consisting of a color B horizon that has been engulfed later by $CaCO_3$ (see discussion in Appendix A). This soil was buried by unit 13, a mudflow. Unit 14 is a dark brown organic-rich soil A horizon. Three $^{14}C$ dates were obtained from samples of organic clay in this A horizon between stations 13-15. The dates, 6100±195 yrs BP, 3975±200 yrs BP, and 2335±150 yrs BP (Appendix B), appear to be reliable indicators of the mean residence time of organic carbon in this soil because they are consistently older with depth. The youngest depositional unit in the trench is active slope colluvium in unit 15 that contains the A and B horizons of the modern soil.

Two surface faulting events are inferred from the stratigraphic evidence. The fault is a vertical contact between units 1A and 6B at station 11 and a zone of vertically oriented cobbles that comprises unit 6B. This loose zone has been disturbed further by burrowing animals as evidenced by a large krotovina west of unit 6B. Units 4 and 5 can be interpreted as the top of a block of alluvial fan deposits displaced about 2-3 m down to the west (the difference in height between the projections of the tops of units 6A and 4). Unit 6 (including 6A and 6B), which overlies this surface, appears to be a wedge shaped deposit of colluvium that covered the free face of the scarp formed in this first event. The debris and mudflows stratigraphically overlying unit 6 were deposited in a depression on the west (uphill) side of the uphill facing scarp. Unit 12 contains a buried soil which formed after the earlier faulting event and prior to the second event. The most recent faulting event displaced the preexisting colluvial wedge (unit 6) about 0.5 m (approximated from the difference in height between the projection of the top of unit 6A with that of unit 6B) and reoriented the cobbles in unit 6B to parallel the fault. After this second event, fine debris-flow sediments, probably partially derived from loess similar to the loess in trench 1, filled the depression adjacent to the new scarp and an organic rich soil A horizon (unit 14) formed within it. Radiocarbon dates from this A horizon, which stratigraphically overlies the fault zone, provide a minimum age of 6 ka for the second surface-faulting event at this location.

In summary, the interpretation of the stratigraphy exposed in trench 3 implies that two surface-faulting events have occurred at this location on the Middle Mountain fault. The total vertical displacement evident in the trench is about 3 m, with 2.5 m having occurred in the first event, and about 0.5 m in the second. The total measured scarp height,

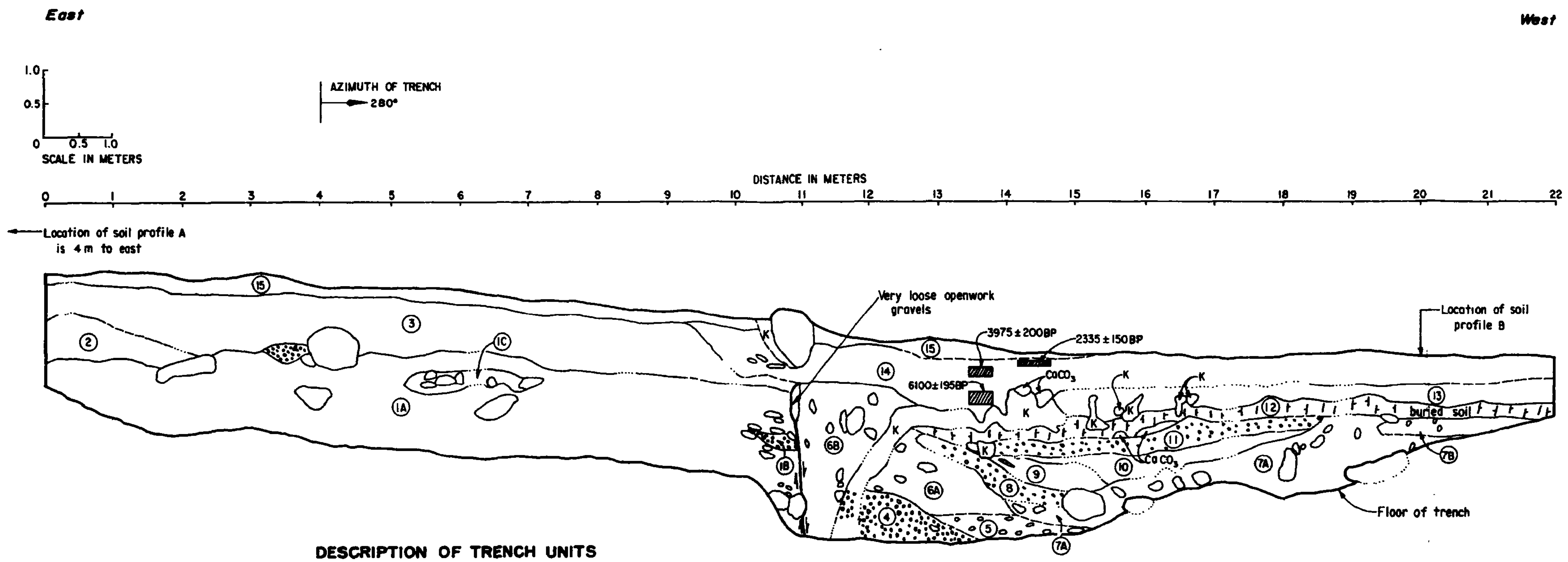


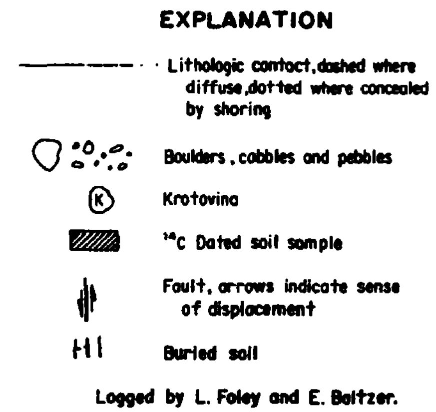


## DESCRIPTION OF TRENCH UNITS

(1A) Alluvium: Very pale brown (10YR 7/3,d) very gravelly silty sand, massive, moderately well sorted, stage I+ carbonate.

(1B) Alluvium: Very pale brown (10YR 7/4,d) very pebbly sand, massive, moderately well sorted, some openwork texture, stage I- carbonate, channel gravel.

(1C) Debris flow: Very pale brown (10YR 7/3,d) very gravelly sandy silt, massive, very poorly sorted.

(2) Alluvium: Very pale brown (10YR 7/3,d) very gravelly sand, moderately well imbricated, moderately well sorted, stage I carbonate.

(3) Debris flow: Very pale brown (10YR 8/3,d) very gravelly sandy silt, massive, moderately well sorted, stage I carbonate.

(4) Alluvium: Very pale brown (10YR 8/3,d) very gravelly silty clay, massive, moderately well sorted, truncated by krotovina at Station 11.5.

(5) Debris flow: Very pale brown (10YR 7/3,d) very gravelly sandy silt, massive, very poorly sorted, stage I+ carbonate.

(6A) Fault-zone gravels: Very pale brown (10YR 7/3,d) very gravelly sandy silt, massive, very poorly sorted, stage I carbonate.

(6B) Fault-zone gravels: Very pale brown (10YR 7/3,d) very gravelly sandy silt, massive, very poorly sorted, stage I carbonate, vertically oriented cobbles, some openwork texture, faulted scarp colluvium.

(7A) Debris flow: Very pale brown (10YR 7/4,d) gravelly sandy silt, massive, poorly sorted, stage I carbonate.

(7B) Mudflow: Very pale brown (10YR 8/4,d) silty clay, massive, moderately well sorted.

(8) Debris flow: Pale yellow (2.5Y 7/4,m) pebbly sandy clay, massive, very poorly sorted.

(9) Debris flow: Light yellowish brown (10YR 6/4,m), gravelly silty sand, massive, moderately well sorted.

(10) Mudflow: Very pale brown (10YR 7/4,m) sandy silt, massive, moderately well sorted.

(11) Debris flow: Very pale brown (10YR 7/4,m) very gravelly sandy silt, massive, very poorly sorted.

(12) Mudflow, buried soil: Strong brown (10YR 7/3,m) sandy silt, massive, well sorted, stage I carbonate, buried soil B horizon.

(13) Mudflow: Strong brown (10YR 7/3,m) sandy silt, massive, poorly sorted, stage I carbonate, soil Bk horizon.

(14) Debris flow: Brown (10YR 4/3,m) very pebbly silty clay, massive, very poorly sorted, soil A horizon.

(15) Colluvium: Brown (10YR 3/2,m) gravelly sandy silt, massive, poorly sorted, soil A and B horizons.

**JOES VALLEY DAM SEISMOTECTONIC STUDY**

LOG OF TRENCH 3

FIGURE 4.10

1.7 m, is lower than the total displacement of the stratigraphic units in the trench because the scarp faces uphill and its height is reduced by the deposition of sediments against it. The two surface-faulting events are chronologically bracketed by the soil formed on the alluvial fan surface (af1) and by the $^{14}C$ age of 6 ka of the organic matter in the A horizon that overlies the fault. The degree of development of the buried soil that formed between the first and second events is an indication of the amount of time that elapsed between them.

4.5.2.3 Trench 2

Trench 2 is located on an en echelon segment of the Middle Mountain fault 200 m west of and parallel to the scarp where trenches 1 and 3 were sited (fig. 4.2). The west-facing 0.5 m high scarp is discontinuous and barely discernible on the ground but forms an easily visible north-trending photolineament on the intermediate age af3 surface.

Trench 2 exposes af3 alluvial fan deposits consisting of poorly sorted debris flows and gravelly alluvium. The deposits have been disturbed by bioturbation as evidenced by numerous krotovinas (fig. 4.11). Near the center of the trench (stations 6 to 7) is an area, interpreted to be a fault zone, containing very loose gravel that has been extensively disturbed by krotovinas on both sides of the trench. Another vertically oriented very loose zone and crack is located between stations 3 and 4. This appears to be an extensional crack. There is no evidence in the trench either for displacement of stratigraphic units or for the existence of a fault scarp at some time in the past. This lack of evidence is attributed to the coarse nature of the deposits and to a relatively small amount (<1 m) of displacement inferred on this portion of the fault. The loose colluvium and soil in the upper 0.5 m of the trench overlie the faulted gravels, although the krotovina extends to the surface, obscuring this relationship. However, oriented $CaCO_3$ rinds (stage I-) on gravels in the fault zone indicate that soil formation postdates the disturbance caused by faulting. This alluvial fan is interpreted to be of late Pleistocene age based on the degree of soil development on its surface (see discussion in Appendix A). The single faulting event recorded in trench 2 appears similar in the small amount of displacement and relative age to the most recent event recorded in trenches 1 and 3.

4.5.2.4 Trench 5

The reservoir scarps are a series north-trending small (<2 m), subdued, west-facing scarps and photolineaments on the west side of Joes Valley Reservoir (fig. 4.2) that are visible on aerial photographs taken before construction of Joes Valley Dam. Some of the scarps are above the level of the reservoir in a large debris flow deposit which originated from Seely Canyon to the west. The scarps that are presently beneath the reservoir cut alluvium that is inset into this debris flow, but no scarps are evident on the youngest alluvial terrace (Qt3 on fig. 4.2) on Seely Creek.

Trench 5 is situated on the west side of the reservoir where a scarp crosses debris flow deposits. At this site the west-facing scarp is

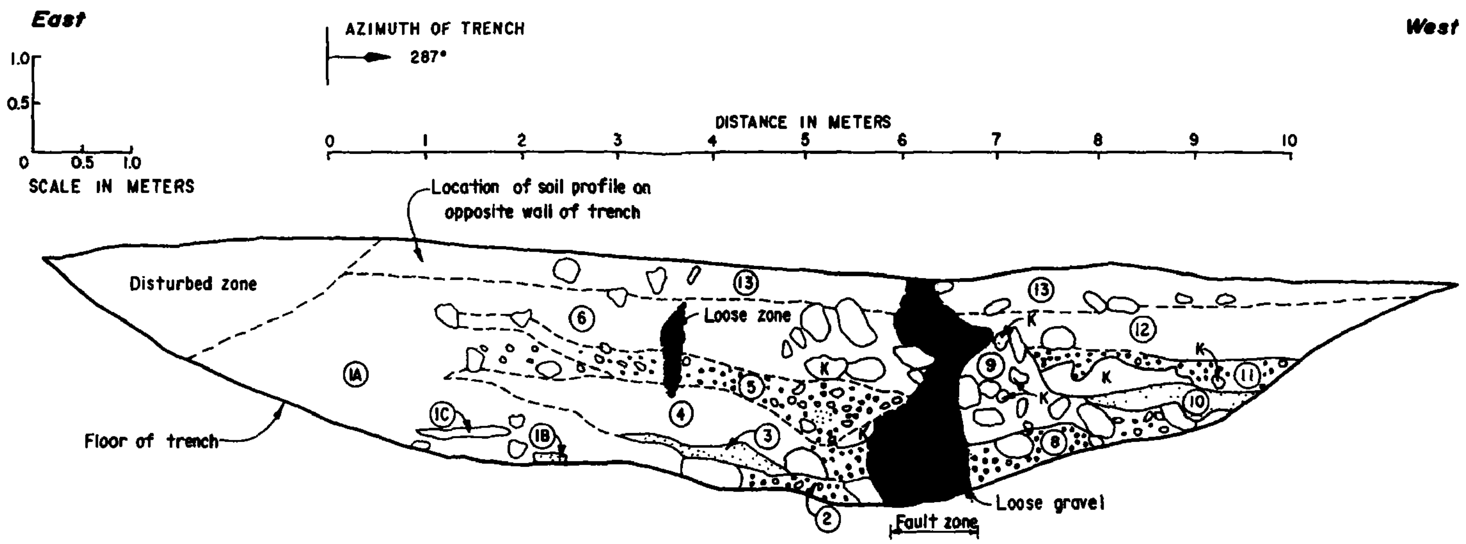


## DESCRIPTION OF TRENCH UNITS

(1A) **Alluvium**: Yellowish brown (10YR 5/4,d) very gravelly medium sand, moderately imbricated, moderately well sorted, stage I+ carbonate, grades into unit 6 at east end of trench.

(1B) **Alluvium**: Light yellowish brown (2.5Y 6/4,m) sandy silt, massive, well sorted, occurs as a thin lens within unit 1A.

(1C) **Alluvium**: Pale brown (10YR 6/3,d) fine sand, finely laminated, very well sorted, occurs as a thin lens within unit 1A.

(2) **Alluvium**: Yellowish brown (10YR 5/4,d) very gravelly silty sand, well imbricated, moderately well sorted.

(3) **Alluvium**: Pale brown (10YR 6/3,d) fine and medium sand, laminated, well sorted.

(4) **Alluvium**: Light yellowish brown (10YR 6/4,d) very gravelly silty sand, moderately imbricated, poorly sorted, stage I- carbonate.

(5) **Alluvium**: Light brownish gray (2.5YR 6/2,d) very gravelly coarse sand, well imbricated, moderately well sorted, some openwork texture.

(6) **Debris flow**: Light gray (2.5Y 7/2,d) very gravelly sandy silt, massive, poorly sorted, stage I- carbonate.

(7) **Fault-zone gravels**: Light yellowish brown (10YR 6/4,d) very gravelly sandy silt, massive, poorly sorted, stage I- carbonate, loose with some openwork texture.

(8) **Colluvium**: Light yellowish brown (10YR 6/4,d) very gravelly sandy silt, massive, moderately well sorted, stage I- carbonate.

(9) **Colluvium**: Light gray (10YR 7/2,d) very gravelly sandy silt, massive, very poorly sorted.

(10) **Alluvium**: Light gray (10YR 7/2,d) sandy silt, massive, well sorted, stage I+ carbonate.

(11) **Alluvium**: Very pale brown (10YR 7/3,d) very pebbly sandy silt, massive, moderately sorted, stage II carbonate, soil Bk horizon.

(12) **Debris flow**: Light gray (2.5Y 7/2,d) very gravelly sandy silt, massive, poorly sorted, stage I- carbonate, soil Bk horizon.

(13) **Loose colluvium, soil**: Brown (10YR 4/3 to 5/3,d) sandy loam, moderately well sorted, soil A and B horizons.

## EXPLANATION

- - - - Lithologic contact, dashed where diffuse

Boulders, cobbles, pebbles

(K) Krotovina

Fault zone or loose zone

Logged by C. Krinsky, E. Baltzer, and L. Foley

**JOES VALLEY DAM SEISMOTECTONIC STUDY**

**LOG OF TRENCH 2**

**FIGURE 4.11**

1.6 m high and very subdued. The stratigraphic units distinguished in the trench (fig. 4.12) consist of unstratified debris flow deposits (units 3,5,7) derived from the Cretaceous and Tertiary rocks up Seely Canyon interbedded with poorly to moderately stratified alluvial gravels (units 1,2,4,6). A layer of active colluvium (unit 9) is draped over the surface of these deposits. The soil developed on the surface contains stage II carbonate and in inferred to be late Pleistocene in age (14-30 ka, Appendix A). Between stations 12 and 13 is an area of loose, disturbed and bioturbated gravel distinguished as unit 8. This zone is interpreted to be a fault zone. The faulting which displaced the gravels apparently did not create a free-face large enough to shed material into a colluvial wedge since none is observed in the trench. This lack of evidence for a scarp suggests that the amount of surface displacement was not very great, certainly less than 1 m. A step in the lower boundary of the calcareous part of the modern soil is evident over the fault zone at station 12.5 suggesting that a second small event may have occurred after the initiation of soil profile development on this surface. The interpretation of two small events, each producing less than 1 m of displacement, is consistent with the total scarp height of 1.6 m measured on the surface.

### 4.5.3 Chronology of surface-displacement on the Middle Mountain fault

Four trenches were excavated across en echelon segments of the Middle Mountain fault: two in older (af1) alluvial fan deposits (trench 1 and 3), one on a younger (af4) fan surface (trench 2), and one on a debris flow surface (trench 5). Each of the three trenches on the oldest surfaces contains evidence for two surface-faulting events separated by a soil. The timing of these events can be estimated from interpretations of the relative age of the surface based on soils data presented in Appendix A and from radiocarbon dates in trench 3. The soil is estimated to be at least 14-30 ka in age and therefore the first surface faulting event occurred after this time. Radiocarbon dates from colluvium deposited after the second and most recent surface displacement in trench 3 provide a minimum age of roughly 6 ka. The length of time that elapsed between these two events can be estimated from the amount of soil development that occurred during this interval. The buried soils in trench 1 and 3, and the surface soil in trench 5 are considered to represent an interval of not less than appoximately 10 ka. The single small event inferred from trench 2, which is on an upper Pinedale fan surface, can be logically correlated with the second small event on the older surfaces.

### 4.5.4 Bald Mountain faults

At the extreme northern end of Joes Valley graben are two intragraben faults with scarps in Quaternary deposits on either side of Bald Mountain horst block (plate 2). Quaternary displacement in the northernmost portion of the Joes Valley graben appears to be restricted to Bald Mountain since neither of the main graben-bounding faults appears to have had surface displacement in the Quaternary at this location. The 2.5 km long scarp on the East Bald Mountain fault is about 3-5 m

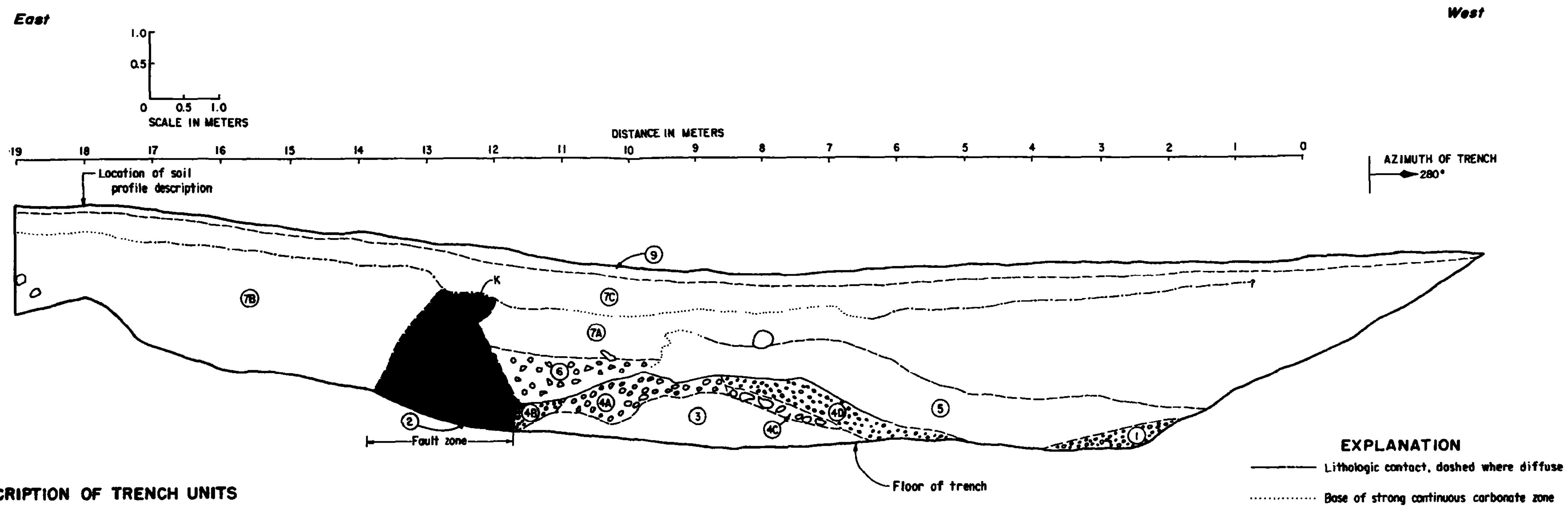


## DESCRIPTION OF TRENCH UNITS

(1) Alluvium: Pale brown (10YR 6/2) pebbly coarse sand, massive, well sorted, channel gravels.

(2) Alluvium: Light brownish gray (10YR 6/2,d) pebbly sand, massive, moderatley sorted, channel gravels in fault-zone.

(3) Debris flow: Light gray (10YR 7/2,d) very gravelly sandy clay, massive, very poorly sorted.

(4A),(4B) Alluvium: Very pale brown (10YR 7/3,d) very gravelly silty sand, massive, well sorted, 4A gravel coarser than 4B.

(4C),(4D) Alluvium: Light gray (10YR 6.5/2) very gravelly clayey coarse sand, moderately well sorted, some openwork structure, channel gravels, stage II carbonate, 4C gravel coarser than 4D.

(5) Debris flow: Light gray (10YR 7/2,d) gravelly fine sandy clay, massive, very poorly sorted.

(6) Alluvium: Light gray (10YR 7/2,d) very gravelly sandy clay, massive, moderately well sorted, channel gravels.

(7A) Debris flow: Light gray (10YR 7/2,d) gravelly fine sandy clay, massive, very poorly sorted.

(7B) Debris flow: Light gray (10YR 7/2,d) gravelly sandy clay, massive, very poorly sorted.

(7C) Debris flow: Pale brown (10YR 6/3,d) silty clay, massive, very poorly sorted, stage II carbonate.

(8) Fault-zone: Light brownish gray (10YR 6/2,d) very gravelly sandy clay, very poorly sorted, very loose.

(9) Slope colluvium: Brown (10YR 5/3,d) sandy silt, massive, moderately well sorted, partly of eolian origin, soil A horizon.

## EXPLANATION

- Lithologic contact, dashed where diffuse
- Base of strong continuous carbonate zone
- Base of weak discontinuous carbonate zone
- Boulders, cobbles and pebbles
- (K) Krotovina
- Fault Zone

Logged by E. Baltzer and C. Krinsky

**JOES VALLEY DAM SEISMOTECTONIC STUDY**

**LOG OF TRENCH 5**

**FIGURE 4.12**

high in an upper Pleistocene outwash terrace, while the West Bald Mountain fault appears to be covered by upper Pleistocene moraines at its south and north ends. A relatively small (<2 m) scarp is present in colluvium on the hillslope north of Miller Flat Reservoir and in a small alluvial fan where Staker Canyon crosses the west side of Bald Mountain horst. These small scarps either have not been preserved in the morainal material to the north and south, are younger than the moraines, or the faults do not extend as far as the moraines.

### 4.5.5 Intragraben faults, summary

Several faults associated with horst blocks have been mapped previously within Joes Valley graben (Spieker, 1931; Kucera, 1954; Witkind and others, 1978; 1982; Kitzmiller, 1982). Fault scarps are present in Quaternary deposits along three of these intragraben faults, the Middle Mountain fault and the two faults bounding Bald Mountain. Evidence from the mapping and relative age-dating of these Quaternary deposits suggests that the scarps are the result of recurrent surface faulting since the Pinedale (11-30 ka). Data from the four trenches excavated on the Middle Mountain fault scarps provide more detailed interpretations of the nature of surface faulting in the Joes Valley graben.

## 4.6 Northern Joes Valley graben: summary

The northern Joes Valley graben, which extends from Ferron Canyon in the south to Electric Lake in the north, is bounded by two major faults, the East and West Joes Valley faults. Geomorphic evidence for recurrent late Quaternary displacement in this graben is limited to the main central segments of these faults, where total stratigraphic displacement is greatest, and to faults located within the graben from the vicinity of Joes Valley Reservoir to the northern end of the graben. The geomorphic characteristics indicative of late Quaternary surface rupture include fault scarps in upper Quaternary deposits, active and/or upper Quaternary alluvial fans at the base of the bedrock escarpment, and a linear near-vertical bedrock escarpment. The lengths of the segments exhibiting these characteristics form the basis for estimating the potential length of surface rupture on these faults, which is approximately 45 km.

The 42 km long central (Straight Canyon) segment of the East Joes Valley fault is located beneath the reservoir 0.12 km west of Joes Valley Dam. Evaluating the late Quaternary activity of this fault segment is difficult since direct evidence is available at only one locality, Scad Valley, 22 km north of Joes Valley Dam, where the relationship of the fault scarps in the alluvial fans to the main bedrock escarpment is unclear. Trench data from this locality indicate recurrent events of relatively small displacement in the late Quaternary. An estimate of the recurrence interval of surface faulting events based on data from trench 6 is discussed in the following section.

The central (Seely) segment of the West Joes Valley fault, 2.5 km west of Joes Valley Dam, is composed of two en echelon sections with a total length of 42 km. Fault scarps are present in upper Pleistocene deposits at the mouths of several east-flowing drainages that cross the fault trace. Field investigations of the West Joes Valley fault included detailed mapping of these scarps and terraces, scarp height measurements, relative age dating of geomorphic features using soil profiles, and the excavation of a trench on the Littles Canyon scarp. Data acquired from five localities along the West Joes Valley fault indicate that approximately 12 m of displacement has occurred in deposits dated at 11-30 ka. Stratigraphic evidence from trench 4 suggests that at least two surface faulting events, at least one prior to about 23 ka and a smaller event prior to 6.5 ka have occurred on the Seely segment. At Black Canyon there is evidence for at least two events, one prior to 14 ka (23-30 ka?) followed by at least one from 11-14 ka. The presence of 12-14 m high scarps in 11-14 ka moraines on the northern part of the segment suggests that greater Holocene displacements have occurred at the northern end of the Joes Valley graben.

The Middle Mountain fault is a major intragraben structure that extends from Reeder Creek to Scad Valley, a distance of 25 km. En echelon scarps beneath Joes Valley Reservoir are on trend with the Middle Mountain fault and may be an extension of it. Three trenches were excavated on en echelon segments of the Middle Mountain fault and one on a reservoir scarp. Data from these four trenches indicate that two late Pleistocene-Holocene surface faulting events have occurred on the Middle Mountain fault since 14-30 ka, the most recent one prior to 6.5 ka.

### 4.7 Estimated length of recurrence intervals for surface faulting in northern Joes Valley graben

The geologic data acquired from trenches, soil pits, detailed geologic maps and scarp profile measurements in the northern part of the Joes Valley graben can be combined in order to estimate recurrence intervals for surface faulting events on the East and West Joes Valley faults and the Middle Mountain fault. The pertinent data are summarized in table 4.2.

The average recurrence interval of surface faulting derived from stratigraphic evidence in trench 6, which is located on a scarp that may be related to movement on the East Joes Valley fault, is an upper limit because the number of faulting events is considered a minimum. The most recent displacement interpreted from the trench data is more likely the result of several small faulting events rather than one large (2.5 m) displacement. This interpretation leads to the conclusion that several small surface faulting events have occurred since the late Pleistocene with a total vertical displacement at this locality of 2.5 m, the most recent having occurred prior to 1.5 ka. Whether this conclusion is representative of this fault segment is questionable since the trench is in an ambiguous location relative to the East Joes Valley fault and because the style of deformation observed in the trench may not be representative of the fault segment as a whole.

The evaluation of the recurrence interval of surface displacement on the West Joes Valley fault is based on data from four locations where the

Table 4.2: Average recurrence interval of surface faulting events on major faults in the northern Joes Valley graben inferred from scarp height measurements and stratigraphic evidence in trenches

| FAULT | LOCALITY | FAULTING EVENT | DISPLACEMENT (m) /1 | AGE OF FAULTING (kyrs) /2 | ESTIMATED AVERAGE RECURRENCE INTERVAL (kyrs) |
|---|---|---|---|---|---|
| East Joes Valley | Trench 6 | 4 | 2.5 (>1 event?) | 1.5*-14 | <60 |
| | | 3 | 0.5 | 14-130 | |
| | | 2 | 1.5-2 (scarp north of trench) | >(130-250@) | |
| | | 1 | n.d. | >(130-250@) | |
| West Joes Valley | Trench 4 | 2 | 0.5 | 6.5*-23* | 10-20 |
| | | 1 | >5.5 (>1 event?) | 23* | |
| | Black Canyon | 2 | 3 (>1 event?) | <10 - (11-14) | |
| | | 1 | 3 | < (14-30) | |
| | Bennets-Seely-Jordan Canyons | ? | 12-14 (>1 event?) | < (11-14) | n.d. |
| Middle Mountain | Trench 1 | 2 | 0.5 | < (14-30) | 10-15 |
| | | 1 | >2 (2->3.5) | < (14-30) | |
| | Trench 3 | 2 | 0.5 | > 6* | 10-15 |
| | | 1 | 2.5 | 6* - (14-30) | |
| | Trench 2 | 1 | <1 | < (14-30) | n.d. |
| | Trench 5 | 1 | <1 | < (14-30) | n.d. |

/1 Amount of displacement is estimated from scarp heights and stratigraphic relationships in trenches.
/2 Unless otherwise noted, age estimate is based on a soil relative age (see section A2)
* Age estimate is based on a radiocarbon date.
@ Age estimate is based on amino acid analysis of shells in trench 6.

fault cuts upper Quaternary deposits. The interpretation of the stratigraphic evidence in trench 4 indicates at least two surface faulting events separated by an interval of about 10-20 kyrs. This estimate is supported by observations at the Black Canyon locality. The northern part of this segment appears to have had greater Holocene displacement since 12-14 m high scarps are found in moraines attributed to the latest Pleistocene glaciation (11-14 ka). This observation is consistent with other indications that the northernmost part of the graben has been more recently active with a higher rate of activity than others.

The Middle Mountain fault has been evaluated at four localities. Data from four trenches indicate that two late Pleistocene-Holocene surface faulting events have occurred on the Middle Mountain fault between 14-30 ka and 6.5 ka. The amount of vertical displacement in the earlier event was about 3 m and the later was about 1 m or less. The recurrence interval for surface faulting derived from these limited chronologic data averages about 8-24 kyrs. A noticable similarity exists between the Middle Mountain and the West Joes Valley faults in the number of late Quaternary surface faulting events, their timing, and the relative amount of estimated vertical displacement. This similarity suggests that the Middle Mountain fault is antithetic to the West Joes Valley fault and that displacement on both occurs synchronously.

## 5.0 Pleasant Valley fault zone

The Pleasant Valley fault zone is a system of north-trending normal faults transected by minor southeast-trending faults in the Cretaceous and Tertiary rocks of the northeastern Wasatch Plateau (plate 1). This fault zone extends for a distance of 50 km from south to north, and includes faults from 8 km west of Scofield Dam to the east edge of the Wasatch Plateau, for a total width of 20 km (plate 3). The total length and vertical displacement on these faults is generally smaller than on the Joes Valley faults which parallel these to the west and southwest. Spieker (1931) estimated the maximum displacement in the Pleasant Valley fault zone to be 450 m versus 750 m in the Joes Valley fault zone. Unlike the Joes Valley fault zone, which for the most part is composed of two major graben-bounding faults, the Pleasant Valley fault zone consists of several overlapping and roughly parallel faults with comparatively small displacements and short lengths.

Mapping of the geology and structure of the Pleasant Valley fault zone was originally accomplished by Spieker (1931) at a scale of 1:62,500 for the purpose of defining the effect of the faults on the location of coal seams in the Blackhawk formation. Later, Spieker (1946, 1949) studied lateral facies changes in the sedimentary rocks and revised the late Mesozoic-early Cenozoic stratigraphy of the Wasatch Plateau. Further work addressing the stratigraphy of the northern Wasatch Plateau was performed by Walton (1954) based on and pertaining to natural gas drilling in the area. More recently, Witkind and others (1978) compiled a geologic map of the Price 1°x 2° quadrangle (scale 1:250 000) which includes the Pleasant Valley fault zone.

Quaternary deposits with which to evaluate faults are not as abundant in the Pleasant Valley area as they are in the Joes Valley area. Therefore the assessment of the Quaternary activity on the Pleasant Valley faults is based on a comparison of the topographic expression of these structures with those in Joes Valley.

Our investigation of the Pleasant Valley fault zone included the analysis of aerial photographs, geologic mapping in the vicinity of Scofield Dam, and field reconnaissance to assess the possibility of Quaternary faulting.

The study was initiated by viewing aerial photographs of the region containing the Pleasant Valley fault zone, locating mapped faults, and identifying photolineaments. Stereo pairs of black and white aerial photographs were obtained at scales of 1:60 000 and 1:15 840. A map was then compiled which included faults from previously published maps (Spieker, 1931; Witkind and others, 1978) and photolineaments observed on the aerial photographs. Field mapping was then conducted in the vicinity of Scofield Dam and Reservoir in order to clarify the location of faults and their relationship to the bedrock and surficial geology. The resulting maps are presented in plate 3 and figure 5.1.

The Pleasant Valley fault zone contains several north-trending grabens and a southeast-trending graben. The faults differ from those in the

Joes Valley fault zone in that they tend to be curvilinear and shorter in length. These structures will be discussed in order of their significance to Scofield Dam.

## 5.1 Pleasant Valley graben.

The Pleasant Valley graben, the central structure of the Pleasant Valley fault zone and one of the few structures in the Pleasant Valley fault zone that has topographic relief, is an asymmetric graben bounded by the East Pleasant Valley fault on the east and by two parallel and partially overlapping faults on the west referred to in this report as the West Pleasant Valley faults (plate 3). The graben is widest in the central and northern areas, where Scofield Reservoir is located, narrowing to the south until it terminates 8.5 km south of the reservoir.

### 5.1.1 East Pleasant Valley fault

The East Pleasant Valley fault, 1.3 km west of Scofield Dam (plate 3), is the east-bounding fault of the Pleasant Valley graben. At the southern end of the Pleasant Valley graben, both bounding faults die out in the Blackhawk Formation, approximately 300 m thick in this area, showing little topographic relief. The maximum displacement of 400 m on the East Pleasant Valley fault occurs along the section closest to Scofield Dam (Spieker, 1931). The fault in this area is characterized by a 250 m high bedrock esscarpment along the east side of Scofield Reservoir exposing the gently (5°) northeast-dipping rocks of the Blackhawk, Castlegate and Price River Formations.

Geologic mapping at the northern end of the East Pleasant Valley fault was undertaken in order to measure the total length of the fault and to determine its relationship to the Dry Valley graben to the north (Plate 3). The resulting map (figure 5.1) shows that the fault terminates 1.5 km north of Scofield Reservoir (total length is 17 km) since it does not displace rocks of the Castlegate Formation in roadcuts perpendicular to a northerly projection of the fault trace. Near the northern end of the fault, the Castlegate Sandstone is nearly horizontal on both sides of the fault while farther to the south the dip of the beds in the footwall gradually increases to 10°N. The bedrock on either side of the fault in the central area near Scofield Dam is relatively undisturbed with one notable exception: in sec 34-T11S-R7E the bedrock (Castlegate?) in the footwall of the fault is folded in an arch dipping into the fault plane with an attitude of 40°W.

Quaternary deposits consisting of colluvium and alluvium overlie the East Pleasant Valley fault with no evidence for displacement. Alluvial fans occur at the mouths of small canyons that drain into the graben and overlie the fault at some localities. These fans are similar in size, degree of incision, and height above the modern drainages to fans of latest Pleistocene and Holocene age in Joes Valley (Appendix A). The area within and around the margins of the central graben, where one would expect to find Pleistocene alluvial deposits, is covered by Scofield Reservoir, making it difficult to assess the possibility of

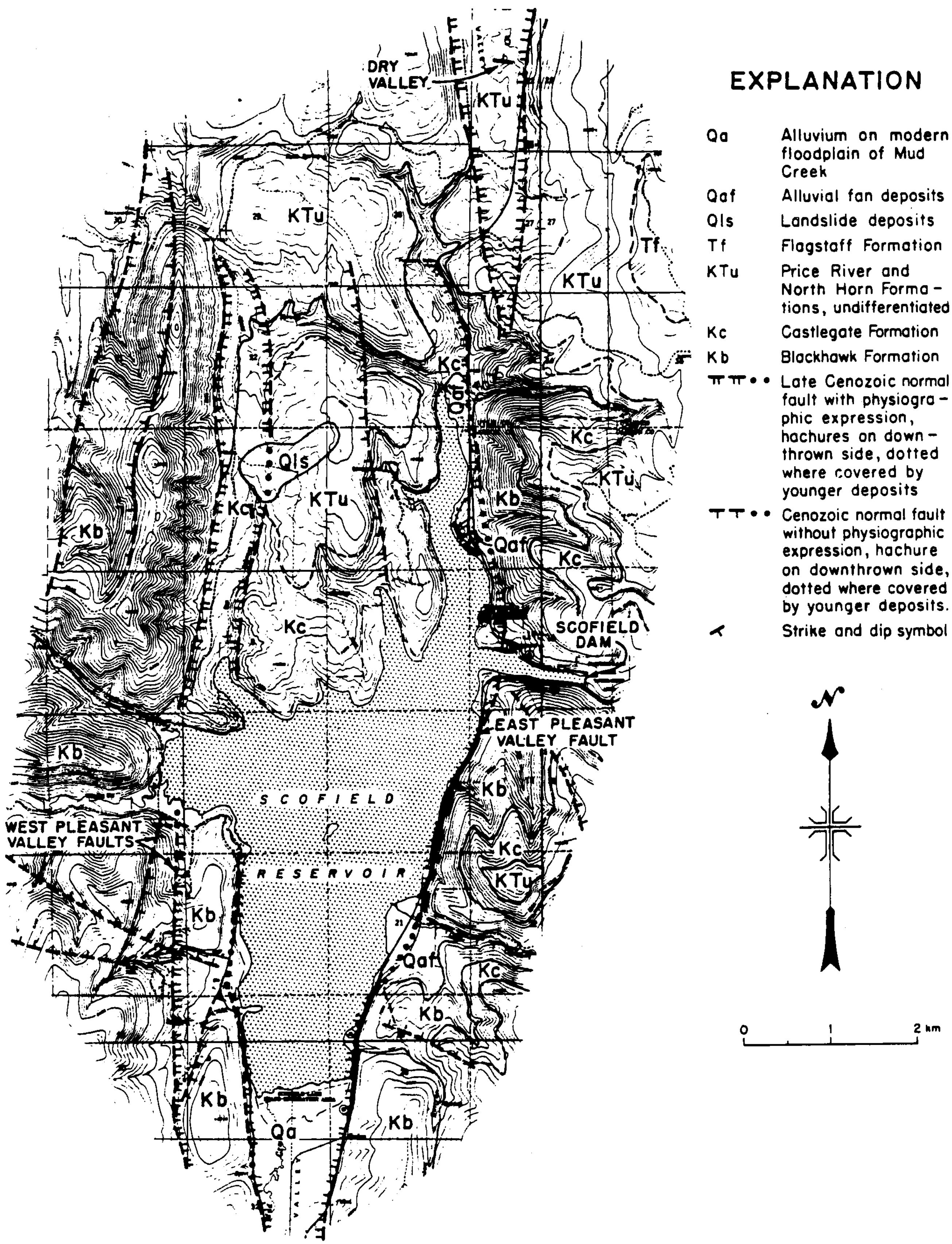


Figure 5.1: Geology in the vicinity of Scofield Dam and Reservoir (mapped by Ed Baltzer). Bedrock units compiled from Spieker (1931).

Quaternary faulting and because the reservoir has existed since 1906, there are no aerial photographs available that show these deposits. Because of the lack of data with which to evaluate Quaternary activity on the East Pleasant Valley fault, its general geomorphic characteristics are compared to those on the Joes Valley faults where data are available (section 4.0). The scarp along the East Pleasant Valley fault is less steep and more eroded than the scarps on the main Joes Valley faults, and as a result appears older than the Joes Valley scarps. The difference could be due to the lower height of the scarp and the composition of the rocks that comprise it since the cliff-forming Castlegate Sandstone crops out higher than in Joes Valley exposing the less resistant Blackhawk Sandstone and Shale in the lower part of the scarp. The degree of incision by creeks flowing perpendicular to the scarp is comparable to Joes Valley.

Although there is no evidence, such as scarps in Quaternary deposits, to indicate recent displacement on the East Pleasant Valley fault, it has similar geomorphic characteristics to Quaternary faults in the Joes Valley fault zone. Although the more eroded appearance of the escarpments may be due to lower slip rates and longer recurrence, displacements possibly as recent as 10 to 20 ka cannot be precluded on the basis of the evidence available.

5.1.2 West Pleasant Valley faults

The west side of the Pleasant Valley graben is bounded by two parallel north-trending faults that overlap for 5 km on the west side of Scofield Reservoir (plate 3) with stratigraphic displacements of up to 310 m in the Blackhawk and Castlegate Formations. The 15 km long southern fault of the pair bounds the southern end of the Pleasant Valley graben and dies out in the Blackhawk Formation 8 km south of the reservoir. The northern fault parallels it for a distance of 5 km, and then continues for another 5 km to the north of the reservoir. Topographic relief on the southern fault is about 450 m on a scarp in the Blackhawk Sandstone and about 250 m on the northern fault. The northern fault is buried by alluvium (Holocene?) on the west bank of the reservoir. There are no fault scarps evident either in this alluvium or on the colluvial slopes on the escarpment.

The West Pleasant Valley faults are similar to the East Pleasant Valley fault in that they form dissected linear escarpments in the Blackhawk Formation and have no direct evidence for surface displacement in late Pleistocene deposits. For the same reasons as the East Pleasant Valley faults, Quaternary displacement cannot be precluded. Because the West Pleasant Valley faults have similar characteristics and closely parallel each other they are treated as a single fault with a combined length of 20 km.

5.2. Dry Valley graben

Immediately to the northeast of Pleasant Valley is the 12 km long Dry Valley graben, a north-trending basin bounded by two faults that converge at the north and south ends. The graben has a maximum displacement of about 200 m in the Price River and North Horn Formations. At the north end of the valley, Flagstaff Limestone crops out in the graben and also caps the North Horn/Price River Formations on both upthrown sides. The North Horn and Price River Formations are undifferentiated on figure 5.1 because they are both relatively thin and difficult to distinguish in this area (Spieker, 1931).

Our field mapping revealed that the East Dry Valley fault is actually located about 500 m west of the bedrock escarpment on the east side of the valley (plate 3). The fault was identified by an abrupt change in dip and a subtle change in lithology (from a coarse sandstone to a fine conglomerate) within the North Horn/Price River Formations. This relationship suggests that considerable erosion of the eastern escarpment has taken place since the principal period of displacement on the fault, suggesting that little or no Quaternary dsplacement has occurred on this fault.

Dry Valley contains very few Quaternary deposits except a thin veneer of colluvium overlying North Horn/Price River deposits within the valley and landslide deposits (Holocene?) covering the scarp on the west side of the graben. No scarps were found in these landslide deposits. Dry Valley is presently drained by a small channel at its south end that flows into Scofield Reservoir (plate 3). A former outlet for Dry Valley appears to be a canyon on the east side that drains into the Price River. In contrast to Pleasant Valley where the major drainage has maintained a course across the graben, in Dry Valley this drainage has been interrupted by the Dry Valley faults and has not incised the graben. This difference could be attributed to a higher slip rate in Dry Valley graben, but is more likely a result of the smaller size of the drainage basin.

Dry Valley is similar to Pleasant Valley in that it is well defined topographically, is bounded by linear escarpments, and has no scarps in Quaternary deposits.

5.3 Other north-trending faults

The Pleasant Valley fault zone includes numerous other north-trending faults which are included on plate 3. These are divided into two groups on the basis of their physiographic expression. The first group is composed of those faults exhibiting little or no topographic expression and small (less than 100 m) total displacements in Cretaceous-Tertiary bedrock. These have been compiled from Spieker (1931) who recognized these structures in coal mine tunnels. This group includes several faults in the southern part of the Pleasant Valley fault zone included on the map on plate 1.

The second group consists of faults recognizable on aerial photographs because of their association with topographic features such as bedrock scarps and linear drainages, although they are less prominent than the Pleasant and Dry Valley faults. These faults have displacements similar to the faults in Pleasant and Dry Valleys (ranging from 100 m to 450 m) although their physiographic expression is less prominent. Quaternary deposits with which to evaluate the age of last movement on these faults are non-existent. Because of their less prominent geomorphic characteristics, this group of faults is considered to be older than the Pleasant and Dry Valley faults.

### 5.4 East-west-trending faults

The Fish Creek fault zone is a zone of faults that trends WNW-ESE through Scofield Reservoir. The relationship between these faults and the Pleasant Valley faults has not been unequivocally resolved although Walton (1954) states that they offset and are therefore younger than the north-trending faults. We found no field evidence to determine which set is younger. These faults generally have small total displacement (less than 200 m, Spieker, 1931) and most lack physiographic expression. This latter characteristic strongly suggests that they are older than the Pleasant Valley faults. Considering the length, amount of total displacement, and apparent relative age of the Fish Creek faults, leads to the conclusion that they are relatively less active than structures in the Pleasant Valley fault zone, if they are indeed active at all in the present tectonic environment.

### 5.5 Pleasant Valley fault zone: summary

The Pleasant Valley fault zone consists of a network of parallel overlapping north-trending normal faults that extends for 50 km from south to north. Many of the faults comprising the Pleasant Valley fault zone do not exhibit topographic relief, presumably a result of small displacement and antiquity. For these reasons they are not considered to be capable of generating large earthquakes. These faults, which displace Eocene rocks, are included on plate 3 as "Cenozoic faults".

The remaining north-trending faults, mapped as "late Cenozoic" on plate 3, are visible as linear scarps in the Cretaceous and Tertiary rocks in the vicinity of Scofield Dam and Reservoir. Due to the scarcity of Quaternary deposits in the Pleasant Valley area, the Quaternary activity rates of these faults are evaluated indirectly on the basis of geomorphic similarities to faults in Joes Valley. The late Quaternary displacement and recurrence rates estimated for the Joes Valley fault zone are consistent with the geomorphic characteristics of these Pleasant Valley faults. However, shorter fault lengths and smaller total displacement suggest smaller magnitude MCE's for the Pleasant Valley faults (see discussion in section 9.3.2).

## 6.0 Snow Lake graben

The Snow Lake graben is a prominent 25 km long north-south trending valley bounded by near vertical 25-45 m high escarpments located on the crest of the Wasatch Plateau 15 km west of Joes Valley Dam (plate 1). Although this narrow valley in the Flagstaff Limestone is incised by streams flowing perpendicular to its length, erosion has not significantly modified the appearance of the graben suggesting that the faulting is relatively recent and, other than thin colluvial deposits at the base of the bounding scarps, Quaternary deposits are rare. Therefore, assessing the Quaternary activity rates of the graben-bounding faults is difficult.

The Snow Lake graben was first mentioned by Spieker and Billings (1940) in their study of glaciation on the Wasatch Plateau. They noted that cirque-like basins along the east side of the plateau crest are beheaded by the East Snow Lake fault and suggested that the graben is therefore a result of post-glacial displacement. The Snow Lake faults are included on geologic maps of the region (Witkind and others, 1982) and are mapped as "suspected Quaternary faults" on the Quaternary fault map of Utah (Anderson and Miller, 1979).

Our work in the Snow Lake graben included a study of aerial photographs and limited field reconnaissance. The review of aerial photographs had the purpose of identifying areas that might contain Quaternary deposits that could elucidate the age of last movement on this structure. Field reconnaissance consisted of estimating the amount of displacement in the Flagstaff Limestone by differentiating stratigraphic units within it and examining sites with possible Quaternary deposits. Unfortunately, these sites contained no more than a thin (<1m) layer of colluvium over the limestone bedrock.

The Snow Lake faults extend for a distance of about 25 km on the crest of the plateau and are characterized by near vertical escarpments 25 to 45 m high in the upper beds of the Flagstaff Formation. A locality where the age and amount of total displacement in the graben can be assessed is at Snow Lake, a small lake for which the graben is named, where the East Snow Lake fault has truncated the head of an east-flowing drainage basin, impounding Snow Lake against the west facing scarp. The original configuration of the drainage basin can be reconstructed and is similar to the unfaulted basins to the north. The drainage basins north of Littles Creek on the east side of the plateau appear to have been glaciated (Spieker and Billings, 1940) because they have U-shaped cross sections and contain deposits inferred to be moraines. Those to the south of Littles Creek, including Snow Lake basin, appear to be nivation basins rather than true cirques because they are wider and shallower than the cirques and the valleys below them are narrow and V-shaped. In any case, the beheaded drainage basin at Snow Lake was probably eroded primarily in the Pleistocene with comparatively minor mass wasting and erosion in the Holocene. The only deposits overlying the East Snow Lake fault at this locality are colluvium at the base of the fault scarp and debris flows and slides at the base of the new headscarp of the basin on the upthrown (east) side of the fault. Total stratigraphic displacement in the flat-lying Flagstaff Limestone at Snow Lake is approximately 75 m and the fault scarp on the east side of Snow Lake is about 30 m high. Therefore the pre-Pleistocene displacement of the bedrock that occurred prior to erosion of the basin is about 45 m. In the absence of any datable deposits in or adjacent to the graben, we assume that some of the 30 m of Quaternary displacement on the East Snow Lake fault is Holocene (<10 ka) because erosion of the basin headwall is presumably primarily Pleistocene in age.

In summary, the Snow Lake valley is a symmetrical graben displacing the upper units of the Flagstaff Formation a total of 75 m and beheading the heads of Pleistocene drainage basins with 30 m of displacement. The scarps that bound the graben are similar to the bounding scarps in Joes Valley in that they are linear, symmetrical, north-trending and near vertical. These characteristics suggest that the Snow Lake graben is structurally similar to the Joes Valley graben although it has formed more recently and appears to have higher slip rates on the bounding faults. The rupture length of 25 km is much less than the Joes Valley fault segments. Because of its distance from Joes Valley Dam (15 km) compared to the Joes Valley graben (1.2 km), the Snow Lake graben, although it must be considered capable of producing large earthquakes, is not considered further in this report.

## 7.0 Gooseberry graben

### 7.1 Introduction

The Gooseberry graben is located near the northwestern margin of the Wasatch Plateau, 15 km west of Scofield Dam and 35 km north of Joes Valley Dam. The graben is part of a 30 km long network of north-trending normal faults that transects the northwestern Wasatch Plateau displacing the Cretaceous and Tertiary rocks from 100 to 450 m. This system of faults parallels the Pleasant Valley system 6 km to the east and the northern end of the Joes Valley system 4 km to the east. The Gooseberry graben is situated near the margin of the Wasatch monocline where the nearly flat-lying sedimentary rocks of the plateau begin to dip west toward the Sanpete Valley.

#### 7.1.1 Previous work

Oberhansley (1980) mapped the Fairview Lakes quadrangle (scale 1:24 000) which includes most of the Gooseberry graben with a focus on the coal, natural gas and petroleum potential of the area. Spieker and Billings (1940) included the Gooseberry area in a study of the glaciation of the Wasatch Plateau and discussed the possibility of Quaternary faulting in the graben. Anderson and Miller (1979) did not include the Gooseberry graben faults on the Quaternary fault map of Utah. The Gooseberry faults are included on the preliminary geologic map of the Price 1°x2° quadrangle (Witkind and others, 1978).

#### 7.1.2 Work by USBR

Our study of the Gooseberry graben included a review of the available literature and maps for the area, a study of color aerial photographs at a scale of 1:19 000, and limited field reconnaissance.

### 7.2 Bedrock geology

The stratigraphy exposed in the vicinity of Gooseberry graben includes, from bottom to top, the Upper Cretaceous Blackhawk, Castlegate, and Price River Formations, the Cretaceous-Paleocene North Horn Formation and the Paleocene Flagstaff Limestone. The total thickness of these nearly flat-lying sedimentary rocks exposed in the vicinity of Gooseberry graben is approximately 1 km (Oberhansley, 1980). With the exception of the Flagstaff Limestone, these rocks are best exposed on the east side of the graben where they form a prominent 300 m high escarpment on the footwall of the East Gooseberry fault. To the west, within the graben, the North Horn and the Flagstaff Formations are on the hanging wall of the fault and are partially covered with glacial deposits and alluvium. The Cretaceous and Tertiary rocks on both the upthrown and downthrown blocks are dipping gently (3°-18°) in a westward direction. To the west of the Gooseberry graben, this westward dip steepens toward the Sanpete Valley forming the Wasatch monocline.

## 7.3 Quaternary deposits

Oberhansley (1980) has differentiated several types of Quaternary deposits on the geologic map of the Fairview Lakes quadrangle. The most significant deposits to an assessment of the activity rates on the Gooseberry faults are the end moraines and alluvial fans that occur along the East Gooseberry fault scarp.

Two terminal moraines are prominent in the Gooseberry area and an assessment of their age is important to an interpretation of the age of last movement on the faults in Gooseberry graben. These moraines are made up of several parallel ridges which are separated into a maximum of four discrete moraines.

These moraines can be compared with those in the northern Joes Valley graben on the basis of their geomorphic position and elevation, hummockiness of the surface, and degree of dissection, in order to estimate their relative age. The Gooseberry moraines extend down two valleys to elevations near 2600 m and have hummocky, irregular surfaces containing numerous kettles. Small ponds are impounded on the inside of the moraines which consist of a series of well-defined sharp-crested ridges. These surface characteristics are consistent with the moraines in Joes Valley which, on the basis of geomorphic and pedologic criteria as well as radiocarbon dates from peat in kettles on their surfaces, are correlated with the Pinedale glaciation in the Rocky Mountains (11-30 ka).

Three alluvial fans are mapped along the base of the East Gooseberry fault scarp (Oberhansley, 1980). These fans are similar in size, gradient, and degree of dissection to fans in Joes Valley that are latest Pleistocene (< 30 ka) and Holocene (< 10 ka). No evidence of surface displacement was found in these alluvial fans during field reconnaissance.

## 7.4 Faults

Superimposed on the gently west-dipping structure of the northwestern Wasatch Plateau are two systems of faults: the faults related to the post-Flagstaff Formation (Eocene) development of the Gooseberry graben and older faults related to the pre-Flagstaff development of the monoclinal flexure to the west (Spieker, 1946). These older faults are visible in roadcuts along the highway between the crest of the plateau and the town of Mt. Pleasant where they juxtapose the Castlegate Formation against the North Horn Formation. The topography in this area does not reflect the position of these faults suggesting that much more erosion has taken place since movement on these faults ceased than has occurred on the Gooseberry faults. Oberhansley (1980) distinguishes four major normal faults: the East and West Gooseberry faults, the Cottonwood Ridge fault, and the Fairview Lakes fault.

The East Gooseberry fault is characterized by a prominent 20 km-long west-facing scarp along the east side of the graben exposing the slightly ($3°$-$8°$) west-dipping sandstones of the Upper Cretaceous units.

These scarps range in height from 180-250 m and, as noted by Spieker and Billings (1940), have disrupted the original drainage pattern by beheading two east-flowing drainages. Gooseberry Creek flows north along the base of the scarp and then flows east, crossing the fault in a narrow 350 m deep canyon incised into the Price River, Castlegate and Blackhawk Sandstones. The East Gooseberry fault scarp was carefully examined both on aerial photographs and in the field for evidence of Quaternary faulting since this scarp has geomorphic characteristics (linearity, near-vertical faces, steep alluvial fans) suggestive of relatively recent activity. Not only are the Quaternary deposits not displaced, but also moraines from the last major glaciation on the Wasatch Plateau (11-30 ka) clearly postdate the beheading of Boulger Canyon by the East Gooseberry fault.

The Fairview Lakes fault, a down-to-the-west normal fault, parallels the East Gooseberry fault 1 km to the west for a total displacement of 450 m on the east side of the graben. At its southern end is a 120 m high west-facing scarp in North Horn rocks which is overlain by the series of moraines that impound Fairview Lakes. As mentioned above, these moraines are correlated with Pinedale (11-30 ka) moraines in Joes Valley. Therefore the most recent movement on the two faults which bound the east side of Gooseberry graben occurred prior to 30 ka.

The Cottonwood Ridge and West Gooseberry faults are two parallel down-to-the-east faults which together define the west boundary of the Gooseberry graben. Total displacement of the Flagstaff and North Horn Formations across these faults is about 100 m (Oberhansley, 1980). These faults do not have the same degree of surface expression as the East Gooseberry fault either because the amount of total displacement is considerably less, or due to the fact that the displacement evident on the surface is entirely within the Flagstaff and more erodible North Horn Formations and the more resistant Cretaceous section is not exposed.

## 7.5 Summary

The Gooseberry graben is the northwesternmost part of a system of north-trending Cenozoic normal faults that transect the Wasatch Plateau. The graben is bounded by two pairs of parallel faults: the East Gooseberry and Fairview Lakes faults on the east and the West Gooseberry and Cottonwood Ridge faults on the west. It is similar to the northern Pleasant Valley fault zone, where Scofield Reservoir is located, in its structural and geomorphic characteristics. The structural similarities include the asymmetry of the graben with the most displacement occurring on the east-bounding faults and the occurrence of sets of parallel faults instead of single bounding faults. The asymmetric nature of the graben is reflected in the geomorphic expression of the bounding faults. The east side of the graben is bounded by a prominent escarpment exposing resistant sandstone stata of the Blackhawk and Castlegate Formations, while the west side of the graben is poorly expressed topographically since the more erodible North Horn Formation is exposed at the surface. The difference in the erodibility of the footwall blocks and the greater displacement on the East Gooseberry fault may account for the younger appearance of the eastern escarpment compared to the escarpment on the west bounding faults.

The Quaternary activity rates of the faults in the Gooseberry graben can be estimated by comparing their geomorphic appearance with faults in the northern Joes Valley graben where more data have been acquired through trenching and geologic mapping. Although they are geomorphically similar, shorter fault lengths and smaller total displacement suggest smaller magnitude MCE's for the Gooseberry faults. Recurrence intervals for surface faulting events in the Gooseberry graben appear to be longer than in Joes Valley because no Quaternary deposits are displaced. The minimum age of last displacement on a major bounding fault is inferred to be 11-30 ka because upper Pinedale moraines overlie it with no evidence for displacement.

## 8.0 Microseismic investigation of the eastern Wasatch Plateau

### 8.1 Previous Work in the BR-CP Transition Zone

As discussed in the section on historic seismicity (sec. 2.3), the operation of the UU (University of Utah) telemetered seismic network has resulted in useful information regarding general patterns of earthquake epicenters and recurrence rates for small-magnitude events occuring in the Utah portion of the ISB. Station spacing within the BR-CP transition zone in central Utah, however, has not been adequate to resolve the finer details of earthquake occurrence, including three-dimensional spatial distribution of earthquake foci and associated source mechanics.

Motivated by increasing interest in the geodynamics of the BR-CP transition zone, and the possible significance of low-angle and listric faults in assessing earthquake hazards in central Utah, the UU has carried out a systematic program of six microearthquake field studies in the transition zone since 1979. These studies have involved temporary arrays of portable seismographs that served to supplement the telemetered network and greatly improved the ability to accurately determine focal depths and reliable focal mechanisms. The primary objectives of this series of field studies were to: 1) determine the subsurface geometry of seismically active faults, 2) correlate diffuse seismicity with geologic structure, 3) determine the relationship between underground coal extraction and shallow seismicity, and 4) investigate the nature of a transitional stress state between the BR and CP provinces. A summary of the results of these studies can be found in Arabasz and Julander (1986). Detailed discussions of the data and subsequent analysis can be found in McKee (1982), McKee and Arabasz (1982), and Julander (1983).

Four of these studies targeted specific sites in the western portion of the transition zone in the following general areas: Goshen Valley; in the vicinity of the southern end of the Wasatch fault; and Sevier Valley. One study was concentrated in the area of active coal mining on the eastern Wasatch Plateau, and the final study covered a broad area including the eastern Basin and Range Province and the Wasatch Plateau.

Numerous attempts have been made to demonstrate a direct relationship between both ongoing background seismicity and mainshock-aftershock sequences and late Cenozoic faults within the ISB (e.g. Westphal, 1963; Westphal and Lange, 1966; Sbar and others, 1972; Langer and others, 1979; Trimble and Smith, 1975; Smith, 1978). Little success has resulted from these efforts, however, and negative results are the rule rather than the exception. These detailed studies across the BR-CP transition zone in central Utah by the University of Utah have also failed to demonstrate more than just a spatial relationship, despite excellent focal depth control and broad focal sphere coverage.

In particular, seismologic observations in Goshen Valley (figures 8.1, 8.2) and further south near the terminus of the Wasatch fault (figures 8.3, 8.4), argue against a simple correlation between well recorded seismicity and the Wasatch fault. Epicenters located west of the Wasatch

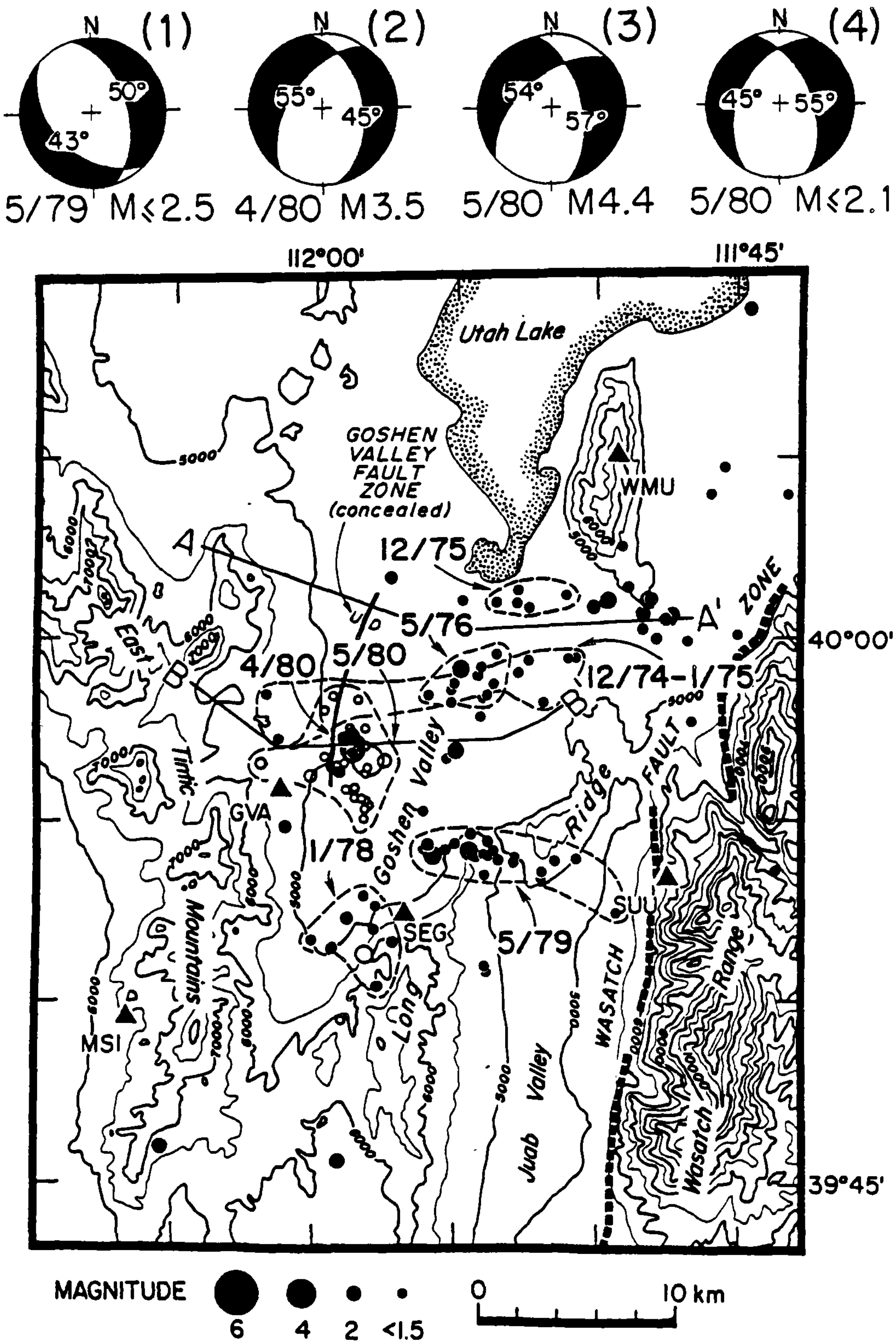


Figure 8.1: Map of Goshen Valley showing representative seismicity (October 1, 1974 - September 30, 1980) and associated focal mechanisms, location of concealed Goshen Valley fault zone (Davis, 1983), and location of cross sections shown in figure 8.2 (from Arabasz and Julander, 1986).

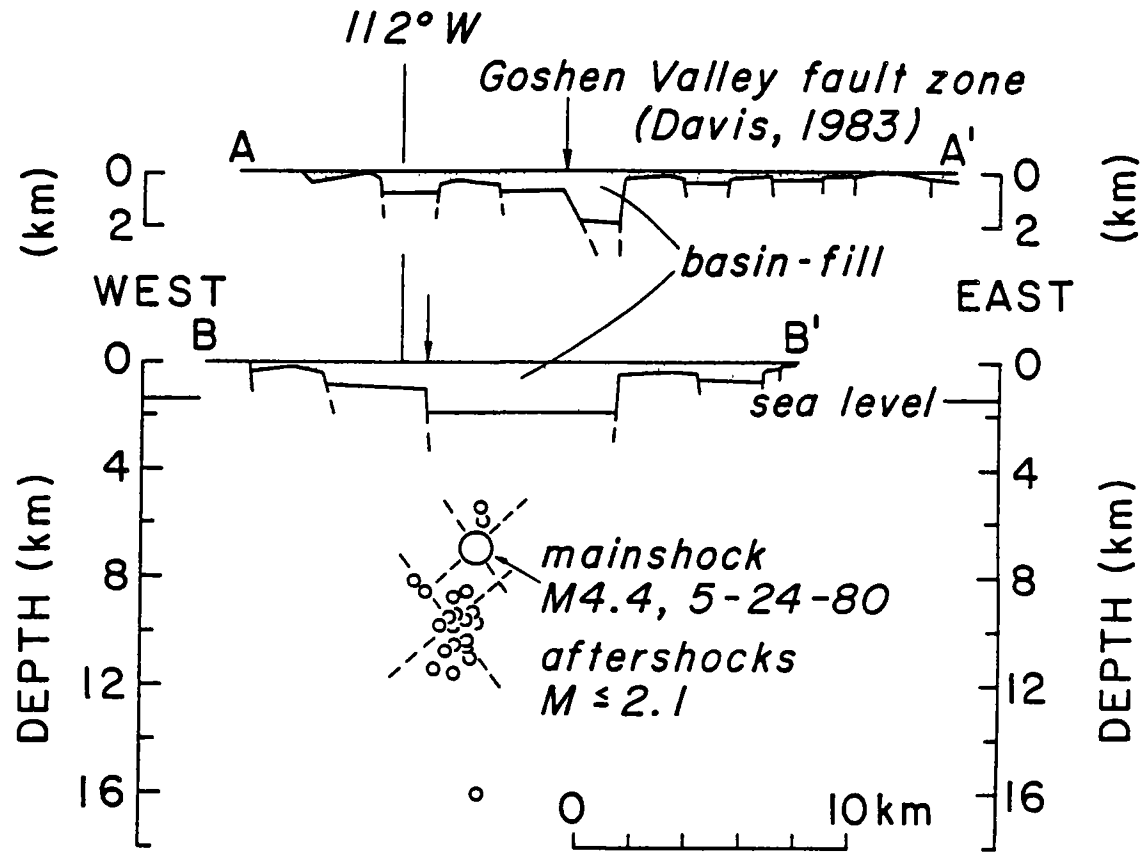


Figure 8.2: Cross sections (keyed to figure 8.1) showing subsurface basin structure interpreted from gravity data by Davis (1983), together with earthquake foci (circles) located by McKee and Arabasz (1982). Datum level is 1,470 m above sea level. Dashed lines are the projection of nodal planes from fault plane solutions 3 and 4 (figure 8.1) (from Arabasz and Julander, 1986).

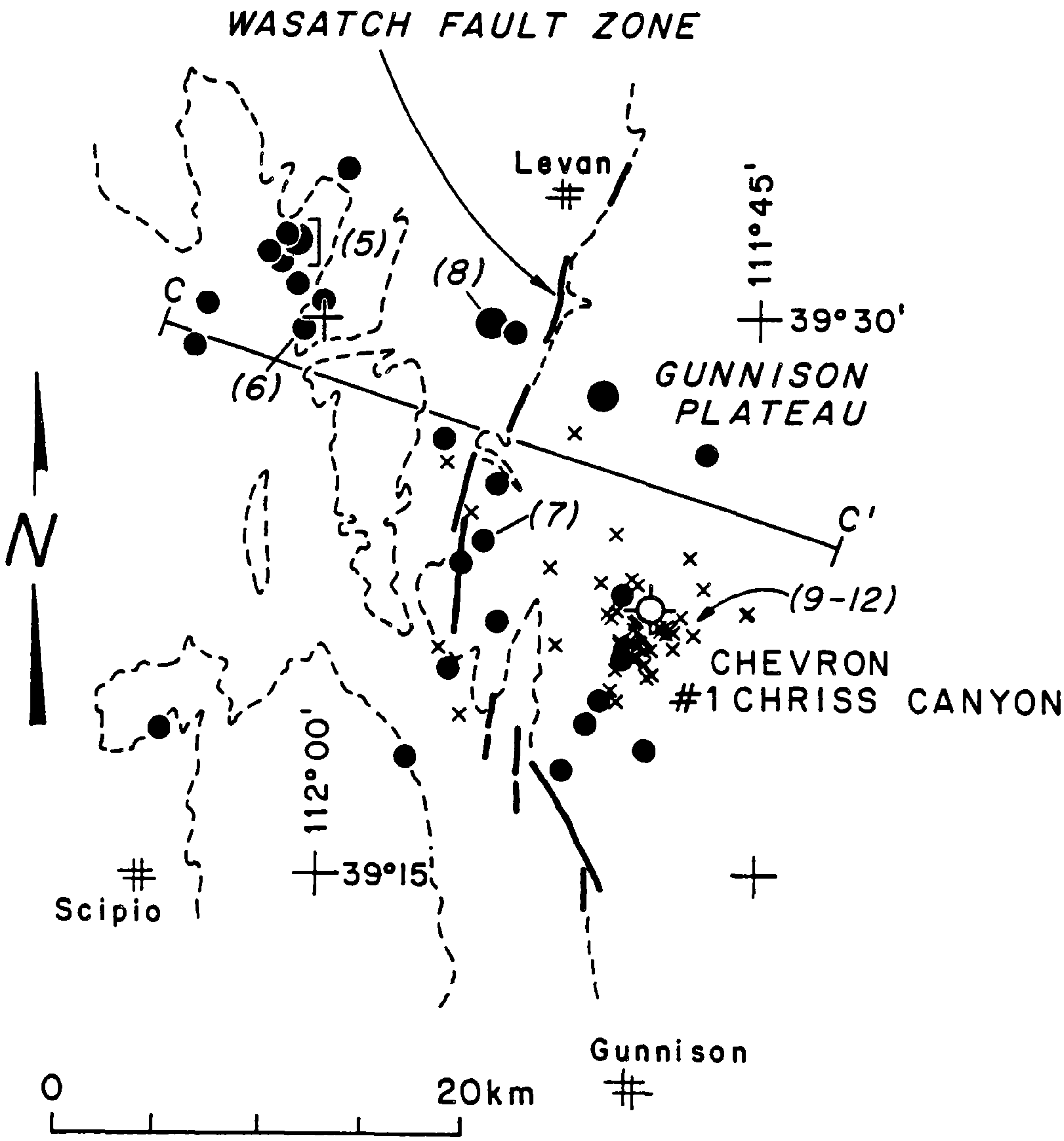


Figure 8.3: Sketch map of southern Wasatch fault zone showing epicenters of earthquakes located in special studies by McKee and Arabasz (1982) (solid circles) and Arabasz (1984) (X's). Magnitudes for smaller circles are less than 1.5; for larger circles, 1.5-1.8; for X's, less than or equal to 2.1. Numbers in parentheses identify earthquakes associated with fault plane solutions from Arabasz and Julander (1986; figure 9) and specially indicated in cross section C-C' (figure 8.4). Mean epicentral precision is 1.23 (+/-0.72) km for the circles and 1.00 (+/-0.84) km for the X's (from Arabasz and Julander, 1986).

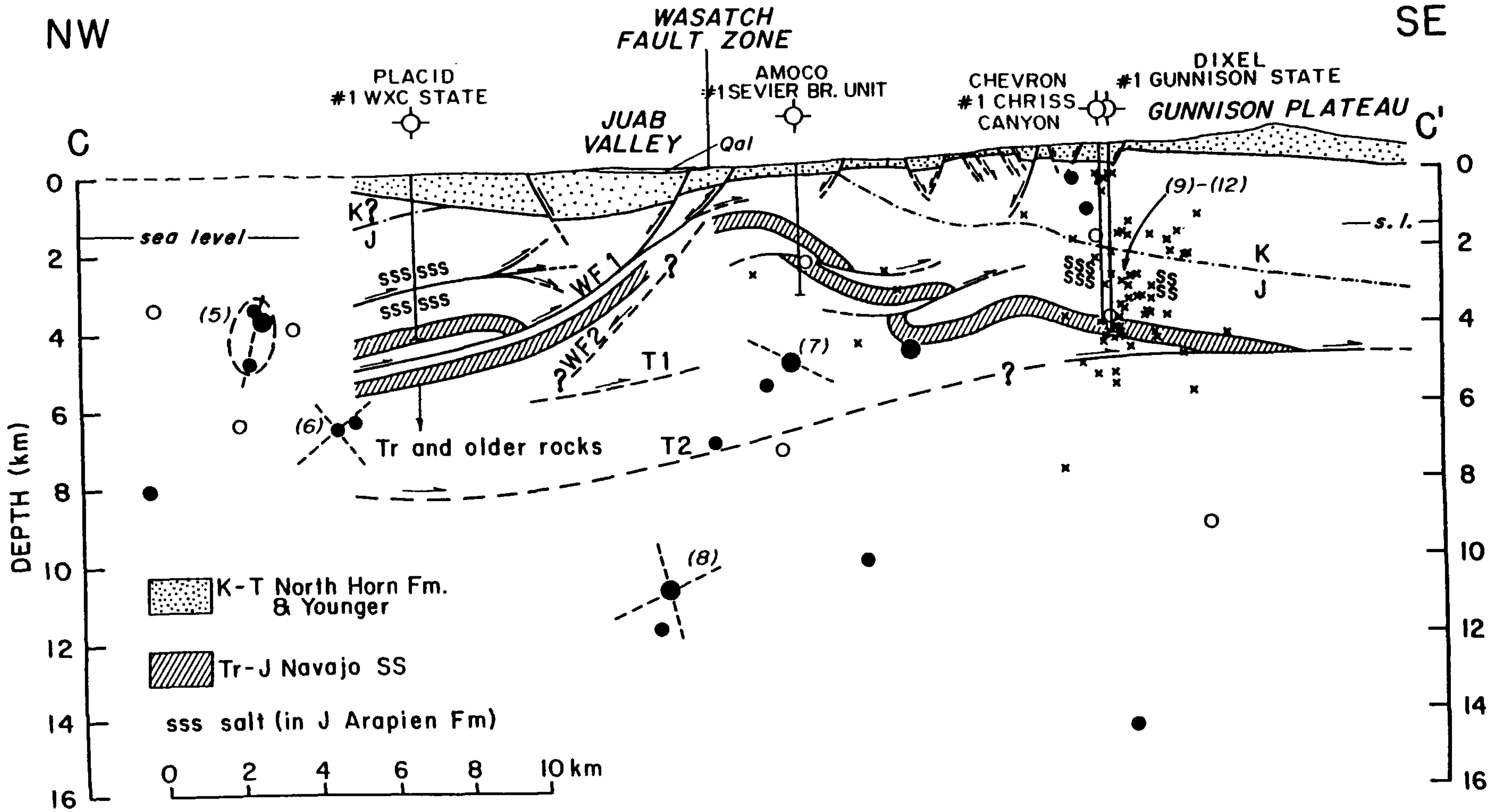


Figure 8.4: Cross section of Arabasz and Julander (1986) (keyed to figure 8.3) showing earthquake foci (located within 14 km normal distance to line of section) superposed upon interpretations of subsurface geology from Standlee (1982), and seismic reflection interpretations from Smith and Bruhn (1984). Foci having depth locations with a standard error exceeding 2.5 km are shown as open circles. Mean focal depth precision for solid circles and X's is 1.47 (+/-0.62) km and 1.39 (+/-1.01) km, respectively. Datum level is 1.47 km above sea level. WF1 and WF2 are respective interpretations of the Wasatch fault at depth by Standlee (1982), and Smith and Bruhn (1984). T1 and T2 are major thrust faults interpreted by Smith and Bruhn (1984). Dashed lines are nodal planes for fault plane solutions of Arabasz and Julander (1986; fig. 9).

fault in Goshen Valley cannot be associated with either a moderate-to-high-angle planar, or low-angle or listric west-dipping Wasatch fault (figure 8.2). In addition, earthquakes spatially clustered near the surface trace of the Wasatch fault do not correlate with the fault at depth (figure 8.4)(Arabasz and Julander, 1986).

Aftershock monitoring of the 1982 M 4.0 earthquake in Sevier Valley and data recorded during 5 weeks of monitoring in 1981 reveal an apparent relationship between an inferred low-angle detachment beneath the transition zone and the depth distribution of microearthquakes. Figure 8.5 shows the epicentral distribution of earthquakes recorded in 1981 and 1982. Figure 8.6 shows the depth distribution of the dense cluster of earthquakes near Elsinore and the 1982 aftershocks southeast of Richfield. The aftershocks cluster in a well defined zone striking about north-northeast beneath the similarly striking surface trace of the Sevier fault. Note that the aftershocks are restricted to depths less than about 4.5 km. This depth coincides with the approximate location of the inferred detachment as determined by seismic reflection data (Smith and Bruhn, 1984; Standlee, 1982). The Elsinore earthquakes cluster near the southern end of the Elsinore fault and similarily suggest an apparent seismicity discontinuity at the approximate depth of the detachment.

Focal mechanisms computed for many of these earthquakes are shown in figure 8.7 and argue against a simple correlation between these earthquakes and the major Sevier and Elsinore faults. Strike slip motion on high-angle faults predominate in this data set and include both right-lateral and left-lateral motion on faults trending north east. Arabasz and Julander (1986) have no fully satisfactory explanation for this observation and believe the right lateral motion to be anomalous and not reflective of the regional stress field. Figure 8.8 summarizes the results of a reconnaissance study conducted in 1979 by McKee and Arabasz (1982) in the East Mountain area of the Wasatch Plateau. Intense spatial clustering of microearthquakes at and beneath the level of active coal mine workings predominated. Some foci were located in the 6 to 16 km depth range. In addition, a composite fault plane solution was computed for 21 earthquakes in the 1.5 to 2.8 km depth range that indicates reverse faulting and northwest-trending nodal planes. This result contrasts sharply with the north-to-northeast-trending, post-Eocene normal faulting mapped at the surface.

Though these detailed studies have failed to directly demonstrate that earthquakes are occurring on major faults, important information about the state of stress in the upper crust across the transition zone for small- to moderate-magnitude earthquakes has resulted from these studies. Data available prior to these more recent studies demonstrated that the contemporary stress field in the Basin and Range province is predominantly east-west extension with earthquakes occurring on moderate- to high-angle north-trending normal faults in response to vertically directed maximum principle stresses (Zoback and Zoback, 1980). The interior of the Colorado Plateau has been shown to be characterized by a compressional stress field with maximum principle

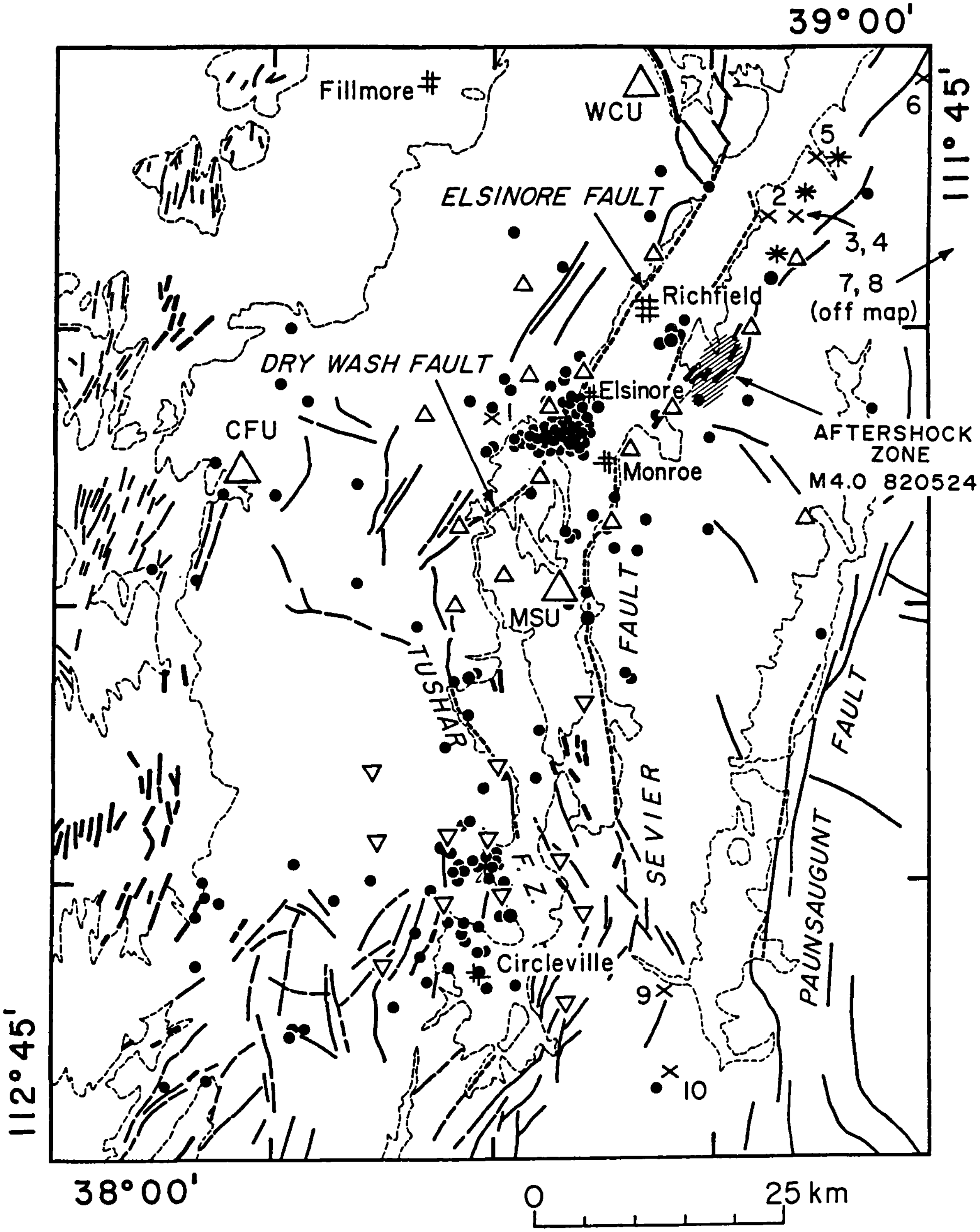


Figure 8.5: Summary map of earthquake field experiments in the Sevier Valley area during 1981 and 1982. Solid circles are epicenters (with mean epicentral precision of 2 km); triangles are seismograph stations (larger ones - permanent stations; smaller ones - temporary stations associated with two separate arrays represented by upright and inverted small triangles). Cenozoic faulting shown by heavy lines (from Arabasz and Julander, 1986).

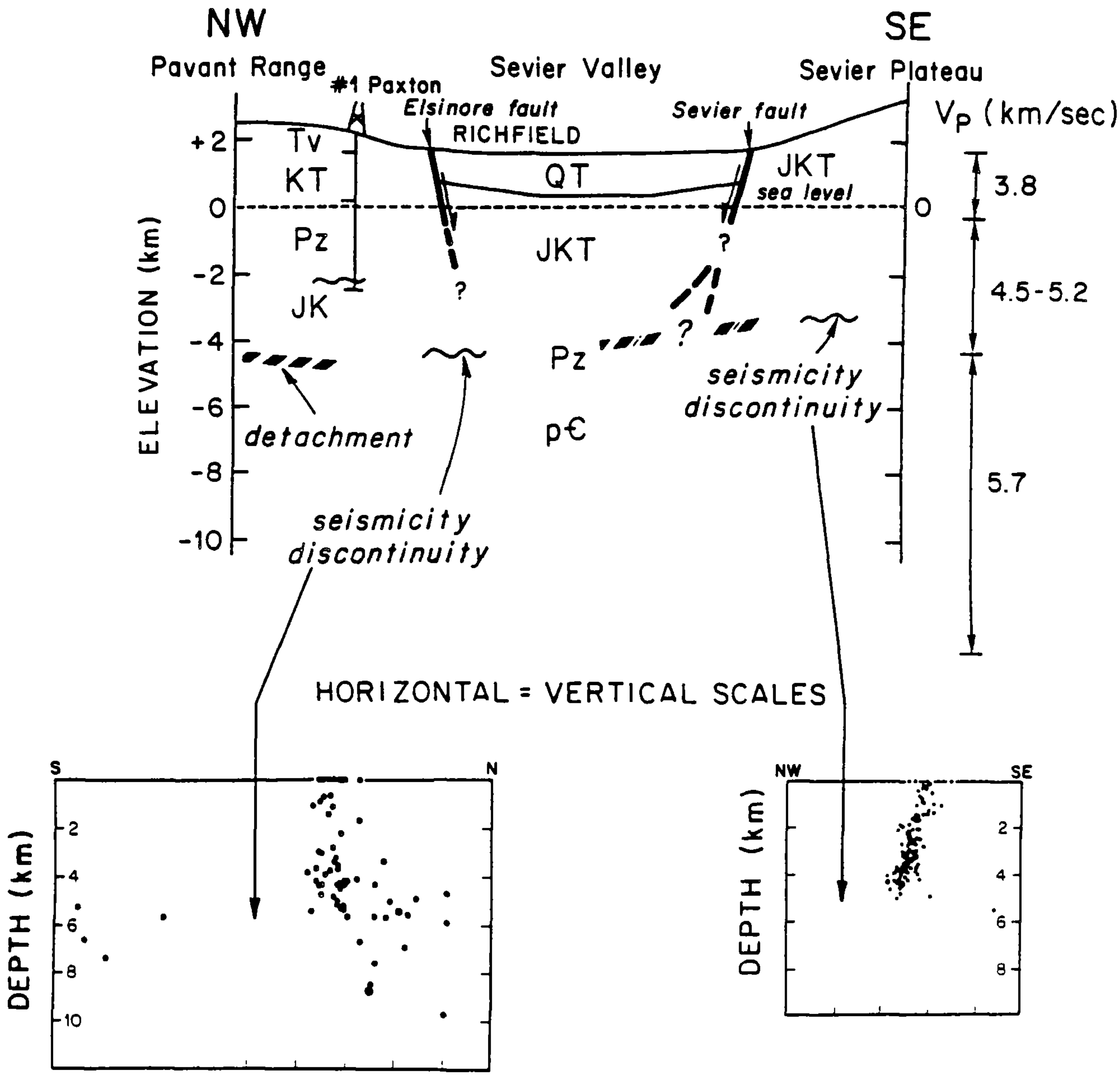


Figure 8.6: Schematic section across the Sevier Valley near Richfield, Utah, illustrating key results from local earthquake studies. Datum for earthquake cross sections is 1,500 m above sea level (from Arabasz and Julander, 1986).

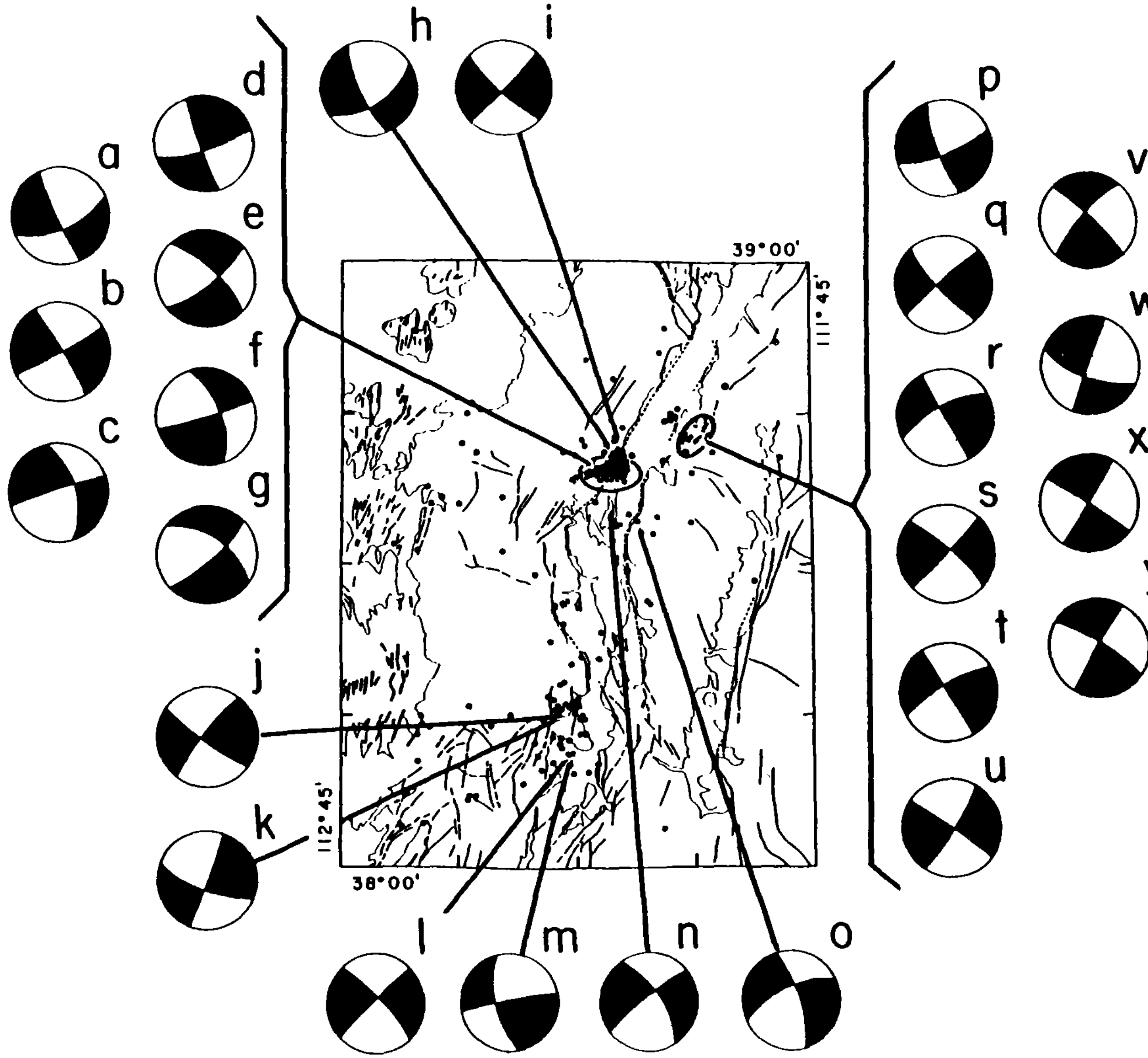


Figure 8.7: Summary of focal mechanisms (lower-hemisphere, compressional quadrants black) determined from studies in the Sevier Valley area during 1981-1982 (from Arabasz and Julander, 1986).

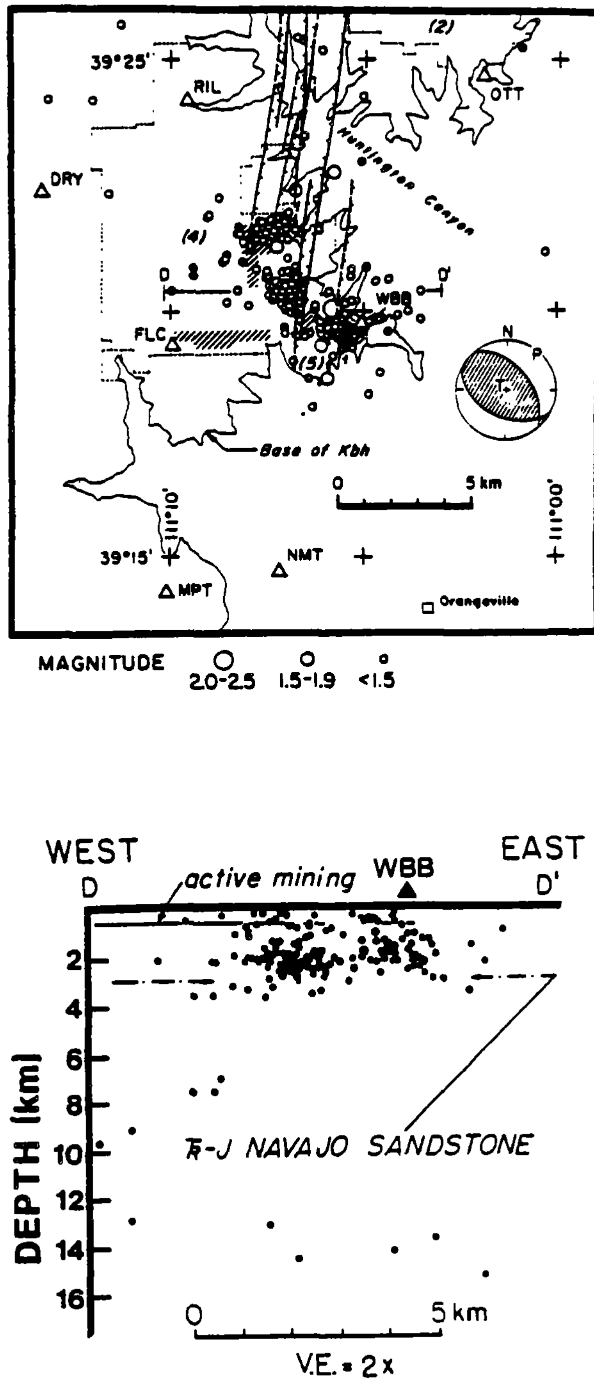


Figure 8.8: Results from reconnaissance earthquake studies in the eastern Wasatch Plateau. Triangles indicate temporary seismograph sites. Open and closed circles - foci shallower and deeper, respectively, than 3.9 km below datum of 2,750 m above sea level. Hachured regions - areas of active underground coal mining during study period. Cross section illustrates location of microearthquake foci with respect to level of active mining and position of Tr-J Navajo Sandstone (from Arabasz and Julander, 1986).

stress in the horizontal plane and directed approximately WNW-ESE (McGarr, 1982).

Figure 8.9 shows the available stress information for the transition zone including the recent work of Arabasz and Julander (1986). Within the transition, the style of faulting, as determined for small- to moderate-magnitude earthquakes from available focal mechanism solutions, changes in an easterly direction from normal to strike-slip to mixed faulting, including compressional reverse faulting (Arabasz and Julander, 1986). Precisely where these changes in upper-crustal stress and preferred mode of faulting occur within the transition zone has not been established.

Arabasz and Julander (1986) have determined that both normal and strike-slip faulting are occurring in the Sevier Valley region. They have also established that compressional reverse faulting is prevalent in the northeast portion of the transition near the active coal mining on the eastern Wasatch Plateau.

Existing data from these prior studies do not establish the current state of crustal stress in the immediate vicinity of the Joes Valley and Pleasant Valley fault systems, leaving open to question whether these normal fault systems are now in a state of horizontal compression, and thus, less likely to generate future large magnitude dip-slip type earthquakes.

## 8.2 1984 Eastern Wasatch Plateau experiment

In the summer of 1984, a multi-institutional microearthquake monitoring program was conducted on the eastern Wasatch Plateau in the vicinity of Joes Valley, East Mountain, and Gentry Mountain. The objectives of this monitoring relative to the seismotectonic study were to: 1) determine the state of stress in the crust beneath Joes Valley, 2) map the depth distribution of earthquakes in the eastern Wasatch Plateau, and 3) determine the relationship between ongoing seismicity and geologic structure.

Up to 40 analog and digital seismographs were operated simultaneously within a 40 by 25 km area by researchers from the USBR, the UU (University of Utah), and WCC (Woodward-Clyde Consultants) (fig. 8.10). Field recording was carried out during a 9-week period between June 21 and August 25, 1986. In order to resolve the fine details of shallow mining-related seismicity, dense seismograph coverage was maintained in the East Mountain area by the UU and in the Gentry Mountain area by WCC. However, broad-aperture network coverage of the eastern Wasatch Plateau was in effect for the period July 6 to August 12, 1984 with the installation of the USBR's instrumentation in and around Joes Valley. During this 38 day period station spacing was everywhere less than 10 km, thus providing an adequate geographic distribution of stations for uniform detection throughout the study area, good azimuthal control for earthquake epicenters, and adequate focal-depth and focal-sphere control for earthquakes that might occur in the 5-15 km depth range.

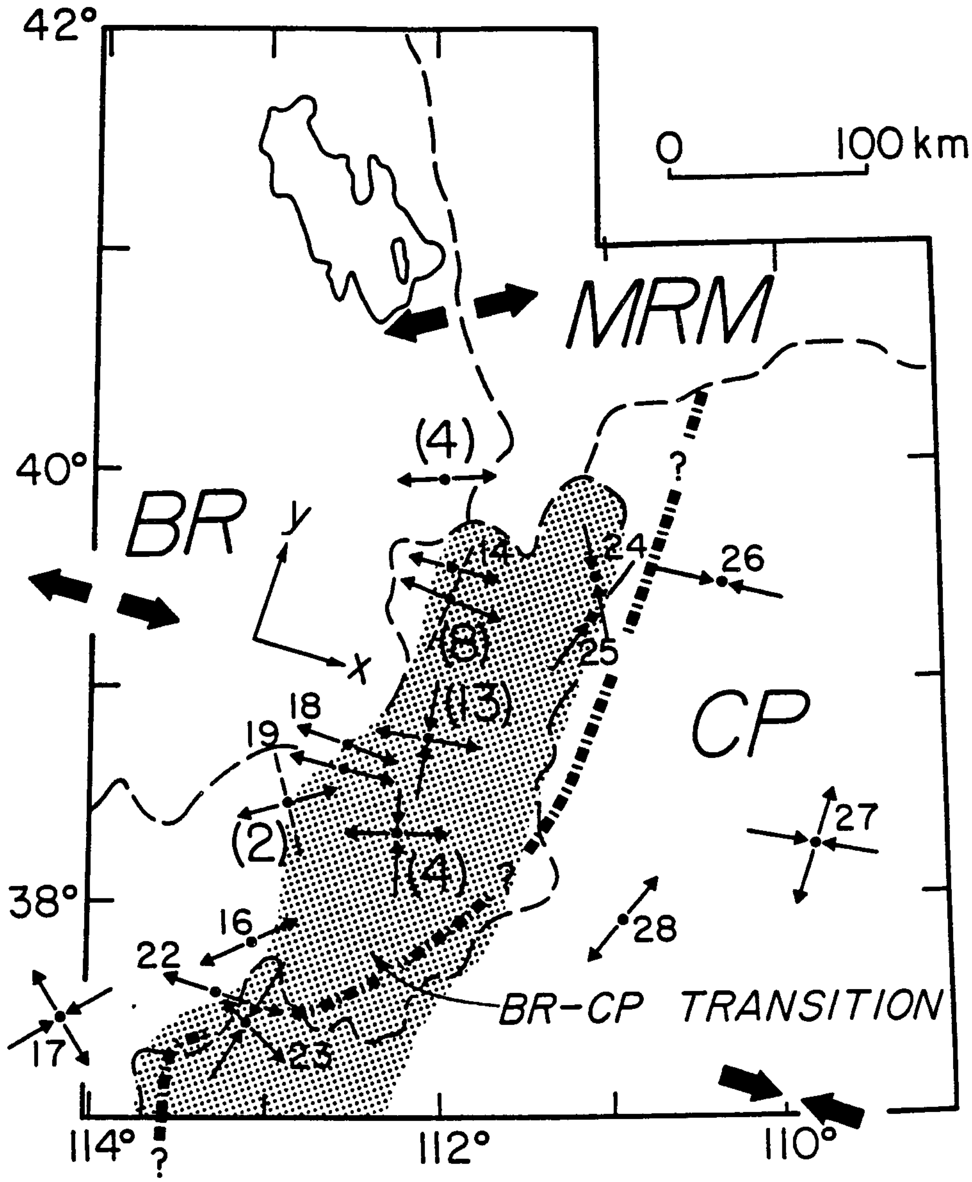


Figure 8.9: Schematic summary of stress-orientation data for the Basin and Range - Colorado Plateau transition zone. Large arrows indicate regional directions of greatest (inward directed) or least (outward directed) principal horizontal compressive stress (from Zoback and Zoback, 1980; Zoback, 1983). Small arrows indicate inferred stress-orientation directions from P and T axes of fault plane solutions: outward directed arrows for normal faulting mechanisms, inward directed arrows for thrust or reverse faulting, a combination of inward and outward directed arrows for strike-slip faulting, and outward directed arrows with perpendicular dashed lines for mixed normal and strike-slip faulting (from Arabasz and Julander, 1986).

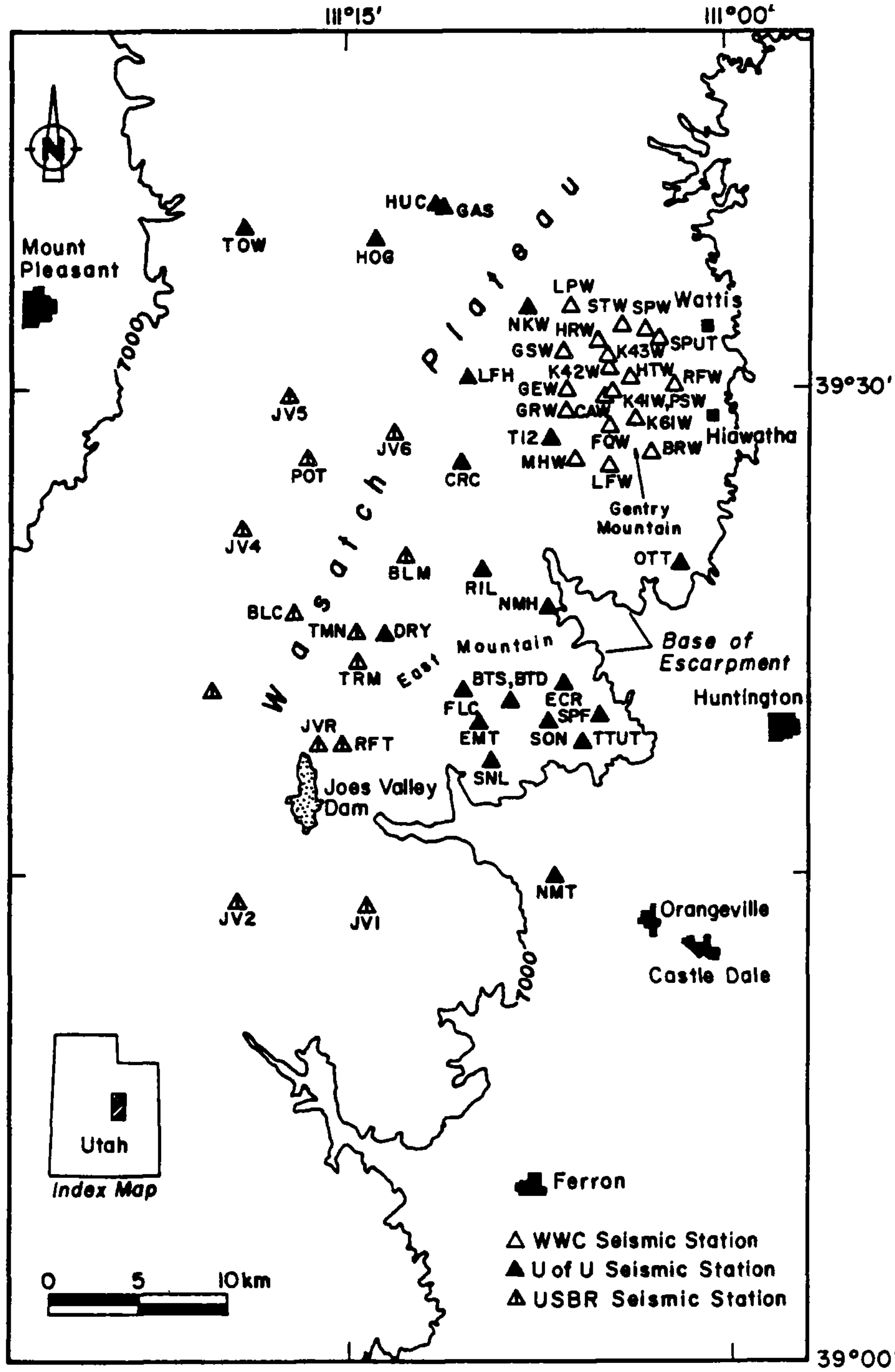


Figure 8.10: Map of seismograph stations (triangles) occupied during the EWP-84 experiment.

The UU was contracted by the USBR to analyze the resulting data from USBR seismographs in conjunction with data recorded by them and WCC for this 38 day period, and provide interpretations relative to the seismotectonics of the eastern Wasatch Plateau based on these data and data from their regional network. The results of this effort will be summarized in the next section. Detailed discussions of these data can be found in Arabasz (1986) and Arabasz and Williams (1986) (see Appendices D and E, this report).

### 8.2.1 Results

Figure 8.11 is an epicenter map summarizing the results of the analysis of 38 days of seismic monitoring in the eastern Wasatch Plateau. A total of 475 seismic events ranging in magnitude from about 0 to 2.1 were located during this recording period. The great majority of earthquakes occurred in the area of active coal mining beneath and near East Mountain. A secondary concentration of epicenters lies within another area of active coal mining near Gentry Mountain. A distinct paucity of seismic activity is noted west of the areas of active mining. Only 16 earthquakes were located in this region despite repeated attempts to identify and locate more events. These earthquakes are numbered on figure 8.12 and corresponding hypocenter summaries are presented in table 8.1.

Table 8.1 Seismic events in western part of EWP-84 study area

| event | yr | date | orig | time | lat-n | long-w | depth | mag | no | gap | dmn | rms |
|---|---|---|---|---|---|---|---|---|---|---|---|---|
| 1 | 84 | 708 | 1825 | 22.58 | 39-22.50 | 111-14.87 | 3.0 | 0.8 | 20 | 127 | 2 | 0.17 |
| 2 | 84 | 713 | 819 | 2.17 | 39-17.53 | 111-11.04 | 0.0 | 0.7 | 14 | 145 | 3 | 0.80 |
| 3 | 84 | 714 | 1901 | 37.94 | 39-13.57 | 111-16.01 | 4.0 | 0. | 3 | 345 | 13 | 0.35 |
| 4 | 84 | 715 | 56 | 10.87 | 39-18.06 | 111-11.43 | 0.1 | 0.4 | 13 | 153 | 3 | 0.15 |
| 5 | 84 | 715 | 607 | 9.06 | 39-17.10 | 111-11.15 | 0.9 | 0. | 7 | 175 | 3 | 0.53 |
| 6 | 84 | 715 | 1222 | 9.70 | 39-19.30 | 111-11.10 | 0.8 | 0. | 5 | 266 | 2 | 0.11 |
| 7 | 84 | 715 | 1601 | 42.79 | 39-18.57 | 111-11.69 | 0.1 | 0.1 | 10 | 100 | 4 | 0.10 |
| 8 | 84 | 717 | 1108 | 39.33 | 39-17.30 | 111-10.31 | 0.8 | 0.1 | 9 | 91 | 2 | 1.69 |
| 9 | 84 | 724 | 1630 | 25.76 | 39-18.17 | 111-10.90 | 5.0 | 0.4 | 12 | 201 | 2 | 0.40 |
| 10 | 84 | 725 | 643 | 17.81 | 39-17.81 | 111-10.84 | 0.9 | 0. | 13 | 96 | 3 | 0.22 |
| 11 | 84 | 730 | 2149 | 0.85 | 39-16.54 | 111-10.72 | 4.0 | 1.3 | 15 | 170 | 6 | 0.20 |
| 12 | 84 | 804 | 39 | 9.38 | 39-16.56 | 111-10.39 | 3.8 | 0.4 | 11 | 174 | 7 | 0.29 |
| 13 | 84 | 806 | 34 | 46.87 | 39-23.79 | 111-15.12 | 4.3 | 1.5 | 26 | 51 | 3 | 0.17 |
| 14 | 84 | 808 | 1543 | 32.93 | 39-17.78 | 111-11.28 | 4.0 | 1.0 | 16 | 167 | 7 | 0.23 |
| 15 | 84 | 809 | 2135 | 2.05 | 39-22.19 | 111-12.05 | 4.0 | 0.6 | 6 | 130 | 5 | 0.56 |
| 16 | 84 | 811 | 220 | 15.60 | 39-13.71 | 111-11.99 | 4.2 | 0.3 | 8 | 288 | 11 | 0.33 |

Events No. 1 and No. 13 in figure 8.12 occur directly within Joes Valley and were recorded by a large number (no) of stations with the closest

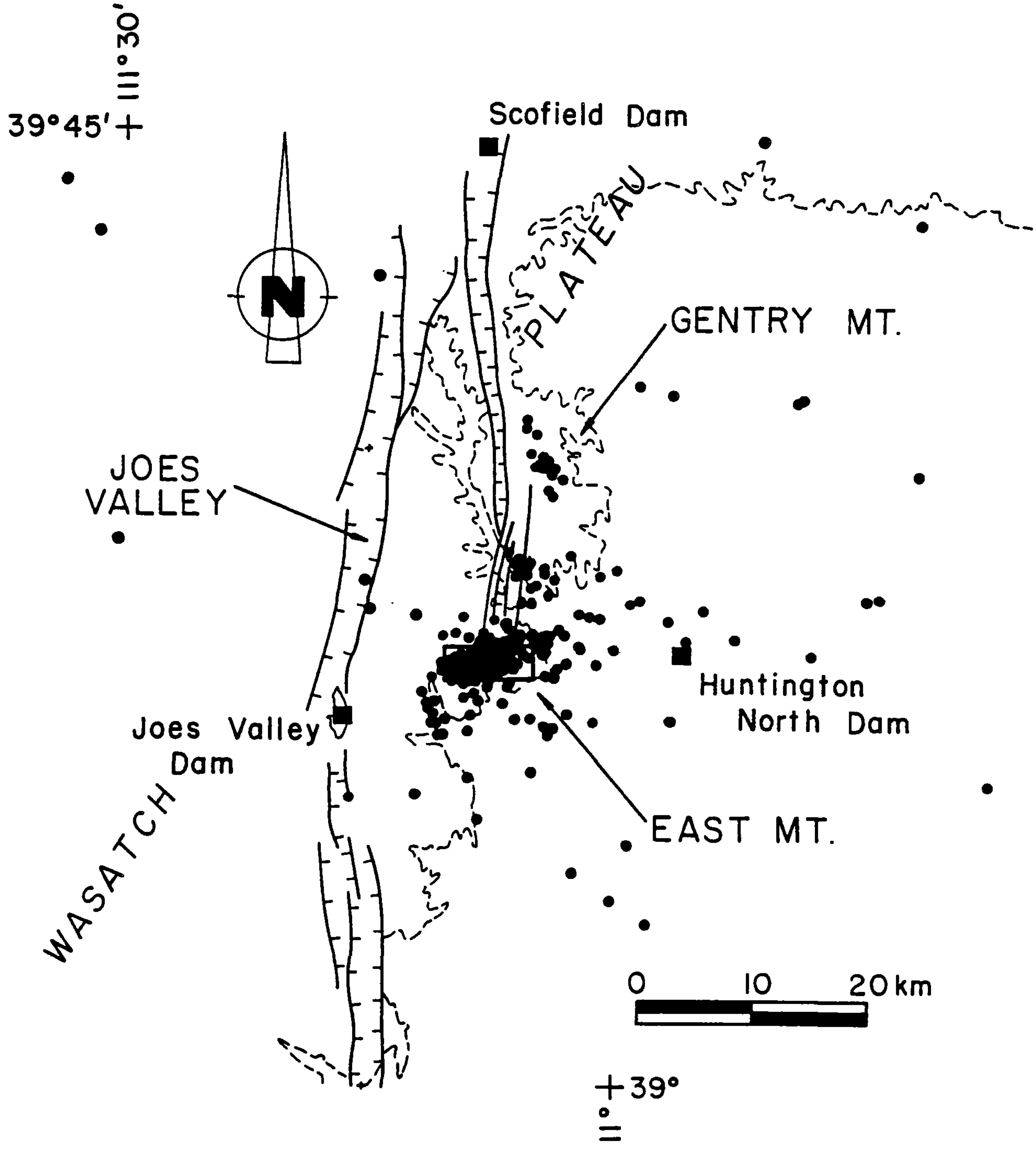


Figure 8.11: Epicenter map of seismic events (solid circles) located as part of the EWP-84 experiment. Joes Valley, Scofield, and Huntington North Dams indicated by solid squares.

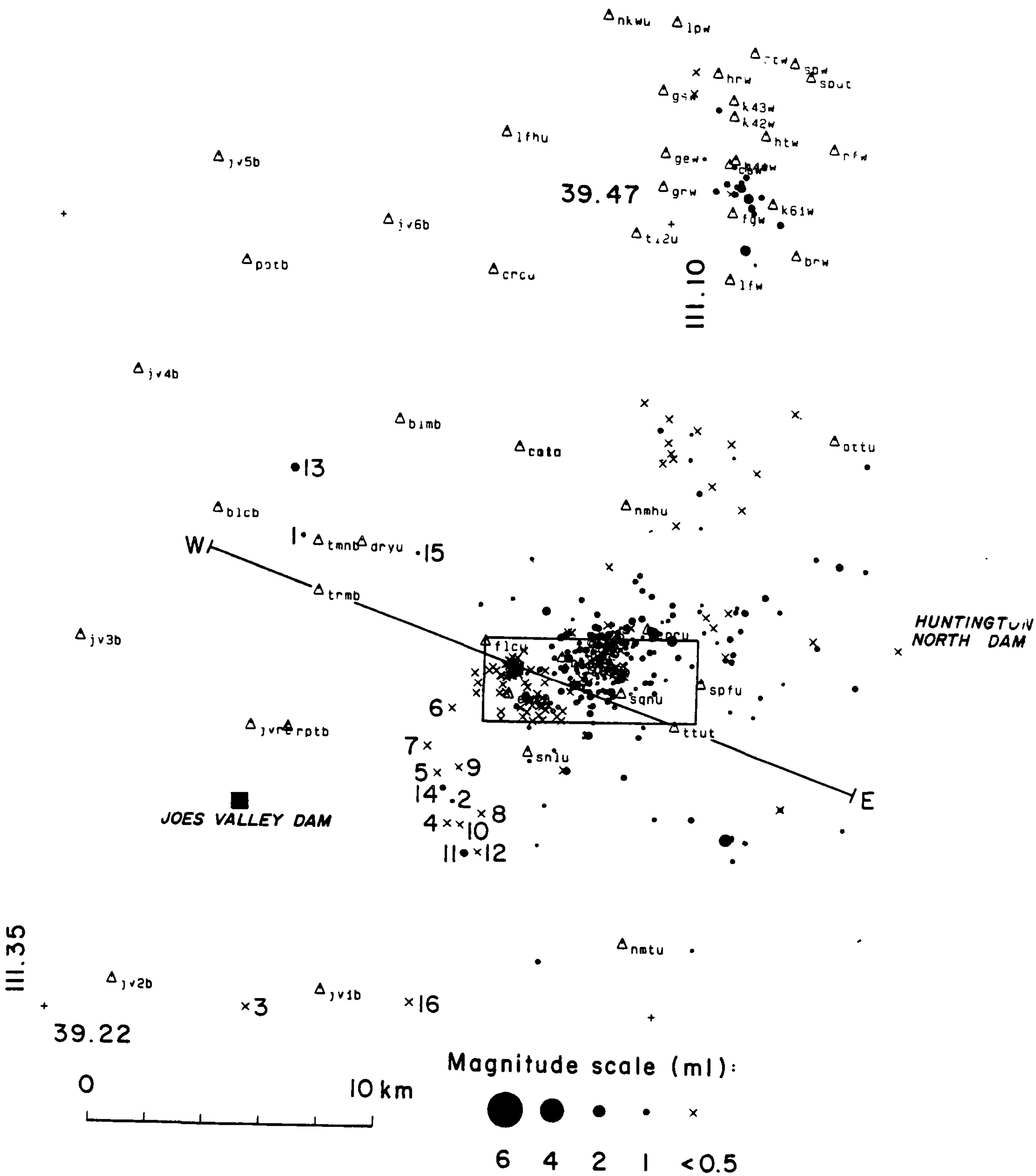


Figure 8.12: Map of station locations (triangles) and epicenters (solid circles and X's) located during the EWP-84 experiment. Special events discussed in text and listed in table 8.1 are indicated by number.

station being less than the computed focal depth (km). Therefore, the computed focal depths of these earthquakes are well constrained and can be assumed to be accurate. Event No. 15, located to the east of station DRYU, is of poor quality and has a relatively large RMS (root mean square) error. Events No. 3 and No. 16, near the southwestern boundary of the array, are also of poor quality and have large azimuthal separations (gap) and large distances to the closest recording station (dmn).

The remaining events, No. 4 through No. 12, are clustered southwest of station SNLU in the vicinity of Cottonwood Creek near an active but small coal mine, and near where a seismic exploration line was shot during the recording period. Though the possibility exists that some of these events may be artificial or mining related, Arabasz and Williams (1986) conclude that this cluster of events include genuine tectonic earthquakes.

Figure 8.13 is an epicenter map of 201 well-located seismic events used for investigation of focal depth distribution and focal mechanisms.

The depth distribution of the 201 foci projected onto the line of section W-E in figure 8.13 is illustrated in figures 8.14a and 8.14b. Two sets of data are shown; figure 8.14a shows all the data and figure 8.14b shows only those foci for which the validity of computed focal depths were critically tested using a procedure outlined in Arabasz and Williams (1986). Figure 8.14a shows a predominance of shallow foci with the majority having focal depths less than 2.0 km; the deepest earthquake occurred at a depth of 4.4 km. Mine level in figure 8.14a is at 0.6 km below datum. The intense near-surface clustering of foci in the vicinity of the active mining in figure 8.14a can not be verified because there generally is inadequate focal depth resolution for these very shallow events. There is, however, adequate focal depth control to verify that earthquakes are indeed occurring below mine level beneath the active mine workings. Figure 8.14b more accurately illustrates the real distribution of earthquakes with depth and indicates well-resolved foci within 1 km below mine level. The two western-most foci in figures 8.14a and 8.14b correspond to events NO. 1 and No. 13 that occurred within Joes Valley. These earthquakes were well-located and indicate that earthquakes are occurring in the vicinity of the Joes Valley faults down to at least 4.4 km.

Fault plane solutions were computed for those earthquakes with well constrained focal depths and adequate focal sphere coverage using both standard P-wave first motion polarity methods and also an amplitude ratio technique. Seventeen single-event solutions and two composite solutions were computed from the well-located data set. The epicenters for these 19 events are indicated in figure 8.13. Thirteen of the best resolved focal mechanisms are shown schematically in figures 8.14a and 8.14b.

The most critical result of these efforts relative to this seismotectonic study is the documentation of contemporary normal faulting in the vicinity of the Joes Valley faults. Focal mechanism solutions No. 1 and

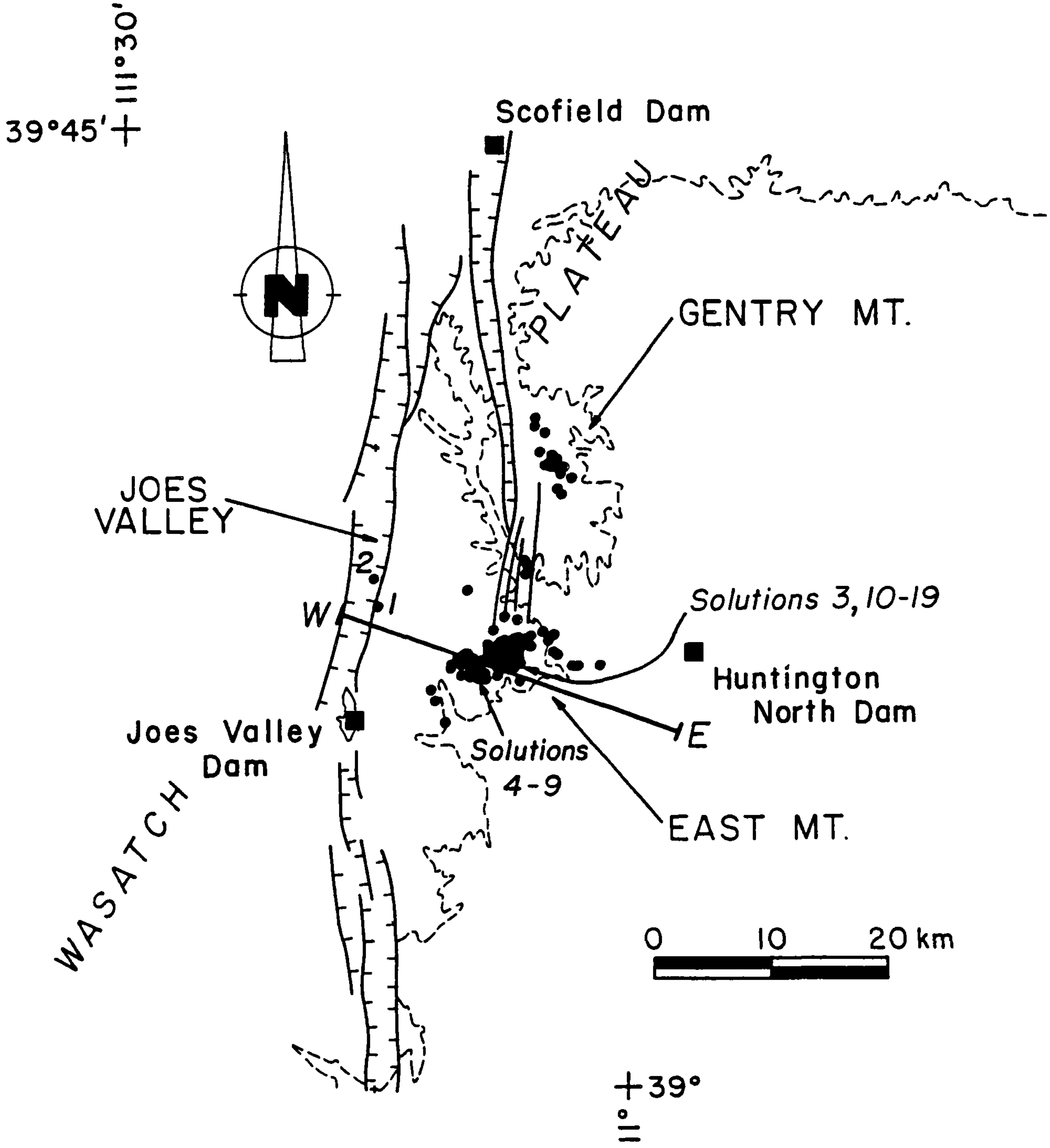


Figure 8.13: Epicenter map of best located earthquakes recorded during the EWP-84 experiment. Specially numbered events and cross section W-E are keyed to figure 8.14. Dams are indicated by squares.

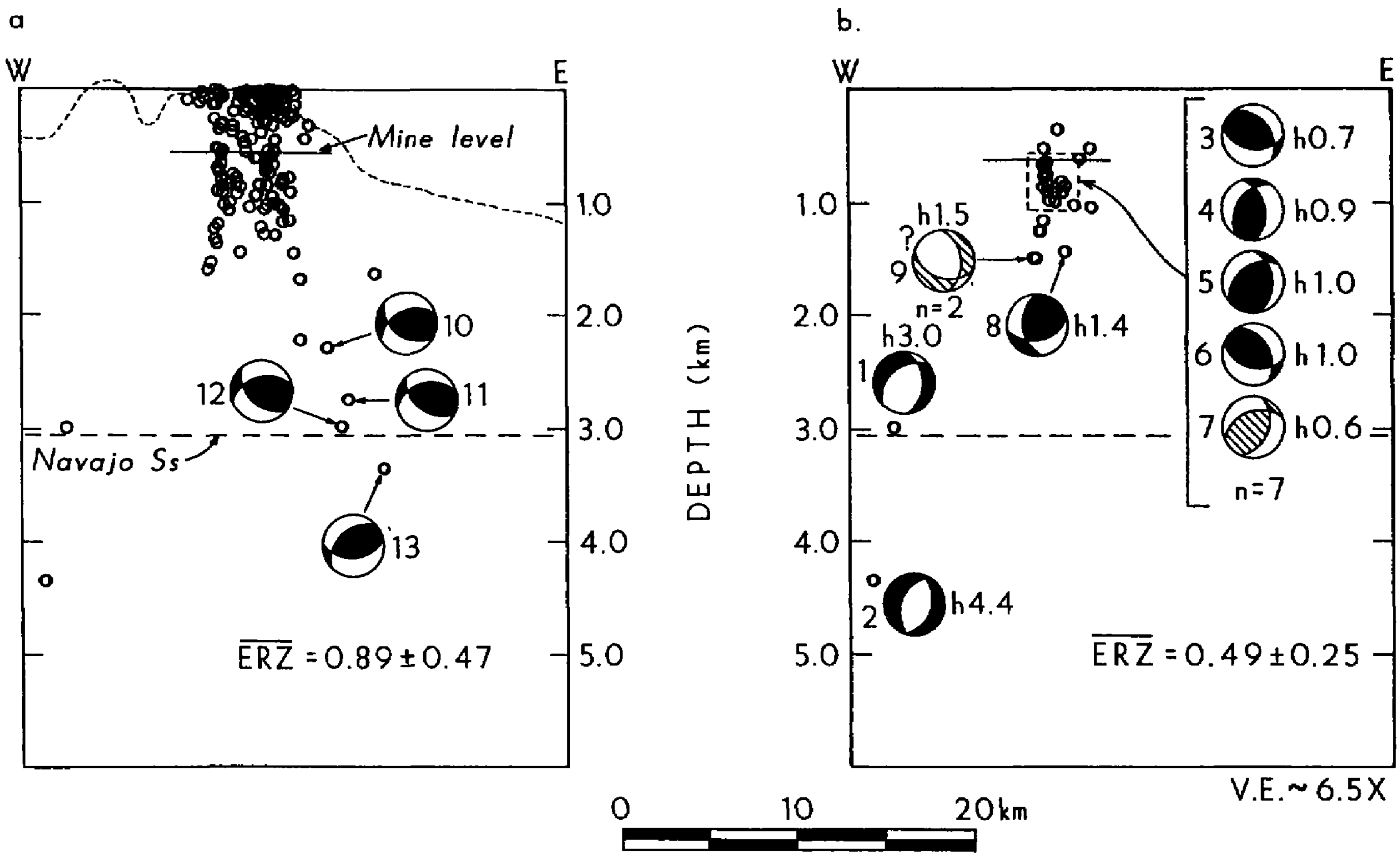


Figure 8.14: Cross section W-E (keyed to figure 8.13) showing depth distribution of foci located within 5.0 km normal distance of line of section. Figure 8.14a shows all earthquakes; figure 8.14b shows only those foci for which the validity of the computed focal depth was critically tested. Numbered fault plane solutions (lower-hemisphere, compressional quadrant black) correspond to numbered events on figure 8.13.

No. 2 (for earthquakes No. 1 and No. 13 from figure 8.12 and table 8.1) demonstrate that these earthquakes occurred in response to nearly pure dip-slip motion on one or more faults that have a general north-south trend. The WNW-ESE orientation of T-axes for these two focal mechanisms is consistent with a mean orientation in the 102°-282° direction of T-axes for fault plane solutions in the BR-CP transition zone west of the Wasatch Plateau. Though it is not possible to unequivocally conclude that these earthquakes occurred on the Joes Valley faults, these data indicate that the current stress field in the vicinity of Joes Valley is characterized by generally east-west extension and not compressional reverse faulting. The inescapable conclusion from these seismologic data, therefore, is that this region is susceptible to further stress release similiar to that which resulted in the formation of the Joes Valley faults and other north-trending normal faults.

To the east, focal mechanism solutions indicate that the extreme eastern Wasatch Plateau is presently within a compressional stress regime, a result consistent with previous work in this area (Arabasz and Julander, 1986). The change in upper crustal stress state from extension to compression must, therefore, occur within the region between Joes Valley and East Mountain.

## 9.0 Fault activity and maximum credible earthquakes

This section summarizes the geologic and seismologic data presented in previous sections and provides MCE's for the major faults on the Wasatch Plateau.

### 9.1 Contemporary tectonics of the Wasatch Plateau

#### 9.1.1 Geologic evidence for late Quaternary normal faulting

Four major fault zones on the northern Wasatch Plateau exhibit characteristics associated with late Quaternary surface faulting: Joes Valley, Pleasant Valley, Snow Lake, and Gooseberry fault zones. Of these four, the northern Joes Valley graben is the only structure with direct evidence, in the form of scarps in upper Quaternary deposits, for recurrent late Quaternary surface displacement. The geologic evidence from the other three structures is equivocal in terms of the age of most recent surface faulting, and therefore general geomorphic comparisons with northern Joes Valley are used to assess Quaternary activity rates on these structures.

##### 9.1.1.1 Joes Valley fault zone

Stratigraphic evidence indicates that the Joes Valley fault zone is a symmetric structure with little net displacement of the Cretaceous-Tertiary bedrock across it. This lack of tectonic displacement combined with a lack of rotation of hanging wall or footwall beds combined with the presence of vertical apparent dips of the fault planes both at the surface and in the reflection sections (discussed in the following section) contrast with late Quaternary normal faults in the ISB (Smith and Bruhn, 1984; Dixon, 1982; Royse and others, 1975) and suggest that the north-trending Wasatch Plateau fault zones may be principally the result of en echelon strike-slip displacement. However, no obvious geomorphic characteristics usually associated with strike-slip faults such as pull-apart basins or shutter ridges are present, and major drainages cross the graben with no evident offset. Although basins such as the one containing Joes Valley Reservoir might be interpreted as pull apart basins, the amount of lateral slip to produce a 1 km deep basin would be in the range of 2-3 km (Aydin and Nur, 1982). This amount of slip would probably result in visible offset of geomorphic features such as alluvial fans or incised drainages. Therefore the mode of relative displacement on the Joes Valley faults is inferred to be predominantly normal.

In the Joes Valley fault zone evidence for late Quaternary surface displacement is limited to faults in the northern part of the Joes Valley graben. Segments of the two main graben-bounding faults, the East and West Joes Valley faults, the Middle Mountain fault, and minor intragraben faults at the northernmost end of the fault zone, exhibit geologic evidence for recurrent late Quaternary surface displacement. The geomorphic characteristics indicative of late Quaternary movement include fault scarps in upper Quaternary deposits, upper Quaternary alluvial fans at the base of the bedrock escarpment, and a linear near-vertical bedrock escarpment. The lengths of the segments exhibiting these characteristics form the basis for estimating the potential length of surface rupture on these faults.

The 42 km long central (Straight Canyon) segment of the East Joes Valley fault is located beneath the reservoir 0.12 km west of Joes Valley Dam. Evaluating this fault segment for late Quaternary activity is difficult since direct evidence is available at only one locality, Scad Valley, where the relationship of the fault scarps in the alluvial fans to the main bedrock escarpment is unclear. Trench data from this locality indicate recurrent events of relatively small displacement in the late Quaternary, with the most recent having occurred prior to 1.5 ka.

The central (Seely) segment of the West Joes Valley fault, 2.5 km west of Joes Valley Dam, is composed of two en echelon sections with a total length of 42 km. Fault scarps are present in upper Pleistocene deposits at the mouths of several east-flowing drainages that cross the fault trace. Field investigation of the West Joes Valley fault included detailed mapping of these scarps and terraces, scarp height measurements, relative age dating of geomorphic features using soil profiles, and the excavation of a trench on the Littles Canyon scarp. These data acquired from five localities along the West Joes Valley fault indicate that approximately 12 m of displacement have occurred in 11-30 ka deposits. Stratigraphic evidence from trench 4 suggests that two surface faulting events, a larger (>5 m) one at about 20 ka and a smaller event prior to 6 ka have occurred on the Seely segment. The presence of 12-14 m high scarps in 11-14 ka moraines on the northern part of the segment suggests that greater Holocene displacements have occurred at the northern end of the Joes Valley graben.

The Middle Mountain fault is a major intragraben fault that extends from Reeder Creek to Scad Valley, a distance of 25 km. En echelon scarps beneath Joes Valley Reservoir are on trend with the Middle Mountain fault and may be an extension of it. Three trenches were excavated on en echelon segments of the Middle Mountain fault and one on a reservoir scarp. Data from these four trenches indicate that two late Pleistocene/Holocene surface faulting events have occurred on the Middle Mountain fault between 14-30 ka and 6.5 ka. The amount of apparent vertical displacement in the earlier event was about 3 m and the later was about 1 m or less.

9.1.1.2 Pleasant Valley fault zone

The Pleasant Valley fault zone consists of a network of curvilinear faults bounding asymmetric graben with vertical displacement of the bedrock usually less than 100 m. This structure differs from that of the Joes Valley fault zone described in the previous section. Two topographically well-defined graben are Pleasant Valley and Dry Valley.

The evidence for late Quaternary surface displacement in the Pleasant Valley fault zone is more difficult to assess than in the Joes Valley fault zone because there are very few deposits of Quaternary age with which to evaluate the Pleasant Valley faults. Many of these faults exhibit no topographic relief. This lack of surface expression is interpreted to be the result of small total displacement and a lack of Quaternary surface displacement.

The rest of the faults in the Pleasant Valley fault zone are visible in the vicinity of Scofield Dam and Reservoir as north-trending linear escarpments in the bedrock. Although there is no evidence in the form of scarps in Quaternary deposits, these faults have similar geomorphic characteristics to faults in the Joes Valley fault zone that have demonstrable Quaternary surface displacement. The faults closest to Scofield Dam that have these characteristics are the East and West Pleasant Valley faults and the bounding faults of the Dry Valley graben.

The East and West Pleasant Valley faults, 1.3 and 4.0 km west of Scofield Dam, respectively, lie beneath the reservoir, and have a maximum of 400 m of vertical displacement in the bedrock (Spieker, 1931), which is about half the amount of the main Joes Valley faults, and are about one third their length (17 km). The bedrock escarpments associated with these faults appear to be more eroded than the Joes Valley fault escarpments, but this may be an artifact of lithologic differences. The presence of upper Pleistocene/Holocene alluvial fans at the base of the escarpments suggests an active tectonic environment although no scarps are evident in deposits that directly overlie the faults.

Dry Valley graben, a 12 km long north-trending basin, is in an east-stepping en echelon pattern relative to the Pleasant Valley graben and, although the amount of vertical displacement (about 200 m) in the Cretaceous and Tertiary bedrock is approximately half that of the Pleasant Valley faults, it is well defined topographically and is bounded by linear escarpments. Quaternary deposits are absent in Dry Valley, a possible indication that this closed basin formed relatively recently and has not had time to fill.

#### 9.1.1.3 Snow Lake and Gooseberry grabens

The Snow Lake and Gooseberry grabens are two prominent structures on the crest of the Wasatch Plateau. The Snow Lake graben is a 25 km long narrow valley with near vertical sidewalls in the Flagstaff Limestone that is 15 km (west) of Joes Valley Dam. Displacement of the Eocene-Paleocene Flagstaff Formation is about 75 m at Snow Lake where the east-bounding fault beheads a Pleistocene cirque-like basin. Quaternary deposits are sparse in the graben rendering it difficult to assess the rate of Quaternary displacement on this structure.

The Gooseberry graben is an asymmetric structure on the crest of the plateau near its northwestern margin. Geomorphically and stucturally, the Gooseberry graben resembles the northern Pleasant Valley graben where Scofield Reservoir is located. The Gooseberry graben has a prominent bedrock escarpment on its eastern margin where the fault has beheaded a subsequently glaciated valley and where total displacement is about 450 m, while it is bounded on the west by two faults, with a combined total displacement of about 100 m (Oberhansley, 1980). Because upper Pleistocene moraines overlie the east-bounding faults with no evidence for displacement, there does not appear to have been Holocene surface displacement as in the northern Joes Valley graben. The minimum age of most recent surface displacement on the most prominent Gooseberry fault is therefore 11-30 ka, the minimum age of the moraines. Due to the structural and geomorphic similarities mentioned above, the suggestion of longer recurrence on the Gooseberry faults may be applicable to the evaluation of the recurrence of surface faulting on the Pleasant Valley faults (discussed in section 9.3).

### 9.1.2 Inferred style of faulting based on seismologic data

Data from seismic monitoring conducted on and/or near the Wasatch Plateau indicate that, with the exception of the region involving active coal mining, the background level of seismic activity is extremely low. Earthquakes are occurring sporadically both in time and space, and the resulting distribution of earthquakes appears diffuse on epicenter maps (fig. 2.8, 2.9, 8.1, 8.3, 8.5, and 8.11). Apparent clustering of epicenters (in northern Joes Valley, for example) reflects cumulative backgound seismicity rather than isolated and intense activity (Arabasz and Julander, 1986). As in other areas of the ISB, the significance of background seismicity on the Wasatch Plateau in relation to tectonic processes is confusing. No conclusive association with geologic structure is possible with the available data. However, certain characteristics of expected future faulting can be inferred from the data.

Seismologic observations resulting from microseismic monitoring conducted as part of this study and from previous studies discussed in chapter 8 demonstrate that, with the exception of the extreme eastern margin, the Wasatch Plateau, and in particular the region including Joes Valley, is currently within a WNW-ESE extensional stress regime. Earthquakes in the small- to moderate-magnitude range are occurring due to predominantly normal dip-slip motion with varying amounts of oblique-slip on northerly trending faults. The degree to which the resulting displacement involves oblique-slip is dependent on the actual strike of the fault and the relative values of the minimum and intermediate principal stresses in the region of the faults. Focal mechanism solutions computed for earthquakes throughout the BR-CP transition zone in central Utah indicate that these normal faults are moderate- to high-angle.

Microearthquake foci have been documented to depths of about 16 km across the Wasatch Plateau, the approximate base of the seismogenic layer of the crust. In Joes Valley, one well recorded microearthquake was located at a depth of 4.4 km placing this earthquake below the Navajo Sandstone and the inferred low-angle detachment. Without evidence to the contrary, it must be assumed that there exists some rupture pathway connecting the surface scarps in Joes Valley with seismogenic depths. The available seismicity data do not confirm the nature of this rupture pathway, but the nodal planes of the focal mechanism solutions computed for the two microearthquakes that occurred beneath Joes Valley are moderate- to high-angle suggesting that the causative faults are not shallow-dipping structures. The spatial relationship of the epicenters to the Joes Valley faults, the northerly trend and moderate-to steep-dips of the computed nodal planes, and the normal-type focal mechanisms all suggest that these earthquakes could have occurred on the Joes Valley faults.

Normal faulting on the Wasatch Plateau has been inferred to be related to westward displacement on a reactivated, formerly east-directed blind thrust in the Arapien Shale above the Jurassic Nugget Sandstone. This inferred low-angle detachment would occur at a depth of 4-5 km below the western Wasatch Plateau and at a depth of about 3 km below Joes Valley (Standlee, 1982; Royse, 1983) implying that these faults do not extend to mid-crustal, seismogenic depths. As verification of this hypothesis would have significant effect on the conclusions of this hazard study, we requested and received permission to review proprietary seismic reflection records across Joes Valley. These data were acquired by CGG (Compagnie Generale de Geophysique) for speculation purposes in the early 1980's and are of very good quality. On the time sections the reflectors are all gently west-dipping including the prominent reflector inferred to be the top of the Navajo Sandstone that is evident on all the lines. The normal faults bounding Joes Valley appear near-vertical on all the sections and clearly interrupt this prominent reflector as well as the rest of the sedimentary section down to a depth of about 5 to 6 km (2.4 sec) below datum (1.7 km above sea level). Data below these reflectors correspond to the basement and are incoherent both below Joes Valley and away from the graben to the east and west. On the more recent, clearer seismic lines, coherent fault blocks can be defined within the Joes Valley graben. Thus the reflection lines provide no evidence that the Joes Valley fault zone is terminated by a horizontal detachment and they indicate that the faults are near-vertical to a depth of at least 5-6 km. Though the faults cannot be traced into the basement, their continuation to depths consistent with that required to generate large, surface-faulting earthquakes (12-15 km) cannot be precluded.

9.1.3 Summary

Based on these seismicity data and the proprietary reflection data, the preferred model of contemporary tectonics for the Wasatch Plateau is the one involving large scarp-forming earthquakes occurring on moderate- to steeply-dipping faults. Therefore, the most likely mode of faulting to be expected in the future would include predominantly normal dip-slip motion with varying amounts of oblique-slip on northerly trending faults. This style of faulting can be expected anywhere on the plateau where the state of crustal stress is predominantly east-west extension including both the Joes Valley and Pleasant Valley fault zones. Seismologic and geologic studies indicate that large-magnitude historical earthquakes in the Basin and Range and ISB occur at the base of the seismogenic zone at focal depths of 12-15 km on 45°-60° dipping normal faults, and are associated with surface ruptures of 1-6 m (section 2). The association of fault scarps in upper Quaternary deposits with the Joes Valley faults is interpreted as evidence that recurrent, large-magnitude earthquakes have occurred on these structures during the late Quaternary.

In the following sections we discuss the recurrence intervals of these scarp-forming earthquakes and assign MCE's to the Quaternary normal faults on the Wasatch Plateau on the basis of geologic evidence.

9.2 Earthquake recurrence estimates from geologic data

Estimates of the recurrence interval of surface faulting earthquakes on the three major faults in the northern Joes Valley graben are based on the interpretation of data from six trenches, relative age dating of upper Quaternary (<150 ka) deposits, and the measurement of scarp heights in datable deposits. Because the available chronologic data are not definitive, and because of the limited number of trenches per fault, the average recurrence interval for each locality is merely a rough estimate of activity on that fault segment relative to other segments.

Data for the West Joes Valley and Middle Mountain faults indicate similar displacement histories and the possibility that the Middle Mountain fault is antithetic to the West Joes Valley fault. The average recurrence interval for these two faults falls within the 10-20 kyr range.

The East Joes Valley fault is difficult to evaluate because only one locality (Scad Valley) yielded chronologic information. The relationship of the Scad Valley scarp to the East Joes Valley fault is ambiguous and the style of deformation on this scarp as observed in trench 6 is unique among the six trenches in the northern Joes Valley graben. Since the symmetry of the graben suggests similar activity rates on the opposing bounding faults and because of the paucity of reliable data pertaining to the displacement history of the east-bounding fault, the recurrence interval inferred for the West Joes Valley and Middle Mountain faults (10-20 kyrs) is applied to the East Joes Valley fault. However, if each of these three major faults were considered as a separate seismic source, then the average recurrence interval for large magnitude surface-faulting earthquakes in the northern Joes Valley fault zone would be reduced to 3-6 kyrs. The trench data indicate that the most recent of these surface rupture events occurred prior to 1-6 ka.

Recurrence intervals are difficult to determine for the bounding faults of the Pleasant Valley graben since there are so few Quaternary deposits exposed in their vicinity. Although the limited data from the Gooseberry graben that suggest longer recurrence intervals for large earthquakes on faults on the northernmost Wasatch Plateau may apply also to the East and West Pleasant Valley faults, a similar displacement history to the Joes Valley faults cannot be precluded. Therefore, because of gross geomorphic similarities and a lack of definitive evidence to the contrary, the average recurrence interval inferred for the northern Joes Valley fault zone is applied to the Pleasant Valley fault zone.

### 9.3 Maximum credible earthquakes

This section provides MCE's (Maximum Credible Earthquakes) for seismic sources on the Wasatch Plateau that are considered to be potentially significant to Joes Valley, Scofield, and Huntington North Dams. Potential rupture lengths on these faults discussed below are estimated on the basis of geologic criteria discussed in sections 4.0, 5.0, 6.0, and 7.0.

#### 9.3.1 Joes Valley fault zone

Although the origin of the normal faults on the Wasatch Plateau remains uncertain, geologic and geophysical evidence suggest that three faults in the Joes Valley fault zone are potential sources of large magnitude earthquakes: the East and West Joes Valley faults and the Middle Mountain fault. Evidence for surface rupture on these faults corresponds in segment length and single event vertical displacement to surface rupture associated with large magnitude (7 - 7-1/2) historical earthquakes in the Basin and Range and the ISB. Seismologic evidence indicates that these historical earthquakes occur at the base of the seismogenic zone with focal depths of 12-15 km. Based on these comparisons, the Joes Valley fault zone is assigned an MCE of $M_S$ 7.5.

#### 9.3.2. Pleasant Valley fault zone

Faults in the Pleasant Valley fault zone inferred to be capable of generating surface-faulting earthquakes are the East and West Pleasant Valley faults and the Dry Valley faults. Because of their smaller total displacement, shorter fault lengths and greater distance from Scofield Dam, the Dry Valley faults are not assigned MCE's. Based on comparisons of estimated length of surface rupture with the Joes Valley faults, and with normal faults in the ISB and the Basin and Range, the Pleasant Valley fault zone is assigned an MCE of $M_S$ 7.0.

#### 9.3.3 Snow Lake and Gooseberry fault zones

Major late Quaternary surface faulting earthquakes on the Snow Lake and Gooseberry faults cannot be precluded from the available data, although the length of these faults suggests smaller magnitude earthquakes than on the Joes Valley faults. For this reason and the relative distance of these structures from the three dams considered in this study, no MCE's are assigned to the the Snow Lake and Goosebery faults.

#### 9.3.4 ISB - random earthquake

As discussed in section 2.4.1, the seismologic data base indicates that within the ISB it is presently impossible to accurately predict the locations of future earthquakes that have magnitudes below the level required to produce surface displacements. Equivocally, it is not possible to predict where these so-called moderate-magnitude earthquakes will not occur. Therefore, for the purposes of hazard assessment in the ISB, it is necessary to include a random or floating earthquake as a potential seismic source. The MCE for this random seismic source is judged to be $M_L$ 6.5 based on the historic record of seismicity which suggests that earthquakes in the ISB must have magnitudes greater than $M_L$ 6.5 to produce measurable surface displacements.

CONCLUSIONS

## 10.0 Conclusions

The following conclusions are based on current understanding of the present tectonic regime of the Basin and Range - Colorado Plateau Transition Zone and the eastern Wasatch Plateau, the historic seismicity of this region, and detailed geologic and seismologic investigations conducted in the vicinity of Joes Valley, Scofield, and Huntington North Dams.

### 10.1 Site specific conclusions for Joes Valley Dam

#### 10.1.1 Maximum credible earthquakes

Maximum credible earthquakes are assigned to the seismic sources that, based on their proximity to Joes Valley Dam, and their inferred capability to generate moderate- to large-magnitude earthquakes, are considered significant to evaluating the safety and stability of the dam and reservoir. The pertinent data are summarized in Table 10.1.

Table 10.1 Maximum credible earthquakes for Joes Valley Dam

| Seismic source | MCE | Closest approach to dam (km) | Focal depth (km) |
|---|---|---|---|
| ISB- random earthquake | 6.5 ($M_L$) | Local | 7-10 |
| Joes Valley fault zone | 7.5 ($M_S$) | 0.12 | 10-15 |

#### 10.1.2 Slope stability

The steep slope along the eastern escarpment of the Joes Valley graben and in Straight Canyon, where the dam is located, are potential sources of landslides and rockfall in the event of seismic shaking. Small landslides have occurred in the colluvium in the dam abutments (USBR, 1983b) and could be remobilized.

#### 10.1.3 Liquefaction

The dam is founded in Blackhawk Formation sandstones and shales with intermittent coal seams overlain by up to 10 m of alluvium in the channel of Straight Canyon and approximately 10 m of colluvium on the abutments. Available records indicate that excavation of the foundation included removing most of these unconsolidated deposits and that the cutoff trench was excavated to bedrock (USBR, 1980b). Though there is no indication that liquefiable deposits exist in the dam foundation, the available information is not adequate to preclude their existence. Further examination of the deposits in the dam foundation is required to resolve this question.

### 10.1.4 Surface faulting in the dam foundation

No faults are located in the dam foundation so surface faulting does not pose a hazard to the stability of the dam.

### 10.1.5 Surface-faulting in the reservoir

Joes Valley Reservoir occupies part of the northern Joes Valley graben where the steeply-dipping East Joes Valley and Middle Mountain faults are beneath the reservoir and the West Joes Valley fault is within 1 km of its western shore. Surface displacements associated with large-magnitude earthquakes on these three faults have the potential to generate waves on the reservior. A similar effect occurred at Hebgen Lake, Montana in association with the 1959 M 7.5 Hebgen Lake earthquake. Surges generated in the Hebgen Reservior by subsidence and surface displacement overtopped Hebgen Dam by as much as 3 m (Myers and Hamilton, 1964). Because we cannot specify the temporal or structural relationships between surface faulting events on the East and West Joes Valley faults, alternate scenarios are presented. Maximum surface displacements for these events are based on trench data from the Littles Canyon site (discussed in section 4.4) on the West Joes Valley fault (2.5 km from Joes Valley Dam) and a comparison to historic earthquakes in the ISB. Based on these data, maximum surface displacements are estimated to be 5.5 m (largest event at Littles Canyon trench) to 6.7 m (maximum subsidence at Hebgen Lake).

Figure 10.1 contains a generalized east-west cross section depicting the spatial relationship between the three major faults and Joes Valley Dam. The structure of the Joes Valley graben is unusual in that normal faults with opposing dips are located within 3 km of each other. In contrast, most historic surface-faulting events have occurred on asymmetric grabens and the widths of areas with significant subsidence in historic events is typically on the order of 5 to 10 km (Gilbert and others, 1983; Myers and Hamilton, 1964). The four scenarios that we include in this assessment attempt to encompass both the unique structure of the Joes Valley graben, and the effects noted in historic earthquakes in the Basin and Range and the ISB. There is no provision for tilting of the downdropped block because geologic evidence from within the graben (Kitzmiller, 1982) suggests only very slight amounts of tilting in an easterly direction. Thus within the reservoir area we would expect predominantly vertical block displacements with negligible tilting and relatively uniform displacements on the bounding faults along the length of the reservoir.

1) The first scenario is that surface displacement occurs simultaneously on both the East and West Joes Valley faults. In this case we would expect normal displacements of up to 5.5 to 6.7 m to occur on both faults along the full length of the reservoir. The net effect of these displacements would be the lowering of most of the reservoir relative to Joes Valley Dam.

2) A second possibility is that surface displacements occur as separate events on either the East or the West Joes Valley faults. Maximum

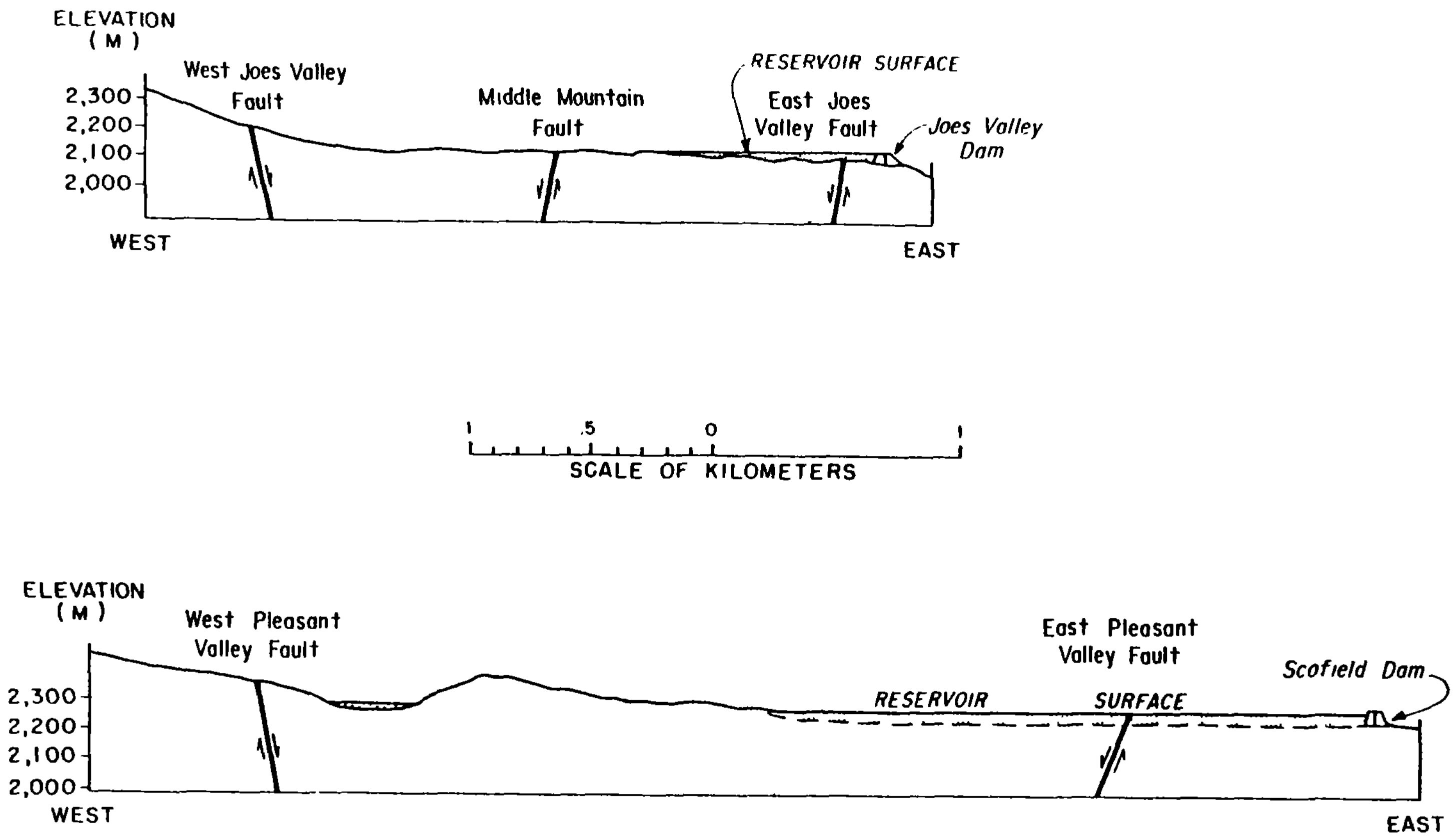


Figure 10.1: Generalized cross-section, showing the location of inferred active faults in relation to Joes Valley Dam and Reservoir (above) and Scofield Dam and Reservoir (below).

single event displacements on either fault would be 5.5 to 6.7 m in a normal sense.

3) The third case is one where surface displacement occurred simultaneously on the opposing West Joes Valley and Middle Mountain faults, a possibility inferred from data from trenches across both faults (discussed in section 4.6). In this event, maximum displacements would be 5.5-6.7 m down to the east on the West Joes Valley and about 3 m down to the west on the Middle Mountain fault. The reservoir would be lowered between the two faults with the possibility of very slight tilting toward the West Joes Valley fault.

4) The fourth possibility is that surface displacement would occur simultaneously on all three faults at once. In this case maximum displacements on the East and West Joes Valley faults would be the same as in case (1) with similar effects. Maximum surface displacement on the Middle Mountain fault would be 3 m.

The nature of waves generated by these displacements is the subject of a separate analysis and is beyond the scope of this report.

10.1.6 Reservoir-induced seismicity

Reservoir-induced seismicity has been empirically related to reservoirs with the following general characteristics: (1) water depth in excess of 92 m, (2) water volume in excess of 1.2 x $10^9$ $m^3$, and (3) active faults in the reservoir (Woodward-Clyde Consultants, 1977). Joes Valley Reservoir, with a maximum water depth of about 57 m and a volume of 7.704 x $10^7$ $m^3$, does not meet the depth or volume criteria. The East Joes Valley fault, however, is a potentially active fault and passes beneath the reservoir just west of the dam. Therefore, the potential for reservoir-induced seismicity exists. In the event earthquakes are induced by the presence of the reservoir, however, we believe they would not exceed the $M_S$ 7.5 MCE proposed for the Joes Valley faults.

10.2 Site-specific conclusions for Scofield Dam and Reservoir

10.2.1 Maximum credible earthquakes

Maximum credible earthquakes are assigned to the seismic sources that, based on their proximity to Scofield dam, and their inferred capability to generate moderate- to large-magnitude earthquakes, are considered significant to the safety and stability of the dam and reservoir. The pertinent data are summarized in Table 10.2.

Table 10.2 Maximum credible earthquakes for Scofield Dam

| Seismic source | MCE | Closest approach to dam (km) | Focal depth (km) |
|---|---|---|---|
| ISB-random earthquake | 6.5 ($M_L$) | Local | 7-10 |
| Pleasant Valley fault zone | 7.0 ($M_s$) | 1.3 | 10-15 |
| Joes Valley fault zone | 7.5 ($M_s$) | 22 | 10-15 |

### 10.2.2 Slope stability

The steep slopes in the canyon where the dam is located are potential sources of landslides and rockfall under seismic loading conditions. A landslide was reported to have occurred in the right abutment in 1952 (USBR, 1984).

### 10.2.3 Liquefaction

The dam is founded in Blackhawk Formation sandstones and shales with intermittent coal seams overlain by about 20 m of alluvium and colluvium. The cutoff trench extends to bedrock. The liquefaction potential of the unconsolidated deposits in the dam foundation under seismic loading should be evaluated.

### 10.2.4 Surface-faulting in the dam foundation

No active faults are located in the dam foundation so surface-faulting does not pose a hazard to the stability of the dam.

### 10.2.5 Surface-faulting in the reservoir

Scofield Reservoir occupies part of the Pleasant Valley graben where the East and West Pleasant Valley faults are beneath the reservoir. Surface displacements associated with large-magnitude earthquakes on these faults have the potential to generate waves on the reservior. A similar effect occurred at Hebgen Lake, Montana in association with the 1959 M 7.5 Hebgen Lake earthquake (Myers and Hamilton, 1964). Surges generated in the Hebgen Reservoir by subsidence and surface displacement overtopped Hebgen Dam by as much as 3 m (Myers and Hamilton, 1964). Because we cannot specify the temporal or structural relationships between surface-faulting events on the East and West Pleasant Valley faults, alternate scenarios are presented. Surface displacements calculated from inferred fault lengths of 17 and 20 km for the East and West Pleasant Valley faults, respectively, are 0.8 and 0.9 m (Bonilla and others, 1984; Slemmons, 1982). A comparison of these inferred fault lengths with faults in the Joes Valley graben where surface displacements of more than 2 m are documented on the 25 km long Middle Mountain fault (discussed in section 4.5) suggests the possibility of greater surface dislacements. Based on these data, maximum surface displacements on the East and West Pleasant Valley faults would most likely be in the 2 to 3 m range.

Figure 10.1 contains a generalized cross section depicting the spatial relationship between the two major faults and Scofield Dam. The structure of the Pleasant Valley graben is unusual in that normal faults with opposing dips are located within 3 km of each other. In contrast, most historic surface-faulting events have occurred on asymmetric graben and the widths of areas with significant subsidence in historic events is typically on the order of 5 to 10 km (Gilbert and others, 1983; Myers and Hamilton, 1964). The scenarios that we include in this assessment attempt to encompass both the unique structure of the Pleasant Valley graben, and the effects noted in historic earthquakes in the Basin and Range and the ISB. The displacements on the bounding faults are relatively uniform along the length of the reservoir.

1) The first scenario is that surface displacement occurs simultaneously on both the East and West Pleasant Valley faults. In this case we would expect normal displacements of up to 3 m to occur on both opposing faults along the full length of the reservoir. The net effect of these displacements would be the lowering of most of the reservior relative to Scofield Dam.

2) A second possibility is that surface displacements occur as separate events on either the East or the West Pleasant Valley faults. Maximum single event displacements on either fault would be 3 m in a normal sense.

The nature of waves generated by these displacements is the subject of a separate analysis and is beyond the scope of this report.

10.2.6 Reservoir-induced seismicity

Reservoir-induced seismicity has been empirically related to reservoirs with the following general characteristics: (1) water depth in excess of 92 m, (2) water volume in excess of $1.2 \times 10^9$ $m^3$, and (3) active faults in the reservoir (Woodward-Clyde Consultants, 1977). Scofield Reservoir, with a maximum water depth of about 17 m and a volume of $9.078 \times 10^7$ $m^3$, does not meet the depth or volume criteria. The East and West Pleasant Valley faults, however, are active faults and pass beneath the reservoir. The potential for reservoir-induced seismicity, therefore, exists. In the event earthquakes are induced by the presence of the reservoir, however, we believe they would not exceed the $M_s$ 7.0 MCE proposed for the Pleasant Valley faults.

### 10.3 Site specific conclusions for Huntington North Dam

#### 10.3.1 Maximum credible earthquakes

Maximum credible earthquakes are assigned to inferred seismic sources in the vicinity of the dam that are considered significant to the safety and stability of the dam and reservoir because of their inferred capability to generate moderate to large magnitude earthquakes. The pertinent data are summarized in Table 10.3.

Table 10.3 Maximum credible earthquakes for Huntington North Dam

| Seismic source | MCE | Closest approach to dam (km) | Focal depth (km) |
|---|---|---|---|
| ISB-random earthquake | 6.5 ($M_L$) | 16 | 7-10 |
| Joes Valley fault zone | 7.5 ($M_S$) | 28 | 10-15 |
| Pleasant Valley fault zone | 7.0 ($M_S$) | 35 | 10-15 |

The ISB has been shown in this report to be characterized by the predominant occurrence of extensional-type, normal faulting earthquakes. The eastern boundary of the ISB is at present, however, ill defined. In the vicinity of East and Gentry Mountains, earthquakes appear to be occurring in response to a compressional stress field. Therefore, a reasonable conclusion is that the eastern limit of the ISB lies west of East and Gentry Mountains. Since an exact boundary cannot be delineated on the basis of seismicity alone, a more reasonable approach is to define the boundary of the ISB based on the easternmost geologic expression of extensional tectonics west of the known compressional stress field. With regard to Huntington North Dam, the epicentral distance of 16 km from the dam to the ISB-random earthquake corresponds to the closest distance to the southern end of the Pleasant Valley fault zone, the easternmost geologic expression of extensional deformation on the Wasatch Plateau within the BR-CP transition zone, and the ISB.

#### 10.3.2 Slope stability

Since the area surrounding the reservoir is relatively flat and of low relief, landslides do not pose a hazard to the dam or reservoir.

10.3.3 Liquefaction

The dam is founded in Mancos Formation siltstone and mudstone with a veneer of silty pediment gravels (USBR, 1983b). The potential of liquefaction of these materials under seismic loading conditions should be studied.

10.3.4 Surface-faulting in the dam foundation

No faults are located in the dam foundation so surface-faulting poses no hazard to the dam.

10.3.5 Surface-faulting in the reservoir

Since there are no active faults located in the reservoir, surface-faulting and resultant waves on the water surface do not pose a hazard to the dam.

10.3.6 Reservoir-induced seismicity

Reservoir-induced seismicity has been empirically related to reservoirs with the following general characteristics: (1) water depth in excess of 92 m, (2) water volume in excess of $1.2 \times 10^9$ $m^3$, and (3) active faults in the reservoir (Woodward-Clyde Consultants, 1977). Huntington North Reservoir, with a maximum water depth of about 17 m and a volume of $6.686 \times 10^6$ $m^3$, does not meet the depth or volume criteria. There are no known active faults passing beneath the reservoir. Therefore, reservoir-induced seismicity is not considered a hazard to Huntington North Dam.

## 11.0 REFERENCES


Allen, C. R., 1968, The tectonic environments of seismically active and inactive areas along the San Andreas fault system, in Dickinson, W. R., and Grantz, A., eds., Proceedings of the Conference on Geologic Problems of the San Andreas Fault System: Stanford, California, Stanford University Publications, Geological Sciences, v. XI.

Allmendinger, R. W., Sharp, J. W., Tish, D. V., Serpa, L., Kaufman, S., Oliver, J., and Smith, R. B., 1983, Cenozoic and Mesozoic structure of the eastern Basin and Range province, Utah, from COCORP seismic reflection data: Geology, v. 11, no. 9, p. 532-536.

Anderson, L. W., and Miller, D. G., 1979, Quaternary fault map of Utah: Long Beach, California, Fugro, Inc., 39 p., 1:1,000,000.

Anderson, R. E., 1971, Thin-skinned distention in Tertiary rocks of south-eastern Nevada: Geological Society of America Bulletin, v. 82, p. 43-58.

Anderson, R. E., and Barnhard, T. P., 1984, Late Cenozoic fault and fold patterns in Sevier County, Utah, and their relationship to seismicity in the area: Geological Society of America Abstracts with Programs, v. 16, no. 6, p. 430.

Anderson, R. E., and Bucknam, R. C., 1979, Map of fault scarps in unconsolidated sediments, Richfield 1° X 2° Quadrangle, Utah: U.S. Geological Survey Open File Report 79-1236, 15 p., 1 pl.

Anderson, R. E., Zoback, M. L., and Thompson, G. A., 1983, Implications of selected subsurface data on the structural form and evolution of some basins in the northern Basin and Range province, Nevada and Utah: Geological Society of America Bulletin, v. 94, no. 9, p. 1055-1072.

Arabasz, W. J., 1986, Interpretation of instrumental seismicity and contemporary tectonics of the eastern Wasatch Plateau relevant to seismic exposure of the Joes Valley and Scofield Dams: Technical Report to U.S. Bureau of Reclamation, Engineering and Research Center, Denver, Colorado.

Arabasz, W. J., and Julander, D. R., 1986, Geometry of seismically active faults and crustal deformation within the Basin and Range - Colorado Plateau Transition in Utah, in Mayer, L., ed., Extensional tectonics of the Basin and Range Province: A perspective: Geological Society of America Special Paper no. 208.

Arabasz, W. J., and Smith, R. B., 1979, Introduction: What you've always wanted to know about earthquakes in Utah, in Arabasz, W. J., Smith, R. B., and Richins, W. D., eds., Earthquake studies in Utah 1850 to 1978, University of Utah Seismograph Stations: Department of Geology and Geophysics, University of Utah, Salt Lake City, Utah, p. 1-14.

---- 1981, Earthquake prediction in the Intermountain seismic belt -- An intraplate extensional regime, in Simpson, D. W., and Richards, P. G., eds., Earthquake Prediction -- An International Review: American

Geophysical Union, Maurice Ewing Series, v. 4, p. 238-258.

Arabasz, W. J., and Williams, D. J., 1986, Analysis and summary of seismographic data recorded in vicinity of Joes Valley Dam, Emery County Project, Eastern Wasatch Plateau, Utah: Technical Report to U.S. Bureau of Reclamation, Seismotectonic Section, Engineering and Research Center, Denver, Colorado.

Arabasz, W. J., Smith, R. B., and Richins, W. D., 1979, Earthquake studies along the Wasatch Front, Utah: Network monitoring, seismicity, and seismic hazards, in Arabasz, W. J., Smith, R. B., and Richins, W. D., eds., Earthquake studies in Utah 1850 to 1978: University of Utah Seismograph Stations, Department of Geology and Geophysics, University of Utah, Salt Lake City, Utah, p. 253-285.

Arabasz, W. J., Richins, W. D., and Langer, C. J., 1981, The Pocatello Valley (Idaho-Utah border) earthquake sequence of March to April, 1975: Seismological Society of America Bulletin, v. 71, p. 803-826.

Armstrong, R. L., 1968, Sevier orogenic belt in Nevada and Utah: Geological Society of America Bulletin, v. 79, p. 429-459.

---- 1974, Magmatism, orogenic timing, and orogenic diachronism in the Cordillera from Mexico to Canada: Nature, v. 247, p. 348-351.

Atwater, T., 1970, Implications of plate tectonics for the Cenozoic tectonic evolution of western North America: Geological Society of America Bulletin, v. 81, p. 3513-3536.

Aydin, A., and Nur, A., 1982, Evolution of pull-apart basins and their scale independence: Tectonics, v. 1, p. 91-105.

Bache, T. C., Lambert, D. G., and Barker, T. G., 1980, A source model for the March 28, 1975 Pocatello Valley earthquake from time-domain modeling of teleseismic P-waves: Bulletin of the Seismological Society of America, v. 70, p. 405-418.

Bachman, G. O., and Machette, M. N., 1977, Calcic soils and calcretes in the southwestern United States: U.S. Geological Survey Open-File Report 77-794.

Baker, A. A., Huddle, J. W., and Kinney, D. M., 1949, Paleozoic geology of the north and west sides of the Uinta Basin, Utah: American Association of Petroleum Geologists Bulletin, v. 33, p. 1161-1197.

Barrientos, S. E., Ward, S. N., Gonzalez-Ruiz, J. R., and Stein, R. S., 1985, Inversion for moment as a function of depth from geodetic observations and long period body waves of the 1983 Borah Peak, Idaho Earthquake, in Stein, R. S., and Bucknam, R. C., eds., Proceedings of Workshop XXVIII on the Borah Peak, Idaho, earthquake: U. S. Geological Survey Open-File Report 85-290, v. A, p. 485-518.

Beutner, E., 1977, Causes and consequences of curvature in the Sevier orogenic belt in Utah and Montana: Wyoming Geological Association

Guidebook, 29th Annual Field Conference, p. 353-366.

Birkeland, P. W., 1984, Soils and Geomorphology: New York, Oxford University Press, 372 p.

Birkeland, P. W., and Shroba, R. R., 1974, The status of the concept of Quaternary soil-forming intervals in the western United States, in Mahaney, W. C., ed., Quaternary Environments, Proceedings of a Symposium: Toronto, Canada, York University Geographic Monograph no. 5, p. 241-276.

Bolt, B. A., 1984, The magnitudes of the Hebgen Lake 1959 and Idaho 1983 earthquakes [abstr.]: Earthquakes Notes, v. 55, p. 13.

Bonilla, M. G., Mark, R. K., and Lienkaemper, J. J., 1984, Statistical relations among earthquake magnitude, surface rupture length, and surface fault displacement: Bulletin of Seismological Society of America, v. 74, p. 2379-2411.

Bucknam, R. C., and Anderson, R. E., 1979, Estimation of fault-scarp ages from a scarp-height-slope-angle relationship; Geology, v. 7, p. 11-14.

Bull, W. B., and McFadden, L. D., 1977, Tectonic geomorphology north and south of the Garlock fault, California, in Doehring, D. O., ed., Geomorphology in arid regions: Proceedings, 8th Annual Geomorphology Symposium, State University of New York, Binghamton, NY, p. 115-138.

Christiansen, R. L. and McKee, E. H., 1978, Late Cenozoic volcanic and tectonic evolution of the Great Basin and Columbia intermontane region, in Cenozoic Tectonics and Regional Geophysics of the Western Cordillera: Geological Society of America Memoir 152, p. 283-311.

Cluff, L. S., Glass, C. E., and Brogan, G. E., 1974, Investigation andevaluation of the Wasatch fault north of Brigham City and Cache Valley faults, Utah and Idaho: A guide to land use planning with recommendations for seismic safety: Oakland, California, Woodward-Lundgren and Associates, 147 p.

Coffman, J. L., Von Hake, C. A., and Stover, C. W., 1982, Earthquake history of the United States: U.S. Department of Commerce.

Colman, S. M., and Pierce, K. L., 1981, Weathering rinds on andesitic and basaltic stones as a Quaternary age indicator, western United States: U.S. Geological Survey Professional Paper 1210, 56 p.

---- 1986, Glacial sequence near McCall, Idaho: Weathering rinds, soil development, morphology, and other relative-age criteria: Quaternary Research, v. 25, no. 1, p. 25-42.

Crone, A. J. and Harding, S. T., 1984, Relationship of late Quaternary fault scarps to subadjacent faults, eastern Great Basin, Utah: Geology, v. 12, no. 5, p. 292-295.

Crone, A. J., and Machette, M. N., 1984, Surface faulting accompanying the

Borah Peak earthquake, central Idaho: Geology, v. 12, p. 664-667.

Das, S., and Scholz, C. H., 1983, Why large earthquakes do not nucleate at shallow depths: Nature, v. 305, p. 621-623.

Davis, G. H., 1978, Monocline fold pattern of the Colorado Plateau, in Matthews, V., III, ed., Laramide folding associated with basement block faulting in the western United States: Geological Society of America Memoir 151, p. 215-234.

Dixon, J. S., 1982, Regional structural synthesis, Wyoming salient of western overthrust belt: American Association of Petroleum Geologists Bulletin, v. 66, no. 10, p. 1560-1580.

Doser, D. I., 1980, Earthquake recurrence rates from seismic moment rates in Utah [M.S. thesis]: Salt Lake City, University of Utah, 163 p.

---- 1984, Source parameters and faulting processes of the August 1959 Hebgen Lake, Montana, earthquake sequence [Ph.D. thesis]: Salt Lake City, University of Utah, 165 p.

Doser, D. I., and Smith, R. B., 1983, Seismicity of the Teton-southern Yellowstone region, Wyoming: Seismological Society of America Bulletin, v. 73, p. 1369-1394.

---- 1985, Source parameters of the 28 October 1983 Borah Peak, Idaho, earthquake from body wave analysis: Bulletin of the Seismological Society of America, v. 75, p. 1041-1051.

Eaton, G. P., 1982, The Basin and Range Province: Origin and tectonic significance: Annual Review of Earth and Planetary Sciences, v. 10, p. 409-440.

Effimoff, I. and Pinezich, A.R., 1981, Tertiary structural development of selected valleys based on seismic data: Basin and Range province, northeastern Nevada: Royal Society of London, Philosophical Transactions, Series A, v. 300, p. 435-442.

Ekstrom, G., and Dziewonski, A. M., 1985, Centroid-moment tensor solutions for 35 earthquakes in western North America (1977-1983): Bulletin of the Seismological Society of America, v. 75, p. 23-40.

Ellis, E. G., 1981a, Geologic map and coal sections of the Ferron Canyon quadrangle, Sanpete and Emery counties, Utah: U.S. Geological Survey Open File Report 81-319.

---- 1981b, Geologic map and coal sections of the Cap quadrangle, Emery county, Utah: U.S. Geological Survey Open-File Report 81-612.

Ellis, E. G., and Frank, J. R., 1981, Geologic map and coal sections of the Mahogany Point quadrangle, Emery county, Utah: U.S. Geological Survey Open File Report 81-718.

Fenneman, N. M., 1931, Physiography of the western United States: McGraw-Hill

Book Company, New York.

Folk, R. L., 1974, Petrology of Sedimentary Rocks: Austin, Texas, Hemphill Publishing Company, 170 p.

Gilbert, J. D., Ostenaa, D., and Wood, C., 1983, Seismotectonic study for Jackson Lake Dam and Reservoir, Minidoka Project, Idaho-Wyoming: Boise, Idaho, and Denver, Colorado, U.S. Bureau of Reclamation, Pacific Northwest Regional Office, and Engineering and Research Center, Seismotectonic Report 83-8, 123 p.

Gile, L. H., Peterson, F. F., and Grossman, R. B., 1966, Morphological and genetic sequences of carbonate accumulation in desert soils: Soil Science, v. 101, p. 347-360.

Godfrey, A. E., 1978, Land surface instability on the Wasatch Plateau, central Utah: Utah Geology, v. 5, no. 2, p. 131-141.

Greensfelder, R. W., Kinter, F. C., and Somerville, M. R., 1980, Seismotectonic regionalization of the Great Basin, and comparison of moment rates computed from Holocene strain and historic seismicity - summary: Geological Society of America Bulletin, Part I, v. 91, p. 518-523.

Gutenberg, B., and Richter, C. F., 1954, Seismicity of the earth and associated phenomena, second edition: Princeton, New Jersey, Princeton University Press, 310 p.

Haimson, B. C., 1981, Hydrofracturing studies, Drillhole DH-101, Fifth water underground powerplant site, Diamond Fork Power system - Bonneville unit, Central Utah Project, Report to the U.S. Bureau of Reclamation, 29 p.

---- 1984, Stress measurements in the Wasatch Hinterland complement existing tectonic and seismic data: EOS, v. 65, no. 45, p. 1118-1119.

Haimson, B. C., and Lee, M. Y., 1985, Stress measurements at the Jordanelle Damsite, Central Utah Project, using wireline hydrofracturing: Report to the U.S. Geological Survey, 34 p.

Hait, M. H., Jr., and Scott, W. E., 1978, Holocene faulting, Lost River Range, Idaho: Geological Society of America Abstracts with Programs, v. 10, p. 217.

Harden, D. R., Biggar, N. E., and Gillam, M. L., 1985, Quaternary deposits and soils in and around Spanish Valley, Utah, in Weide, D. L., ed., Soils and Quaternary geology of the southwestern United States: Geological Society of America Special Paper 203, p. 43-64.

Harden, J. W., 1982, A quantitative index of soil development from field descriptions -- Examples from a chronosequence in central California: Geoderma, v. 28, p. 1-28.

Harden, J. W., and Taylor, E. M., 1983, A quantitative comparison of soil development in four climatic regimes: Quaternary Research, v. 20, no. 3, p. 342-359.

Hayes, P. T., and Sanchez, J. D., 1979, Geologic map and coal resources of the Emery West quadrangle, Emery and Sevier Counties, Utah: U.S. Geological Survey Coal Investigations map C-82, 1:24,000.

Jackson, S. M., 1985, Acceleration data from the 1983 Borah Peak, Idaho, earthquake recorded at the Idaho National Engineering Laboratory, in Stein, R. S., and Bucknam, R. C., eds., Proceedings of Workshop XXVIII on the Borah Peak, Idaho, earthquake: U. S. Geological Survey Open-File Report 85-290, v. A, p. 385-400.

Jackson, S. M., and Boatwright, J., 1985, The Borah Peak earthquake of October 28, 1983 -- strong ground motion: Earthquake Spectra, v. 2, p. 51-69.

Jenny, H., 1941, Factors of Soil Formation -- A System of Quantitative Pedology: New York, McGraw-Hill, 281 p.

Julander, D. R., 1983, Seismicity and correlation with fine structure in the Sevier Valley area of the Basin and Range-Colorado Plateau transition, south-central Utah [M.S. thesis]: Salt Lake City, University of Utah, 143 p.

Keller, G. R., Smith, R. B., and Braile, L. W., 1975, Crustal structure alongthe Great Basin-Colorado Plateau transition from seismic refraction studies: Journal of Geophysical Research, v. 80, no. 8, p. 1093-1098.

Keller, G. R., Braile, L. W., and Morgan, P., 1979, Crustal structure, geophysical models and contemporary tectonism of the Colorado Plateau: Tectonophysics, v. 61, p. 131-147.

Kitzmiller, J. M., II, 1982, Preliminary geologic map of the Joes Valley Reservoir quadrangle, Emery and Sanpete counties, Utah: Utah Geological and Mineral Survey Map no. 67.

Kucera, R. E., 1954, Geology of the Joes Valley and North Dragon Area, Central Utah (M.S. thesis): Columbus, Ohio State University, 185 p.

Langer, C. J., Keller, G. R., amd Smith, R. B., 1979, A study of aftershocks of the October 1, 1972, $m_b$ = 4.7, Heber City, Utah earthquake, in Arabasz, W. J., Smith, R. B., and Richins, W. D., eds., Earthquake studies in Utah, 1850-1978: University of Utah Seismograph Stations, Department of Geology and Geophysics, Salt Lake City, Utah, p. 383-394.

MacDonald, R. E., 1976, Tertiary tectonics and sedimentary rocks along the transition -- Basin and Range province to Plateau and Thrustbelt province, Utah, in Hill, J.G. (ed) Symposium on the Geology of the Cordilleran Hingeline: Rocky Mountain Association of Geologists, 1976 Symposium, p. 281-317.

Machette, M. N., 1985, Calcic soils of the southwestern United States, in

Weide, D. L., ed., Soils and Quaternary geology of the southwestern United States: Geological Society of America Special Paper 203, p. 1-21.

Madole, R. F., 1986, Lake Devlin and Pinedale glacial history, Front Range, Colorado: Quaternary Research, v. 25, no. 1, p. 43-54.

Madole, R. F., and Shroba, R. R., 1979, Till sequence and soil development in the north St. Vrain drainage basin, east slope, Front Range, Colorado, in Ethridge, F. G., ed., Geological Society of America, Rocky Mountain Section, Guidebook for Fieldtrips, 32nd Annual Meeting: Fort Collins, Department of Earth Resources, Colorado State University, p. 124-178.

Madsen, D. B., and Currey, D. R., 1979, Late Quaternary glacial and vegetation changes, Little Cottonwood Canyon area, Wasatch Mountains, Utah: Quaternary Research, v. 12, no. 2, p. 254-270.

Mahaney, W. C., 1978, Late Quaternary stratigraphy and soils in the Wind River Mountains, western Wyoming, in Mahaney, W. C., ed., Quaternary Soils: Norwich, England, Geo Abstracts, p. 223-264.

Malde, H. E., 1971, Geologic investigation of faulting near the National Reactor Testing Station, Idaho, with a section on microearthquake studies by Pitt, A. M., and Eaton, J. P.: U.S. Geological Survey Open File Report 71-338, 167 p.

Martin, R. A., Jr., Nelson, A. R., Weisser, R. R., and Sullivan, J. T., 1986, Seismotectonic study for Taskeech Dam and Reservoir Site, Upalco Unit, and Upper Stillwater Dam and Resevoir Site, Bonneville Unit, Central Utah Project, Utah: U.S. Bureau of Reclamation Seismotectonic Report 85-2.

McCalpin, J. R., Robison, R. M., and Garr, J. D., in press, Neotectonics of the Hansel Valley-Pocatello Valley Corridor, northern Utah and southern Idaho, in Hayes, W. W., and Gori, P., eds., Assessment of regional earthquake hazards and risk along the Wasatch Front, Utah: U.S. Geological Survey Professional Paper.

McGarr, A., 1982, Analysis of states of stress between provinces of constant stress: Journal of Geophysical Research, v. 87, p. 9279-9288.

McKee, M. E., 1982, Microearthquake studies across the Basin and Range-Colorado Plateau transition in central Utah [M.S. thesis]: Salt Lake City, University of Utah, 117 p.

McKee, M. E. and Arabasz, W. J., 1982, Microearthquake studies across the Basin and Range - Colorado Plateau transition in central Utah, in Nielson, D. L., ed., Overthrust Belt of Utah: Utah Geological Association Publication no. 10, p. 137-149.

Myers, W. B., and Hamilton, W., 1964, Deformation accompanying the Hegben Lake eartquake of August 17, 1959, in The Hegben Lake, Montana, earthquake of August 17, 1959: U.S. Geological Survey Professional Paper no. 435, p. 55-98.

National Earthquake Information Service, 1983, Preliminary determination of epicenters, monthly listing: U.S. Geological Survey, October, 1983, 20 p.

National Oceanic and Atmospheric Administration (NOAA), 1985, Earthquake data file: U.S. Department of Commerce.

Nelson, A. R., and Taylor, E. M., 1985, Automated calculation of soil profile development indices using a microcomputer and integrated spreadsheet: Geological Society of America Abstracts with Programs, v. 17, no. 4, p. 258.

Oberhansley, G. G., 1980, Fairview Lakes Quadrangle: Utah Geological and Mineralogical Survey Map no. 56, 1:24,000.

Pardee, J. T., 1926, The Montana earthquake of June 27, 1925: U.S. Geological Survey Professional Paper 147-B, 17 p.

Peterson, R. E., 1979, Tectonic geomorphology of the northern Sangre de Cristo Mountains near Villa Grove, Colorado [M.S. thesis]: Tucson, University of Arizona, p.

Pierce, K. L., 1979, History and dynamics of glaciation in the northern Yellowstone National Park area: U.S. Geological Survey Professional Paper 729-F, 90 p.

---- 1985, Quaternary history of faulting on the Arco segment of the Lost River fault, central Idaho, in Stein, R. S., and Bucknam, R. C., eds., Proceedings of Workshop XXVIII on the Borah Peak, Idaho, earthquake: U.S. Geological Survey Open-File Report 85-290, v. A, p. 195-206.

Pierce, K. L., Obradovitch, J. D., and Friedman, I., 1976, Obsidian hydration dating and correlation of Bull Lake and Pinedale glaciations near West Yellowstone, Montana: Geological Society of America Bulletin, v. 87, p. 703-710.

Porter, S. C., Pierce, K. L., and Hamilton, T. D., 1983, Late Wisconsin mountain glaciation in the western United States, in Wright, H. E., Jr., Late Quaternary environments of the western United States, Porter, S. C., ed., The Late Pleistocene, v. 1: Minneapolis, Minn., University of Minnesota Press, p. 71-111.

Powers, M. C., 1953, A new roundess scale for sedimentary particles: Journal of Sedimentary Petrology, v. 23, p. 117-119.

Proffett, J. M., Jr., 1971, Late Cenozoic structure in the Yerington district, Nevada, and the origin of the Great Basin: Geological Society of America Abstracts with Programs, v. 3, no. 2, p. 181.

Royse, Frank, 1983, Extensional faults and folds in the Foreland Thrust Belt, Utah, Wyoming, and Idaho: Geological Society of America Abstracts, v. 15, no. 5, p.295.

Royse, F., Jr., Warner, M. A., and Reeves, D. L., 1975, Thrust belt structural geometry and related stratigraphic problems -- Wyoming, Idaho, and northern Utah: Rocky Mountain Association of Geologists Symposium -- Deep Drilling Frontiers of the Rocky Mountains, p. 41-54.

Sanchez, J. D., and Brown, T. L., 1983, Stratigraphic framework and coal resources of the Upper Cretaceous Blackhawk Formation in the Muddy Creek and Nelson Mountain areas of the Wasatch Plateau coal field, Manti 30' X 60' Quadrangle, Emery, Sevier, and Sanpete counties, Utah: U.S. Geological Survey Coal Investigations Map C-94-A, 1:24,000.

Sanchez, J. D., and Hayes, P. T., 1979, Geologic map and coal resources of the Flagstaff Peak quadrangle, Emery, Sanpete, and Sevier Counties, Utah: U.S. Geological Survey map C-83, 1:24,000.

Sbar, M. L., Barazangi, M., Dorman, J., Scholz, C. H., and Smith, R. B., 1972, Tectonics of the Intermountain seismic belt, western United States: microearthquake seismicity and composite fault plane solutions: Geological Society of America Bulletin, v. 83, p. 13-28.

Schwartz, D. P., and Coppersmith, K. J., 1984, Fault behavior and characteristic earthquakes -- examples from the Wasatch and San Andreas fault zones: Journal of Geophysical Research, v. 89, n. B7, p. 5681-5698.

Shenon, P.J., 1936, The Utah earthquake of March 12, 1934, (extracts from unpublished report), in Newman, F., United States Earthquakes, 1934: U.S. Coast and Geodetic Survey Serial 4593, p. 43-48.

Shroba, R. R., 1980, Influence of parent material, climate, and time on soils formed in Bonneville-shoreline and younger deposits near Salt Lake City and Ogden, Utah: Geological Society of America, Abstracts with Programs, v. 12, no. 6, p. 304.

Shroba, R. R., and Birkeland, P. W., 1983, Trends in late-Quaternary soil development in the Rocky Mountains and Sierra Nevada of the western United States, in Porter, S. C., ed., Late Quaternary Environments of the United States, the Late Pleistocene: Minneapolis, University of Minnesota Press, p. 145-156.

Slemmons, D. B., 1982, Determination of design earthquake magnitudes for microzonation, in Proceedings, Third International Earthquake Microzonation Conference: Seattle, v. 1, p. 119-130.

Smith, R. B., 1977, Regional geophysics and intraplate tectonics of the Wyoming-Idaho-Utah thrust belt: Joint Wyoming-Montana-Utah Geological Associations, 29th Annual Field Conference and Symposium, Rocky Mountain Thrust Belt Geology and Resources.

---- 1978, Seismicity, crustal structure, and intraplate tectonics of the interior of the western Cordillera, in Smith, R. B. and Eaton, G. P., eds., Cenozoic tectonics and regional geophysics of the western Cordilleran: Geological Society of America Memoir 152, p. 111-144.

Smith, R. B. and Arabasz, W. J., 1979, Seismicity, tectonics and crustal structure in Utah: Important aspects from new data; in Earthquake studies in Utah 1850 to 1978: Seismograph Stations, Salt Lake City, University of Utah, p. 395-408.

Smith, R. B., and Bruhn, R. L., 1984, Intraplate extensional tectonics of the eastern Basin-Range: Inferences on structural style from seismic reflection data, regional tectonics, and thermal-mechanical models of brittle-ductile deformation: Journal of Geophysical Research, v. 89, p. 5733-5762.

Smith, R. B. and Sbar, M. L., 1974, Contemporary tectonics and seismicity of the western United States with emphasis on the intermountain seismic belt: Geological Society of America Bulletin, v. 85, p. 1205-1218.

Smith, R. B., Richins, W. D., Doser, D. I., Pechman, J. C., Leu, L. L., and Chen, G. J., 1984, The 1983, $M_S$ 7.3 Borah Peak, Idaho earthquake: A model for active crustal extension: EOS (American Geophysical Union Transactions), v. 65, p. 989.

Smith, R. B., Richins, W. D., and Doser, D. I., 1985, The 1983 Borah Peak, Idaho, earthquake: Regional seismicity, kinematics of faulting, and tectonic mechanism, in Stein, R. S., and Bucknam, R. C., eds., Proceedings of Workshop XXVIII on the Borah Peak, Idaho, earthquake: U.S. Geological Survey Open-File Report 85-290, v. A, p. 236-263.

Soltanpour, P. N., and Workman, S. M., 1981, Soil-testing methods used at Colorado State University Soil Testing Laboratory: Colorado State University Experiment Station of Fort Collins Technical Bulletin 142, 22 p.

Spieker, E. M., 1931, The Wasatch Plateau coal field, Utah: Geological Society of America Bulletin, v. 819, 210 p.

---- 1946, Late Mesozoic and early Cenozoic history of central Utah: U.S. Geological Survey Professional Paper no. 205-D, p. 117-161.

---- 1949, Transition between the Colorado Plateaus and the Great Basin in central Utah: Utah Geological Society Guidebook no. 4, p.

Spieker, E. M., and Baker, A. A., 1928, Geology and coal resources of the Salina Canyon district, Sevier County, Utah: U.S. Geological Survey Bulletin 796, p. 125-170.

Spieker, E. M. and Billings, M. P., 1940, Glaciation in the Wasatch Plateau: Geological Society of America Bulletin, v. 51, p. 1173-1198.

Spieker, E. M., and Reeside, J. B., Jr., 1925, Cretaceous and Tertiary formations of the Wasatch Plateau, Utah: Geological Society of America Bulletin, v. 36.

Standlee, L. A., 1982, Structure and stratigraphy of Jurassic rocks in central Utah: Their influence on tectonic development of the Cordilleran foreland thrustbelt, in Geologic Studies of the Cordilleran Thrustbelt, Powers, R. B., (ed): Rocky Mountain Association of Geologists, p. 357-

382.

Stein, R. S., and Barrientos, S. E., 1985, The 1983 Borah Peak, Idaho earthquake--geodetic evidence for deep rupture on a planar fault: U.S. Geological Survey Open-File Report 85-290, p. 459-484.

Stewart, J. H., 1971, Basin and Range structure: a system of horsts and grabens produced by deep-seated extension: Geological Society of America Bulletin, v. 82, p. 1019-1043.

---- 1978, Basin-Range structure in western North America: areview: Geological Society of America Memoir 152, p. 1-32.

Stokes, W. L., 1952, Salt-generated structures of the Colorado Plateau and possible analogies [abstr.]: American Association of Petroleum Geologists Bulltin, v. 36, no. 5, p. 961.

---- 1956, Tectonics of Wasatch Plateau and near-by areas [abstr.]: American Association of Petroleum Geologists Bulletin, v. 40, no. 4, p. 790.

---- 1977, Subdivisions of the major physiographic provinces in Utah: Utah Geology, v. 4, no. 1, p. 1-17.

Sullivan, J. T., Nelson, A. R., Martin, R. A., Jr., Foley, L. L., Baltzer, E. M., and Krinsky, C. M., 1986, Regional seismotectonic study for the Central Utah Project, Utah: Seismotectonic Section Report 86-3 [unpublished], U.S. Bureau of Reclamation, Denver, Colorado, (in press).

Suppe, J., Powell, C., and Berry, R., 1975, Regional topography, seismicity, Quaternary volcanism, and the present-day tectonics of the western United States: American Journal of Science, v. 275-A, p. 397-436.

Swan, F. H., III, Schwartz, D. P., Cluff, L. S., Hanson, K. L., and Knuepfer, P. L., 1979, Study of earthquake recurrence intervals on the Wasatch fault at the Hobble Creek site, Utah: U.S. Geological Survey Open-File Report, 40 p.

Swan, F. H., III, Schwartz, D. P., and Cluff, L. S., 1980, Recurrence of moderate to large magnitude earthquakes produced by surface faulting on theWasatch fault zone, Utah: Bulletin Seismological Society of America, v. 70, no. 5, p. 1431-1462.

Swan, F. H., III, Schwartz, D. P., Hanson, K. L., Knuepfer, P. L., and Cluff,L. S., 1981a, Study of earthquake recurrence intervals on the Wasatch fault at the Kaysville site, Utah: U.S. Geological Survey Open-File Report 81-228, 33 p.

Swan, F. H., III, Schwartz, D. P., Cluff, L. S., Hanson, K. L., and Knuepfer, P. L., 1981b, Study of earthquake recurrence intervals on the Wasatch fault at the Hobble Creek site, Utah: U.S. Geological Survey Open-File Report 81-229, 40 p.

Toucher, D., 1962, The earthquake at Hebgen Lake, Montana, on August 18, 1959

(GCT) -- Introduction: Bulletin of the Seismological Society of America, v. 52, p. 153-162.

Trimble, A. B., and Smith, R. B., 1975, Seismicity and contemporary tectonics of the Hebgen Lake - Yellowstone Park region: Journal of Geophysical Research, v. 80, no. 5, p. 733-741.

U.S. Bureau of Reclamation, 1962, Preconstruction Geologic Report, Joes Valley Dam and Reservoir Site, Emery County Project, Utah: U.S.B.R. Report G-180.

---- 1980a, Engineering geology report for Scofield Dam, Carbon County, Utah, Upper Colorado Region: Converse, Ward and Dixon, Inc.

---- 1980b, Geologic report, field examination and safety evaluation, Joes Valley Dam: G. S. Rasmussen and Associates, Inc., Contract no. 0-07-DV-00096.

---- 1983a, Palisades Dam seismotectonic study - preliminary conclusions - Palisades Project, Idaho: Denver, Colorado, Memorandum from Head, Seismotectonic Section to Chief Design Engineer, July 14, 1983, 2 p.

---- 1983b, Geologic data collection report for field investigations for the right abutment and downstream embankment for safety of dams modification decision analysis for Joes Valley Dam, Emery County Project, Utah.

U.S. Department of Agriculture, Soil Survey Staff, 1951, Soil Survey Manual: Washington, D.C., U.S. Department of Agriculture Handbook no. 18, 503 p.

---- 1975, Soil Taxonomy: Washington, D.C., U.S. Department of Agiculture Handbook no. 436, 754 p.

---- 1982, Soil Survey Manual: Soil Conservation Service, U.S. Department of Agriculture (in review).

U.S. Forest Service, 1983, Storage rain gauge precipitation data, Straight Canyon barometer watershed, 1967-1978, Manti-La Sal National Forest: File 2530, Barometer watersheds.

U.S. Geological Survey, 1976, "Fault scarps - Joes Valley, Utah": Memorandum from R. C. Bucknam, Branch of Earthquake Hazards, to A. Viksne.

University of Utah, 1982, Earthquake data file (magnetic tape through December 1981): University of Utah Seismograph Stations, Department of Geology and Geophysics, Salt Lake City, Utah.

Wallace, R. E., 1981, Active faults, paleoseismology, and earthquake hazards in the western United States, in Simpson, D. W., and Richards, P. G., eds., Earthquake Prediction - An International Review: American Geophysical Union, Washington, D.C., p. 209-216.

Walton, P. T., 1954, Wasatch Plateau gas fields, Utah, in Geology of portions of the high plateaus and adjacent canyonlands of central and south central Utah: Intermountain Association of Petroleum Geologists 5th

Annual Field Conference, p. 79-85.

Wecshler, D. J., 1979, An evaluation of hypocenter location techniques with applications to southern Utah: Regional earthquake distributions and seismicity of geothermal areas [M.S. thesis]: Salt Lake City, University of Utah, 225 p.

Wernicke, B., 1981, Low angle normal faults in the Basin and Range province: nappe tectonics in an extending orogen: Nature, v. 291, p. 645-648.

Wesnousky, S. G., Scholz, C. H., Shimazaki, K., and Matsuda, T., 1983, Earthquake frequency distribution and the mechanics of faulting: Journal of Geophysical Research, v. 88, no. B11, p. 9331-9340.

Westphal, W. H., 1963, Seismic aftershock investigations -- Project Vela Uniform; Juab Valley, Utah, earthquake of 7 July 1963: Technical Report no. 4, SRI Project PHU-4322, prepared for Advanced Research Projects Agency by Stanford Research Institute.

Westphal, W. H., and Lange, A. L., 1966, Local seismic monitoring: final technical report: Stanford Research Institute Report, 242 p.

Witkind, I. J., 1982, Salt diapirism in central Utah, in Overthrust Belt of Utah, D. L. Nielson (ed): Utah Geological Association Publication no. 10, p. 13-30.

Witkind, I. J., and Page, W. R., 1984, Origin and significance of the Wasatch and Valley Mountains monoclines, Sanpete-Sevier Valley area, central Utah: The Mountain Geologist, v. 21, no. 4, p. 143-156.

Witkind, I. J., and Sprinkel, D. A., 1982, Salt diapirism in central Utah: Utah Geological Association Publication no. 10, p. 315-330.

Witkind, I. J., Lidke, D. J., and McBroome, L. A., 1978, Preliminary Geologic Map of the Price 1¶ x 2¶ quadrangle: U.S. Geological Survey Open File Report 78-465.

Witkind, I. J., Weiss, M. P., and Brown, T. L., 1982, Preliminary geologic map of the Manti 30o X 60o quadrangle, Carbon, Emery, Juab, Sanpete, and Sevier counties, Utah: U.S. Geological Survey Open File Report 82-654.

Zoback, M. L., 1983, Structure and Cenozoic tectonism along the Wasatch fault zone, Utah, in Tectonic and Stratigraphic studies of the eastern Great Basin: Geological Society of America Memoir 157, p. 3-27.

Zoback, M. L., and Zoback, M. D., 1980, State of stress in the conterminous United States: Journal of Geophysical Research, v. 85, p. 6113-6156.

Zoback, M. L., Anderson, R. E., and Thompson, G. A., 1981, Cenozoic evolution of the state of stress and style of tectonism of the Basin and Range province of the western United States: Philosophical Transactions of the Royal Society of London, series A, v. 300, p. 407-434.

## APPENDICES

A. Quaternary geology of the northern Joes Valley graben

B. Radiocarbon dates

C. Amino-acid analyses

D. Analysis and summary of seismographic data recorded in the vicinity of Joes Valley Dam, Emery County Project, eastern Wasatch Plateau, Utah

E. Interpretation of instrumental seisimicity and contemporary tectonics of the eastern Wasatch Plateau relevant to seismic exposure of the Joes Valley and Scofield Dams

## Appendix A: Quaternary geology and chronology of the northern Joes Valley graben

Available literature on the Quaternary geology of the northern Joes Valley graben consists of a general study of the glaciation of the Wasatch Plateau by Spieker and Billings (1940), a study of the geology of the area surrounding Joes Valley Reservoir (Kucera, 1954), and a map of a portion of the Gooseberry graben (Oberhansely, 1980). These studies provide only minimal information on the chronology of glaciation and geomorphic development of the graben. This seismotectonic study includes detailed mapping and age-dating of Quaternary deposits and landforms in the northern part of the graben, between Joes Valley Reservoir and Lake Canyon (plate 2), in order to evaluate the timing of surface displacements on the Joes Valley faults. The deposits that are important to this chronologic assessment, and that were studied in detail, include end moraines, outwash gravels, debris flows, landslides, and alluvial deposits in fans and on mainstream terraces. These deposits are divided into four relative age groups (RAGs), numbered 1 through 4 from oldest to youngest. The relative age group assignments for the moraines and landslide deposits are primarily based on their geomorphic position and topographic expression, whereas the alluvial deposits are assigned to RAGs primarily on the basis of their height above the modern drainages. The degree of soil development on the surfaces of these deposits is also used to assess their relative ages. Amino-acid racemization (see Appendix C) provides a limiting age for deposits at one locality (trench 6) and radiocarbon dates (see Appendix B) from trenches 3, 4, and 6 and from kettles on moraine surfaces set numerical age constraints for RAGs 2 and 3. The following sections provide a description of 1) the general characteristics of the deposits of northern Joes Valley, 2) the four relative age groups, 3) the soils formed on the deposits, and 4) the correlation of the RAGs with age-dated deposits elsewhere.

### A.1 Description of deposits

The glaciation of the Wasatch Plateau was initially recognized by Spieker and Billings (1940) who identified cirques in the valleys heading on the east side of the plateau from Boulger Canyon south to Bulgur Canyon (plate 2), and attributed the deposits within these valleys to glacial processes. In Joes Valley graben they recognized three end moraine complexes from the coalescence of glaciers from valleys draining the east side of the plateau. Moraines were also recognized in Reeder and Black Canyons, at elevations similar to the moraines within the graben to the north. Kucera (1954) examined the southernmost area of glacial deposits in the graben and mapped three moraines which he attributed to three "Wisconsin" glacial advances. Other deposits important to this study that were mapped by Kucera (1954) are the large landslide masses and debris flows around the margins of Joes Valley Reservoir and the alluvial fan remnants at Reeder Canyon.

End moraines are mapped at five localities in the Joes Valley study area (plate 2). The northernmost moraine is at the mouths of Lake and Spring

Canyons and is formed by converging glaciers from these two drainages. To the south is another moraine at the mouths of Rolfson and Staker Canyons. These moraines are prominent ridges with a relief of approximately 150 m and are characterized by a hummocky surface with numerous kettles, some containing ephemeral ponds, and steep (25° to 35°) outer margins. The moraines overlie traces of the northernmost (Huntington) segment of the West Joes Valley fault without evidence for displacement. These moraines are correlated with the Qm2 moraines to the south (see following section) based on their size, position relative to the source canyons, and surface characteristics (hummockiness, kettles, steep outer margins).

Six kilometers to the south, at the mouths of Jordan, Seeley, and Bennets Canyons is an extensive outer moraine (Qm2) with three connected lobes deposited by glaciers from each of the three source canyons and a smaller inner moraine (Qm3) at the mouths of Jordan and Seeley Canyons. The outer and inner moraines have similar surface morphology with sharp crests and numerous closed depressions. A pit excavated in one of these kettles (soil pit 22 on plate 2) on the Qm2 moraine contained a 60-cm-thick cumulic A horizon overlying 60 cm of interstratified clay and organic matter with unstratified poorly sorted gravelly clay (till) at a depth of 120 cm. Radiocarbon ages from layers of organic matter 100 and 110 cm deep are 4590±90 yrs BP and 5860±100 yrs BP, respectively, provide a minimum age estimate for the underlying till. These ages suggest that thousands of years elapsed between the retreat of the glacial terminus from this position and the initiation of organic matter accumulation in the kettles; this may reflect the long time required to revegetate the area following glacial retreat.

The southernmost moraine within the graben consists of three separate but overlapping moraines of different ages adjacent to the mouth of Potters Canyon. This moraine complex is in the form of a north-trending ridge about 5 km long. The two higher moraines, Qm2 and Qm3, are similar to the Bennets-Seely-Jordan moraines in surface morphology, areal extent and position relative to the mouth of Potters Canyon. A soil pit (21 on plate 2) excavated in a kettle on the Qm2 surface contained an A horizon 35 cm thick overlying 85 cm of stratified clay and organic matter, with till at a depth of 120 cm. Radiocarbon ages obtained from the lowest organic layers within the lacustrine clays are 9220±130 BP (90 cm deep) and 7300±170 BP (50 cm deep) (Appendix B). These ages indicate that organic material began to accumulate in these kettles earlier than material in kettles on the Qm2 moraine to the north. However, this moraine is probably also late Pleistocene (<130 ka) in age.

The lowest moraine, Qm1, exposed at the southern end of the moraine complex where it juts out from beneath the Qm2 margin, appears to be substantially older than the Qm2 and Qm3 moraines because Qm1 has a smooth surface lacking kettles and a gently sloping (<15°) outer margin in contrast to the steep (>20°) outer margins of the younger moraines.

The fifth terminal moraine of significance to this study is in Black Canyon, 0.6 km up the canyon, west of the graben. This moraine has similar surface morphology and terminates at approximately the same elevation (2440 m) as the Qm2 moraines to the north.

In summary, we map three RAGs of terminal moraines in the graben, consistent with Kucera's (1954) findings. The oldest moraine, from the most extensive glacial advance in southern extent in the graben, has a smooth surface morphology. The younger moraines, Qm2 and Qm3, have hummocky surface morphology. The intermediate (Qm2) moraines extend farther into the graben from the canyon mouths than the Qm3 moraines. The Qm3 were deposited at the canyon mouths overlying the West Joes Valley fault. These latter two groups have distinctly different surface morphology from the first.

Alluvial terraces that are close to the same height above the present creek as the moraines are inferred to be outwash terraces. These terraces are present at two localities in the graben (Qt on plate 2). Two outwash terraces about 25 m and 50 m above the modern creek level are found in the small graben between the Bald Mountain and the East Joes Valley faults. These outwash gravels were deposited by meltwater from the three northernmost glaciers that extended into the graben. The meltwater apparently found outlets from the graben through Rolfson and Miller Flat Canyons on the east side of the graben. The southernmost glacier in Joes Valley appears to have drained to the south into Lowry Water because a 75 m high terrace is adjacent to the Qm2 terminal moraine at Mill Canyon.

Two of the drainages on the west side of the graben contain sets of terraces that reflect progressive lowering of base level. Seely Creek has a sequence of three terraces incised into an older debris flow (figure 4.2). Because these terraces do not extend above the mouth of the canyon at the West Joes Valley fault, they cannot be used to assess late Quaternary activity rates on this fault. In contrast, Littles and Black Canyons have terraces at their mouths that are cut by fault scarps. At the mouth of Littles Canyon is a set of three terraces 2, 6, and 15 m above the creek (figure 4.6). The highest of these terraces is composed of debris flow deposits that are $^{14}C$ dated at >23 ka in trench 4 (see section 4.4.4).

Alluvial fans are common at the base of the main escarpments, as well as toward the center of the graben where they are graded to the modern creek. The fans vary in size, surface gradient, and degree of dissection; the older fans are larger and more dissected. These differences are well illustrated at Reeder Creek on the west side of the graben, where there is a sequence of four alluvial fans of different heights (figure 4.2). To the north of Reeder Creek, between the West Joes Valley fault and the Middle Mountain fault, the graben is filled with alluvium from steep gullies on the escarpment and colluvium from the surrounding slopes. At Black Canyon a large fan heads at the West Joes Valley fault. The relationship of these fans to the West Joes Valley and Middle Mountain faults is discussed in sections 4.4 and 4.5.1.

A fan that is similar in size and geomorphic position to the older surfaces at Reeder Creek occurs immediately north of the dam and heads at the base of the escarpment formed by the East Joes Valley fault. In Upper Joes Valley is a series of small, steep (8-9° slope), active alluvial fans which head at the base of the East Joes Valley fault. This graben is filled to an unknown depth with sediment, probably mostly outwash deposited by the glacial terminus located immediately to the west. The alluvial fans overlie this outwash.

An alluvial fan at Scad Valley contains the only direct evidence, in the form of scarps, for late Quaternary surface rupture on the East Joes Valley fault (figure 4.3). A trench (JVT-6) across these scarps revealed that the fan has been active from at least the mid-Pleistocene through the Holocene (section 4.3.4).

South of the glaciated portion of the graben, some of the more prominent Quaternary landforms consist of unsorted, unstratified, gravelly clays that have a fan-shaped configuration and hummocky surface topography. These features are debris flows which emanated from Black, Littles and Seely Canyons.

The Black Canyon debris flow (Qdf on figure 4.7) is an eroded remnant of a deposit that at one time extended from the mouth of the canyon across the graben to Middle Mountain. The surface of this debris flow falls on a projection of the surface of the moraine located in Black Canyon (Qm2 on plate 2) when measured with a Kern PG-2 photogrammetric plotter. This relationship implies that the debris flow is composed of material originally deposited in the moraine which was later remobilized and flowed out of the canyon and into the graben.

The most extensive area of debris flow deposits in the graben is located west of Joes Valley Dam (fig.4.2). The debris flows, which originated in Seely and Littles Canyons, form a prominent fan-shaped area of unsorted unstratified deposits with an irregular hummocky surface that partly underlies the reservoir. Erosion by Lowry Water and Seely Creek has left small island-like remnants of these deposits that are surrounded by younger alluvium. One of these remnants is about 200 m west of Joes Valley Dam (figure 4.2). Kucera (1954) attributes these large debris flows to mass wasting induced by greater effective precipitation during the late Pleistocene. The correlation of the Black Canyon debris flow with the intermediate (Qm2) terminal moraine supports this interpretation and suggests that the flows in the vicinity of the reservoir may be the same age as the moraines. A radiocarbon date of 23 140±350 yrs BP (Appendix B) obtained from debris flow sediments in trench 4 provides a minimum age (see discussion in section 4.4.4) for the debris flow deposits. The degree of soil development on these deposits, although not definitive, supports a late Pleistocene (10-30 ka) age for them.

Landslides are common and widespread on the Wasatch Plateau, especially in those areas where slopes are underlain by the unstable North Horn Formation (Godfrey, 1978). Erosion and undercutting of the soft shales in the North Horn below vertical cliffs formed in the resistant Flagstaff Limestone has led to large-scale block-sliding and rotational slumping. Several large landslide masses dominate the landscape in the area surrounding Joes Valley Reservoir: between Littles and Reeder Canyons and south of Seely Creek on the west side of the graben, and on the east side of the graben south of the dam (plate 2). The age of these landslides and their relationship to underlying faults is difficult to assess. The hummocky surface morphology of the landslides suggests that they are at least as old as the Qm2 and Qm3 moraines and the large debris flows, although the degree of dissection of the major portion of these landslides suggests that they may be much older.

A.2 Relative age groups (RAGs)

The deposits in the area are divided into four RAGs (relative age groups) (tables A1 and A2) defined by their topographic position (height above the present base level and/or position relative to canyon mouth), surface morphology, and stratigraphic relationships exhibited in trenches. Soil characteristics including maximum carbonate stage or depth of carbonate leaching and B horizon development distinguish only three RAGs. In this section the characteristics of each RAG will be discussed beginning with the oldest (RAG 1) and proceeding to the youngest (RAG 4). Section A.3 will discuss the soils developed on the surfaces of these deposits.

The oldest group, RAG 1, is recognized at only one location, the outermost moraine (Qm1) near the mouth of Mill Canyon (plate 2). This moraine has a smooth surface without kettles and a gently sloping (<15°) outer margin.

RAG 2 deposits are distinguished in the northern part of the study area by relative geomorphic position and in the southern part by geomorphic and stratigraphic position and by the relative degree of soil development.

The deposits in the southern area include three alluvial fan remnants at Reeder Canyon (af1, af2, and af3), a high terrace (t1) at the mouth of Littles Creek in the southern part of the study area, the Littles and Seely Creek debris flows, an alluvial fan on the east side of the graben that heads at the escarpment along the East Joes Valley fault, and the large landslide separating the drainages of Littles and Reeder Creeks.

RAG 2 at Black Canyon is represented by the highest terrace (t1) and by the debris flow within the graben. This terrace falls on a projected surface extending from the Qm2 moraine farther up the canyon to the debris flow in the graben (figure 4.7) suggesting that these three landforms are approximately equivalent in age, and similar in age to the Qm2 moraines to the north. The height of the terrace above the creek and the soil profile development (see section A.2) suggest that t1 is the same age as the high terrace at the mouth of Littles Creek. In the northern part of the study area RAG 2 includes the intermediate moraines mapped as Qm2 on plate 2.

RAG 3 deposits are the youngest fan surface (af4) and loessial material that overlie the older (af1, af2, af3) surfaces at Reeder Creek (figure

Table A1: Relative age groups and soil properties of selected landforms in the southern part of the Joes Valley study area.

| Relative age group | Geomorphic unit /1 | Profile | Max. carb. stage /2 | Cs (g/cm2) /3 | Non-arid index /4 | Arid index /4 | All properties index /4 |
|---|---|---|---|---|---|---|---|
| 2 | Qdf: Seely Creek debris flow /5 | JVT-5 | II | 61.49 | 0.0427 | 0.0423 | 0.0654 |
| 2 | " | JVS-6 | II+ | n.d. | 0.0843 | 0.0933 | 0.1028 |
| 2 | Qt1: highest terrace adjacent to Littles Canyon /6 | JVS-13 | II+ | 64.86 | 0.0957 | 0.1099 | 0.1247 |
| 2 | Qaf: alluvial fan, east side of Joes Valley reservoir /5 | JVS-3 | II+ | 27.33 | 0.0675 | 0.1177 | 0.1334 |
| 2 | Qls: landslide between Littles and Reeder Canyons /5 | JVS-5 | I+ | 46.86 | 0.1175 | 0.1309 | 0.1602 |
| 2 | Qaf1: oldest alluvial fan adjacent to Reeder Canyon /5 | JVT-1A | III | 41.70 | 0.0673 | 0.0912 | 0.1142 |
| 2 | " | JVT-3A | II+ | 27.58 | 0.0784 | 0.0896 | 0.1110 |
| 2 | " | JVS-8 | II | n.d. | 0.0901 | 0.1174 | 0.1312 |
| 2 | Qaf3: intermediate alluvial fan adjacent to Reeder Canyon /5 | JVS-7 | III | n.d. | 0.0720 | 0.1178 | 0.1323 |
| 2 | Qt1: highest terrace adjacent to Black Canyon /7 | JVS-18 | II | n.d. | 0.1789 | 0.1443 | 0.1752 |
| 2 | Qdf: debris flow adjacent to Black Canyon /7 | JVS-1 | I+ | 58.69 | 0.0526 | 0.0512 | 0.0726 |
| 3 | Qaf1: loess overlying oldest alluvial fan at Reeder Canyon /5 | JVT-1B | I+ | n.d. | 0.1260 | 0.1251 | 0.1636 |
| 3 | " | JVT-1C | II | -18.47 | 0.1096 | 0.0850 | 0.1177 |
| 3 | " | JVS-12 | II | n.d. | 0.1928 | 0.1862 | 0.2076 |
| 3 | Qaf4: lowest alluvial fan adjacent to Reeder Canyon /5 | JVT-2 | II | 24.38 | 0.0836 | 0.0736 | 0.1043 |
| 3 | " | JVT-3B | III | 38.64 | 0.0924 | 0.937 | 0.1394 |
| 3 | Qaf: alluvial fan adjacent to Black Canyon /7 | JVS-4 | I+ | 10.37 | 0.0640 | 0.0562 | 0.0799 |
| 3 | Qt2: intermediate (13 m) terrace adjacent to Black Canyon /7 | JVS-19 | I | n.d. | 0.1285 | 0.0832 | 0.1390 |
| 3 | Qt3: intermediate (4 m) terrace adjacent to Black Canyon /7 | JVS-20 | I | n.d. | 0.1005 | 0.0830 | 0.1136 |
| 4 | Qt3: 7 m high terrace adjacent to Seely Canyon /5 | JVS-9 | I+ | 37.13 | 0.0211 | 0.0219 | 0.0352 |
| 4 | Qc: colluvium on scarp adjacent to Littles Canyon /6 | JVT-4 | I | n.d. | 0.0341 | 0.0183 | 0.0350 |

/1 Geomorphic units as designated on plate 2 and figures 4.2, 4.6, and 4.7.
/2 Maximum stage of carbonate development in the profile, terminology of Gile and others (1966) and Bachman and Machette (1977).
/3 Secondary carbonate (g/cm2), after Machette (1978, 1985). Bulk density was estimated from texture (Rawls, 1983).
/4 Numbers are weighted means of horizon indices following the methods of Harden (1982) and Harden and Taylor (1983) and modified by Nelson and Taylor (1985).
/5 Figure 4.2
/6 Figure 4.6
/7 Figure 4.7

Table A2: Relative age groups and selected soil properties of landforms in the northern part of the Joes Valley study area.

| Relative age group | Geomorphic unit /1 | Soil Profile | Depth of CO3 leaching (cm) /2 | Rubification | Non-arid index /3 | Arid index /3 | All properties index /3 |
|---|---|---|---|---|---|---|---|
| 1 | Qm1: outermost moraine adjacent to Potters Canyon | JVS-10 | 88 | 0.2381 | 0.2761 | 0.2237 | 0.2930 |
| 1 | " | JVS-10b* | --- | 0.2441 | 0.2772 | 0.2260 | 0.2958 |
| 1 | " | JVS-15 | 68 | 0.2811 | 0.2457 | 0.1952 | 0.2590 |
| 2 | Qm2: intermediate moraine adjacent to Potters Canyon | JVS-14 | 21 | 0.2779 | 0.1335 | 0.1166 | 0.1620 |
| 2 | Qm2: outer moraine adjacent to Bennets, Seeley, and Jordan Canyons | JVS-17 | 5 | 0.1263 | 0.1263 | 0.1315 | 0.1588 |
| 3 | Qm3: inner moraine adjacent to Bennets, Seeley, and Jordan Canyons | JVS-16 | 66 | 0.1160 | 0.1815 | 0.1641 | 0.1943 |
| 4 | included in Qu: terrace 4 m above Lowry Water | JVS-11 | 33 | 0.0297 | 0.0390 | 0.0246 | 0.0398 |
| unassigned /4 | Qaf: alluvial fan on east side of Scad Valley, all profiles are in trench 6 (fig. 4.5). | JVT-6A | 90 | 0.3123 | 0.1234 | 0.0780 | 0.1373 |
| | | JVT-6Ab* | --- | 0.3193 | 0.1334 | 0.0845 | 0.1472 |
| | | JVT-6B | 79 | 0.3059 | 0.1667 | 0.1256 | 0.1868 |
| | | JVT-6Bb* | --- | 0.3384 | 0.1674 | 0.1328 | 0.1881 |
| | | JVT-6C | 98 | 0.2519 | 0.1954 | 0.1507 | 0.2154 |
| | | JVT-6Cb* | --- | 0.2377 | 0.2146 | 0.1783 | 0.2432 |

/1 Units as designated on plate 2

/2 Depth of carbonate leaching is the depth at which there is a significant increase in the amount of $CaCO_3$ in the profile (see tables A3 and A4). Because it is measured from the surface it is not included for the buried profiles.

/3 Numbers are weighted means of horizon indices following the methods of Harden (1982), Harden and Taylor (1983), and Nelson and Taylor (1985).

/4 Because the alluvial fan contains deposits spanning the late Pleistocene and Holocene, and because the soil profiles in trench 6 contain a sequence of buried soils, the fan does not fit into a relative age group.

* Numbers are calculated for the buried soils within these profiles, excluding the overlying horizons.

4.2), the intermediate terraces (Qt2 and Qt3, figure 4.7) the alluvial fan at the mouth of Black Canyon, and the Qm3 moraines at the northern end of the Joes Valley graben (plate 2).

In the northern part of the study area, RAG 3 contains the innermost moraines that are located the mouths of the canyons, mapped as Qm3 on plate 2. The similar surface morphology of the Qm2 and Qm3 moraines suggests that there is relatively little age difference between them.

RAG 4 contains the lowest set of terraces along the major drainages (Lowry, Seely, Reeder, Black Creeks) and the lowest alluvial fans along the margins at the graben. The terraces range in height from 2 m to 7 m.

In summary, the deposits in the Joes Valley area fall into four relative age groups based on a combination of descriptive criteria which include geomorphic characteristics and stratigraphic relationships exhibited in trenches. The oldest group, RAG 1, contains only one deposit exposed at the surface, the Qm1 moraine. The next younger group, RAG 2, includes the high terraces at Littles and Black Creeks, the older Reeder Creek alluvial fans (af1,af2,af3) the large landslide between Reeder and Littles Creeks, and the Qm2 moraines. RAG 3 includes the fine deposits on the af1 surface at Reeder Creek, the debris flows from Seely, Littles and Black Canyons, and the Qm3 moraines. The youngest group, RAG 4, contains the lowest alluvial terraces along Seely, Reeder, Black and Lowry Creeks and alluvial fans along the margins of the graben.

A.2 Soils on Quaternary deposits

The degree of soil profile development on the surfaces of the deposits discussed in the previous section provides supporting data with which to determine relative age groups and a means of comparing the deposits with age-dated sequences elsewhere in central Utah and the Rocky Mountains. Despite the many problems associated with attempting chronocorrelation based on relative soil development (Pierce, 1979; Birkland, 1984; Sullivan and others, 1986), the comparison of soils data combined with geomorphic characteristics and some independent age data allows for an approximately dated framework to be formulated for the deposits in the Joes Valley area. Futhermore, the correlation of glacial deposits in the Rocky Mountains (Pierce, 1979; Colman and Pierce, 1981; 1986; Porter and other, 1983) provides a chonologic point of reference for this framework.

A total of 31 soil profiles were studied in excavated pits, trenches, and pre-existing exposures on landforms significant to the displacement history of the graben. These landforms include terminal moraines, alluvial terraces and fans, debris flows, and landslides. In this section the soil forming factors in the study area are discussed, followed by a description of the field and laboratory methods, and finally the descriptive and numerical soils data are presented.

The degree of soil development in an area is the result of the five soil-forming factors of climate, organisms, topographic position, time, and parent material (Jenny, 1941). In order to compare the degree of profile development among soils within the study area and with soils of known age in other areas, the time factor (the amount of time during which the soil has formed) is isolated as a variable while the remaining factors are held constant. In the Joes Valley study area this condition is difficult to achieve because precipitation varies with elevation, increasing from south to north: in the vicinity of Joes Valley Reservoir (el. 2100 m) m.a.p. (mean annual precipitation) is 35.5 cm and increases to 70.7 cm at Scad Valley (el. 2650 m), 20 km to the north (U.S. Forest Service, 1983). Soil temperature presumably decreases with increased elevation, although no data are readily available. The soils reflect the dramatic difference in m.a.p. in the degree of accumulation or leaching of $CaCO_3$, in B horizon chroma, and in the amount of illuvial clay in the B horizon. These variations make it difficult to compare soils in the southern part of the study area (south of Black Canyon) with soils of the same age in the northern part. The parent material is lithologically similar throughout the study area although the gravel content varies according to the origin of the sediments. Topographic position is maintained as a constant among the profiles described by choosing sites on level surfaces and moraine crests.

An important soil forming factor in calcareous soils is the rate at which calcareous particles infiltrate the profile, which is related to the carbonate influx rate in the region. The prevailing westerly winds in the region would transport dust from the Sevier Basin and Wasatch Front. Influx rates on the Wasatch Plateau, therefore, are probably similar to those on the Wasatch Front reported by Shroba (1980) (0.5 $g/cm^2/kyr$) but may be slightly lower due to greater distance from the source. Sullivan and others (1986) use 0.5 $g/cm^2/yr$ as a maximum influx rate for the back valleys.

Soil profiles were described and classified according to the Soil Survey Staff (1951, 1975, 1980). A total of 31 profiles were described and sampled in the Joes Valley area: 11 profiles from backhoe trenches, 15 from excavated soil pits, and 5 from either natural exposures or road-cuts. Selected field properties and laboratory data for these profiles are summarized in tables A3 and A4. Soil colors are from the Munsell color chart. Carbonate stages are assigned according to Gile and others (1966). Percentages of greater than 2mm material (gravel) by volume were visually estimated as well as roundness (Powers, 1953). For the gravel fraction, the following size categories are derived from Folk (1974): pebbles (2-64 mm), cobbles (64-156 mm), and boulders (>256 mm).

Samples from selected soil profiles were submitted for analysis to the Colorado State University Soils Testing Laboratory, Fort Collins, Colorado. Sand fractions were determined by dry sieving; silt and clay fractions were determined by pipette with prior removal of organic matter and $CaCO_3$. The percent of organic matter and $CaCO_3$ were determined by methods described in Soltanpour and Workman (1981).

Because of the elevation-related climatic gradient that exists in the graben, and the effect that it has on soil formation, the soils are distinguished as being from the more arid southern sites or the less

Table A3: Selected horizon properties of soil profiles described in trenches

| Profile | Horizon | Depth (cm) | Munsell color (dry) | Texture | % Clasts >2mm pebbles | % Clasts >2mm cobbles | % Clasts >2mm boulders | Carb. stage /1 | Cs /2 horizon | Cs /2 profile | % CO3 /3 | % O.M. /4 | % sand /5 | % silt /5 | % clay /5 |
|---|---|---|---|---|---|---|---|---|---|---|---|---|---|---|---|
| JVT-1A | A | 0-9 | 7.5YR 4/4 | sl | 2 | 1 | 0 | | 0.52 | 41.70 | 14.6 | 2.9 | 61.4 | 22.4 | 16.2 |
| | 2Ak | 9-18 | 10YR 5/3 | l | 6 | 4 | 0 | I- | 1.92 | | 28.2 | 3.3 | 48.8 | 29.0 | 22.2 |
| | 3K | 18-34 | 10YR 8/3 | l | 50 | 20 | 4 | III | 3.43 | | 53.6 | 1.1 | 46.4 | 28.0 | 25.6 |
| | 3Bk | 34-59 | 10YR 8/3 | l | 50 | 20 | 4 | I+ | 5.55 | | 55.8 | 0.4 | 45.9 | 27.4 | 26.7 |
| | 4Bk | 59-97 | 10YR 7/3 | scl | 25 | 35 | 4 | I | 10.51 | | 54.0 | 0.4 | 51.6 | 23.7 | 24.7 |
| | 5Bk | 97-152 | 10YR 7/5 | cl | 35 | 15 | 4 | I | 19.77 | | 54.8 | 0.2 | 43.2 | 25.6 | 31.2 |
| JVT-1B | A1 | 0-4 | 10YR 5/3 | cl | 5 | 0 | 0 | | n.d. | n.d. | n.d. | n.d. | n.d. | n.d. | n.d. |
| | A2 | 4-16 | 10YR 5/3 | cl | 8 | 0 | 0 | | n.d. | | n.d. | n.d. | n.d. | n.d. | n.d. |
| | B1 | 16-28 | 10YR 4/3 | cl | 5 | 0 | 0 | | n.d. | | n.d. | n.d. | n.d. | n.d. | n.d. |
| | B2 | 28-42 | 7.5YR 5/4 | cl | 5 | 0 | 0 | | n.d. | | n.d. | n.d. | n.d. | n.d. | n.d. |
| | B3 | 42-57 | 7.5YR 4/4 | cl | 5 | 0 | 0 | | n.d. | | n.d. | n.d. | n.d. | n.d. | n.d. |
| | Bk | 57-80 | 10YR 7/4 | cl | 10 | 0 | 0 | I+ | n.d. | | n.d. | n.d. | n.d. | n.d. | n.d. |
| | 2Bk | 80-107 | 10YR 8/3 | cl | 5 | 0 | 0 | | n.d. | | n.d. | n.d. | n.d. | n.d. | n.d. |
| | 3Bk | 107-140 | 10YR 7/4 | cl | 15 | 3 | 0 | I+ | n.d. | | n.d. | n.d. | n.d. | n.d. | n.d. |
| JVT-1C | A | 0-23 | 10YR 4/3 | cl | 5 | 0 | 0 | | -5.45 | -18.47 | 0.8 | 2.4 | 33.0 | 35.4 | 31.6 |
| | B1 | 23-52 | 7.5YR 5/4 | cl | 0 | 0 | 0 | | -8.03 | | 0.2 | 1.4 | 40.6 | 28.7 | 30.7 |
| | B2 | 52-73 | 7.5YR 5/4 | cl | 0 | 0 | 0 | I | -5.75 | | 0.4 | 0.9 | 43.9 | 25.8 | 30.3 |
| | Bk1 | 73-92 | 7.5YR 5/4 | cl | 0 | 0 | 0 | I | -1.15 | | 12.6 | 0.7 | 44.1 | 26.5 | 29.4 |
| | Bk2 | 92-160 | 7.5YR 6/4 | cl | 0 | 0 | 0 | II | 6.47 | | 20.8 | 0.6 | 44.0 | 28.6 | 27.4 |
| | Bk3 | 160-200 | 7.5YR 6/4 | cl | 0 | 0 | 0 | II | -4.55 | | 9.8 | 0.3 | 41.8 | 28.1 | 30.1 |
| JVT-2 | A | 0-5 | 10YR 4/3 | ls | 10 | 10 | 5 | | -0.56 | 24.38 | 8.6 | 4.0 | 83.2 | 9.7 | 7.1 |
| | Bw1 | 5-12 | 10YR 4/3 | sl | 10 | 10 | 5 | I- | -0.32 | | 14.2 | 3.3 | 69.7 | 20.2 | 10.1 |
| | Bw2 | 12-32 | 10YR 5/3 | sl | 10 | 10 | 5 | I- | 1.35 | | 25.0 | 2.8 | 67.5 | 22.7 | 9.8 |
| | Btk | 32-65 | 10YR 6/3 | sl | 30 | 10 | 10 | I- | 5.15 | | 37.0 | 1.3 | 66.1 | 20.8 | 13.1 |
| | 2Bk1 | 65-150 | 10YR 7/4 | sl | 15 | 30 | 20 | II | 16.29 | | 44.6 | 0.8 | 63.3 | 16.4 | 14.3 |
| | 2Bk2 | 150-178 | 10YR 5/4 | sl | 15 | 40 | 20 | I | 2.48 | | 34.4 | 0.3 | 67.9 | 15.8 | 16.3 |
| JVT-3A | A | 0-9 | 10YR 5/2 | sl | 3 | 2 | 4 | | 0.78 | 27.58 | 17.3 | 3.1 | 58.8 | 25.3 | 15.9 |
| | 2Ak | 9-25 | 10YR 5/3 | sl | 15 | 30 | 4 | I | 1.67 | | 27.6 | 3.6 | 55.2 | 25.9 | 18.9 |
| | 2Bk1 | 25-55 | 10YR 7/3 | scl | 15 | 30 | 4 | II+ | 12.36 | | 50.4 | 1.2 | 58.6 | 20.3 | 21.1 |
| | 2Bk2 | 55-79 | 10YR 7/3 | sl | 15 | 30 | 4 | I+ | 8.07 | | 42.6 | 0.9 | 60.3 | 19.7 | 20.0 |
| | 3Bk | 79-133 | 10YR 7/3 | sl | 45 | 20 | 4 | I | 3.15 | | 17.8 | 0.8 | 58.2 | 23.3 | 18.5 |
| | 4Bk | 133-159 | 10YR 6/4 | sl | 25 | 25 | 5 | I- | 1.36 | | 13.8 | 0.4 | 71.2 | 15.4 | 13.4 |

Table A3 continued

| Profile | Horizon | Depth (cm) | Munsell color (dry) | Texture | % Clasts >2mm pebbles | % Clasts >2mm cobbles | % Clasts >2mm boulders | Carb. stage /1 | Cs /2 horizon | Cs /2 profile | % CO3 /3 | % O.M. /4 | % sand /5 | % silt /5 | % clay /5 |
|---|---|---|---|---|---|---|---|---|---|---|---|---|---|---|---|
| JVT-3B | A1 | 0-4 | 10YR 4/2 | l | 5 | 0 | 0 | | -0.46 | 38.64 | 9.0 | 5.5 | 39.9 | 40.6 | 19.5 |
| | A2 | 4-12 | 10YR 4/2 | cl | 5 | 0 | 0 | | -1.27 | | 4.8 | 3.9 | 24.7 | 39.1 | 36.2 |
| | Bt1 | 12-25 | 10YR 4/2 | c | 5 | 0 | 0 | | -2.77 | | 1.2 | 2.8 | 18.2 | 40.5 | 41.3 |
| | Bt2 | 25-37 | 10YR 4/3 | cl | 10 | 0 | 0 | | -2.23 | | 2.6 | 1.7 | 21.6 | 43.9 | 34.5 |
| | Bk | 37-53 | 10YR 5/3 | cl | 5 | 5 | 0 | II | -0.12 | | 14.8 | 1.5 | 34.1 | 33.9 | 32.0 |
| | 2Bk1 | 53-67 | 10YR 6/5 | scl | 10 | 2 | 0 | II | 6.93 | | 46.8 | 0.9 | 50.6 | 28.8 | 20.6 |
| | 2Bk2 | 67-86 | 10YR 7/5 | scl | 15 | 0 | 0 | II | 7.67 | | 40.8 | 0.6 | 52.6 | 24.0 | 23.4 |
| | 3Kb | 86-108 | 10YR 7/5 | scl | 10 | 0 | 0 | III | 8.66 | | 38.8 | 0.7 | 60.6 | 19.0 | 20.4 |
| | 4Kb | 108-127 | 10YR 8/3 | sl | 5 | 12 | 0 | III | 13.49 | | 60.8 | 0.6 | 59.2 | 22.6 | 18.2 |
| | 5Kb | 127-146 | 10YR 8/4 | sl | 15 | 5 | 10 | III | 6.75 | | 50.4 | 0.4 | 66.3 | 20.1 | 13.6 |
| JVT-4 | A | 0-15 | 2.5Y 6/2 | cl | 10 | 5 | 5 | | n.d. | n.d. | n.d. | n.d. | n.d. | n.d. | n.d. |
| | Bk1 | 15-37 | 2.5Y 7/2 | cl | 10 | 10 | 5 | I | n.d. | | n.d. | n.d. | n.d. | n.d. | n.d. |
| | Bk2 | 37-125 | 2.5Y 7/2 | c | 10 | 15 | 5 | I | n.d. | | n.d. | n.d. | n.d. | n.d. | n.d. |
| JVT-5 | Ak | 0-10 | 10YR 5/3 | sil | 10 | 0 | 0 | | 2.74 | 61.49 | 45.4 | 2.5 | 32.7 | 55.0 | 12.3 |
| | Bk | 10-24 | 10YR 6/3 | scl | 12 | 0 | 0 | I | 7.96 | | 55.4 | 1.9 | 27.4 | 39.5 | 33.1 |
| | 2Bk1 | 24-50 | 10YR 8/2 | cl | 35 | 5 | 0 | II | 13.48 | | 57.2 | 0.7 | 31.7 | 35.6 | 32.7 |
| | 2Bk2 | 50-86 | 10YR 6/2 | cl | 30 | 10 | 2 | I+ | 16.04 | | 52.4 | 0.5 | 31.3 | 32.7 | 36.0 |
| | 2Bk3 | 86-155 | 2.5Y 7/2 | cl | 30 | 15 | 5 | I | 21.27 | | 49.8 | 0.3 | 34.2 | 34.1 | 31.7 |
| JVT-6A | A | 0-6 | 10YR 5/3 | cl | 5 | 0 | 0 | | -0.81 | 11.83 | 0.3 | 5.2 | 56.6 | 34.1 | 9.3 |
| | 2B1 | 8-26 | 7.5YR 6/3 | l | 10 | 10 | 0 | | -1.83 | | 0.2 | 1.3 | 60.4 | 31.7 | 7.9 |
| | 2B2 | 26-58 | 7.5YR 7/4 | ls | 10 | 10 | 0 | | -3.55 | | 0.1 | 0.7 | 63.7 | 29.0 | 7.3 |
| | 3Btb1 | 58-90 | 7.5YR 5/6 | sc | 5 | 15 | 0 | | -2.84 | 18.02 | 2.3 | 0.6 | 55.6 | 17.4 | 27.0 |
| | 3Bk | 90-114 | 10YR 6/4 | sl | 10 | 15 | 0 | | 2.95 | | 16.2 | 0.5 | 61.4 | 22.1 | 16.5 |
| | 3Ck | 114-210 | 10YR 6/6 | scl | 15 | 15 | 5 | I | 17.91 | | 23.0 | 0.6 | 60.1 | 23.8 | 16.1 |
| JVT-6B | A1 | 0-10 | 7.5YR 5/3 | sl | 3 | 3 | 5 | | -1.06 | 3.37 | 0.1 | 3.5 | 61.1 | 30.5 | 8.4 |
| | A2 | 10-19 | 7.5YR 6/4 | sl | 3 | 3 | 5 | | -1.02 | | 0.2 | 2.1 | 65.6 | 26.7 | 7.7 |
| | 2B | 19-34 | 7.5YR 6/5 | sl | 5 | 8 | 5 | | -1.83 | 5.44 | 0.1 | 0.6 | 77.0 | 15.5 | 7.5 |
| | 3Btb1 | 34-60 | 10YR 6/6 | sl | 10 | 10 | 5 | | -2.89 | | 0.1 | 0.7 | 61.0 | 21.9 | 17.1 |
| | 3Btb2 | 60-79 | 10YR 6/8 | l | 10 | 10 | 5 | | -1.95 | | 0.2 | 0.7 | 45.1 | 34.7 | 20.2 |
| | 3Btkb | 79-95 | 10YR 6/5 | sl | 10 | 15 | 5 | I | 0.62 | | 11.4 | 0.7 | 55.0 | 27.0 | 18.0 |
| | 4Bkb1 | 95-122 | 10YR 6/4 | sl | 10 | 15 | 10 | I+ | 5.37 | | 24.0 | 0.7 | 59.6 | 25.0 | 15.4 |
| | 4Bkb2 | 122-150 | 2.5Y 6/4 | sl | 10 | 15 | 10 | I | 6.12 | | 25.6 | 0.4 | 57.8 | 26.5 | 15.7 |
| JVT-6C | A1 | 0-15 | 7.5YR 5/3 | sl | 3 | 3 | 0 | | -1.73 | -8.30 | 0.2 | 3.8 | 52.9 | 36.4 | 10.7 |
| | A2 | 15-37 | 7.5YR 5/3 | sl | 3 | 3 | 0 | | -2.63 | | 0.2 | 1.6 | 56.6 | 34.4 | 9.0 |
| | 2B | 37-57 | 7.5YR 6/4 | sl | 5 | 15 | 2 | | -2.02 | | 0.7 | 0.8 | 66.0 | 27.9 | 6.1 |
| | 2Bt1 | 57-80 | 7.5YR 6/4 | sl | 5 | 15 | 5 | | -2.44 | -1.91 | 0.2 | 0.6 | 72.2 | 21.7 | 6.1 |
| | 2Bt2 | 80-98 | 7.5YR 6/5 | sl | 3 | 20 | 5 | | -1.79 | | 0.7 | 0.6 | 64.4 | 19.8 | 15.8 |
| | 3Btb | 98-138 | 7.5YR 5/5 | sl | 3 | 20 | 5 | | -0.21 | | 8.4 | 0.7 | 61.4 | 21.6 | 17.0 |
| | 4C | 138-160 | 10YR 6/4 | ls | 8 | 15 | 0 | I | 1.27 | | 15.0 | 0.3 | 78.0 | 14.5 | 7.5 |
| | 5C | 160-187 | 10YR 6/4 | sl | 40 | 10 | 0 | I | 1.26 | | 16.2 | 0.3 | 66.6 | 22.4 | 11.0 |

/1 Maximum stage of carbonate development in the profile, terminology of Gile and others (1966) and Bachman and Machette (1977).
/2 Secondary carbonate (g/cm2), after Machette (1978, 1985). Bulk density was estimated from texture (Rawls, 1983).
/3 Percent CaCO3 by dilution with sulfuric acid and titration with sodium hydroxide using methods of Soltanpour and Workman (1981).
/4 Percent organic matter by wet titration using methods of Soltanpour and Workman (1981).
/5 Grain-size data are given in percent by weight of the less than 2 mm fraction: sand (>50um), silt (2-50um), clay (<2um).
Sand fractions by dry sieve with prior removal of organic matter and CaCO3. Silt fractions by pipette with prior removal of organic matter and CaCO3.

Table A4: Selected horizon properties of soil profiles described in soil pits

| Profile | Horizon | Depth (cm) | Munsell color (dry) | Texture | ------% pebbles | cobbles | boulders | Carb. stage /1 | Cs /2 horizon | Cs /2 profile | % CO3 /3 | % O.M. /4 | % sand /5 | % silt /5 | % clay /5 |
|---|---|---|---|---|---|---|---|---|---|---|---|---|---|---|---|
| JVS-1 | Ak | 0-10 | 10YR 5/3 | sl | 20 | 0 | 0 | | -0.10 | 58.69 | 19.0 | 3.2 | 54.7 | 29.4 | 15.9 |
| | Bk1 | 10-19 | 10YR 6/4 | l | 20 | 0 | 0 | | 3.25 | | 40.6 | 2.1 | 46.0 | 33.8 | 20.2 |
| | Bk2 | 19-38 | 10YR 7/6 | l | 20 | 0 | 0 | I | 9.53 | | 48.8 | 0.9 | 46.1 | 33.9 | 20.0 |
| | Bk3 | 38-63 | 10YR 6/4 | l | 20 | 5 | 0 | I | 10.88 | | 47.8 | 0.7 | 40.3 | 40.4 | 19.3 |
| | Bk4 | 63-117 | 10YR 5/4 | l | 20 | 5 | 0 | I+ | 26.94 | | 50.8 | 0.5 | 44.6 | 29.4 | 26.0 |
| | Bk5 | 117-145 | 10YR 5/4 | l | 20 | 20 | 5 | I+ | 8.20 | | 43.8 | 0.2 | 48.8 | 32.7 | 18.5 |
| JVS-2 | Ak | 0-6 | 10YR 5/3 | sl | 10 | 10 | 0 | | -0.36 | 9.35 | 4.6 | 2.8 | 71.0 | 13.7 | 15.3 |
| | A | 6-16 | 10YR 4/3 | sl | 15 | 15 | 0 | | -0.86 | | 1.2 | 2.0 | 77.0 | 13.3 | 9.7 |
| | Bk1 | 16-27 | 10YR 4/4 | sl | 30 | 10 | 0 | | -0.50 | | 3.2 | 2.1 | 74.0 | 15.5 | 10.5 |
| | Bk2 | 27-43 | 7.5YR 5/4 | sl | 5 | 45 | 10 | II | 1.59 | | 21.6 | 2.0 | 71.7 | 18.9 | 9.4 |
| | 2K | 43-63 | 10YR 6/4 | ls | 5 | 45 | 10 | III | 2.78 | | 26.2 | 0.8 | 83.3 | 8.5 | 8.2 |
| | 3Bk | 63-138 | 10YR 7/4 | sl | 60 | 20 | 0 | II | 6.70 | | 31.4 | 0.7 | 76.4 | 14.8 | 8.8 |
| JVS-3 | A | 0-16 | 10YR 5/3 | scl | 25 | 2 | 0 | I- | 1.79 | 27.33 | 21.8 | 2.6 | 52.7 | 26.8 | 20.5 |
| | Bk1 | 16-52 | 10YR 8/3 | l | 35 | 20 | 5 | II | 9.54 | | 44.6 | 1.3 | 51.2 | 29.5 | 19.3 |
| | Bk2 | 52-96 | 10YR 7/2 | scl | 35 | 20 | 5 | II+ | 10.55 | | 39.4 | 0.9 | 49.3 | 25.3 | 25.4 |
| | Bk3 | 96-130 | 10YR 7/3 | scl | 40 | 25 | 5 | I | 5.45 | | 36.0 | 0.4 | 50.5 | 24.8 | 24.7 |
| JVS-4 | Ak1 | 0-3 | 10YR 5/3 | sl | 20 | 0 | 0 | | -0.12 | 10.37 | 5.6 | 6.5 | 60.0 | 26.3 | 13.7 |
| | Ak2 | 3-14 | 10YR 3/3 | sl | 18 | 2 | 0 | | -0.87 | | 1.8 | 4.5 | 64.7 | 21.6 | 13.7 |
| | Btk1 | 14-22 | 10YR 4/3 | sl | 20 | 5 | 0 | | -0.66 | | 1.3 | 2.9 | 67.2 | 19.5 | 13.3 |
| | Btk2 | 22-31 | 10YR 4/4 | sl | 20 | 5 | 0 | | -0.23 | | 6.2 | 1.8 | 65.4 | 19.2 | 15.4 |
| | 2Bk1 | 31-41 | 10YR 5/4 | sl | 30 | 10 | 5 | I | 1.91 | | 26.2 | 1.4 | 70.6 | 17.2 | 12.2 |
| | 2Bk2 | 41-73 | 10YR 6/4 | sl | 40 | 10 | 5 | I | 4.24 | | 23.4 | 1.2 | 68.6 | 18.2 | 13.2 |
| | 3Bk | 73-99 | 10YR 6/3 | sl | 40 | 0 | 10 | I+ | 6.09 | | 33.8 | 1.4 | 76.4 | 14.8 | 8.8 |
| JVS-5 | Ak1 | 0-12 | 10YR 5/3 | cl | 8 | 0 | 0 | | -1.32 | 46.86 | 10.0 | 3.0 | 30.9 | 38.3 | 30.8 |
| | Ak2 | 12-25 | 10YR 4/3 | cl | 8 | 2 | 0 | | 0.22 | | 21.6 | 3.2 | 24.8 | 42.4 | 32.8 |
| | 2Bk1 | 25-42 | 10YR 5/3 | c | 8 | 2 | 0 | | 4.45 | | 32.4 | 2.0 | 20.7 | 36.5 | 42.8 |
| | 2Bk2 | 42-60 | 10YR 5/3 | c | 8 | 2 | 0 | I | 6.37 | | 37.4 | 1.6 | 19.6 | 36.0 | 44.4 |
| | 2Bk3 | 60-90 | 10YR 5/2 | c | 8 | 2 | 20 | I | 10.07 | | 42.2 | 1.3 | 17.7 | 38.1 | 44.2 |
| | 3Bk | 90-150 | 10YR 5/2 | c | 8 | 2 | 20 | I+ | 27.06 | | 53.2 | 0.7 | 5.5 | 38.9 | 55.6 |
| JVS-6 | A | 0-9 | 10YR 5/3 | sil | 2 | 0 | 0 | | n.d. | n.d. | n.d. | n.d. | n.d. | n.d. | n.d. |
| | Ak1 | 9-19 | 10YR 6/3 | l | 5 | 1 | 0 | II | n.d. | | n.d. | n.d. | n.d. | n.d. | n.d. |
| | Ak2 | 19-34 | 10YR 7/2 | l | 5 | 1 | 0 | II | n.d. | | n.d. | n.d. | n.d. | n.d. | n.d. |
| | Bk1 | 34-52 | 10YR 8/3 | l | 25 | 10 | 0 | II+ | n.d. | | n.d. | n.d. | n.d. | n.d. | n.d. |
| | Bk2 | 52-85 | 10YR 8/3 | l | 25 | 10 | 0 | II+ | n.d. | | n.d. | n.d. | n.d. | n.d. | n.d. |
| | Bk3 | 85-120 | 10YR 8/3 | l | 15 | 0 | 0 | I | n.d. | | n.d. | n.d. | n.d. | n.d. | n.d. |
| | Bk4 | 120-150 | 10YR 7/3 | l | 30 | 10 | 0 | I | n.d. | | n.d. | n.d. | n.d. | n.d. | n.d. |
| JVS-7 | A | 0-28 | 10YR 4/4 | sl | 3 | 0 | 0 | | n.d. | n.d. | n.d. | n.d. | n.d. | n.d. | n.d. |
| | Btk | 28-44 | 10YR 6/4 | sl | 3 | 5 | 20 | II+ | n.d. | | n.d. | n.d. | n.d. | n.d. | n.d. |
| | K | 44-94 | 10YR 7/4 | sl | 15 | 10 | 10 | III | n.d. | | n.d. | n.d. | n.d. | n.d. | n.d. |
| | Bk | 94-120 | 10YR 7/4 | sl | 15 | 15 | 20 | II | n.d. | | n.d. | n.d. | n.d. | n.d. | n.d. |
| | C | 120-170 | 10YR 5/4 | sl | 40 | 15 | 5 | I+ | n.d. | | n.d. | n.d. | n.d. | n.d. | n.d. |

Table A4 continued

| Profile | Horizon | Depth (cm) | Munsell color (dry) | Texture | ------% pebbles | cobbles | boulders | Carb. stage /1 | Cs /2 horizon | Cs /2 profile | % CO3 /3 | % O.M. /4 | % sand /5 | % silt /5 | % clay /5 |
|---|---|---|---|---|---|---|---|---|---|---|---|---|---|---|---|
| JVS-8 | A | 0-5 | 10YR 5/3 | l | 10 | 5 | 5 | I- | n.d. | n.d. | n.d. | n.d. | n.d. | n.d. | n.d. |
| | AB | 5-14 | 10YR 4/3 | l | 10 | 5 | 5 | I- | n.d. | | n.d. | n.d. | n.d. | n.d. | n.d. |
| | Bk1 | 14-24 | 10YR 6/3 | cl | 25 | 5 | 5 | II | n.d. | | n.d. | n.d. | n.d. | n.d. | n.d. |
| | Bk2 | 24-59 | 10YR 7/2 | sic | 20 | 15 | 15 | II- | n.d. | | n.d. | n.d. | n.d. | n.d. | n.d. |
| | Bk3 | 59-78 | 10YR 8/3 | sic | 20 | 15 | 15 | I | n.d. | | n.d. | n.d. | n.d. | n.d. | n.d. |
| | C | 78-139 | 10YR 7/3 | sic | 10 | 10 | 25 | I- | n.d. | | n.d. | n.d. | n.d. | n.d. | n.d. |
| JVS-9 | A | 0-9 | 10YR 5/3 | l | 20 | 0 | 0 | | 1.94 | 37.13 | 32.4 | 3.3 | 29.0 | 44.6 | 26.4 |
| | Ak | 9-27 | 10YR 6/3 | cl | 30 | 30 | 15 | I+ | 2.43 | | 48.2 | 2.3 | 43.8 | 26.2 | 30.0 |
| | Bk1 | 27-48 | 10YR 6/2 | sl | 25 | 35 | 15 | I+ | 4.06 | | 48.6 | 1.2 | 68.9 | 14.9 | 16.2 |
| | Bk2 | 48-210 | 10YR 7/2 | scl | 25 | 25 | 25 | I+ | 28.71 | | 45.2 | 0.5 | 56.1 | 23.0 | 20.9 |
| JVS-10 | A | 0-5 | 10YR 5/3 | l | 5 | 0 | 0 | | -0.26 | -5.64 | 15.4 | 4.5 | 47.9 | 33.4 | 18.7 |
| | C | 5-14 | 10YR 5/4 | l | 5 | 0 | 0 | | 0.09 | | 20.8 | 2.7 | 47.6 | 29.1 | 23.3 |
| | 2Ab1 | 14-29 | 10YR 5/3 | l | 5 | 0 | 0 | | -3.37 | -5.47 | 1.8 | 2.5 | 48.2 | 34.5 | 17.3 |
| | 2Ab2 | 29-40 | 10YR 5/4 | l | 5 | 0 | 0 | | -2.66 | | 0.4 | 2.0 | 46.0 | 36.6 | 17.4 |
| | 2Ab | 40-51 | 10YR 5/6 | cl | 5 | 0 | 0 | | -2.67 | | 0.3 | 1.5 | 40.3 | 29.1 | 30.6 |
| | 2Btb1 | 51-67 | 10YR 5/6 | cl | 5 | 0 | 0 | | -4.48 | | 0.3 | 1.2 | 44.1 | 22.8 | 33.1 |
| | 2Btb2 | 67-88 | 10YR 5/6 | scl | 5 | 0 | 0 | | -5.88 | | 0.3 | 0.9 | 47.7 | 22.6 | 29.7 |
| | 3Bkb1 | 88-101 | 10YR 5/6 | scl | 30 | 0 | 0 | | 0.23 | | 16.6 | 1.2 | 51.0 | 23.0 | 26.0 |
| | 3Bkb2 | 101-154 | 10YR 6/4 | scl | 5 | 0 | 0 | | 12.00 | | 28.8 | 1.1 | 50.0 | 27.1 | 22.9 |
| | 3Bkb3 | 154-166 | 10YR 6/5 | sl | 5 | 0 | 0 | I+ | 1.37 | | 22.0 | 0.3 | 77.1 | 12.5 | 10.4 |
| JVS-11 | A | 0-2 | 10YR 4/3 | sl | 20 | 0 | 0 | | -0.02 | 7.15 | 9.0 | 5.7 | 62.1 | 25.1 | 12.8 |
| | Bw | 2-33 | 10YR 5/4 | sl | 20 | 20 | 10 | | -1.57 | | 2.6 | 2.4 | 63.7 | 22.5 | 13.8 |
| | Bk | 33-110 | 10YR 6/4 | sl | 30 | 20 | 20 | | 8.74 | | 27.8 | 1.1 | 74.5 | 15.3 | 10.2 |
| JVS-12 | A1 | 0-5 | 10YR 4/4 | sl | 5 | 4 | 0 | | n.d. | n.d. | n.d. | n.d. | n.d. | n.d. | n.d. |
| | A2 | 5-18 | 10YR 4/4 | sl | 5 | 4 | 0 | | n.d. | | n.d. | n.d. | n.d. | n.d. | n.d. |
| | AB | 18-26 | 10YR 6/4 | sl | 5 | 4 | 0 | | n.d. | | n.d. | n.d. | n.d. | n.d. | n.d. |
| | Bt | 26-57 | 10YR 6/4 | scl | 5 | 4 | 0 | | n.d. | | n.d. | n.d. | n.d. | n.d. | n.d. |
| | Btk | 57-95 | 10YR 6/4 | scl | 5 | 4 | 0 | I+ | n.d. | | n.d. | n.d. | n.d. | n.d. | n.d. |
| | Bk1 | 95-120 | 10YR 6/4 | sl | 4 | 0 | 0 | II | n.d. | | n.d. | n.d. | n.d. | n.d. | n.d. |
| | Bk2 | 120-144 | 10YR 6/4 | sl | 4 | 0 | 0 | I | n.d. | | n.d. | n.d. | n.d. | n.d. | n.d. |
| JVS-13 | A1 | 0-4 | 10YR 5/3 | sl | 5 | 10 | 5 | | -0.10 | 64.86 | 17.0 | 6.9 | 55.1 | 34.2 | 10.7 |
| | A2 | 4-26 | 10YR 5/3 | sl | 5 | 10 | 5 | | 1.90 | | 29.0 | 4.1 | 52.9 | 30.8 | 16.3 |
| | 2Bk1 | 26-66 | 10YR 7/3 | l | 10 | 5 | 5 | II | 23.53 | | 56.4 | 2.1 | 44.7 | 32.6 | 22.7 |
| | 2Bk2 | 66-90 | 10YR 7/3 | scl | 10 | 5 | 5 | II+ | 16.06 | | 59.8 | 1.0 | 54.9 | 23.8 | 21.3 |
| | 3Bk | 90-125 | 10YR 6/3 | sl | 0 | 0 | 0 | II | 18.63 | | 43.8 | 0.7 | 75.3 | 14.7 | 10.0 |
| | 4Bk | 125-140 | 10YR 5/4 | sl | 40 | 5 | 5 | I | 4.85 | | 49.8 | 0.5 | 52.6 | 28.4 | 19.0 |

Table A4 continued

| Profile | Horizon | Depth (cm) | Munsell color (dry) | Texture | ------% pebbles | cobbles | boulders | Carb. stage /1 | Cs /2 horizon | Cs /2 profile | % CO3 /3 | % O.M. /4 | % sand /5 | % silt /5 | % clay /5 |
|---|---|---|---|---|---|---|---|---|---|---|---|---|---|---|---|
| JVS-14 | A | 0-21 | 10YR 4/2 | l | 10 | 15 | 2 | | -2.24 | 12.92 | 6.7 | 6.4 | 38.8 | 36.9 | 24.3 |
| | 2Btk1 | 21-38 | 10YR 6/3 | l | 15 | 15 | 10 | I | 1.93 | | 27.6 | 1.0 | 40.8 | 30.3 | 28.9 |
| | 2Btk2 | 38-50 | 10YR 6/3 | cl | 15 | 15 | 10 | I | 1.41 | | 28.0 | 1.1 | 37.6 | 31.6 | 30.8 |
| | 2Bk1 | 50-110 | 10YR 6/4 | cl | 15 | 15 | 20 | I | 10.11 | | 33.0 | 0.4 | 38.3 | 31.9 | 29.8 |
| | 2Bk2 | 110-125 | 10YR 6/4 | scl | 15 | 15 | 10 | I- | 1.71 | | 25.8 | 0.2 | 51.7 | 27.7 | 20.6 |
| JVS-15 | A1 | 0-5 | 10YR 3/3 | cl | 5 | 5 | 0 | | -0.75 | 21.25 | 4.1 | 6.8 | 35.0 | 37.7 | 27.3 |
| | A2 | 5-36 | 10YR 3/3 | l | 5 | 5 | 0 | | -3.38 | | 9.0 | 5.7 | 35.8 | 37.4 | 26.8 |
| | 2Bt | 36-68 | 10YR 4/4 | c | 20 | 10 | 5 | | -2.43 | | 10.2 | 1.8 | 30.5 | 28.6 | 40.9 |
| | 2Btk | 68-118 | 10YR 5/4 | cl | 20 | 10 | 5 | I | 9.85 | | 35.2 | 1.2 | 34.1 | 37.6 | 28.3 |
| | 3Bk | 118-148 | 2.5Y 6/3 | sil | 0 | 0 | 0 | I+ | 17.95 | | 48.8 | 0.6 | 7.1 | 72.7 | 20.2 |
| JVS-16 | A | 0-11 | 10YR 4/2 | c | 10 | 0 | 0 | | -1.90 | -6.46 | 0.8 | 6.8 | 28.9 | 38.9 | 32.2 |
| | 2A1 | 11-31 | 10YR 4/2 | c | 5 | 15 | 0 | | -3.10 | | 0.6 | 6.6 | 29.6 | 37.5 | 32.9 |
| | 2A2 | 31-37 | 10YR 4/4 | c | 5 | 10 | 0 | | -1.09 | | 0.5 | 5.6 | 28.9 | 37.7 | 33.4 |
| | 2Bt1 | 37-66 | 10YR 6/2 | c | 8 | 10 | 10 | | -5.30 | | 0.4 | 1.2 | 22.2 | 40.0 | 37.8 |
| | 2Bt2 | 66-84 | 10YR 6/2 | c | 5 | 10 | 2 | | 1.63 | | 24.6 | 0.9 | 26.4 | 38.4 | 35.2 |
| | 2Bk | 84-130 | 2.5Y 6/3 | c | 10 | 5 | 5 | | 3.31 | | 20.0 | 0.6 | 42.6 | 32.2 | 25.2 |
| JVS-17 | Ak1 | 0-5 | 10YR 4/3 | c | 5 | 5 | 0 | | -0.82 | 43.21 | 3.5 | 6.8 | 44.6 | 36.0 | 19.4 |
| | Ak2 | 5-13 | 10YR 4/3 | c | 5 | 8 | 0 | | 0.28 | | 23.4 | 4.6 | 36.5 | 37.9 | 25.6 |
| | Bk1 | 13-38 | 10YR 5/3 | c | 5 | 5 | 1 | I | 6.62 | | 32.8 | 1.4 | 34.4 | 38.1 | 27.5 |
| | Bk2 | 38-66 | 10YR 5/3 | c | 10 | 5 | 0 | I+ | 9.79 | | 38.4 | 1.1 | 34.8 | 35.9 | 29.3 |
| | Bk3 | 66-85 | 10YR 6/3 | c | 10 | 5 | 0 | I+ | 6.93 | | 39.4 | 0.7 | 36.1 | 36.6 | 27.3 |
| | Bk4 | 85-140 | 10YR 6/3 | c | 10 | 5 | 0 | II | 20.40 | | 39.8 | 0.6 | 36.5 | 36.6 | 26.9 |
| JVS-18 | A | 0-5 | 10YR 5/3 | sl | 5 | 0 | 0 | | n.d. | n.d. | n.d. | n.d. | n.d. | n.d. | n.d. |
| | Bt | 5-24 | 7.5YR 5/5 | cl | 5 | 5 | 5 | | n.d. | | n.d. | n.d. | n.d. | n.d. | n.d. |
| | 2Bt | 24-35 | 7.5YR 5/5 | scl | 40 | 0 | 0 | I | n.d. | | n.d. | n.d. | n.d. | n.d. | n.d. |
| | 3Bk1 | 35-77 | 10YR 5/4 | sl | 10 | 15 | 20 | II | n.d. | | n.d. | n.d. | n.d. | n.d. | n.d. |
| | 3Bk2 | 77-93 | 10YR 5/4 | sl | 20 | 15 | 20 | II- | n.d. | | n.d. | n.d. | n.d. | n.d. | n.d. |
| JVS-19 | A | 0-6 | 10YR 4/4 | l | 3 | 0 | 0 | | n.d. | n.d. | n.d. | n.d. | n.d. | n.d. | n.d. |
| | Bw | 6-38 | 10YR 4/4 | cl | 10 | 5 | 5 | | n.d. | | n.d. | n.d. | n.d. | n.d. | n.d. |
| | 2Bw | 38-64 | 10YR 5/3 | cl | 20 | 10 | 20 | I | n.d. | | n.d. | n.d. | n.d. | n.d. | n.d. |
| | 2C | 64-103 | 10YR 6/4 | sl | 10 | 0 | 40 | I | n.d. | | n.d. | n.d. | n.d. | n.d. | n.d. |
| JVS-20 | Ak1 | 0-4 | 10YR 3/3 | sl | 15 | 5 | 5 | I | n.d. | n.d. | n.d. | n.d. | n.d. | n.d. | n.d. |
| | Ak2 | 4-48 | 10YR 4/3 | scl | 15 | 5 | 20 | I | n.d. | | n.d. | n.d. | n.d. | n.d. | n.d. |
| | Btk | 48-59 | 10YR 5/3 | sc | 15 | 5 | 30 | I | n.d. | | n.d. | n.d. | n.d. | n.d. | n.d. |
| | 2Bk1 | 59-115 | 10YR 6/3 | sl | 30 | 5 | 5 | I | n.d. | | n.d. | n.d. | n.d. | n.d. | n.d. |
| | 2Bk2 | 115-127 | 10YR 6/3 | sl | 20 | 10 | 5 | I | n.d. | | n.d. | n.d. | n.d. | n.d. | n.d. |

/1 Maximum stage of carbonate development in the profile, terminology of Gile and others (1966) and Bachman and Machette (1977).
/2 Secondary carbonate (g/cm2), after Machette (1978, 1985). Bulk density was estimated from texture (Rawls, 1983).
/3 Percent CaCO3 by dilution with sulfuric acid and titration with sodium hydroxide using methods of Soltanpour and Workman (1981).
/4 Percent organic matter by wet titration using methods of Soltanpour and Workman (1981).
/5 Grain-size data are given in percent by weight of the less than 2 mm fraction: sand (>50um), silt (2-50um), clay (<2um).
Sand fractions by dry sieve with prior removal of organic matter and CaCO3. Silt fractions by pipette with prior removal of organic matter and CaCO3.

arid northern sites. Parameters used to distinguish soils on surfaces of different ages in the southern sites where the elevation ranges from 2200 to 2400 m are the amount of translocated clay in the B horizon and the degree of accumulation of $CaCO_3$ in the profile. This latter property is determined by visually assessing the maximum carbonate stage in the profile and by estimating the amount of secondary carbonate ($g/cm^2$) from laboratory data using the method of Machette (1985). The northern soils, ranging from 2450 to 2800 m elevation, are distinguished by the amount of translocated clay in the B horizon, and the depth of carbonate leaching.

Two soil profiles (JVS-10 and 15) were examined on the surface of Qml, the only deposit in RAG 1. They have thick (37-82 cm) argillic horizons with about a 10% increase in clay from that estimated for the parent material, 10YR hues, chromas of 4-6 and low $CaCO_3$ values to a depth of 70 cm (table A4). The low $CaCO_3$ values are attributed to leaching in the upper part of the profile. No deposit considered to be equivalent in age has been recognized in the drier southern part of the study area for comparison.

Soil profiles from three trenches (JVT-1,2,3), one soil pit (JVS-12) and two roadcuts (JVS-7,8) were examined in the Reeder Canyon area (tables A3 and A4). Although the soils data obtained from these profiles discriminate only slightly between geomorphic surfaces of different ages, the data do support the distinction of RAG 2 from RAG 3. Since all of the soils are calcareous and have formed from calcareous parent materials, the most useful relative age indicator is the maximum carbonate stage for each profile. Soils formed in very gravelly parent material on the oldest fan, af1 (profiles JVT-1A,3A; JVS-8), are characterized by an A horizon in gravelly colluvium directly overlying a Bk or K horizon (stage II-III carbonate) in very gravelly alluvium. There is little evidence in these profiles for an argillic horizon. The soil profile in very gravelly alluvium on an intermediate fan surface (af3), exposed in a roadcut (JVS-8), has a K horizon (stage III-) overlying a Btk horizon. The relationship between these horizons suggests that two periods of soil formation are represented in this profile: an early stage characterized by clay translocation and illuviation in the Btk horizon and a later stage when $CaCO_3$ was precipitated. The existence of a two-stage sequence of soil development implies that a significant time interval, on the order of tens to hundreds of thousands of years, has elapsed since soil formation commenced on the af3 surface. The lack of evidence for an argillic horizon on the older af1 surface could be due to its being masked by $CaCO_3$ or to erosion which removed the upper parts of the profile, exposing only the calcareous lower portions of the soil. However, laboratory data for particle size (tables A3 and A4) do not indicate the existence of an engulfed argillic horizon.

Other soils in the southern part of the study area that have similar characteristics (stage I $CaCO_3$ in fine or stage II-III in coarse parent materials) are developed on the following RAG 2 deposits: the high terrace (t1) at the mouth of Littles Creek (JVS-13), the Littles Creek debris flow (JVS-6), the Seely Creek debris flow exposed in trench 5

(JVT-5), an alluvial fan on the east side of the graben that heads at the escarpment along the East Joes Valley fault (JVS-3), and the large landslide separating the drainages of Littles and Reeder Creeks (JVS-5).

However, the soil profile on the landslide surface (JVS-5), formed in fine debris flow sediments overlain by 12 cm of fine colluvium, is not as well developed as the soils in fine parent material on the af1 surface. JVS-5 has only stage I+ carbonate and little evidence of translocated clay (table A2). The discrepency in the degree of development may be due to instability of the surface of the landslide resulting in redeposition of debris flow materials and colluvium on its surface.

A soil profile (JVS-13) on the highest terrace at Littles Canyon (t1 on figure 4.6) is in fine-grained debris flow deposits and contains an A-Bk sequence with a maximum stage II+ carbonate. The carbonate development in this profile suggests that the soil is older than the fine soils on the Reeder Creek af1 surface which have stage I-II.

The soil profile in trench 5 (JVT-5) is similar in the degree of development (stage II) to the Littles Creek debris flow and to the t1 terrace. The large alluvial fan on the east side of Joes Valley Reservoir (fig. 4.2) has an A-Bk profile with stage II carbonate formed in gravelly parent material (JVS-3).

The type of soil development in the Black Canyon area is transitional in nature between the arid conditions near the reservoir to the south and the less arid conditions on the moraines to the north. The resulting soils have weaker calcic horizons than the more southern areas and stronger argillic horizons. RAG 2 at Black Canyon is represented by the highest terrace (t1) and by a debris flow within the graben (location of soil pit JVS-1, plate 2). This terrace falls on a projected surface extending from the Qm2 terminal moraine farther up the canyon to the debris flow in the graben (figure 4.5) suggesting that these three landforms are of approximately equivalent age. The height of the terrace above the creek and the soil profile development suggest that t1 is the same age as the high terrace at the mouth of Littles Creek. The soil profile on the t1 surface (JVS-18) contains a 19 cm thick argillic horizon with reddish hues (7.5 YR) and a maximum stage II carbonate. The soil formed in the debris flow (JVS-1) is in fine parent materials and consists of Ak-Bk horizons with a maximum of stage I+ carbonate. The degree of profile development suggests that redeposition of sediments has occurred on this slope resulting in a younger soil than on the original surface. To the south 1.25 km is a fan that is beheaded by a small (<1m) scarp along the Middle Mountain fault. The soil (JVS-2) formed in colluvium and alluvium over coarse gravel, has a K horizon (stage III carbonate).

In the northern part of the study area RAG 2 includes the intermediate moraines mapped as Qm2 on plate 2. Two soil pits are located on these moraines, JVS-14 and JVS-17. Since JVS-14 is in close proximity to the profiles on the older Qm1 moraine, differences in climate and vegetation are minimized and an accurate comparison between the soils on RAG 1 and

RAG 2 deposits can be made. The JVS-14 profile has an argillic horizon with a 4.6% increase in clay in contrast to the Qm1 soils (JVS-10,15) which have a 13% increase from the A to the B horizon. The depth of carbonate leaching in the younger profile is only 21 cm and soil color is lower in chroma with 10YR hues. The other profile (JVS-17) on the Qm2 surface is on the sharp outer crest of the Jordan Creek moraine. This site appears to be drier than the other soil pit locations and the soil has higher $CaCO_3$ values than JVS-14 and lacks an argillic horizon. Although there is evidence for carbonate leaching in the upper 13 cm of the profile, this soil is considered anomalous and a poor example for the degree of soil development on RAG 2 surfaces.

Soils developed on RAG 3 surfaces were described at Reeder Canyon, Black Canyon, and at the northern end of the Joes Valley graben. At Reeder Canyon, the af4 surface is a continuous surface inset into the older higher fan remnants. The soil on the af4 surface is exposed in trench 2 (profile JVT-2) and has an argillic overlying a Bk horizon with stage II carbonate in very gravelly parent material. There is no evidence for a two-stage soil development sequence on this surface as there is on the older RAG 2 fan surfaces.

Three profiles were described in loess overlying the af1 surface (JVT-1B,1C; JVS-12). Although this fan remnant is inferred to be in RAG 2, the overlying loess is in RAG 3. Stratigraphic relations in trench 1 show that these deposits and soil are younger than the gravelly alluvium that comprises most of af1. The three soil profiles have 7.5 YR and 10YR hues and a maximum of stage I and II carbonate. The two profiles (JVT-1B,1C) for which lab data are available show no significant increase in the percent of clay in the B horizon and no field evidence for clay translocation, although clay films are visible in the third profile (JVS-12). Evidence from trench 1 (see section 4.5.2.1) indicates that this soil was forming during continual loess accumulation with periods of slower deposition indicated by the presence of buried soils.

In trench 3, a soil profile (JVT-3B) in fine deposits is in a stratigraphic position comparable to JVT-1B,1C, and JVS-12 and is presumably similar in age to the three profiles discussed above. This soil has 10YR hue and stage II carbonate. At a depth of 86 cm is a buried B horizon which appears to have been subsequently engulfed by carbonate to form a K horizon.

In summary, the soils on RAG 3 deposits in the Reeder Creek area are characterized by the presence of an argillic horizon and stage II carbonate in coarse materials (JVT-2) and stage I-II carbonate in fine materials.

At Black Canyon, RAG 3 includes the intermediate terraces, t2 and t3, as well as the alluvial fan at the mouth of the canyon. The soils on these surfaces (JVS-4,19,20) have minimal argillic horizons and stage I-I+ carbonate.

In the northern part of the study area, RAG 3 is represented by the innermost terminal moraines that are located at the margin of the graben mapped as Qm3 on plate 2. The only soil profile described on the surface of Qm3 (JVS-16) has a well developed argillic horizon with 10YR hues, a 4.4% increase in clay, and carbonate leaching to a depth of 66 cm. These characteristics which are similar to the profile on Qm2 in pit JVS-14, could be the result of a surface that is substantially younger than the Qm2 moraine with a faster rate of soil development due to higher precipitation or, alternatively, the Qm3 moraine may be only slightly younger than the Qm2 moraine. The similar surface morphology of the Qm2 and Qm3 moraines suggests that there is relatively little age difference between them.

The RAG 4 deposits on which soil profiles were described are alluvial terraces 7 m above Seely Creek and 4 m above Lowry Water. The Seely Creek terrace, at an elevation of 2145 m where the m.a.p. is 35.5 cm, has a soil profile (JVS-9) consisting of an A horizon 27 cm thick that is partially leached of carbonate in the upper 9 cm overlying a zone of stage I+ carbonate that forms thin (<1mm) coatings on the undersides of gravel clasts and extends to a depth of 210 cm. The unexpectedly high $CaCO_3$ content in the lower horizons may be due to the inclusion of fine particles of limestone in the parent material and may not reflect the degree of pedogenesis. The $CaCO_3$ coatings provide a more realistic asessment of pedogenic carbonate accumulation.

The Lowry Water terrace, at an elevation of 2450 m, has a soil profile (JVS-11) that reflects the higher precipitation at this locality than at the Seely Creek terrace with a redder B horizon and leached $CaCO_3$ to a depth of 33 cm (table 2) with stage I carbonate in 1 mm thick coatings on clasts below this depth. A quantitative comparison of the amount of $CaCO_3$ with the JVS-9 profile is not possible since lab data are not available for this profile.

In order to quantitatively compare the degree of soil development among profiles on surfaces of different ages, soil development indices (Harden, 1982; Harden and Taylor, 1983) were calculated for each profile (table A5). These indices give a measure of the degree of soil development using several field properties found to change with time. The index allows comparison of soil properties, either singly or in combination, for the entire profile or the individual horizons. Calculation of these indices takes into account parent material differences but does not compensate for faster rates of soil development in fine-textured parent materials. Soil profile properties used in this study to calculate the all properties index are: clay films, texture, rubification, color-paling, color-lightening, structure, consistence, and melanization. Clay films were absent in most of the profiles described, especially in gravelly parent materials, but this property is included using a zero value in the summation of the profile index so that the profiles could be compared with indices calculated for profiles containing argillic B horizons.

Table A5: Soil development indices for profiles in Joes Valley

| Profile | SOIL PROPERTIES /1 RUBIFI-CATION | MELANI-ZATION | COLOR PALING | COLOR LIGHTENING | TEXTURE | STRUCTURE | DRY CONSISTENCE | CLAY FILMS | HARDEN INDICES /2 NON-ARID INDEX | ARID INDEX | ALL PROPE INDEX |
|---|---|---|---|---|---|---|---|---|---|---|---|
| JVT1A | 0.1070 | 0.0453 | 0.0000 | 0.3199 | 0.0614 | 0.1891 | 0.0329 | 0.0000 | 0.0673 | 0.0912 | .0.1142 |
| JVT1B | ,0.1147 | 0.1319 | 0.1430 | 0.2259 | 0.1143 | 0.3911 | 0.1300 | 0.0000 | 0.1260 | 0.1251 | 0.1636 |
| JVT1C | 0.0817 | 0.1241 | 0.0000 | 0.0338 | 0.0824 | 0.4800 | 0.0000 | 0.0000 | 0.1096 | 0.0850 | 0.1177 |
| JVT2 | 0.0668 | 0.1468 | 0.0000 | 0.0895 | 0.0474 | 0.3118 | 0.0350 | 0.0000 | 0.0836 | 0.0736 | 0.1043 |
| JVT3A | 0.0430 | 0.1103 | 0.0000 | 0.1580 | 0.0804 | 0.3512 | 0.0189 | 0.0000 | 0.0784 | 0.0896 | 0.1110 |
| JVT3B | 0.1650 | 0.1943 | 0.0000 | 0.2192 | 0.1081 | 0.2089 | 0.0281 | 0.0348 | 0.0924 | 0.0997 | 0.1394 |
| JVT4 | 0.0619 | 0.0489 | 0.0000 | 0.0000 | 0.0000 | 0.1280 | 0.0000 | 0.0000 | 0.0341 | 0.0183 | 0.0350 |
| JVT5 | 0.1195 | 0.0228 | 0.0000 | 0.1395 | 0.0000 | 0.1565 | 0.0000 | 0.0000 | 0.0427 | 0.0423 | 0.0654 |
| JVT6A | 0.3123 | 0.0818 | 0.0000 | 0.0762 | 0.0169 | 0.2381 | 0.0152 | 0.1993 | 0.1234 | 0.0780 | 0.1373 |
| JVT6Ab* | 0.3193 | 0.0743 | 0.0000 | 0.0789 | 0.0234 | 0.1930 | 0.0211 | 0.2753 | 0.1334 | 0.0845 | 0.1472 |
| JVT6B | 0.3059 | 0.0384 | 0.0422 | 0.0354 | 0.1726 | 0.3883 | 0.0773 | 0.1636 | 0.1667 | 0.1256 | 0.1868 |
| JVT6Bb* | 0.3384 | 0.0384 | 0.0483 | 0.0406 | 0.1815 | 0.3836 | 0.0885 | 0.1873 | 0.1674 | 0.1328 | 0.1881 |
| JVT6C | 0.2519 | 0.0937 | 0.0330 | 0.0000 | 0.1872 | 0.3378 | 0.1604 | 0.3365 | 0.1954 | 0.1507 | 0.2154 |
| JVT6Cb* | 0.2377 | 0.0163 | 0.0000 | 0.0000 | 0.2376 | 0.3397 | 0.1869 | 0.4840 | 0.2146 | 0.1783 | 0.2432 |
| JVS1 | 0.1256 | 0.0081 | 0.0000 | 0.1241 | 0.0138 | 0.1937 | 0.0269 | 0.0000 | 0.0526 | 0.0512 | 0.0726 |
| JVS2 | 0.1053 | 0.0409 | 0.0000 | 0.2400 | 0.0395 | 0.1135 | 0.0688 | 0.0134 | 0.0545 | 0.0679 | 0.0927 |
| JVS3 | 0.0000 | 0.0362 | 0.1128 | 0.1561 | 0.0000 | 0.3487 | 0.0877 | 0.0000 | 0.0675 | 0.1177 | 0.1334 |
| JVS4 | 0.0489 | 0.0844 | 0.0051 | 0.0732 | 0.0370 | 0.1667 | 0.0515 | 0.0598 | 0.0640 | 0.0562 | 0.0799 |
| JVS5 | 0.1263 | 0.0298 | 0.2000 | 0.0500 | 0.0000 | 0.5922 | 0.0000 | 0.0738 | 0.1175 | 0.1309 | 0.1602 |
| JVS6 | 0.0354 | 0.0804 | 0.0856 | 0.0929 | -0.0156 | 0.4361 | 0.0540 | 0.0000 | 0.0843 | 0.0933 | 0.1028 |
| JVS7 | 0.0817 | 0.0194 | 0.0000 | 0.4221 | 0.1516 | 0.2000 | 0.0512 | 0.0000 | 0.0720 | 0.1178 | 0.1323 |
| JVS8 | 0.0186 | 0.0516 | 0.0420 | 0.2194 | 0.0000 | 0.4083 | 0.0576 | 0.0946 | 0.0901 | 0.1174 | 0.1312 |
| JVS9 | 0.0541 | 0.0370 | 0.0000 | 0.0964 | 0.0095 | 0.0429 | 0.0043 | 0.0000 | 0.0211 | 0.0219 | 0.0352 |
| JVS10 | 0.2381 | 0.1283 | 0.0000 | 0.0000 | 0.9980 | 0.2746 | 0.0867 | 0.2067 | 0.2761 | 0.2237 | 0.2930 |
| JVS10b* | 0.2441 | 0.1146 | 0.0000 | 0.0000 | 1.0080 | 0.2593 | 0.0888 | 0.2257 | 0.2772 | 0.2260 | 0.2958 |
| JVS11 | 0.0297 | 0.0770 | 0.0061 | 0.0000 | 0.0313 | 0.0765 | 0.0582 | 0.0000 | 0.0390 | 0.0246 | 0.0398 |
| JVS12 | 0.0863 | 0.1152 | 0.0046 | 0.1510 | 0.1532 | 0.5365 | 0.0653 | 0.3932 | 0.1928 | 0.1862 | 0.2076 |
| JVS13 | 0.0177 | 0.0655 | 0.0238 | 0.1589 | 0.0786 | 0.4530 | 0.0550 | 0.0000 | 0.0957 | 0.1099 | 0.1247 |
| JVS14 | 0.2779 | 0.0395 | 0.0000 | 0.1995 | 0.0791 | 0.2933 | 0.1432 | 0.1012 | 0.1335 | 0.1166 | 0.1620 |
| JVS15 | 0.2811 | 0.1653 | 0.0000 | 0.0929 | 0.3934 | 0.3964 | 0.1000 | 0.3836 | 0.2457 | 0.1952 | 0.2590 |
| JVS16 | 0.1160 | 0.0950 | 0.0000 | 0.0894 | 0.1590 | 0.4946 | 0.2477 | 0.2183 | 0.1815 | 0.1641 | 0.1943 |
| JVS17 | 0.0914 | 0.0218 | 0.0095 | 0.1402 | 0.0429 | 0.2583 | 0.2221 | 0.2473 | 0.1263 | 0.1315 | 0.1588 |
| JVS18 | 0.1401 | 0.1746 | 0.0045 | 0.0675 | 0.1864 | 0.4713 | 0.1032 | 0.1770 | 0.1789 | 0.1443 | 0.1752 |
| JVS19 | 0.0478 | 0.2696 | 0.0000 | 0.0000 | 0.0000 | 0.4741 | 0.0000 | 0.1083 | 0.1285 | 0.0832 | 0.1390 |
| JVS20 | 0.0182 | 0.2057 | 0.0341 | 0.0669 | 0.0626 | 0.2907 | 0.0000 | 0.1266 | 0.1005 | 0.0830 | 0.1136 |

/1 Numbers are weighted means of normalized properties calculated from field descriptions following the methods of Harden (1982) and Harden and Taylor (1983) and modified methods of Nelson and Taylor (1985).

/2 Numbers are weighted means of horizon indices. Properties used to calculate the non-arid index are rubification, melanization, texture, structure, dry consistence, clay films (Harden and Taylor, 1983). Properties used to calculat the arid index are color-paling, color lightening, texture, structure, dry consistence, clay films (Harden and Taylor 1983). The all properties index was calculated from all of the properties tabulated for each profile.

* Numbers are calculated for the buried soil in these profiles, excluding the overlying horizons.

Carbonate accumulation at depth within the profiles appears to be a major pedogenic characteristic distinguishing the soil profiles in the more arid part of the study area, but, except for the color-paling property, pedogenic carbonate is not taken into account by the Harden indices. The amount of carbonate accumulation in a profile is expressed by the carbonate stage (Gile and others,1966; Bachman and Machette, 1977) and by the estimated amount of secondary carbonate in a $cm^2$ column through the profile (Machette, 1985). The amount of secondary carbonate is estimated in tables A1 and A2 for those profiles with laboratory analyses for percent of $CaCO_3$. Because the soil development indices and the secondary carbonate are calculated relative to the same properties in the parent material, a change in the estimate for the parent material properties could significantly affect the profile indices. Because the soil parent materials in Joes Valley are derived from the calcareous rocks of the Wasatch Plateau, the $CaCO_3$ in the soil is not entirely the result of pedogenesis. The parent material estimates in gravelly materials are based on data from two profiles in gravelly alluvium that extend into the C horizon and from soil profiles in fine parent materials in deep trenches. The estimates for original $CaCO_3$ content are applied as consistently as possible to each profile.

The soil profiles are divided into two groups, calcareous soils from the southern part of the study area (table A1) and those from the northern part where the carbonate has been mostly leached from the profile (table A2). In general, the soils on RAG 2 deposits have a higher value for secondary carbonate than the soils on RAG 3 deposits, although there is some overlap in these values. The RAG 2 and RAG 3 profiles, however, cannot be distinguished by the Harden indices, probably because the soils on these intermediate age surfaces are complex, in some cases resulting from the superposition of a soil profile on a pre-existing one and in other cases the upper part of the soil having been stripped by erosion on the alluvial fan surface.

## A.3 Correlation of the Joes Valley relative age groups with age dated glacial sequences

The stratigraphic terminology and methodology that are used to subdivide deposits of different relative ages in central Utah are reviewed by Sullivan and others (1986) and these can be applied to the deposits in the Joes Valley area. In the Rocky Mountain region relative chronologies are based on weathering characteristics of deposits from the last two major glaciations, the Bull Lake and Pinedale. In this report the terms Bull Lake and Pinedale refer to these glaciations, and the four relative age groups identified in Joes Valley are assigned numerical ages on the basis of correlation of the glacial sequence on the Wasatch Plateau with the Rocky Mountain glacial sequence (Birkeland and Shroba, 1974, 1984; Mahaney, 1978; Madole and Shroba, 1979; Pierce, 1979; Colman and Pierce, 1981; 1983; 1986; Birkeland, 1985). Although characteristics vary somewhat with locality, Bull Lake deposits in the Rocky Mountains often have moderately to strongly developed reddish argillic B horizons, contain weathered clasts, and are often dissected or have subdued surface topography. Bull Lake moraines have been dated at 140 ka at West Yellowstone (Pierce and others, 1976) and may include moraines dated at 60 ka near McCall, Idaho (Colman and Pierce, 1981; 1986). Deposits from the later stages of the Pinedale glaciation, dated at 14 to 30 ka (Pierce, 1979; Porter and others, 1982) have more weakly developed B horizons, few weathered clasts, and are generally undissected and retain an irregular surface topography. Latest Pinedale deposits, about 11 to 14 ka (Porter and others, 1982) have weak cambic B horizons. Soils on Holocene surfaces, <10 ka, also consist of very weakly developed profiles.

Because there are no independently dated glacial deposits on the Wasatch Plateau, we use relative age dating techniques, especially soil development, to compare them with glacial deposits in other areas within the Rocky Mountains that have been independently dated. The closest dated moraine sequence is in Little Cottonwood and Bells Canyons on the west side of the Wasatch Mountains, where moraines interfinger with deposits from Lake Bonneville. The sequence has been interpreted most recently by Madsen and Currey (1979) to include evidence for two canyon-mouth glaciations separated by a period of soil development. The earlier glacial advance is correlated with marine oxygen isotope stage 6 (approximately 130-150 ka), the intervening soil is $^{14}C$ dated at about 26 ka, and the second canyon-mouth glaciation is inferred to have commenced about 19 ka, followed by a "midcanyon deglacial pause prior to 12.3 ka, and an upper canyon deglacial pause prior to 7.5 ka " (Madsen and Currey, 1979).

The subdued surface morphology and thick reddish argillic soils on the surface of the oldest moraine recognized on the Wasatch Plateau (Qm1 on plate 2), included in RAG 1, suggest deposition during the Bull Lake glaciation (130-150 ka). The two younger sets of moraines in Joes Valley (Qm2 and Qm3), included in RAG 2 and RAG 3, are not distinguishable by surface morphology or degree of soil development suggesting that the time between deposition of the outer moraines (Qm2) and deposition of the inner moraines (Qm3) was not sufficiently long to produce a recognizably greater degree of soil development on the older surfaces. These two sets of moraines are similar to Pinedale moraines dated at approximately 20 and 14 ka elsewhere (Pierce, 1979; Colman and Pierce, 1981; 1986; Porter and others, 1983; Birkeland, 1985; Madole, 1986). These age estimates for RAG 2 and RAG 3 deposits in the Joes Valley area are consistent with the lack of distinction of the deposits by characteristics other than geomorphic position. Radiocarbon dates from basal organic material deposited in closed depressions on the surface of Qm2 after the glacier retreated from this position fall in the range 6-9 ka (Appendix B) supporting the latest Pleistocene (10-30 ka) age estimates for the deposition of the two sets of moraines. The age of RAG2 and RAG3 deposits in the southern part of the study area is considered to be a minimum because the correlation of these deposits with moraines is tenuous and because the degree of soil development on these surfaces is greater than one would expect for deposits of latest Pleistocene age. RAG 4 deposits, consisting of alluvial terraces about 2 to 8 m above the modern floodplain, have minimal soil development and are considered to be Holocene, <10 ka.

# Appendix B

# Radiocarbon Dates

Table B.1: Radiocarbon dates for samples from Joes Valley, Utah.

| Sample No. | C-13 corrected age (yrs BP) | C-13/C-12 | Laboratory | Lab. number |
|---|---|---|---|---|
| JVT-4A | 5005 + 215 | -23.8 | Krueger | GX-10051 |
| JVT-4-11-2 | 6525 + 220 | -23.8 | Krueger | GX-9969 |
| JVT-3A | 2335 + 150 | -24.0 | Krueger | GX-10048 |
| JVT-3B | 3975 + 200 | -24.0 | Krueger | GX-10049 |
| JVT-3C | 6100 + 195 | -23.4 | Krueger | GX-10050 |
| JVS-15 | 3310 + 100 | -22.12 | Beta | Beta-10858 |
| JVS-17 | 6390 + 150 | -23.05 | Beta | Beta-10859 |
| JVS-21-A1 | 9150 + 130 | -29.11 | Beta | Beta-10860 |
| JVS-21-B1 | 7300 + 170 | -26.23 | Beta | Beta-10861 |
| JVS-22-A1 | 5860 + 100 | -22.91 | Beta | Beta-10862 |
| JVS-22-B1 | 4590 + 90 | -22.82 | Beta | Beta-10863 |
| JVT-6-18-11 | 1400 + 230 | -28.0 | Beta | Beta-10864 |
| JVT-6-19A | 900 + 70 | -26.00 | Beta | Beta-10865 |
| JVT-6-19B | 1630 + 80 | -25.73 | Beta | Beta-10866 |

# Appendix C

## Amino Acid Analyses

Table C.1: D-alloisoleucine/L-isoleucine ratios in the total (free + peptide-bound) amino acid fraction and calculated ages for Oreohelix cf. strigosa from fine-grained sediments at the base of Trench 6, Scad Valley.

| AAR Lab No. (Univ. of Colo.) | Depth below surface (m) | No. of sample preparations | Mean Total alle/Ile ratio* | Minimum age estimates (ka)# | Sample location in trench 6 (see figure 4.2) |
|---|---|---|---|---|---|
| AAL-4162 | 4.0-4.5 | 6 | 0.1110 + 0.0241 | 180-265 | station 37.5 |
| AAL-4163 | 3.5 | 6 | 0.1183 + 0.0226 | 190-280 | station 31 |
| AAL-4164 | 3.0 | 6 | 0.0942 + 0.0062 | 150-220 | station 33 |

* alle/Ile ratio (peak area) measured using methods of Miller and Hare (1980). Mean ratios include one standard deviation. Extraneous values rejected using methods of Dixon (1965).

# Age calculated using a linear kinetic model of isoleucine racemization (equation 18 in Williams and Smith (1977)) with k' = 0.77, modern ratio of 0.025 for Oreohelix (Nelson, unpub. data), Arrhenius parameters determined for Vallonia by Nelson and others (1984), and values of constants in Arrhenius equation (no. 9 in Williams and Smith, 1977). Age calculated using an EDT (mean effective diagenetic temperature)(Wehmiller, 1977) for the Holocene estimated using instrumental mean annual temperatures in the region (NOAA, 1981), limited soil temperature data (Conrad, 1965, and unpub. data of Lael Harvey, Soil Conservation Service, Coalville, UT), and data of Miller and others (1982). Age calculated using an EDT for the late Quaternary in this region of 8 C less than present mean annual temperature (Nelson and others, 1984)(for example, Wehmiller and Belknap, 1982). Age range calculated using +/-0.25oC range in estimated EDT.

# ANALYSIS AND SUMMARY OF SEISMOGRAPHIC DATA RECORDED IN VICINITY OF JOES VALLEY DAM, EMERY COUNTY PROJECT, EASTERN WASATCH PLATEAU, UTAH

by

Walter J. Arabasz and Donna J. Williams
Department of Geology and Geophysics
University of Utah
Salt Lake City, Utah 84112

Technical Report to

U.S. Bureau of Reclamation
Seismotectonic Section
Denver, Colorado

Contract Monitor
Richard A. Martin

Contract No.: PO# 4 PG 40 13210
Principal Investigator: Walter J. Arabasz
Award Period: October 15, 1984 - June 30, 1985

November 1985
(Revised August 1986)

## Disclaimer

# CONTENTS

Appendix B. Station Data

Appendix C. Chronology of Seismic Events Recorded at Station TTUT with Duration of 30 sec or Greater, July 6-August 12, 1984

Appendix D. Summary of Information Relating to Seismic Exploration Activity (and Plate I) During 1984 Field Experiment

Appendix E. Focal Mechanism Data

Plate 1. Location of Seismic Exploration Lines, Summer 1984, Eastern Wasatch Plateau (submitted separately and reproduced as figure 4.1).

Plate 2. Location of Coal Mining Properties in Eastern Wasatch Plateau (submitted separately and reproduced as figure 5.1).

SUMMARY

During June to August 1984, a collaborative field experiment was carried out in the eastern Wasatch Plateau in central Utah by the University of Utah, the U.S. Bureau of Reclamation, and Woodward-Clyde Consultants. Up to 40 analog and digital seismographs were operated simultaneously within a 40x25 km area located in the eastern part of the Basin and Range-Colorado Plateau transition.

The cooperative earthquake-recording experiment had multiple objectives. Those relevant to this report relate chiefly to an understanding of the seismotectonics of the area and included: (1) hypocentral resolution of abundant mining-related and less abundant tectonic earthquakes (neighboring both vertically and laterally), especially in relation to an inferred subjacent detachment and to Holocene surface faulting in the Joes Valley area; (2) assessment of the level of microseismicity in the Joes Valley area and implications of observational seismology for an earthquake hazards evaluation of the Joes Valley Dam; and (3) confirmation and spatial mapping of variations in stress orientation earlier identified within this part of the Basin and Range-Colorado Plateau transition.

As part of the 1984 field experiment, a sub-array of up to nine analog seismographs was deployed and operated by the U.S. Bureau of Reclamation (USBR) from July 6 to August 12, 1984. The principal focus of this subarray was monitoring of the central and northern parts of Joes Valley and the immediate vicinity of Joes Valley Dam. Funding was subsequently provided by the USBR to the University of Utah for analysis of the analog data

collected by the USBR. The intention was to achieve processing of the USBR-collected data for hypocenter location, source mechanism (where possible), and magnitude of seismic events—in conjunction with the analysis of data recorded by the University of Utah and Woodward-Clyde Consultants.

This report describes and summarizes results of the analysis of seismographic data from the 1984 field experiment undertaken for the USBR. The scope of the report is limited to a description of experimental procedures, methods of analysis, and presentation of results. Data separately submitted to the USBR in computer-tape format include the listing of (1) standard parameters associated with hypocentral solution and size estimation for 475 seismic events located from the data set, and (2) all arrival-time data used for part (1). Interpretation of the results of the 1984 field experiment forms part of a companion report entitled, "Interpretation of Instrumental Seismicity and Contemporary Tectonics of the Eastern Wasatch Plateau Relevant to Seismic Exposure of the Joes Valley and Scofield Dams."

# 1. INTRODUCTION

## 1.1 Background

During June to August 1984, a multi-institutional seismic-monitoring experiment was carried out in the East Mountain-Joes Valley-Gentry Mountain area of the eastern Wasatch Plateau in central Utah (fig. 1.1). For convenience, we will refer to the field experiment as the EWP-84 experiment (for eastern Wasatch Plateau, 1984). The field experiment involved collaborative efforts by the University of Utah (U of U), the U.S. Bureau of Reclamation (USBR), and Woodward-Clyde Consultants (WCC) of San Francisco, California.

The field experiment was conceived as basic research to investigate the seismotectonics of the seismically active eastern Wasatch Plateau. Planning of the experiment dates from submission in August 1983 of a research proposal to the National Science Foundation by W.J. Arabasz of the University of Utah. The proposal entitled, "Characteristics of Coal-Mining-Induced and Tectonic Seismicity, Wasatch Plateau, Utah," included letters of intention from both the USBR and WCC (see Appendix A) to participate with independent funding in the proposed seismic-monitoring experiment in order to pursue objectives of respective engineering interest.

Funding to the University of Utah was awarded by the National Science Foundation in April 1984, and the collaborative field experiment was successfully carried out during the summer of 1984 (Arabasz and others, 1985). Up to 40 analog and digital seismographs were operated simultaneously within a 40 by 25 km area encompassing the central and a

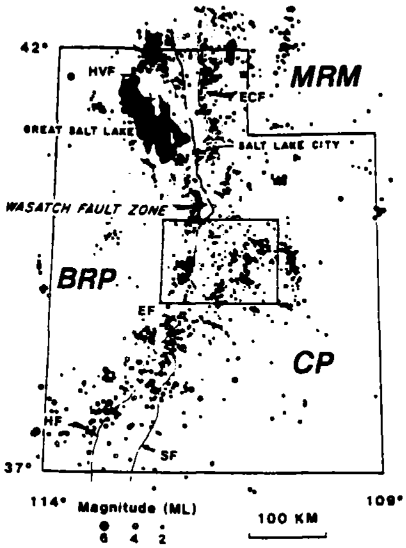


Index map of the Utah region showing the Intermountain seismic belt and the setting of the area of this study (rectangle). Seismicity is for the period July 1962-June 1978, based on University of Utah data (Arabasz et al. 1979). BRP indicates Basin and Range province. CP—Colorado Plateau. MRM—Middle Rocky Mts., HVF—Hansel Valley fault. ECF—East Cache fault. EF—Elsinore fault. HF—Hurricane fault. SF—Sevier fault.

b

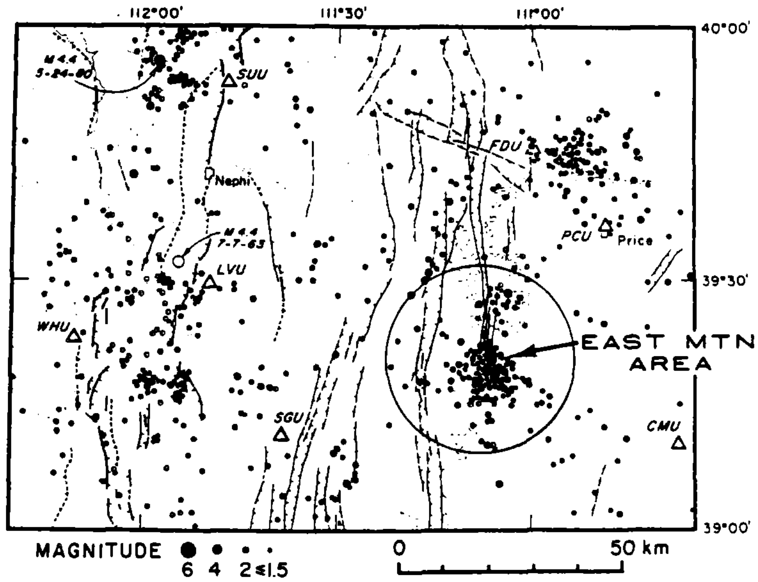


—Seismicity map of study area for the period: October 1, 1974-December 31, 1981, based on network monitoring by the University of Utah.

c

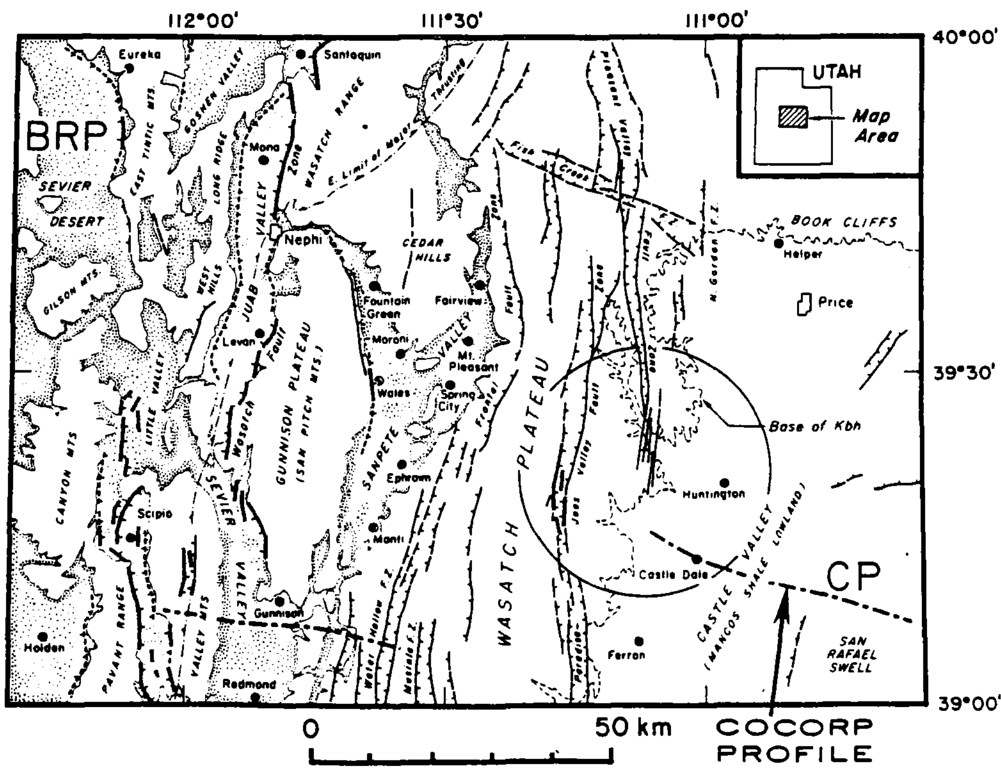


—Geologic sketch map of central Utah study area. Valleys floored with Quarternary alluvium shown by stippled pattern. Cenozoic normal faults shown by heavy lines, hachures on downthrown side; short dashes indicate concealed faults; broad pattern, late Quaternary fault scarps; BRP—Basin and Range province, CP—Colorado Plateau. Outcrop trace of Cretaceous Blackhawk Formation (Kbh) roughly defines erosional eastern boundary of Wasatch Plateau. Geology adapted from Stokes (1963), Witkind et al (1978), Bucknam and Anderson (1979), Doelling (1972), Burchfiel and Hickcox (1972).

Figure 1.1. Index maps showing seismotectonic setting of the study area in the eastern Wasatch Plateau of central Utah (adapted from McKee and Arabasz, 1982).

northern parts of Joes Valley as well as the adjacent areas of East Mountain and Gentry Mountain to the east (fig. 1.2).

Multiple objectives of the cooperative experiment included: (1) precise hypocentral resolution of intense mining-induced seismicity—both at and below levels of active underground coal mining in two target areas; (2) source characterization of mining-induced and tectonic earthquakes (neighboring both vertically and laterally), especially in relationship to an inferred subjacent detachment and to Holocene surface faulting in the Joes Valley area; (3) assessment of the level of microseismicity in the Joes Valley area and implications of observational seismology for an earthquake hazard evaluation of Joes Valley Dam (USBR); (4) digital recording of steeply incident waves, both at underground mine level and at surface, to investigate path/site effects on high-frequency spectral content (U of U); (5) investigation of near-field ground motion at mine level (WCC); and (6) confirmation and spatial mapping of variations in stress orientation earlier identified within this part of the Basin and Range—Colorado Plateau transition.

## 1.2 Purpose and Scope of This Report

As part of the EWP-84 experiment, seismologists from the U.S. Bureau of Reclamation—under the direction of R.A. Martin—deployed and operated a sub-array of up to nine analog and two digital seismographs (described further in section 2) from July 6 to August 12, 1984. The principal focus of the USBR efforts was seismic monitoring of the central and northern parts of Joes Valley and the immediate area of Joes Valley Dam (fig. 1.3).

After completion of the EWP-84 experiment, funding was provided to the

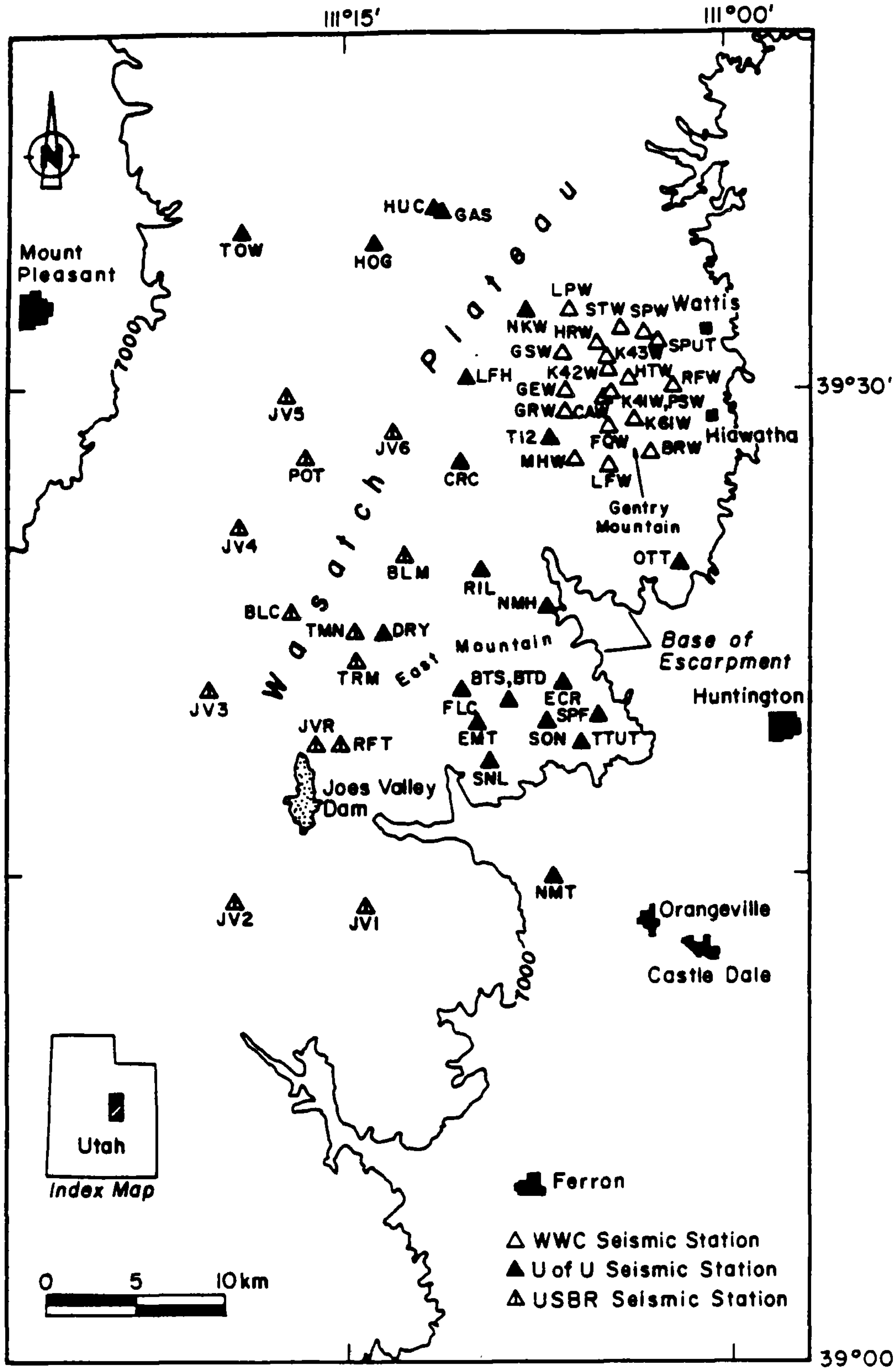


Figure 1.2. Map showing location of all seismograph stations operated during the EWP-84 field experiment.

University of Utah for analysis of the analog data collected by the USBR. Basically, the intention was to achieve processing of the USBR-collected data for hypocenter location, source mechanism (where possible), and magnitude of seismic events—in conjunction with the analysis of data recorded by the University of Utah and Woodward-Clyde Consultants. Efforts were to include the discrimination of artificial seismic events related to seismic exploration in the study area and to active underground coal mining.

The purpose of this report is to describe and summarize results of the analysis of seismographic data from the EWP-84 experiment undertaken for the USBR. Separately, data are being submitted to the USBR in computer-tape format including the listing of (1) standard parameters associated with hypocentral solution and size estimation for 475 seismic events located from the data set, and (2) all arrival-time data used for part (1).

Another aspect of the contractual effort for the USBR is an interpretation of "the resulting microseismicity data together with instrumental earthquake data recorded by the University of Utah Seismograph Stations with regard to contemporary tectonics of the Eastern Wasatch Plateau and implied earthquake hazards relative to Joes Valley & Scofield Dams." This specific task is the focus of a companion report by W.J. Arabasz entitled, "Interpretation of Instrumental Seismicity and Contemporary Tectonics of the Eastern Wasatch Plateau Relevant to Seismic Exposure of the Joes Valley and Scofield Dams." Accordingly, the scope here is limited to a description of experimental procedures, methods of analysis, and presentation of results from the EWP-84 experiment.

# 2. EARTHQUAKE RECORDING EXPERIMENT

## 2.1 Network Design

The EWP-84 experiment involved operation of a temporary network of up to 40 portable analog and digital seismographs in the study area (fig. 1.2). Field recording was carried out during a nine-week period between June 21 and August 25, 1984. Figure 1.2 and Appendix B summarize basic information on the geographic distribution and operational dates of stations included in the temporary network. (In Appendix B, note that stations installed and operated by the U of U have an identification code ending in the suffix U; those installed and operated by the USBR, the suffix B; and those installed and operated by WCC, the suffix W.) Given the collaborative involvement of the three research groups, the basic strategy in the field experiment was to establish three discrete subarrays (focused on three respective targets within the study area) while forming a broad-aperture network to cover the study area with a station spacing of about 10 km or less. Dense station coverage in the East Mountain and Gentry Mountain areas was essential for investigating very shallow, mining-related seismicity, especially for focal-depth control. The broad-aperture network, on the other hand, was designed to ensure an adequate geographic distribution of stations for uniform detection throughout the study area, good azimuthal control for earthquake epicenters, and adequate focal-depth and focal-sphere control for earthquakes that might occur in the 5-15 km depth range.

A primary target area selected by the U of U was the East Mountain area, which includes the Deer Creek Mine and the Wilberg Mine, two major underground coal mines of the eastern Wasatch Plateau. In addition, the U of U assumed the responsibility of deploying seismographs to supplement array coverage by the USBR and to ensure skeletal station coverage throughout the study area. As noted in section 1.2, the focus of USBR attention was the Joes Valley area. The USBR equipment involved telemetry capabilities such that six stations (JV1-JV6, fig. 1.2 and Appendix B) were installed by helicopter along the high-elevation flanks of the Joes Valley graben, and signals were telemetered by radio to two recording sites on Trail Mountain (near the location of station TRM in fig. 1.2). Topographic relief in the study area exceeds 1400 m. The principal target of the WCC subarray was the Gentry Mountain area—the location of the King Mine, another major underground coal mine.

The study area is covered by the University of Utah's regional seismic telemetry network (see triangles, fig. 1.1b) such that seismic events larger than about magnitude 1.5 in the study area are routinely located. As part of the EWP-84 experiment, two seismic telemetry stations were installed at stations TTUT and SPUT (fig. 1.2), and signals were telemetered to the University of Utah campus in Salt Lake City for temporary recording as part of the U of U regional seismic network (see, for example, Richins and others, 1984). Data from stations TTUT and SPUT were recorded continuously on helicorder drum recorders at a recording speed of 60 mm/min from mid-June to the end of August 1984 (see Appendix B).

As outlined in Appendix B, an effective broad-aperture network operated in the study area from about July 6 to August 12, 1984—effectively the same period of operation as the USBR sub-array in the Joes

Valley area. Supplemental coverage of the study area during this period was provided chiefly by U of U stations. Dense-array coverage of the East Mountain area by U of U stations was in place from the last week of June to about July 27. For the Gentry Mountain area, dense-array coverage by WCC stations was in place from about July 13 to August 25.

## 2.2 Instrumentation

The majority of portable seismographs deployed as part of the EWP-84 experiment were analog instruments of the smoked-paper type (Sprengnether Model MEQ-800). Vertical-component, 1-second-period seismometers were used throughout. For six of the USBR stations (JV1-JV6, fig. 1.2 and Appendix B), signals from remote sites were telemetered by radio to two recording sites where data were recorded on groups of smoked-paper type recorders. Analog recordings for the portable seismographs were made at speeds either of 60 mm/min or 120 mm/min. Quartz crystal clocks were synchronized with WWV radio signals for accurate time reference.

In addition to operating smoked-paper type seismographs, each of the research groups deployed a small number of digital-event-recorders (DER's) with 1-second seismometers for supplemental recording of waveform data. The University of Utah deployed three DER's fabricated at the U of U, each in a three-component mode. Two temporary telemetry stations installed by the U of U (stations TTUT and SPUT, fig. 1.2 and Appendix B) were of the standard short-period type, also with 1-second, vertical-component seismometers.

# 3. METHODS OF ANALYSIS

## 3.1 General Strategy

For the purpose of this report, attention is limited to a 38-day sample window from the EWP-84 experiment between July 6 and August 12, 1984. This period corresponds not only to the time frame of operation of USBR-operated stations, but also to the period of effective operation of the broad-aperture network in the study area (see section 2.1).

The general strategy adopted for analyzing the USBR-collected data—and for integrating data recorded by the U of U and WCC groups included the following principal elements:

I. SCANNING

A. Documentation of a complete chronology for the largest events in the EWP-84 study area during the USBR 38-day sample window: Seismograms from station TTUT, a high-performance station operating at an equivalent MEQ gain of approximately 90-96 db, were used as the basis for such a chronology, presented in Appendix C. All seismic events having a total signal duration of 30 sec or longer together with duration exceeding 7 sec from P-wave onset to 5 mm peak-to-peak amplitude decay were timed and measured. Further, the chronology was cross-checked with the USBR seismograms and also with the U of U and WCC data. The estimated magnitude threshold is about $M_L$ 1.0. The majority of the events in this sample appear to be events having mostly dilatational first-motions.

B. Documentation of a chronology above some magnitude threshold for all seismic events recorded at station JVR, located within a few kilometers of the Joes Valley Dam, during the 30-day sample period: 1900h July 13 to 1900h August 12: The extraordinarily large number of seismic events--predominantly mining related--recorded by the USBR stations preclude an exhaustive analysis and tabulation. For 5 days randomly selected from the record sample at station JVR (July 14, July 22, July 25, August 4, August 11), signals were timed at both JVRB and TTUT for all seismic events recorded at JVR with a total signal duration of 7 sec or longer. Hundreds of other readings at JVR have also been made as part of systematic scanning to identify a chronology of all significant events recorded by the USBR stations. Data for both the five special-study days and the general USBR chronology are included within the master phase list accompanying this report.

C. Completion of systematic scanning of USBR records to identify all seismic events above approximately 20 seconds in signal duration that might correspond to earthquakes close to the Joes Valley area and outside the areas of active mining. Here too, resulting data have been folded into the master phase list accompanying this report.

D. Completion of discrimination of all seismic events recorded by the University of Utah's regional seismic network during the EWP experiment: During the period June-August 1984, only 5 seismic events triggered and were located by the U of U network within 50 km of TTUT. As apparent from the following listing, none occurred during the USBR study window, and one recorded by the U of U local net on June 27th appears to have been one of the dilatational-type events.

| | | | | | | |
|---|---|---|---|---|---|---|
| 840608 | 21h52m | M2.5; | 49.2 km | NNE | of | TTUT |
| 840627 | 06h14m | Ml.8; | 3.9 km | SSW | of | TTUT |
| 840827 | 13h30m | Ml.4; | 3.5 km | N | of | TTUT |
| 840829 | 09h09m | M2.8; | 6.5 km | W | of | TTUT |
| 840830 | 10h25m | Ml.6; | 8.3 km | SW | of | TTUT |

II. DISCRIMINATION OF ARTIFICIAL SEISMIC EVENTS

A. Identification and elimination of all known artificial seismic events related to seismic exploration (involving both above-ground and in-hole shooting): Information was acquired from the U.S. Forest Service regarding the location and timing of seismic exploration blasting in the study area. USBR records were scrutinized to identify and correlate events in this category.

B. Identification of artificial seismic events related to active underground coal mining: This represented a massive task because mining-related events were found to make up most of the observed seismic activity in the study area. Discussion is deferred to section 5.

III. EARTHQUAKE LOCATIONS

A. Identification and location of seismic events local to the USBR study area.

B. Identification and location of representative seismic events elsewhere within the EWP-84 study area, including coordination of WCC and U of U data sets: Independently, WCC seismologists located a representative sample of the largest and/or distinctive events during the period July 14-August 12 that were local to their own network in the Gentry

Mountain area. A few dozen of the larger events in that area have been located using all available phase data from the EWP-84 experiment.

C. Development of an appropriate velocity model for hypocentral locations in the study area (see section 3.2).

IV. FOCAL MECHANISMS

A. Determination of a representative sample of focal mechanisms for both tectonic and mining-related seismic events in the study area (see section 5.2).

### 3.2 Velocity Structure

Upper-crustal velocity structure was specially investigated for the EWP-84 study area to provide a refined velocity model for the accurate location of seismic events. The model is based on available results from high-resolution seismic-reflection profiles and borehole sonic logs. Fortunately, the geological make-up of the study area involves a nearly horizontally stratified section of sedimentary rocks (see fig. 3.1). With the exception of the Joes Valley fault zone (fig. 1.1c), which has a reported maximum vertical displacement of 750-900 m, other faults in the study area east of the Joes Valley fault zone have maximum throws in the range of a few hundreds to a few tens of meters or less (Doelling, 1972).

McKee (1982) developed a simplified one-dimensional velocity model for the upper-crust in the eastern Wasatch Plateau by extrapolaton from the Book Cliffs area, 60 km to the east, where reversed refraction profiling

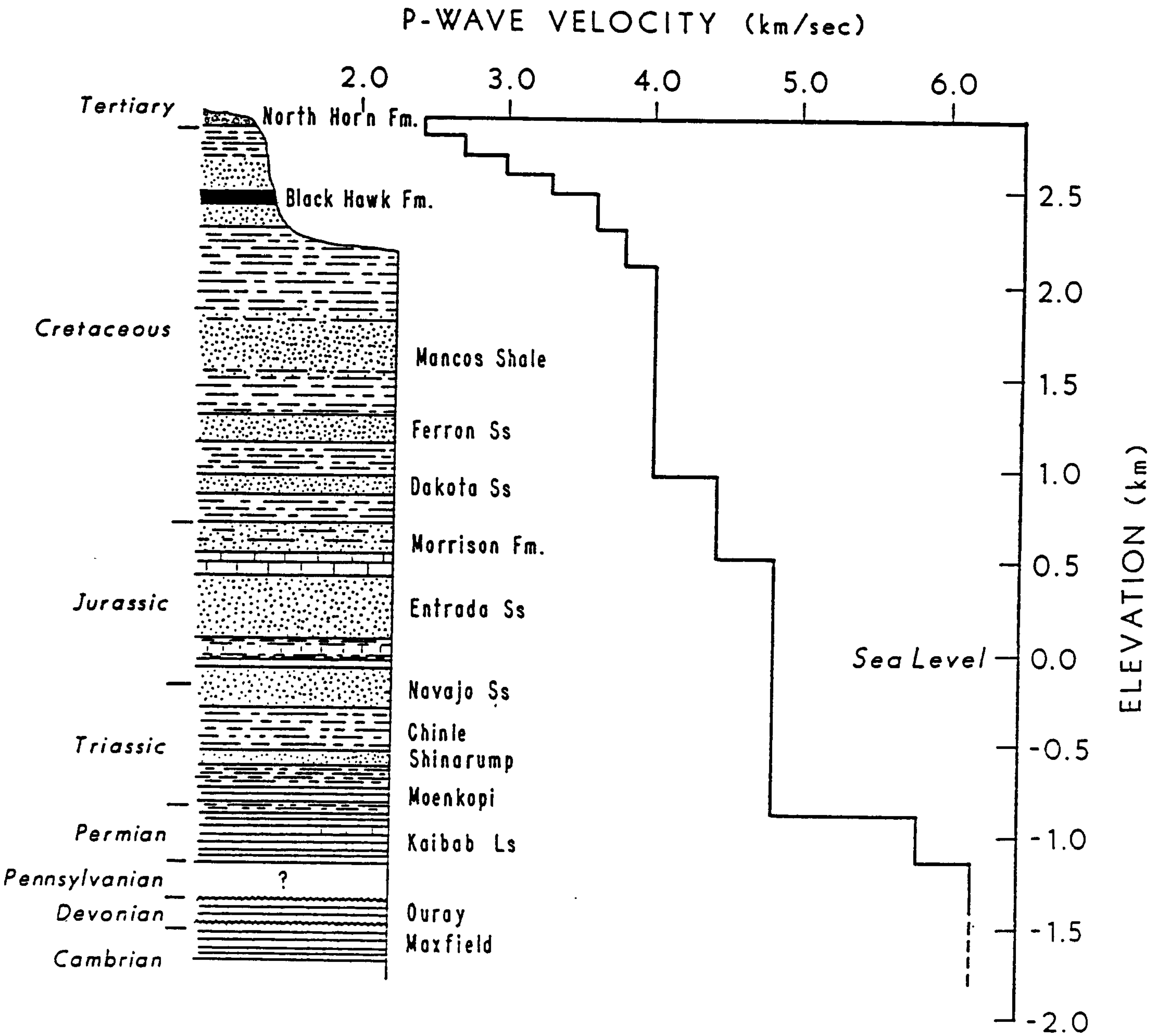


Figure 3.1. P-wave model (right) derived for the eastern Wasatch Plateau study area and the corresponding stratigraphic column (left) from Hintze (1973). Datum for the P-wave velocity model is 2.9 km above sea level.

had been carried out by Tibbetts and others (1966). Assuming a local datum of approximately 2,800 m above sea level for parts of the eastern Wasatch Plateau, McKee's (1982) upper-crustal velocity model has a layer 3.75 km thick with P-wave velocity, $V_p$, of 4.3 km/sec, overlying a layer more than 20 km thick with $V_p$=6.0 km/sec.

Figure 3.2 shows the location of high-resolution seismic-reflection profiles in the East Mountain area contracted by Utah Power and Light Co. and completed during 1980-82. The profiling involved frequencies up to 256 Hz, 6-12 fold coverage, 50-ft trace spacing, and maximum penetration to a two-way travel time of 2.0 sec, or roughly about 4 km below a datum 2,900 m above sea level. From stacking velocities reported for the profiles, vertical interval velocities were approximated by the commonly-used Dix solution (e.g., Landseth, 1982, p. 814).

Figure 3.3 summarizes the interval-velocity data derived from the high-resolution reflection profiling. A relatively steep velocity gradient within the uppermost kilometer is apparent. At depths below about 1 km, the vertical interval velocities are judged to be unreliable because the reflection profiling involved relatively small offsets. Under these circumstances, travel paths for reflections from deeper horizons approach the vertical leading to large uncertainties in resolving vertical interval velocities for the deeper layers (e.g., Landseth, 1982). Accordingly, velocities from 1.1 km to approximately 5 km below datum were determined from sonic logs of the Texas International Petroleum Federal #41-33, which is located in the southern portion of the study area (fig. 3.2). These logs were examined to determine vertical velocity changes. A mean value of velocity was estimated visually from the sonic curve for discrete

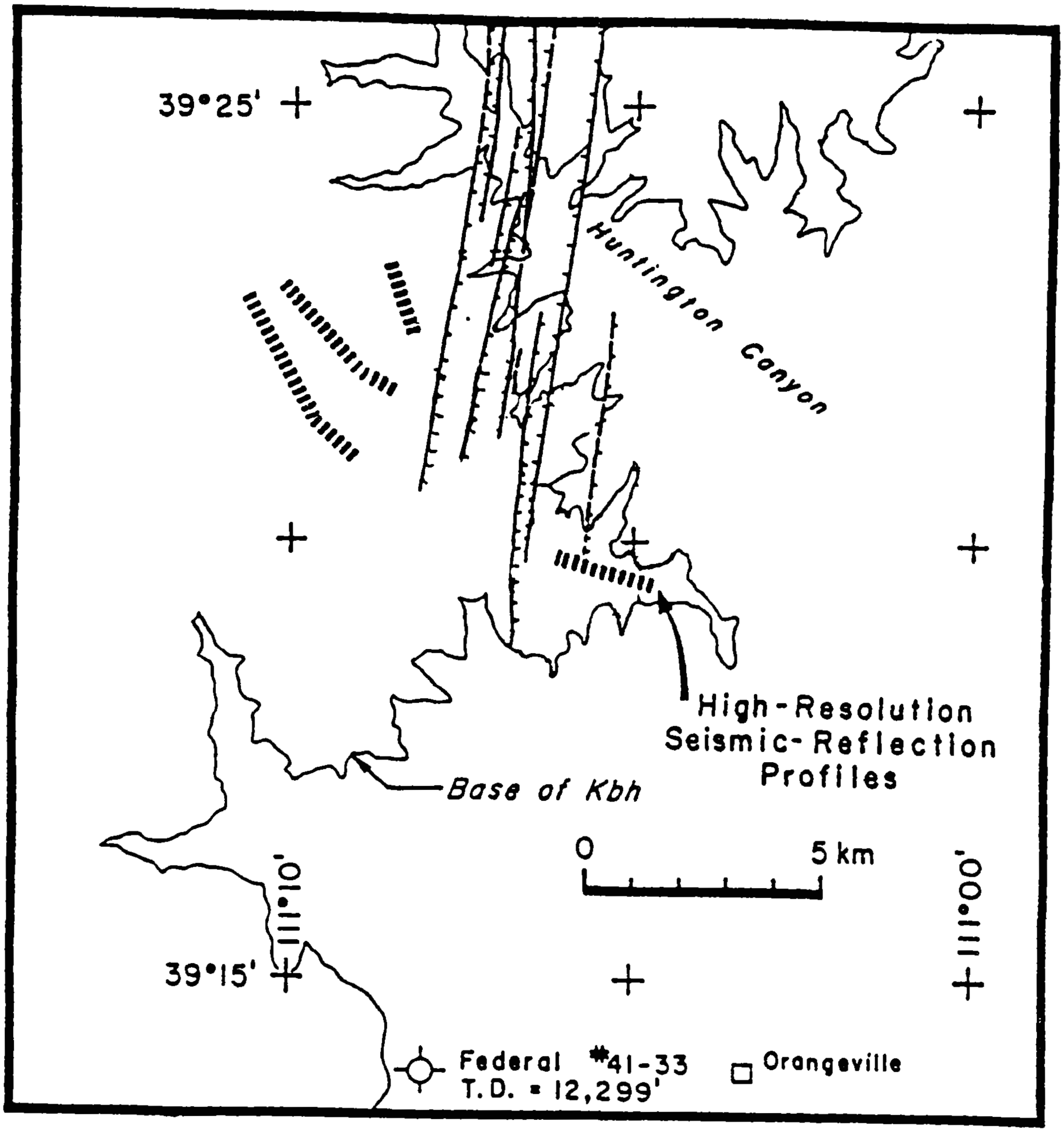


Figure 3.2. Map of the eastern Wasatch Plateau showing the location of high-resolution seismic-reflection profiles and an oil exploration well from which sonic logs were available. Both data sets were used to derive a P-wave velocity model for the study area.

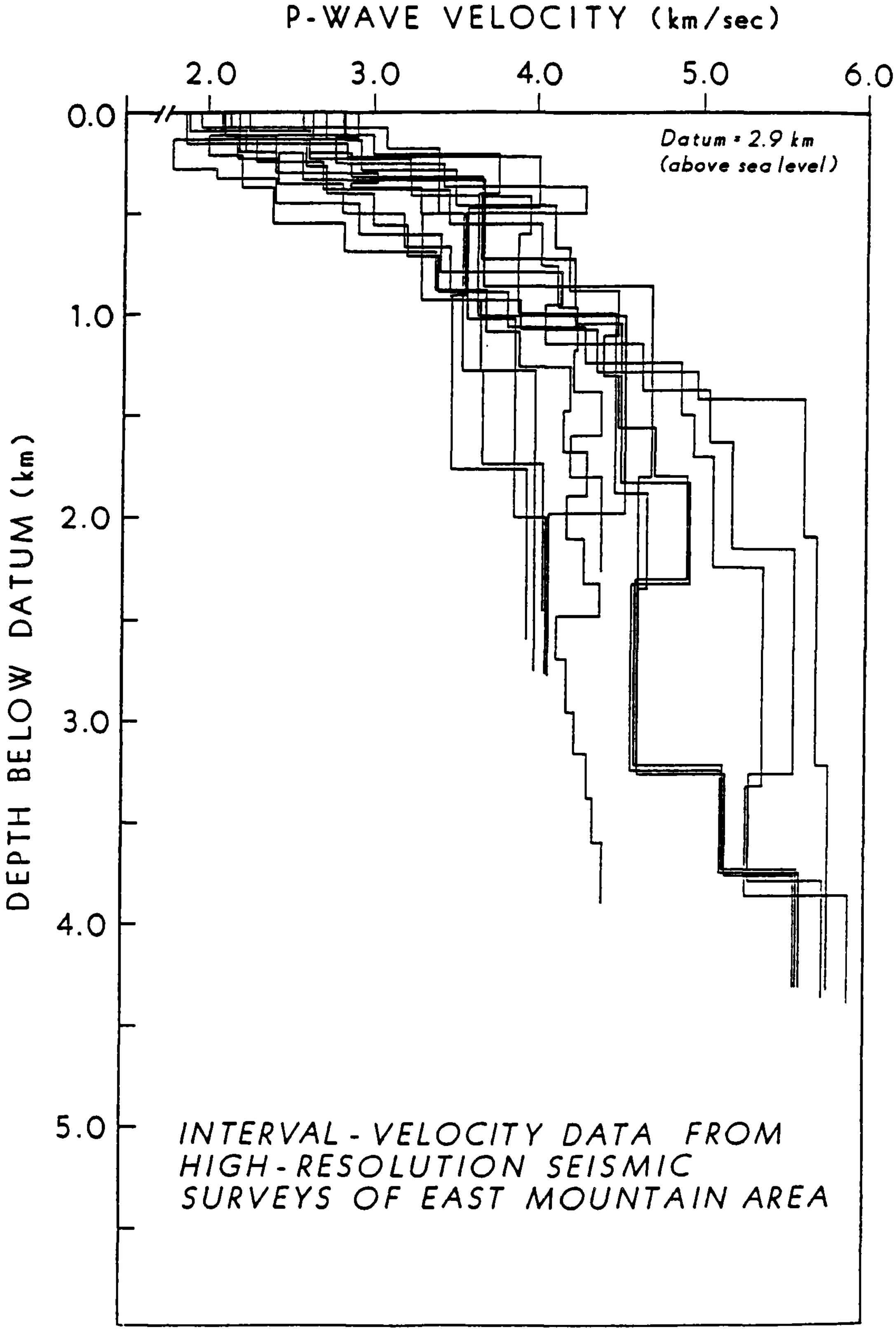

P-WAVE VELOCITY (km/sec)
2.0
3.0
4.0
5.0
6.0
0.0
1.0
2.0
3.0
4.0
5.0
DEPTH BELOW DATUM (km)
Datum = 2.9 km
(above sea level)
INTERVAL-VELOCITY DATA FROM
HIGH-RESOLUTION SEISMIC
SURVEYS OF EAST MOUNTAIN AREA


Figure 3.3

intervals, ranging in thickness from 5 to 250 m, for which the curve could be approximated by straight line segments. From these velocities, an average velocity over a specific depth was calculated by summing the interval travel times corresponding to each mean-value velocity, and dividing by total depth.

The mean-value velocities for the discrete intervals varied less than 35% over the total depth for each average velocity. From a depth of 3.78 km below datum to 4.04 km below datum the interval velocity was constant, so an average velocity was not calculated.

Figure 3.1 summarizes the combination of interval-velocity and sonic-log velocity data from which a generalized velocity model was developed for the study area. In the upper part of the velocity model, the stair-step profile represents an approximation of mean values of the velocity gradient, documented in figure 3.3, to a depth of 1.0 km below datum. Below that depth, interval velocities are generalized from the sonic-log data, as described above.

McKee (1982) empirically determined ratios of P-wave to S-wave velocities from local earthquake travel-times in the Gentry Mountain and East Mountain areas. For the common assumption of Poisson's ratio as 0.25, $V_p/V_s$ is equal to 1.73, which is the average of values of 1.69 and 1.76 determined by McKee (1982) for the Gentry Mountain and East Mountain areas, respectively. Accordingly, Poisson's ratio is simply assumed equal to 0.25 to derive corresponding S-wave velocities from the P-wave velocity structure. The following velocity model (with datum=2,900 m above sea level) is thus assumed as a good approximation for the study area:

| Depth below datum (km) | P-wave velocity(km/sec) | S-wave velocity (km/sec) |
|---|---|---|
| 0.00-0.10 | 2.40 | 1.39 |
| 0.10-0.20 | 2.70 | 1.56 |
| 0.20-0.30 | 3.00 | 1.73 |
| 0.30-0.40 | 3.30 | 1.91 |
| 0.40-0.60 | 3.60 | 2.08 |
| 0.60-0.80 | 3.80 | 2.20 |
| 0.80-1.94 | 4.04 | 2.33 |
| 1.94-2.38 | 4.40 | 2.54 |
| 2.38-3.78 | 4.84 | 2.79 |
| 3.78-4.04 | 5.81 | 3.35 |
| 4.04- | 6.18 | 3.57 |

From the well log, stratigraphic columns, and formation thicknesses in the eastern Wasatch Plateau (Hintze, 1973), the following velocity discontinuities are attributed to formation boundaries: The discontinuity at 1.94 km below datum is interpreted to be the contact between the top of the Dakota Sandstone and the base of the overlying Mancos Shale; at 2.38 km below datum, the boundary between sandstones and shales of the Morrison Formation and the Entrada Sandstone; and at 3.78 km below datum, the boundary between sandstones and siltstones of the Moenkopi Formation and the Kaibab Limestone.

## 3.3 Hypocentral Locations and Focal-Depth Resolution

Hypocenters were determined with version 1 of the computer program HYPOINVERSE (Klein, 1978), using both P-wave and S-wave arrival times. Two approaches were taken to achieve the location of seismic events. First, the best-recorded events were timed on all available seismograms specifically for location purposes. Second, a master file of arrival times that had been compiled as part of the scanning strategy was processed to attempt an event location for all events timed at four or more stations.

Results are described further in section 5.

The issue of focal-depth resolution is a critical one, so special efforts were made to analyze selected seismic events for the uniqueness and stability of hypocentral-depth determination. (The events selected included those well located with 10 or more stations and having a nearest recording station closer than the preliminary focal depth; all events for which focal mechanisms were determined were also investigated.) The procedure used was the following. Each event was located with a range of fixed depths incremented from 0.01 to 20.0 km below datum. Incremental steps varied from 0.2 to 0.5 km and were selected to sample and bracket velocity intervals and steps in the adopted velocity model (section 3.2). RMS travel-time residuals taken from the range of hypocentral solutions were plotted as a function of the fixed focal depth (see fig. 3.5a). Next, the same seismic events were processed again with HYPOINVERSE using the range of incremental depths as trial focal depths, but with the focal depth unconstrained allowing an iterative focal-depth solution. Figure 3.5b illustrates the result of such a procedure in which the final focal depth is plotted as a function of the trial or starting depth.

Detailed information provided by results such as in figure 3.5 allow the evaluation of the uniqueness of a minimum in the RMS function and also the stability of a focal-depth solution as a function of trial focal depth. Where there is a distinctive minimum in the former and stability in the latter (as in fig. 3.5) one can be confident that the solved focal depth is reliable and not an artifact of either an arbitrary trial focal depth or discontinuities within the assumed velocity model.

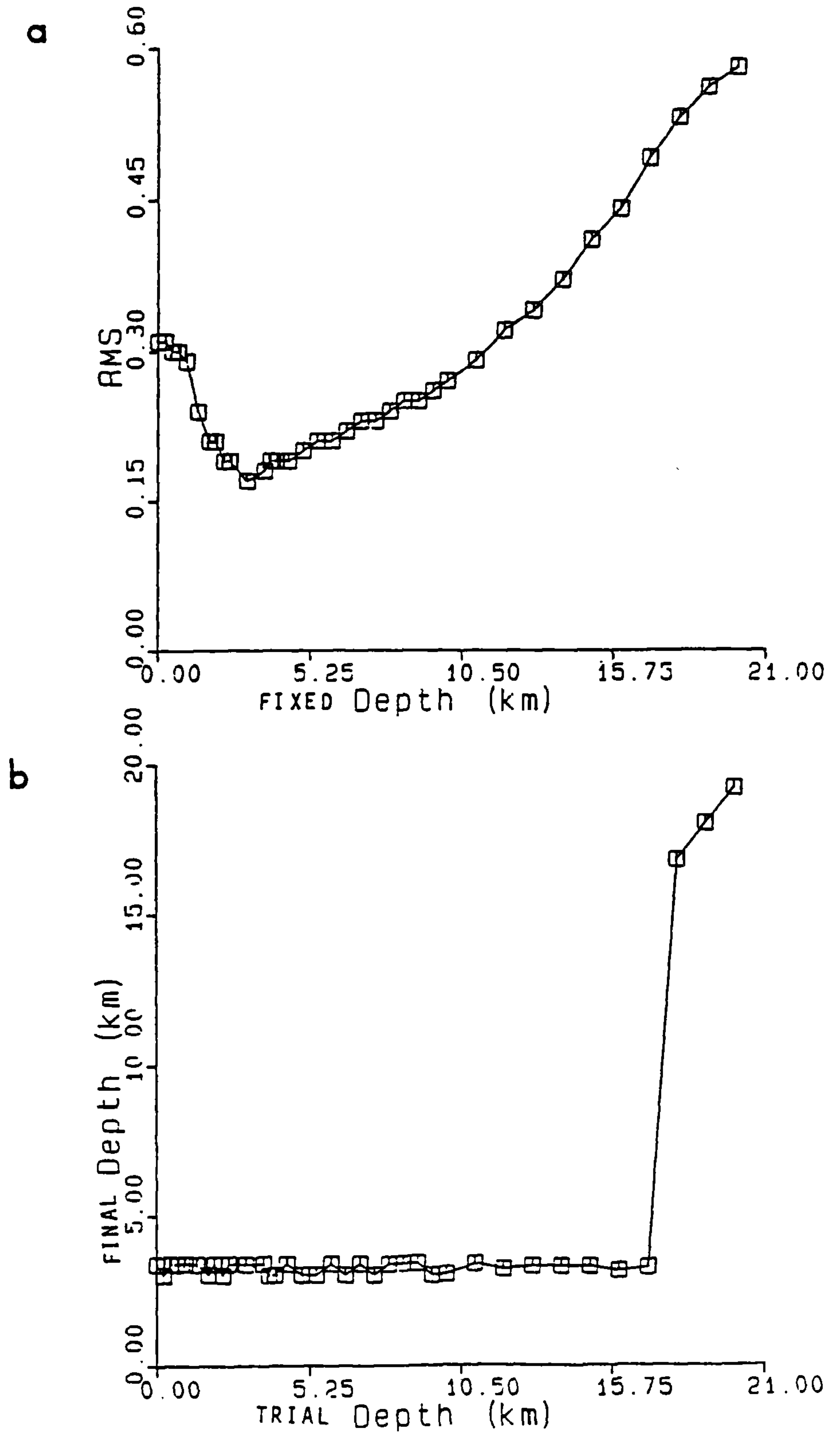


8407081825

Figure 3.5. Examples of plots of RMS versus focal depth (above) and final focal depth as a function of the starting trial depth (below).

## 3.4 Magnitude Estimation

Total signal duration, from P-wave onset to the point where the coda amplitude decreases to the pre-earthquake level, was used as an estimator of earthquake size. Signal durations measured on helicorder seismograms for station TTUT, one of the temporary telemetry stations operated by the U of U, provide the most reliable link to the calibrated scale for coda-magnitude estimates of local magnitude ($M_L$) developed for the University of Utah's regional seismic telemetry network. The relevant equation determined by Griscom and Arabasz (1979) for multiple measurements of coda duration from the U of U seismic network is:

$$M_L = -3.13 + 2.74\overline{\log\tau} + 0.0012\overline{\Delta} \qquad (3\text{-}1)$$

where $\overline{\log\tau}$ is the average logarithm of total signal duration measured in seconds from P-wave onset, and $\overline{\Delta}$ is the average epicentral distance in kilometers. The standard error of estimation is 0.27. Because coda-magnitude scales cannot be extrapolated below about $M_L = 1.5$ without special calibration (Bakun and Lindh, 1977; Suteau and Whitcomb, 1979), magnitudes less than 1.5, indicated in this report, cannot be considered reliable. The smaller values do, however, provide some measure of relative size.

Throughout the analysis of the EWP-84 data, we have consistently documented a measure of signal duration together with every P-wave arrival. In general, there appears to be a consistent relation between signal durations measured on the smoked-paper seismograms and those measured on seismograms for station TTUT. The TTUT measurements are greater, on average, by a factor of 1.5 to 2.0 than those for the smoked-paper seismograms which would cause magnitude estimates based on the latter and equation (3-1) to be systematically lower by 0.2 to 0.3 of a unit of magnitude compared to station TTUT—and presumably the local magnitude scale for the Utah region.

The reliable estimate of earthquake size in terms of local magnitude is both reasonable and feasible for the larger shocks (say, M1.5 to M3.0) recorded in a typical microearthquake field experiment. For the abundant microearthquakes smaller than M1.5, however, magnitude estimates must be considered uncertain in absolute terms (unless extraordinary efforts have been made to account for instrumentation and spectral scaling effects), and the estimates realistically serve little purpose other than providing a crude ranking of size.

## 3.5 Fault-Plane Solutions

Fault-plane solutions were attempted only for events with well constrained focal depths. Two methods were employed. The first was the standard stereographic projection of P-wave first motions. For selected events with appropriate data, we also applied the method of Kisslinger (1980), which involves the inversion of SV-to-P amplitude ratios as measured on vertical-component seismograms. Procedures for application of the latter technique are described in detail by Arabasz and Julander (1986).

Fault-plane solutions based on P-wave first motions are notoriously susceptible to systematic error because of sensitivity to focal-depth error and velocity structure—and often because of interpretive bias when nodal planes are determined by "eye-ball" fitting. Special efforts (described in section 5.2) were made to address uncertainty in focal depth and velocity structure. To minimize bias in nodal-plane determination, the computer algorithm FOCPLT, developed by Whitcomb and Garmany (Whitcomb, 1973), was acquired and implemented at the University of Utah by J.C. Pechmann. As described by Pechmann (1983, p. 27), FOCPLT "...tests a grid of trial mechanisms spaced at approximately 5 degree intervals on the focal sphere and then chooses a mechanism which minimizes the number of first motion readings in error. Less reliable readings are given half the weight of other readings, and a linear function is used to downweight stations within 3 degrees of a nodal plane."

# 4. DISCRIMINATION OF ARTIFICIAL SEISMIC EVENTS

## 4.1 General Statement

Within the study area and during the time period of the EWP-84 experiment, there were three notable sources of artificial seismic events that had to be carefully discriminated from tectonic earthquakes: (1) blasting associated with seismic exploration activities, (2) mining-related seismic events associated with active, and locally intensive, underground coal mining, and (3) blasting associated with development work in some coal mines. First we consider source (1), and then the mining-related sources (2) and (3) together.

## 4.2 Seismic Exploration Activities

During the period of the EWP-84 experiment, from June 18 to August 31, 1984, various geophysical exploration companies were shooting seismic-reflection lines adjacent to and within the study area. Summary information has been compiled from sources (J.F. Niebergall and S. Robison) at the Ferron Ranger District Office of the U.S. Forest Service. Because the study area lies within the Manti-La Sal National Forest, permits for the seismic exploration systematically had to be processed by the Ferron office. Locations of the seismic lines in the study area are shown in plate 1 (submitted separately), and supplementary information is presented in Appendix D. Figure 4.1 shows part of the compilation of plate 1—emphasizing the intensity of exploration activity in the study area during the 1984 field experiment.

Three main field crews were involved in the seismic shooting depicted

Figure 4.1. (following page). Section of plate 1 (submitted separately) showing locations of seismic-reflection lines carried out by geophysical exploration companies in the study area during the summer of 1984.

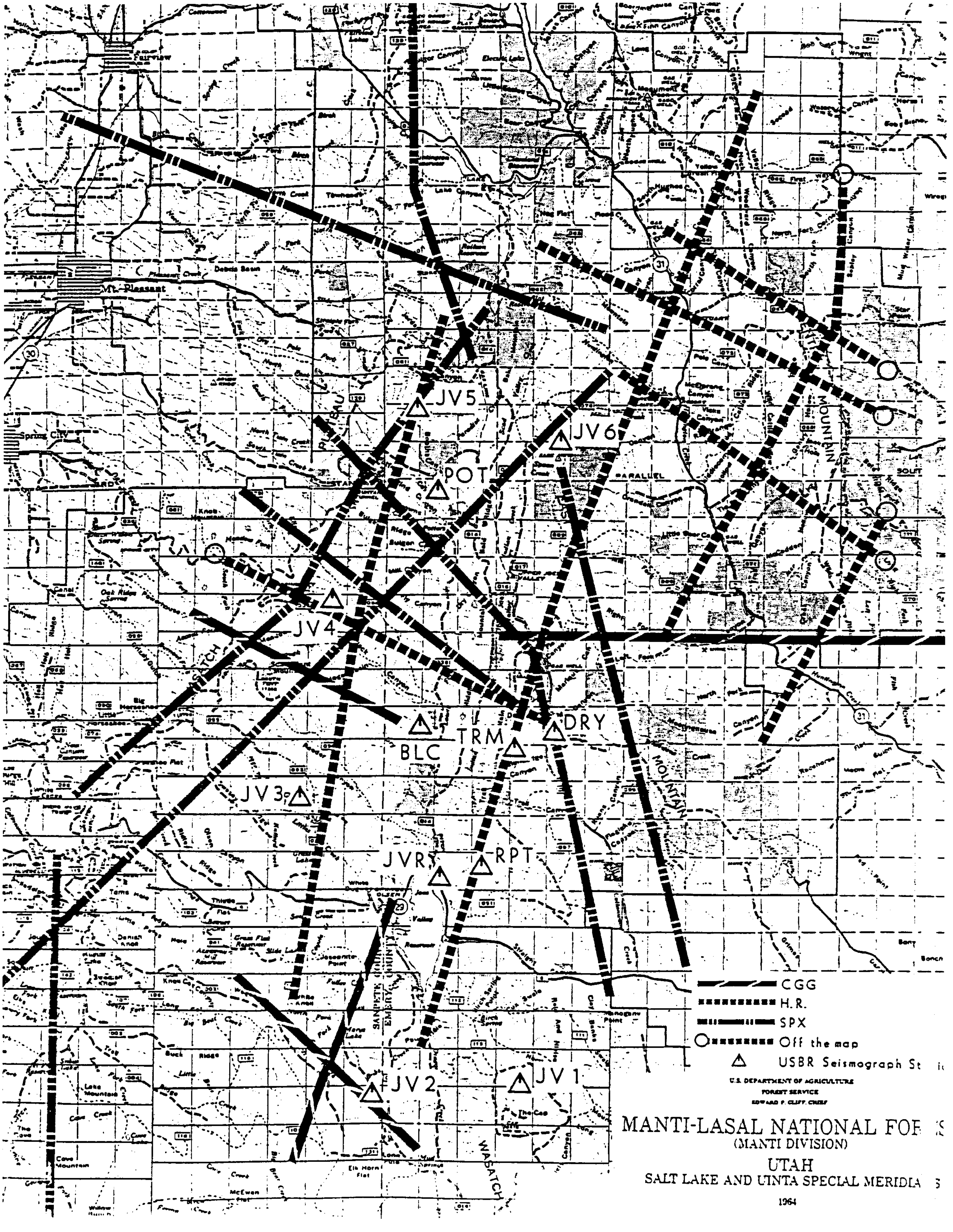

JV5
JV6
POT
JV4
BLC
TRM
DRY
JV3
JVRY
RPT
JV2
JV1
CGG
H.R.
SPX
Off the map
USBR Seismograph St
U.S. DEPARTMENT OF AGRICULTURE
FOREST SERVICE
EDWARD P. CLIFF, CHIEF
MANTI-LASAL NATIONAL FOR
(MANTI DIVISION)
UTAH
SALT LAKE AND UINTA SPECIAL MERIDIA
1964

in figure 4.1 and plate 1: (1) CGG Land Seismic (CGG), (2) Northern Geophysical of America (identified as "HR" by the U.S. Forest Service), and (3) Seis-Port Exploration, Inc. (SPX). Seismic sources included drill-hole and surface explosions. The standard Poulter method (surface shooting) involved approximately 50-pound blasts. Some drill-hole shooting was done by SPX (see Appendix D) involving 20-pound blasts in 60-ft-deep drill holes.

Many of the blasts used as sources for the reflection work were recorded by close seismographic stations of the EWP-84 network—either as direct P-waves or as sonic arrivals (demonstrable from relative arrival times). The artificial events were easily recognized by their character: high-frequency content, large-amplitude onset, total signal duration of only several seconds, and temporal clustering. Typically, the individual exploration blasts were only large enough to have P-waves recorded by one or two very close stations, so epicentral location was impossible. Local earthquakes, in contrast, had discernible shear waves and a coda or tail with gradually increasing period. Even small earthquakes of magnitude less than 0.5 were commonly recorded by several stations.

A total of 26 clusters of artificial seismic events were identified from the seismograms of the Joes Valley subarray (see table 4.1). We are confident that the numerous artificial seismic events associated with the seismic exploration activity in the Joes Valley area have been readily discriminated. There should be no confusion with genuine earthquake activity in the study area.

Table 4.1
LISTING OF ARTIFICIAL SEISMIC EVENTS
(Identified by characteristic appearance)

| DATE | TIME | STATION RECORDING EVENT |
|---|---|---|
| 840705 | 1738 | TRM |
| 840706 | 0135 | TRM |
| 840706 | 1806-1920 | JV1, JV2 |
| 840707 | 0144 | JV3, JV4 |
| 840707 | 1328-1823 | JV1, JV4, JV5, TRM |
| 840708 | 1550-1825 | JV1, JV3 |
| 840709 | 0113 | JV1 |
| 840709 | 1644-2223 | JV1, JV2, JV4, JV5, JV6, TRM |
| 840710 | 1400-1900 | JV2, JV4, JV5, TRM, RPT |
| 840711 | 1511-1926 | JV1, JV2, JV3, JV4 |
| 840712 | 1900-2300 | JV1, JV2, JV4, JV6, RPT |
| 840713 | 1400-2300 | JV1, JV2, JV3, JV4, JV5, JV6 |
| 840715 | 1757-2355 | JV3, JV4, JV5, JV6 |
| 840716 | 1430-2315 | JV6 |
| 840717 | 1649 | JV2 |
| 840727 | 1606 | JV4 |
| 840728 | 1553-2300 | JV4, JV6, DRY |
| 840802 | 1608-2400 | JV3, JV4, JV5, BLC |
| 840803 | 1500-2400 | JV4, JV5, JV6, POT |
| 840804 | 1620-2400 | JV5, POT |
| 840805 | 1500-1600 | JV5 |
| 840806 | 1700-2300 | JV4, JV5 |
| 840807 | 1600-2200 | JV4, JV5, JV6, BLC, POT |
| 840808 | 1350-2300 | JV3, JV4, JV5, JV6, BLC, POT |
| 840809 | 1800-2300 | JV5, DRY |
| 840810 | 1039 | JV5 |

## 4.3 Mining-Related Seismic Events

The second important class of seismic events, many of which might be interpreted to be non-tectonic, is that of mining-related seismic events. A prominent feature of the seismicity of east-central Utah is an intense clustering of epicenters in a horseshoe-shaped pattern (fig. 1.1a) extending northward along the eastern side of the Wasatch Plateau and then eastward around the Book Cliffs escarpment. The association of seismic events (both rockbursts and earthquakes) as large as $M_L$4.5 with active underground coal mining in these areas has been evident since the late 1950's. On the scale of figure 1.1b, seismic events appear to concentrate near mining properties where annual coal extraction is of the order of 500,000 tons or greater. The maximum depth of the mine workings is less than 900 m below surface.

On the basis of reconnaissance microearthquake recording in the eastern Wasatch Plateau coal fields during the summer of 1979, McKee and Arabasz (1982) were able to document: (1) intense spatial clustering of seismicity (depth < 4 km) both at and beneath levels of active underground coal mining, and (2) an average rate of more than 300 microearthquakes per day in the East Mountain coal mining area immediately east of the Joes Valley area.

Without question, the preponderance of seismic events recorded during the EWP-84 experiment were spatially associated with areas of major coal mining (discussed next in section 5). It is difficult *a priori* to determine which of those seismic events are "artificial"--with the exception of known blasting done by the mine operators for developmental work.

Information was compiled on the location and amount of coal extraction in the Wasatch Plateau coal field relevant to the EWP-84 field experiment. Plate 2 (submitted separately), based on information from the U.S. Forest Service (C. Reed, Manti-La Sal National Forest Supervisor's Office, personal communication, 1985) outlines the boundaries of coal-mining properties in the eastern Wasatch Plateau. Figure 4.2 shows part of plate 2. Basic information on those mining properties, keyed to plate 2 and figure 4.2, is summarized in table 4.2. Inspecting figure 4.2 and table 4.2, it is evident that the mines with most significant coal extraction within the study area are located in the East Mountain area (#5 and #13) and the Gentry Mountain area (#8 and #9).

The East Mountain coal-mining area is the one of most direct relevance to the Joes Valley area. For mines in the East Mountain area, information on the location of active coal extraction and blasting during the EWP-84 recording period was acquired from Utah Power and Light Company (D.W. Jense, personal communication, 1985).

Table 4.2 Information on Active Coal Mines of the Wasatch Plateau Coal Field*

| | Company | Mine Name | Underground Equipment Use | 1984 Tonnage |
|---|---|---|---|---|
| 1. | Valley Camp of Utah, Inc. | Belinda #1,#2 | 4 continuous miners | 756,000 |
| 2. | SUFCO | Convulsion Canyon | (information not available) | |
| 3. | Co-op Mining Col. | Co-op | 2 continuous miners | ? |
| 4. | Genwall | Crandall Canyon | | (<80,000)+ |
| 5. | Emery Mining Corp. | Deer Creek | 8 continuous miners<br>2 longwall units | 1,894,317 |
| 6. | Emery Mining Corp. | Des-Bee-Dove | 5 continuous miners | 100,304 |
| 7. | Beaver Creek | Huntington Canyon | | (<200,000)** |
| 8. | United States Fuel Co. | King #4,#5,#6 | 4 continuous miners | 792,500 |
| 9. | Plateau Mining Co. | Starpoint | 6 continuous miners<br>1 longwall unit | 1,200,000 |
| 10. | West APPA | Rilda Canyon | | (no production)** |
| 11. | Coastal States Energy Co. | Skyline | 2 continuous miners | 375,000 |
| 12. | Trail Mountain Coal Co. | Trail Mountain | 2 continuous miners | 137,274 |
| 13. | Emery Mining Corp. | Wilberg | 5 continuous miners<br>2 longwall units | 2,046,840 |

* Source: 1985 Keystone Coal Industry manual (Nielson, 1985).
** Approximate 1983 tonnage, from Utah Geological & Mineral Survey. (Information not available in Keystone Coal Industry Manual.)
\+ Unconfirmed estimate of 1984 tonnage.

Figure 4.2. (following page). Section of plate 2 (submitted separately) showing the boundaries of active coal-mining properties in the eastern Wasatch Plateau. Property numbers keyed to table 4.2.

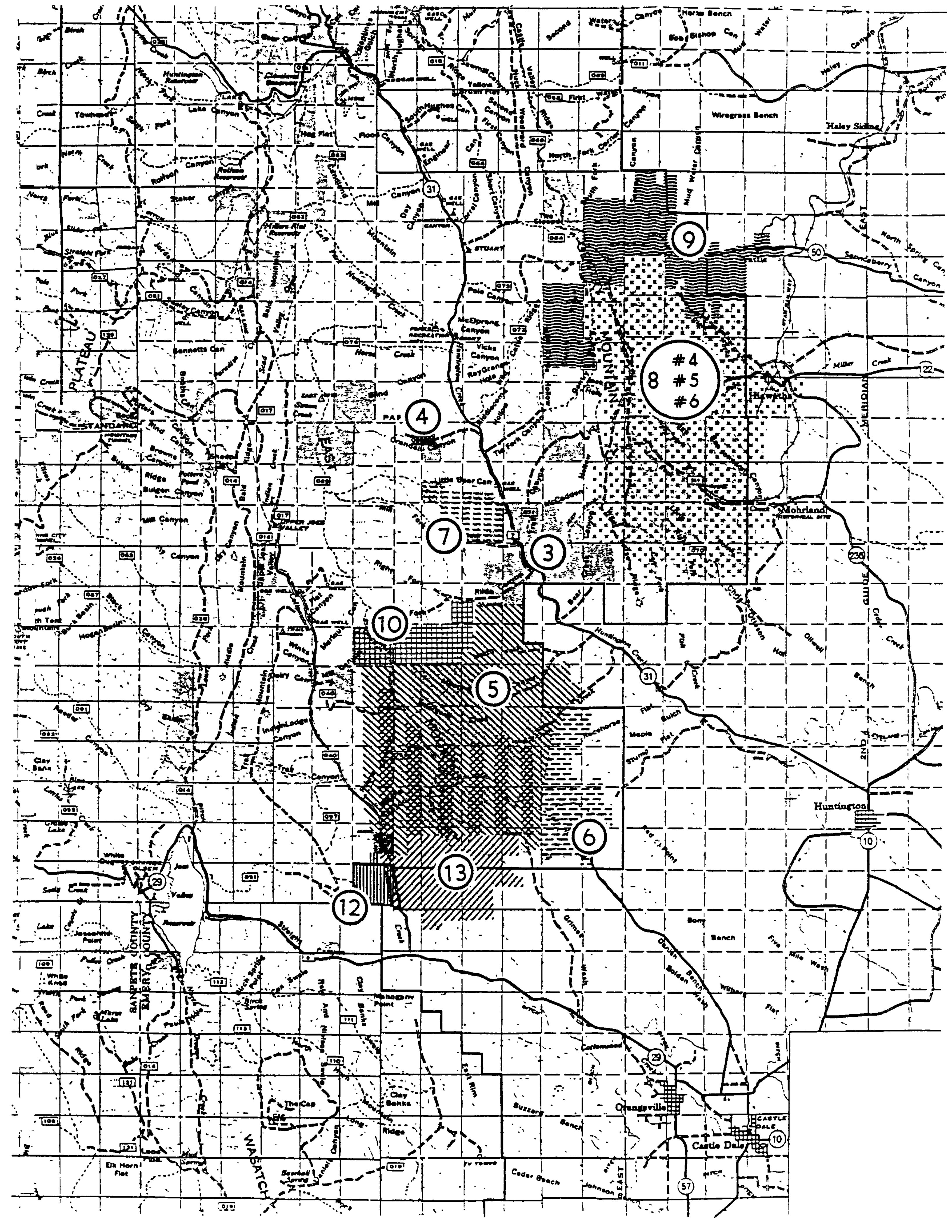

Huntington Reservoir
Cleveland Reservoir
Lake Canyon
Rolfson Canyon
Rolfson Reservoir
Miller Flat Reservoir
Hog Flat
Flood Canyon
Engineer
Mill Canyon
Mountain
Straight Fork
PLATEAU
STANDARD
Bennetts Can
Seeley Canyon
Huntington Creek
McDprong Canyon
Vicks Canyon
Pole Canyon
Horse Creek
Grandall Canyon
Little Bear Can
McCadden
Mill Canyon
Indian Creek
Bald Mountain
Joes Valley
Right Fork
Wales Canyon
Indian Lodge Canyon
Trail Canyon
Clay Bank
Little Lake
Huntington Creek
Huntington
Miller Creek
Hiawatha
Mohrland
HISTORICAL SITE
Haley Siding
Wiregrass Bench
Horse Bench
Mud Water Canyon
Mud Water Canyon
North Spring Canyon
Sandaberry Canyon
MOUNTAIN
GUIDE
MERIDIAN
Cedar Creek
Olsen Bench
Maple Gulch
Stump Flat
Dry Wash
Bench
Five Mile Wash
Wilber Flat
Cottonwood
Orangeville
Castle Dale
CASTLE DALE
Buzzard Bench
Cedar Bench
Johnson
Clay Banks
The Cap
Long Ridge
East Rim
Mahogany Point
Elk Horn Flat
Mud Spring
WASATCH
SANPETE COUNTY
EMERY COUNTY
Reservoir
Valley
Jacobs Point
White Knoll
Grimes Wash
Straight
Canyon
Rock Canyon
31
29
10
57
236
122
50
9
#4
#5
#6
8
4
7
3
10
5
6
13
12

# RESULTS

## 5.1 Locations of Seismic Events

A total of 475 seismic events were located in the EWP-84 study area as part of this contract. The events range in size from approximately magnitude 0 to magnitude 2.1 and cover the period July 6-August 12, 1984. The locations are based chiefly on the integration of arrival times from the USBR and U of U stations—with contributions from the WCC stations for roughly twenty percent of the events. Locations were attempted for all 359 events in the master chronology at station TTUT (Appendix C), representing the largest events recorded in the study area during the USBR 38-day sample window. Of primary concern, however, was the systematic location of events recorded by the USBR stations that might correspond to earthquakes close to the Joes Valley area and outside the areas of active mining (see section 3.1). Repeated efforts were made to identify such events from the USBR data set on the basis of relative arrival times and appearance on the USBR seismograms.

Figure 5.1 shows an epicenter map of the located seismic events throughout the EWP-84 study area. (For convenience, fig. 5.2 includes a transparent overlay, from fig. 4.2, allowing comparison of the seismicity with the boundaries of areas of active mining.) The concentration of seismic activity in the East Mountain area is a first-order feature of the epicenter map. This includes intense clustering beneath East Mountain itself as well as scattered epicenters in its general vicinity. From the relatively larger events sampled in the TTUT chronology, there is a secondary concentration of activity in the Gentry Mountain area, the focus

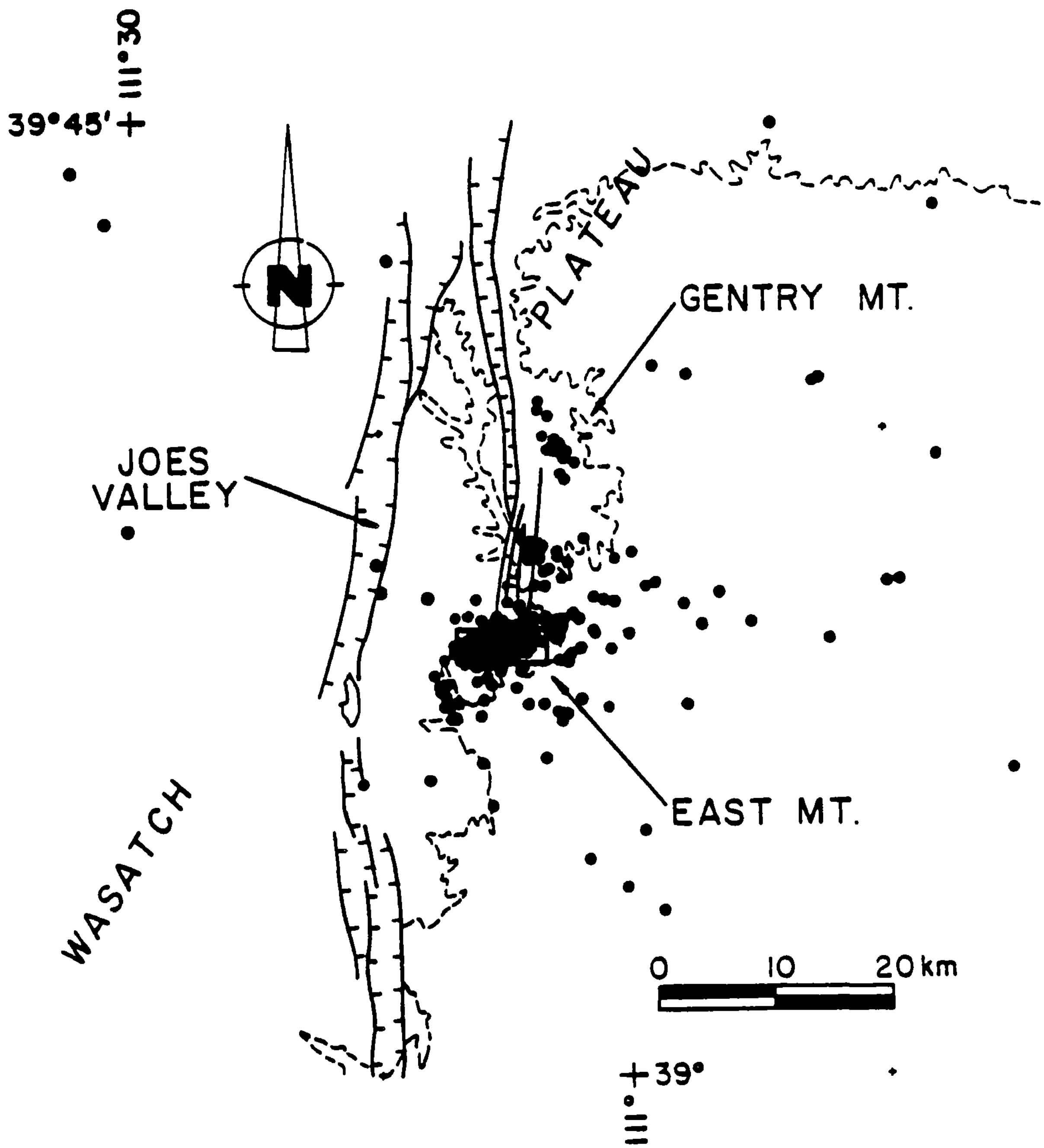


Figure 5.1. Map showing epicenters (solid circles) of 475 seismic events located for this study as part of the EWP-84 experiment.

Figure 5.2. (following page). Map showing epicenters (circles and X's) from figure 5.1 and seismograph stations (triangles) in relation to the boundaries of active coal-mining properties in the eastern Wasatch Plateau.

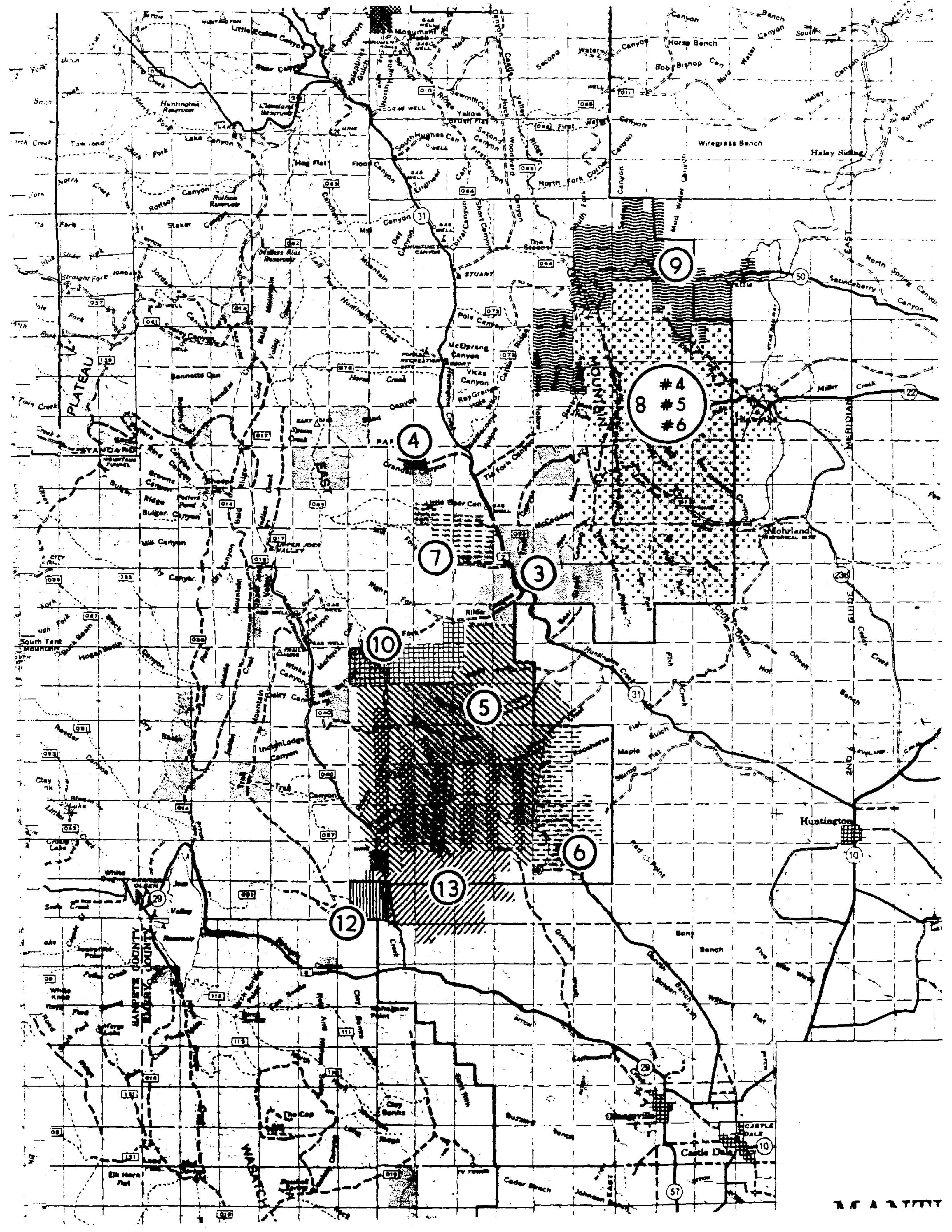

Little Bear Canyon
Bear Canyon
Huntington Reservoir
Cleveland Reservoir
Lake Canyon
Hog Flat
Flood Canyon
South Hughes Can
Engineer Can
Rolfson Canyon
Rolfson Reservoir
Steker Canyon
Millers Flat Reservoir
Mill Canyon
Huntington Creek
Straight Fork
Pole Canyon
McElprang Canyon
Vicks Canyon
Bennetts Can
Horse Creek
Little Bear Can
Grandall Canyon
Mill Canyon
Joes Valley
Indian Canyon
Dairy Can
Horse Bench
Bob Bishop Can
Wiregrass Bench
Haley Siding
North Spring Canyon
Serviceberry Canyon
Miller Creek
Mohrland
Huntington Creek
Huntington
Bony Bench
Cedar Bench
Buzzard Bench
Orangeville
Castle Dale
Elk Horn Flat
The Cap
PLATEAU
EAST MOUNTAIN
WASATCH
SANPETE COUNTY
EMERY COUNTY
MERIDIAN
GUIDE
EAST
31
50
22
10
29
57
236
9
#4
8 #5
#6
4
7
3
10
5
6
13
12

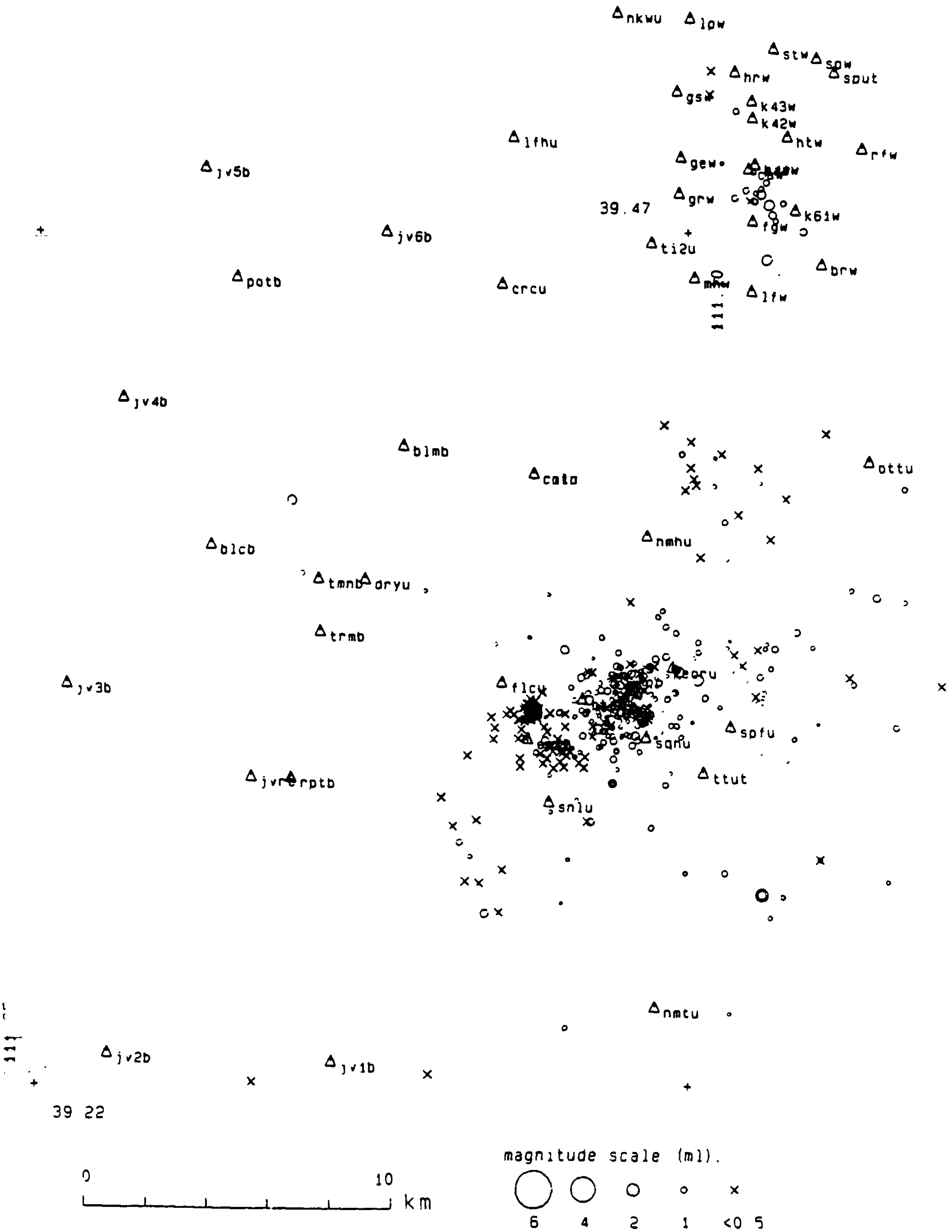
nkwu
lpw
stw
spw
sput
hrw
gs
k43w
k42w
lfhu
htw
rfw
jv5b
gew
grw
39.47
k61w
fgw
jv6b
ti2u
brw
potb
crcu
lfw
111.
jv4b
blmb
ottu
calo
nmhu
blcb
tmnb
dryu
trmb
jv3b
flcu
spfu
sqnu
ttut
rptb
snlu
nmtu
jv2b
jv1b
111
39 22
0
10
km
magnitude scale (ml).
6
4
2
1
<0 5

of study by the WCC group.

The immediate vicinity of Joes Valley is obviously of primary concern in this report, and it is there that we find a distinct paucity of seismic activity reflected in the epicenter summary of figure 5.1. Despite the repeated attempts to identify and locate events occurring to the west of the areas of active mining, a very small number of such events were found. Sixteen of these events are specially indicated in figure 5.3, and corresponding hypocentral summaries are presented in table 5.1. We next scrutinize those sixteen events.

Events No. 1 and No. 13 in figure 5.3 occur directly within the Joes Valley graben and are among the best located events of table 5.1. They were located with a large number of stations and have an epicentral distance to the nearest recording station (dmn) that is smaller than the focal depth. Event No. 15, located to the east of station DRYU, is of poor quality and has a relatively large rms error. Events No. 3 and No. 16, near the southwestern boundary of the study area, are of poor quality. Both have a large azimuthal separation (gap) in degrees between recording stations and a large value of dmn.

The remaining events (No. 4 through No. 12) specially identified in figure 5.3 to the west of the mining area are clustered to the southwest of station SNLU and lie in the vicinity of Cottonwood Creek. Two immediate concerns arise. First, we are aware that a seismic exploration line was shot along Cottonwood Creek (fig. 4.1). Second, the Trail Mountain Mine is located in that area (fig. 4.2) and has a modest but significant level of coal extraction (table 4.2). Events No. 4, 5, 6, 7, 8, and 10 all have very shallow focal depths of less than 1 km, with a nearest recording

Figure 5.3. (following page). Map of epicenters located in the study area as part of the EWP-84 experiment. Numbers (keyed to table 5.1) indicate events of special relevance to the Joes Valley area.

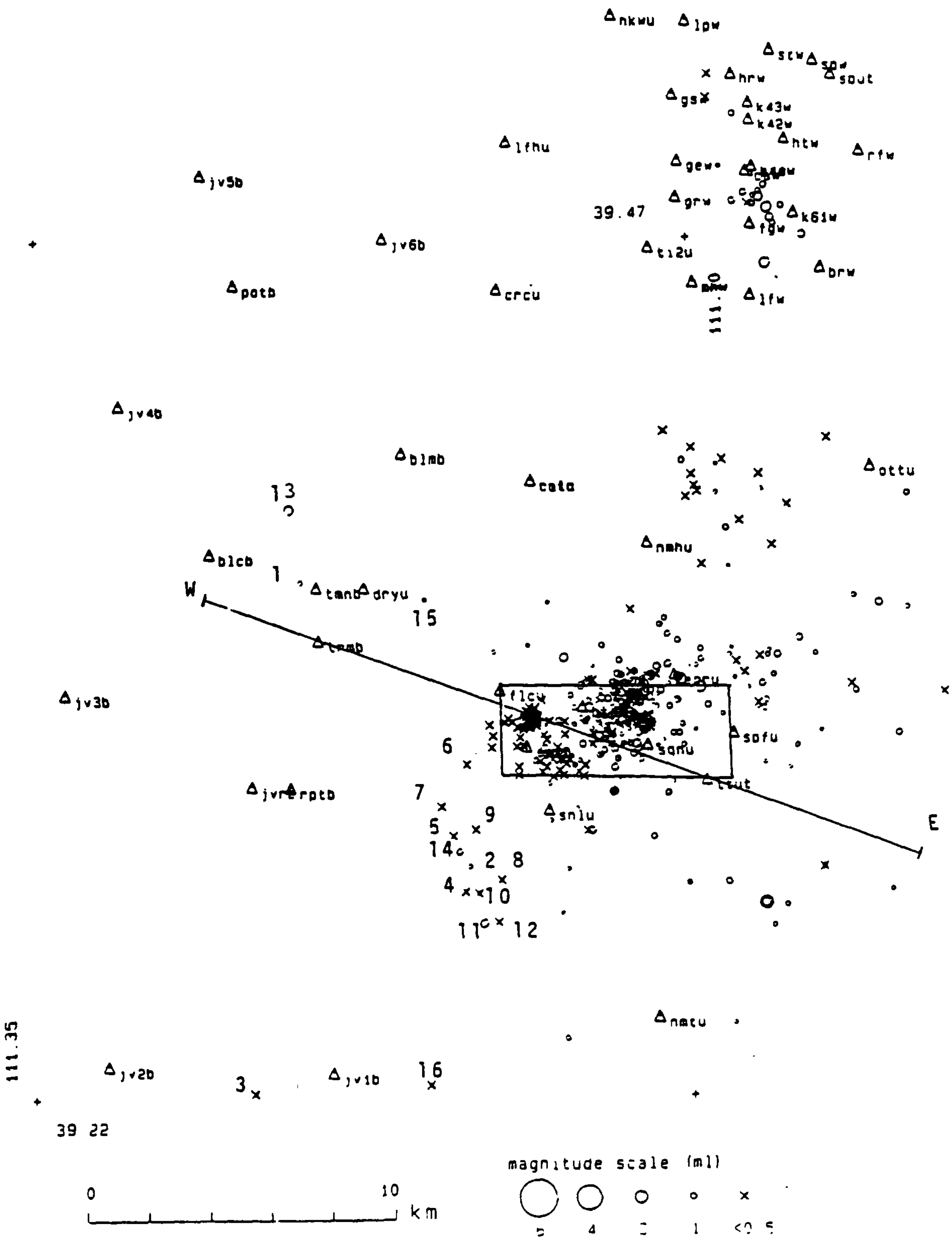
39.47
111.35
39 22
W
E
0
10
km
magnitude scale (ml)

Table 5.1

Seismic Events in Western Part of EWP-84 Study Area

| event | yr | date | orig | time | lat-n | long-w | depth | mag | no | gap | dmn | rms |
|---|---|---|---|---|---|---|---|---|---|---|---|---|
| 1 | 84 | 708 | 1825 | 22.58 | 39-22.50 | 111-14.87 | 3.0 | 0.8 | 20 | 127 | 2 | 0.17 |
| 2 | 84 | 713 | 819 | 2.17 | 39-17.53 | 111-11.04 | 0.0 | 0.7 | 14 | 145 | 3 | 0.80 |
| 3 | 84 | 714 | 1901 | 37.94 | 39-13.57 | 111-16.01 | 4.0 | 0. | 3 | 345 | 13 | 0.35 |
| 4 | 84 | 715 | 56 | 10.87 | 39-18.06 | 111-11.43 | 0.1 | 0.4 | 13 | 153 | 3 | 0.15 |
| 5 | 84 | 715 | 607 | 9.06 | 39-17.10 | 111-11.15 | 0.9 | 0. | 7 | 175 | 3 | 0.53 |
| 6 | 84 | 715 | 1222 | 9.70 | 39-19.30 | 111-11.10 | 0.8 | 0. | 5 | 266 | 2 | 0.11 |
| 7 | 84 | 715 | 1601 | 42.79 | 39-18.57 | 111-11.69 | 0.1 | 0.1 | 10 | 100 | 4 | 0.10 |
| 8 | 84 | 717 | 1108 | 39.33 | 39-17.30 | 111-10.31 | 0.8 | 0.1 | 9 | 91 | 2 | 1.69 |
| 9 | 84 | 724 | 1630 | 25.76 | 39-18.17 | 111-10.90 | 5.0 | 0.4 | 12 | 201 | 2 | 0.40 |
| 10 | 84 | 725 | 643 | 17.81 | 39-17.07 | 111-10.84 | 0.9 | 0. | 13 | 96 | 3 | 0.22 |
| 11 | 84 | 730 | 2149 | 0.85 | 39-16.54 | 111-10.72 | 4.0 | 1.3 | 15 | 170 | 6 | 0.20 |
| 12 | 84 | 804 | 39 | 9.38 | 39-16.56 | 111-10.39 | 3.8 | 0.4 | 11 | 174 | 7 | 0.29 |
| 13 | 84 | 806 | 34 | 46.87 | 39-23.79 | 111-15.12 | 4.3 | 1.5 | 26 | 51 | 3 | 0.17 |
| 14 | 84 | 808 | 1543 | 32.93 | 39-17.78 | 111-11.28 | 4.0 | 1.0 | 16 | 167 | 7 | 0.23 |
| 15 | 84 | 809 | 2135 | 2.05 | 39-22.19 | 111-12.05 | 4.0 | 0.6 | 6 | 130 | 5 | 0.56 |
| 16 | 84 | 811 | 220 | 15.60 | 39-13.71 | 111-11.99 | 4.2 | 0.3 | 8 | 288 | 11 | 0.33 |

number of earthquakes = 16

station within a few kilometers. Noting that local time (MDT) was 6 hours behind Greenwich Mean Time listed in table 5.1, at least two of those events—No. 5 and No.10—occurred between midnight and 1:00 am; both had mixed dilatational and compressional first motions. Inspection of the recordings of Events No. 4, 6, 7, and 8 indicates to us that they are not seismic exploration blasts.

Three events in the Cottonwood Creek group have good indications of not being artificial—No. 9, 10, and 12. No. 9 has a reliable focal depth of 5.0 km and mixed first motions; No. 11 has a depth of of 4.0 km that is not well constrained, but a magnitude of 1.3 and all dilatational first motions; No. 12 has an apparent depth of 3.8 km (with dmn = 7 km) and mixed first motions. In sum, the seismic events clustering in the Cottonwood Creek area appear to include genuine earthquakes; some of the seismic events could conceivably be mining-related.

## 5.2 Focal-Depth Distribution

Of the 475 seismic events located and used for analysis in this study, a subset of 201 well-located events was obtained meeting the following criteria: (1) N, the total number of P- and S-wave arrival times >5; (2) GAP, the largest azimuthal separation between stations < 250 degrees; (3) RMS, the root-mean-square error of the travel-time residuals < 0.40 sec. (4) ERH, the standard error in epicentral determination < 2.0 km; and (5) ERZ, the standard error of focal depth determination < 2.0 km. This subset of events, referred to as subset A, encompasses a 37-day period from July 6 to August 11, 1984. Epicenters for the seismic events in subset A are shown in figure 5.4.

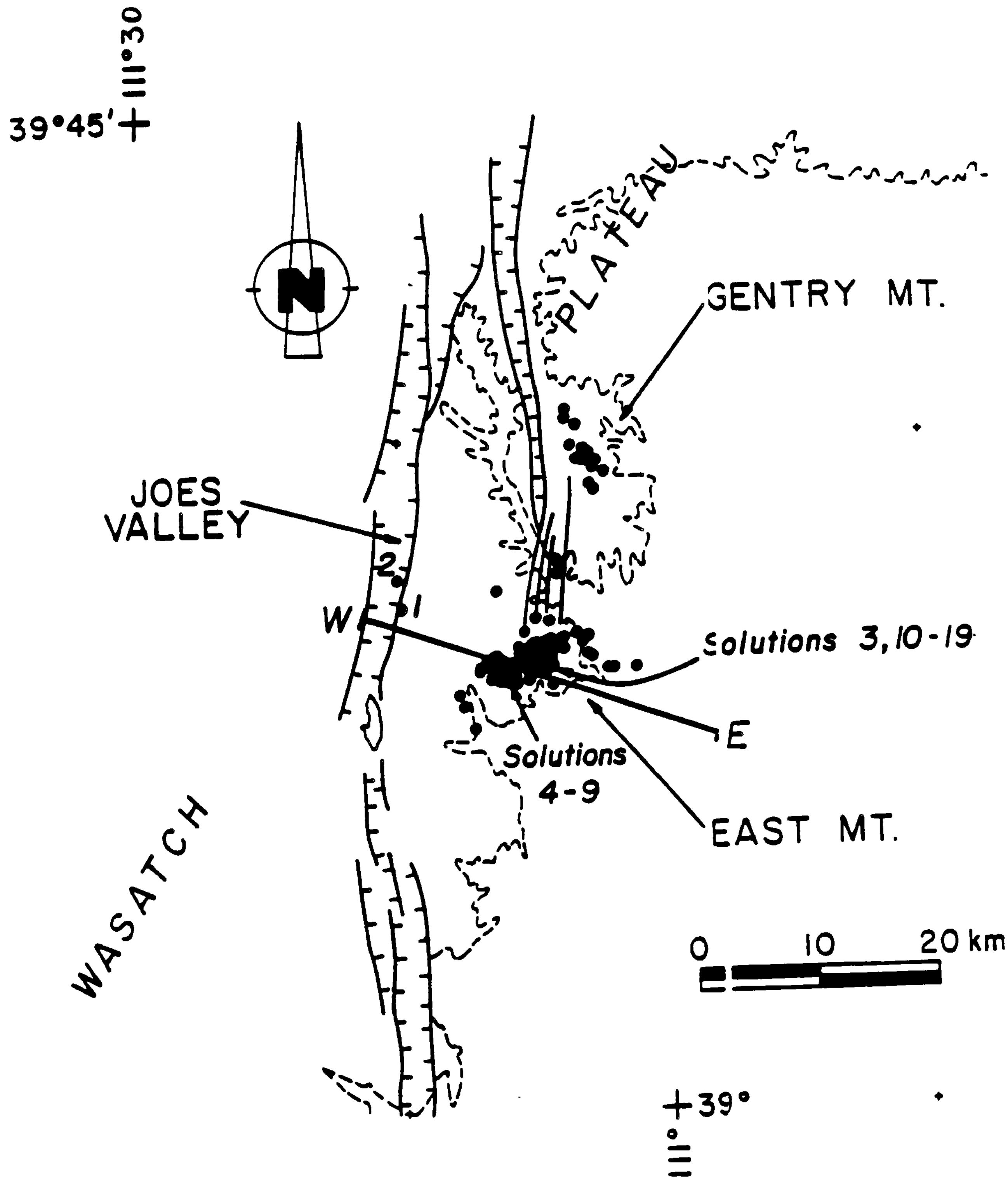


Figure 5.4. Map showing epicenters of 201 well-located seismic events (subset A) used for investigation of focal-depth distribution and focal mechanisms. W-E cross-section line keyed to figure 5.5. Numbers indicate epicenters of events for which focal mechanisms have been determined.

A process of rigorous focal-depth testing was performed on subset A to verify focal-depth reliability for as many events as possible. One of the most important criteria for these data was the epicentral distance in kilometers (DMIN) to a station closest to the event. Criteria to be met were: N≥5, GAP≤200, and RMS≤0.25 second. Next, for each qualifying event an analysis of RMS versus depth and focal-depth stability was completed (see Methods of Analysis). Events for which an RMS minimum and focal-depth stability could be established were grouped into another subset. This refined subset containing events whose focal-depth reliability has been rigorously tested will be referred to as the "best" subset.

Figure 5.5 shows cross-section views, keyed to figure 5.4, of hypocenters belonging respectively to subset A (figure 5.5a) and its corresponding subset having "best" focal depths (figure 5.5b). First the "best" foci are considered. Disregarding for the moment the focal-mechanism information, figure 5.5b shows concentrated foci within 0.5 km below mine level in the East Mountain area. There are relatively few accurately located foci above mine level, but the constraints of this subset must be emphasized. Because of the average station spacing of 2.5 km and the criteria for focal depth reliability, very shallow focal depths are not well controlled. A more dense network would have been required to achieve good focal-depth precision above mine level. None of the foci in figure 5.5b below the mine workings are deeper than 1.5 km below datum. Deeper foci lie to the west corresponding to two Joes Valley events (no. 1 and no. 13 in fig. 5.3 and table 5.1). The reliable depths of 3.0 km and 4.35 km for these seismic events imply that they are tectonic earthquakes. In the Gentry Mountain area, the WCC group located abundant seismicity extending to about 2 km below mine level, and more sparse activity down to

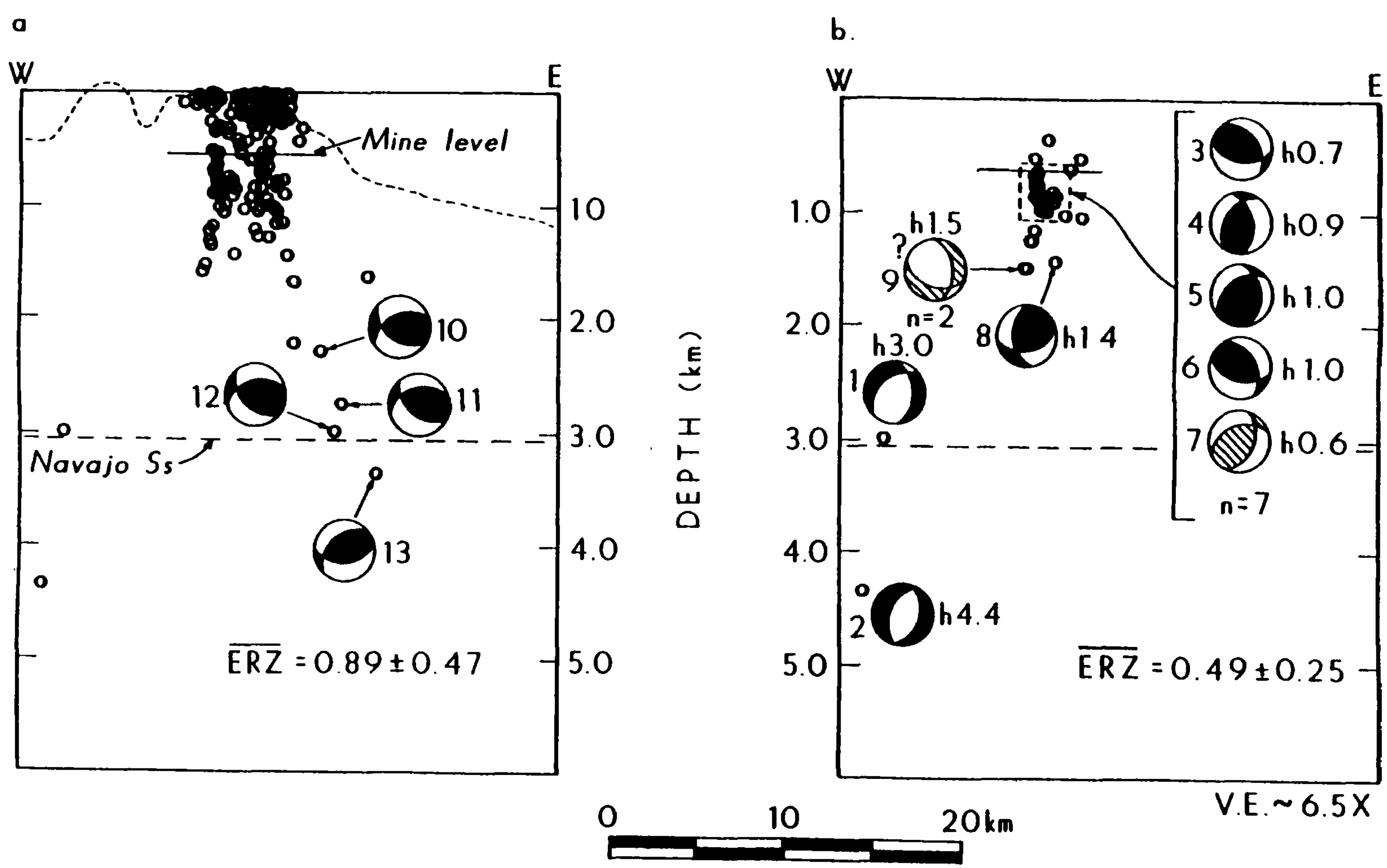


Figure 5.5. West-East cross sections (keyed to Figure 5.4) showing distribution of focal depths for (a) subset A and (b) for "best" subset. Schematic focal mechanisms shown for solutions 1-13. Dilatational quadrants are white, compressional quadrants black (for single events), hachured (for composite solutions). Dashed line in (a) is an approximation of the topography.

about 3.5 km below mine level (I.G. Wong Woodward-Clyde Consultants, personal communication, 1985).

Given the relatively small number of events in the "best" subset, all data of subset A are plotted for comparison in figure 5.5a. Obvious differences with figure 5.5b are the clustering of very shallow events above mine level in the East Mountain area and location of foci beneath mine workings in the 2 to 3 km depth range below datum. In both plots the majority of sub-mine seismicity lies within 1.0 km of mine level. The deepest reliably located event is at a depth of 4.4 km. The location of the top of the Navajo Sandstone is shown in figure 5.5 for reference. If a detachment surface lies close to that level, then only a single event has been located confidently below it.

## 5.3 Fault-Plane Solutions

We have seen that the majority of seismic events located from the EWP-84 experiment cluster in the areas of active coal mining in the eastern Wasatch Plateau. One of the basic goals of the experiment was to determine fault-plane solutions for earthquakes occurring outside and/or sufficiently below the areas of active mining so that important information could be gathered about the regional stress field.

The following basic strategy was used. First, attention was placed on the subset of seismic events in the "best" focal-depth group. These foci included events clustered in the immediate vicinity of East Mountain together with the two earthquakes in Joes Valley. Thus it was straightforward to consider them in cross-section view (as done in fig. 5.5b) along the line of section shown in figure 5.4. Some seismic events were later selected from the remainder of subset A (fig. 5.5a) to gain additional information on focal mechanisms for the relatively deepest events directly below the area of mining. Finally, another group of seismic events was selected, chiefly from subset A, to study a class of events having all dilatational first motions.

A total of seventeen single-event and two composite fault-plane solutions were determined. Epicenters for the corresponding events are labeled in figure 5.4; all lie within 3 km of the line of section. In addition to data illustrated in the following text, Appendix E contains a summary of hypocentral information for the 19 fault-plane solutions, stereographic plots for solutions 1-13, and data for RMS and depth-stability tests for selected earthquakes.

All fault-plane solutions herein are equal-area, lower-hemishpere stereographic projections of the focal sphere. Filled-in circles correspond to compressional first motions; open circles indicate dilatational first motions. With the exception of solution 2e (fig. 5.7), which was determined with the computer program AMPRAT, all solutions were determined with the computer program FOCPLT (see Methods of Analysis). For the FOCPLT solutions, triangles indicate the locations of the P-axis, T-axis, and the alternative slip vectors (corresponding to the poles of the auxiliary nodal planes). The P-axis and T-axis respectively bisect the dilatational and compressional quadrants of the focal sphere.

Figure 5.5b gives an overview of focal mechanism data for the "best" focal depth set. This includes (1) five fault-plane solutions sampled from the 0.6 km to 1.0 km depth range at or slightly below mine level, (2) two solutions for events roughly one km below mine level, and (3) two solutions for the deeper earthquakes west of the mining area beneath Joes Valley. Figure 5.6a shows the first-motion information for solution 1 at its free depth of 3.0 km. This solutions shows oblique slip with a predominance of normal faulting. To test the sensitivity of the solution to focal depth, and hence velocity structure, alternative solutions were determined by fixing the depth at 3.1 km (fig. 5.6b), 2.3 km (fig 5.6c), and 3.7 km (fig. 5.6d). The first two alternatives (b,c) indicate the predominance of normal faulting, but the third (d) involves a significantly different pattern of take-off directions on the focal sphere corresponding to critically-refracted ray paths. The resulting focal mechanism (fig. 5.6d) has reversed quadrants such that the mechanism is compressional with nearly pure reverse slip on either nodal plane. From the results for the nearby second earthquake in Joes Valley, presented next, one can argue that the normal-fault-type solutions for this first earthquake is more likely.

Solution 2 (fig. 5.7a) is for the 4.4-km-deep event beneath Joes Valley and shows a normal-faulting mechanism with nearly pure dip slip. Again, to test the sensitivity of the solution to focal depth, alternative solutions were determined assuming focal depths of 5.0 km (fig. 5.7b), 3.5 km (fig. 5.7c), and 2.5 km (fig. 5.7d). The consistency of a normal-fault-type mechanism is apparent, with slightly rotated, but generally northerly-trending nodal planes. An independent fault-plane solution for this same event was determined from SV/P amplitude ratios, using the computer algorithm LAMPRAT. Figure 5.7e shows the result of this procedure. The solution violates a few of the first-motions but is consistent with the previous results in that the focal sphere has a dilatational cap. The consistency of a normal-fault-type mechanism between 2.5 km and 5.0 km makes it unlikely that the compressional alternative for

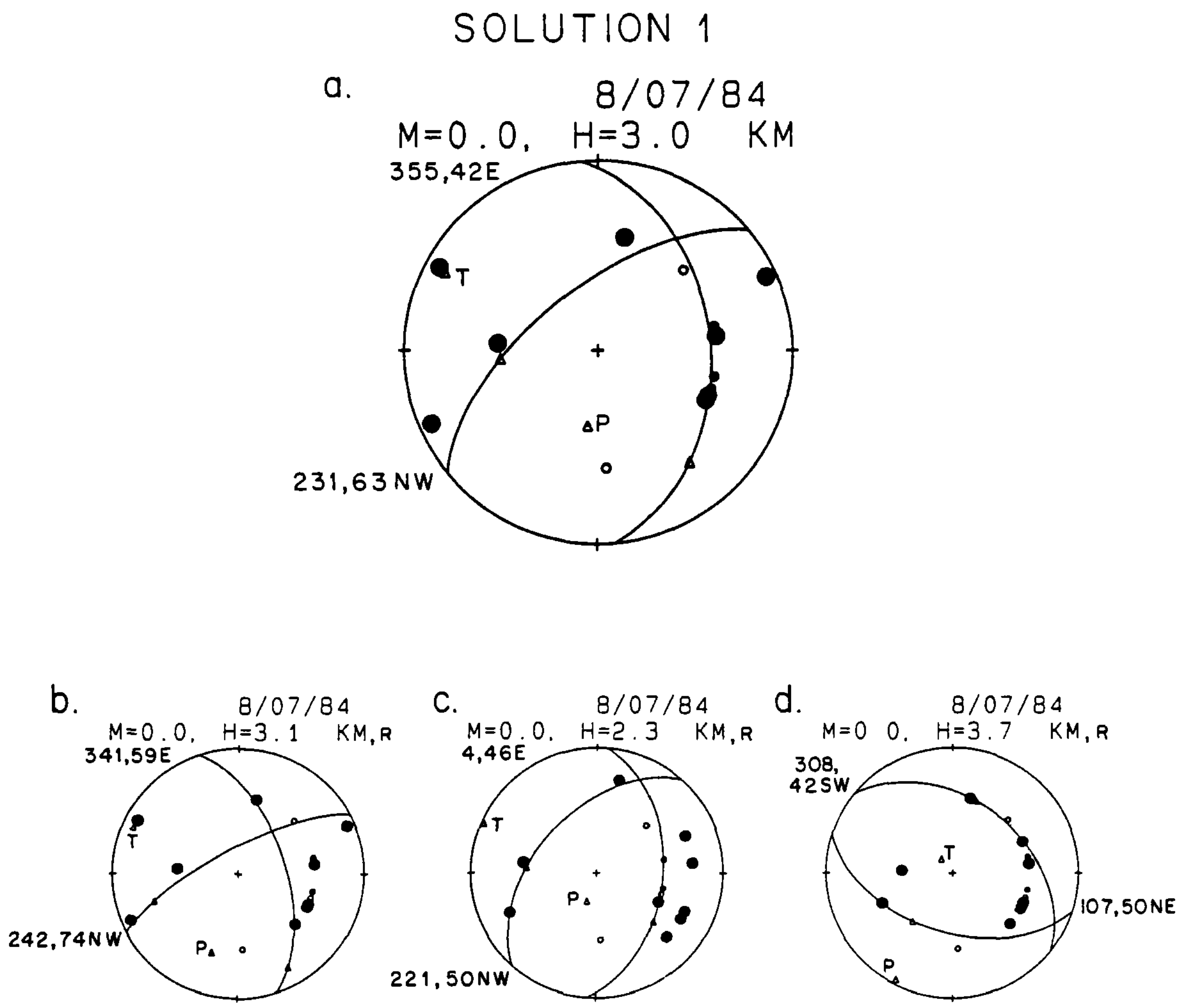


Figure 5.6. Focal mechanisms for solution 1. Projections are lower-hemisphere, equal-area. Filled in circles represent compressions, open dilatations. Triangles represent P-axis, T-axis, and alternative slip vectors. Symbol h represents focal depth, R, restricted fixed depth solutions. Numbers are the strike and dip of the nodal planes.

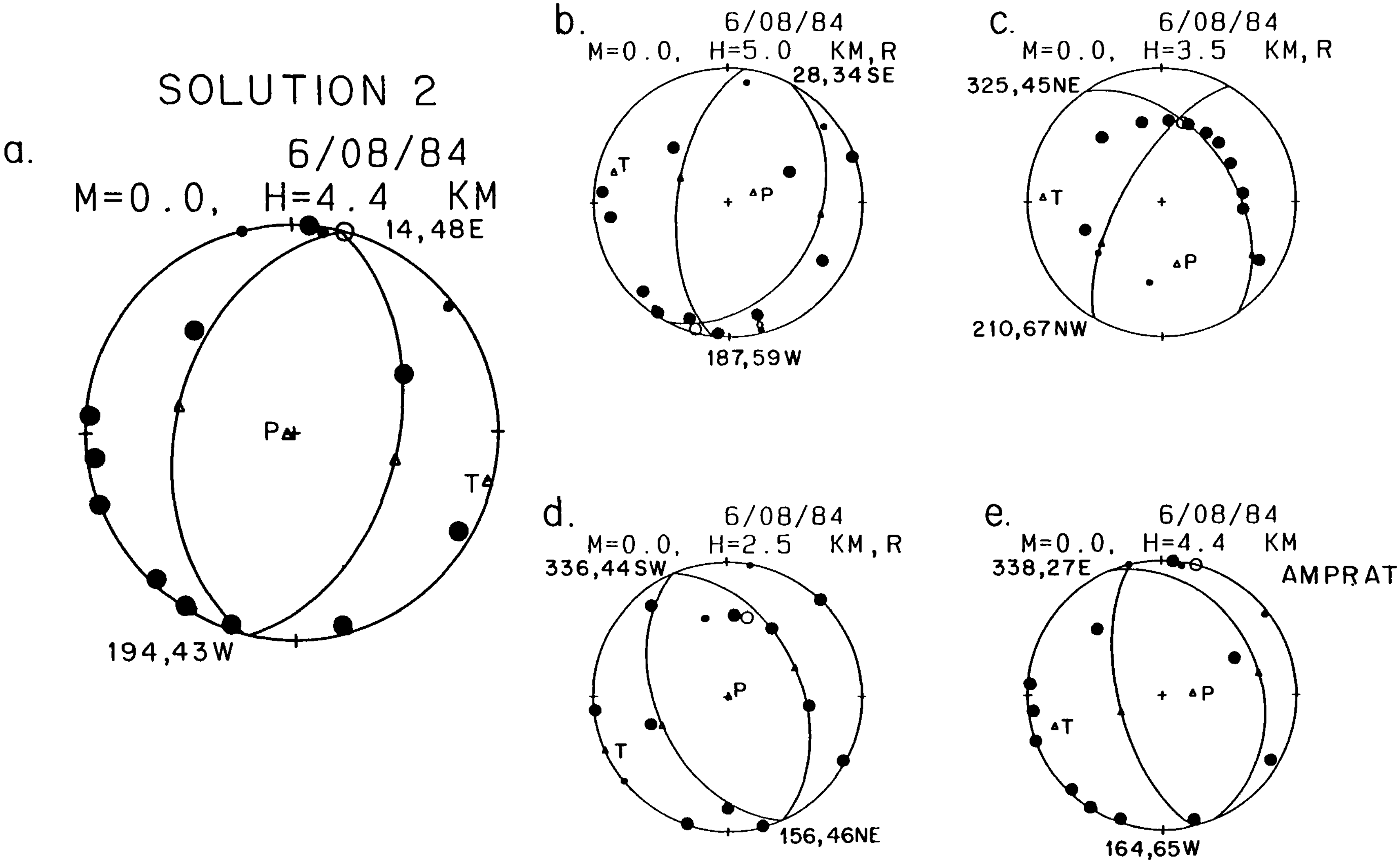


Figure 5.7. Focal mechanisms for solution 2 at its free depth (a) and restricted depths (b,c,d), e is the AMPRAT solution at the free depth. Symbols as in figure 5.6.

solution 1 at 3.7 km depth (fig 5.6) is valid. The free-depth solutions of normal-faulting type (solutions 1a and 2a) are preferred.

In figure 5.5b thirteen events in the outlined box range in depth from mine level (0.6 km) down to 1.0 km. Five fault-plane solutions for events sampled from this box are systematically shown as solutions 3 through 7 (see Appendix E). In general, mechanisms 3-6 are consistent in that all are compressional mechanisms with an implied predominance of reverse slip on planes of moderate dip. Solution 7, a composite of seven events at 0.6 (+,-0.1) depth is of the same type. Inconsistency of these events is seen in the fact that they have divergent orientations of P-axis, presumably approximating the direction of maximum horizontal compression.

Solutions 8 and 9 in figure 5.5b show a contradiction in the first-motion quadrants. Solution 8 has a free depth of 1.4 km. The data quality is good and there are no first motions in disagreement with the solution (Appendix E). To test the stability of the mechanism to focal depth, the depth sequentially was held at depths of 0.6 km, 1.0 km, 1.6 km, and 2.0 km. The resulting mechanism was consistently compressional, with only minor change in P-axis orientation for each depth (see Appendix E).

Solution 9 (fig. 5.5b, Appendix E) is a composite of two events, each well constrained to be at 1.5 km depth. This solution was also analyzed for its sensitivity to focal depth. The focal mechanism stays dilatational for depths of 2.0 km, 1.6 km, 1.4 km, and 1.0 km. At a fixed depth at 0.6 km, however, the focal depth becomes compressional, showing a change in the pattern of take-off directions on the focal sphere. The data of figure 5.5b show convincing evidence for compressional-type mechanisms at or slightly below mine level. Whether or not there is a change in stress orientation below mine level cannot be simply resolved by solutions 8 and 9, although solution 8 of the compressional type is more reliable.

Next, focal mechanism information was added from subset-A events in the 2 km to 4 km depth range below the mining area (fig. 5.5a). The focal depths for these events are not strictly as reliable as for the "best" set, but the solutions are informative. Four events beneath the mining area in figure 5.5a between 2.3 km and 3.4 km depth had an adequate number of first-motion observations and were systematically tested for focal-depth reliability. Results presented in Appendix E show variable quality in terms of distinct RMS minima and focal depth stability. Event 11 at 2.7 km depth has the highest-quality focal depth; for the other three events the depth stability was good, but RMS-versus-depth profiles would allow events 10 and 12 to have a depth less than 1 km, while event 13 might be as shallow as 1.7 km. The resulting fault-plane solutions (10 to 13) for the free focal depths are schematically shown in figure 15a. As a group the mechanisms are consistent and of compressional type. Alternative fault-plane solutions for a range of focal depths are included in Appendix E. For each event the mechanism is not sensitive to depth. Solution 11 at 2.7 km depth and solution 13 at 3.4 km depth (perhaps as shallow as 1.7 km) provide a good basis for inferring reverse-type faulting 1 km to 2 km below mine level. Solutions 10 and 12 show the same type mechanism but their precise depth location must be considered uncertain.

An unexpected result of the data analysis from the EWP-84 data set was the observation that the majority of located events appeared to have ubiquitous, dilatational P-wave first motions. A similar result was observed by the WCC group for data in the Gentry Mountain area. There, only about three events of more than 200 located in that mining area had mixed first motions, and those were not of high quality (I.G. Wong, Woodward-Clyde Consultants, personal communication, 1985). The observations are enigmatic but similar to observations made by Kusznir and others (1980) in a study of longwall coal mining in England where the source mechanisms were interpreted to be implosional. The important point is that the abundant seismic events recorded during the EWP-84 experiment did not simply lead to abundant focal-mechanism information. On the contrary, extensive efforts had to be made to find events with both compressional and dilatational first motions—that at the same time were well recorded and amenable to reliable hypocentral location. More complete discussion of the investigation of these seismic events with dilatational first motions is given by Williams (1986).

Further discussion of these results of the EWP-84 experiment is pursued in a companion report. We refer the reader to Arabasz (1985), "Interpretation of Instrumental Seismicity and Contemporary Tectonics of the Eastern Wasatch Plateau Relevant to Seismic Exposure of the Joes Valley and Scofield Dams."

## ACKNOWLEDGMENTS

Numerous individuals made contributions relating to various aspects of the acquisition, analysis, and interpretation of data presented in this report. R.A. Martin, of the U.S. Bureau of Reclamation (USBR), I.G. Wong of Woodward-Clyde Consultants (WCC), and J.C. Pechmann of the University of Utah (U of U) were primary co-investigators (together with W.J. Arabasz) in the 1984 Eastern Wasatch Plateau field experiment. We gratefully acknowledge their help through all stages leading to this report.

The following individuals were part of the respective field groups: D.C. Martin, E. McPherson, T.L. Olson, J.F. Peinado, K.A. Poulson, and J.K. Whipp (U of U); R. LaForge, R.A. Hansen, and C.K. Wood (USBR); and J.A. Adams and I.G. Humphrey (WCC). D.T. Loeb, T.L. Olson, J.F. Peinado, and R.M. Smith helped at the University of Utah in the analysis of data for this report; W.D. Richins, D. Cameron, and E.D. Brown kindly provided computer assistance.

The cooperation of officials of Utah Power & Light Company was crucial to the 1984 field experiment—notably in connection with investigations of mining-related seismic activity in the East Mountain area; we are especially indebted to R.C. Fry for key assistance, and T.W. Lloyd for help with subsurface operation of seismographs. J.F. Niebergall, W.E. Nowak, C. Reed, and S. Robison of the U.S. Forest Service provided useful help relating to site selection for the temporary network and especially to compilation of information on seismic exploration activity and active mining in the study area.

Data analysis and preparation of this report was supported by U.S. Bureau of Reclamation Contract No. 4PG 40 13210. Field work and companion research at the University of Utah was supported by the National Science Foundation, Grant No. EAR-8319661. Woodward-Clyde Consultants participated in the 1984 field experiment with support from the Office of Nuclear Waste Isolation, Battelle Memorial Institute, and the U.S. Department of Energy.

## REFERENCES

Arabasz, W.J., and Julander, D.R., 1986, Geometry of seismically active faults within the Basin and Range-Colorado Plateau transition in Utah, in Mayer, L., ed., Extensional tectonics of the southwestern United States: A perspective on processes and kinematics: Geological Society of America Special Paper 208, in press.

Bakun, W.H., and Lindh, A.G. 1977, Local magnitudes, seismic moments, and coda durations for earthquakes near Oroville, California: Bulletin of the Seismological Society of America, v. 67, p. 615-629.

Griscom, M, and Arabasz, W.J., 1979, Space-time seismicity patterns in the Utah Region: A 300-km-long seismicity gap in the Intermountain seismic belt: Earthquake Notes, v. 50, no. 4, p. 69.

Hintze, L.F., 1973, Geologic history of Utah: Brigham Young University Geological Studies, v. 20, pt. 3, 181 pp.

Klein, F.W., 1978, Hypocenter location Program: HYPOINVERSE: U.S. Geological Survey Open-File Report 78-694.

Kusznir, N.J., Ashwin, D.P., and Bradley, A.G., 1980, Mining induced seismicity in the North Staffordshire Coalfield, England: International Journal of Rock Mechanics, Mineral Sciences & Geomechanical Abstracts, v. 17, p. 45-55.

Lindseth, R.O., 1982, Digital processing of geophysical data a review: Calgary, Canada, Teknica Resource Development Ltd.

Suteau, A.M., and Whitcomb, J.H., 1979, A local earthquake coda magnitude and its relation to duration, moment $M_o$, and local Richter magnitude $M_L$: Seismological Society of America Bulletin, v. 69, p. 353-368.

McKee, M.E., 1982, Microearthquake studies across the Basin and Range-Colorado Plateau transition zone in central Utah: Salt Lake City, Utah, University of Utah, M.S. thesis, 118 p.

McKee, M.E., and Arabasz, W.J., 1982, Microearthquake studies across the Basin and Range-Colorado Plateau transition in central Utah, in Nielson, D.L., ed., Overthrust belt of Utah: Salt Lake City, Utah Geological Association Publication 10, p. 137-149.

Tibbets, B.L., Dunrud, C.R., and Osterwald, F.W., 1966, Seismic-refraction measurements at Sunnyside, Utah: U.S. Geological Survey Professional Paper 550-D, p. D132-D137.

Whitcomb, J.H., 1973, The 1971 San Fernando earthquake series focal mechanisms and tectonics: Pasadena, California, California Institute of Technology, Ph.D thesis (Part II).

Williams, D.J., 1986, Mining-related and tectonic seismicity in the East Mountain area, Wasatch Plateau, central Utah: Salt Lake City, Utah, University of Utah, M.S. thesis.

# Appendix A.

## CORRESPONDENCE RELATING TO COLLABORATIVE INVOLVEMENT OF THE UNIVERSITY OF UTAH, THE U.S. BUREAU OF RECLAMATION, AND WOODWARD-CLYDE CONSULTANTS

APPENDIX A

# United States Department of the Interior

BUREAU OF RECLAMATION

ENGINEERING AND RESEARCH CENTER

P O BOX 25007
BUILDING 67, DENVER FEDERAL CENTER
DENVER, COLORADO 80225-0007

IN REPLY REFER TO: D-1630

AUG 26 [illegible]

Dr. Walter J. Arabasz
Research Professor of Geology and Geophysics
Department of Geology and Geophysics
University of Utah
Salt Lake City, Utah 84112

Dear Dr. Arabasz:

Recent discussions between you and Mr. Richard A. Martin Jr. of this office have revealed your desire and proposed intention to conduct a 6-week seismic monitoring program in the vicinity of the Bureau's Joes Valley Dam which is located within the eastern Wasatch Plateau, Utah. It is our understanding that your primary objective is to simultaneously sample the tectonic earthquakes occurring naturally within the eastern Wasatch Plateau as well as the mining induced seismicity occurring beneath the adjacent coal fields to the east. We also understand that you are attempting to secure funding for this research effort through a proposal to the NSF (National Science Foundation).

The Seismotectonic Section, Geologic Services Branch, is in the process of performing a seismic hazard evaluation for Joes Valley Dam. Our investigations to date have shown that there currently exists a less than desirable understanding of the tectonic processes in effect in the eastern Wasatch Plateau. We believe that an earthquake monitoring experiment like the one that you are proposing is needed to improve the earthquake generation model for that area of Utah.

In support of your attempt to secure funding from NSF, we would like to make known our desire to participate in a joint earthquake monitoring effort in the eastern Wasatch Plateau should such a program materialize by the 1984 field season. The stipulation that the monitoring be conducted during the summer of 1984 reflects our scheduled completion date of December 1984 for the Joes Valley Dam seismic hazard evaluation. The scope of Bureau involvement can not be defined at this time because specific budgetary commitments cannot be made before Federal appropriations are in hand for FY 1984. Nevertheless, the Bureau has a definite interest in collaborating in the proposed earthquake recording experiment, particularly relating to the investigation of tectonic earthquake activity in the vicinity of Joes Valley. We have the capability to field seven Sprengnether MEQ 800 analog portable seismographs and two Sprengnetner DR-100 digital portable seismographs. The digital event recording system can operate in a telemetry mode and was successfully field tested during a 5-month monitoring program the Bureau conducted in 1982 near Palisades Dam in southeastern Idaho.

Earthquake activity beneath the Wasatch Plateau in central Utah is of considerable interest to the Bureau. In addition, intense mining-induced seismicity in the East Mountain area lies within 10 to 20 km of the Joes Valley Dam and thus is also of concern to us. A more accurate and complete definition of the stress orientation and the state of stress in the eastern Wasatch Plateau would greatly aid in our interpretation of the earthquake potential in this portion of the Intermountain Seismic Belt.

Although many of your proposed objectives are academic in nature and are properly aimed at NSF funding, the experiment planned by you provides a unique opportunity for Bureau involvement in terms of facilitating dense network monitoring of seismicity local to Joes Valley Dam and the eastern Wasatch Plateau. We are sincerely hopeful that NSF will approve your seismic monitoring experiment and look forward to the possible opportunity for a joint field effort in 1984.

Sincerely yours,

D. W. Webber

Darrell W. Webber
Assistant Commissioner
Engineering and Research

One Walnut Creek Center
100 Pringle Avenue
Walnut Creek CA 94596
415-945-3000

**Woodward-Clyde Consultants**

August 26, 1983

PBP-WCC-MS-3170
17000 - 2520, 3122.2

Dr. Walter Arabasz
Seismograph Stations
Department of Geology and Geophysics
University of Utah
Salt Lake City, Utah 84112

Dear Dr. Arabasz:

Since 1979, Woodward-Clyde Consultants has been conducting seismological investigations in the Colorado Plateau of eastern Utah, supported by the Office of Nuclear Waste Isolation, Battelle Memorial Institute and the Department of Energy. The objective of our studies has been to assess the earthquake hazard to a proposed underground nuclear waste repository in the Paradox Basin in the southeastern portion of the state. As part of our studies, we have been keenly interested in the problem of mining-induced seismicity in the eastern Wasatch Plateau and Book Cliffs because of the potential of such seismicity in the excavation of a repository. We have also attempted to refine the boundary between the Basin and Range and Colorado Plateau tectonic provinces in Utah in order to characterize the seismicity and tectonics of the Plateau for maximum earthquake and recurrence assessments. On this basis, Woodward-Clyde Consultants would be interested in joint participation with the University of Utah and the Bureau of Reclamation in the dense network earthquake recording experiment that you are proposing to the National Science Foundation.

Because this study is scheduled for the summer of 1984, in the next fiscal year, it is difficult at this time to determine the amount of manpower and instrumentation that can be committed to this experiment. However, we anticipate that we will be participating at some yet undefined level of effort. Woodward-Clyde Consultants has the capability of deploying 18 analog instruments and 14 digital instruments.

It should be emphasized that a large number of instruments and manpower are required to meet the objectives of this experiment. This can only be achieved by joint cooperation among several organizations. The large size of this experiment and cost involved would prohibit Woodward-Clyde Consultants from pursuing this project on a sole basis. We hope that the National Science Foundation will consider your proposal favorably, because it will be beneficial to our efforts in the Paradox Basin.

Very truly yours,

Ivan G. Wong
Ivan G. Wong
Senior Project Seismologist

Fred R. Conwell
Fred R. Conwell
Project Manager

# Appendix B.

## STATION DATA

## WASATCH PLATEAU STATION DATA

| Station | Lat. (N) | Long. (W) | Elevation (m) | Operating Dates (1984) | Polarity |
|---|---|---|---|---|---|
| JV1B | 39-13.94 | 111-14.19 | 2914 | Jul 6 - Aug 11 | N |
| JV2B | 39-14.07 | 111-19.35 | 3036 | Jul 6 - Aug 11 | N |
| JV3B | 39-20.57 | 111-20.31 | 3048 | Jul 6 - Aug 11 | N |
| JV4B | 39-25.61 | 111-19.06 | 3377 | Jul 6 - Aug 11 | N |
| JV5B | 39-29.66 | 111-17.18 | 3231 | Jul 6 - Aug 11 | N |
| JV6B | 39-28.52 | 111-12.97 | 3274 | Jul 7 - Aug 11 | N |
| BLCB | 39-23.02 | 111-16.99 | 2566 | Jul 29 - Aug 10 | N |
| POTB | 39-27.71 | 111-16.42 | 2853 | Jul 28 - Aug 10 | N |
| TRMB | 39-21.49 | 111-14.46 | 3002 | Jul 2 - Jul 10 | N |
| RPTB | 39-18.92 | 111-15.13 | 2670 | Jul 10 - Jul 12 | R |
| JVRB | 39-18.94 | 111-16.04 | 2249 | Jul 13 - Aug 12 | N |
| BLMB* | 39-24.76 | 111-12.56 | 3133 | Jul 31 - Aug 10 | ? |
| TMNB* | 39-22.42 | 111-14.50 | 3030 | Jul 24 - Aug 10 | ? |
| BTDU* | 39-20.31 | 111- 8.43 | 2920 | Jul 4 - Jul 12 | N |
| BTSU | 39-20.31 | 111- 8.43 | 2920 | Jun 26 - Jul 27 | N |
| CRCU | 39-27.61 | 111-10.34 | 2463 | Jul 27 - Aug 11 | R |
| DRYU | 39-22.41 | 111-13.43 | 2676 | Jun 26 - Aug 10 | N |
| (EMTB)* | 39-19.61 | 111- 9.71 | 2292 | Jul 6 - Jul 9<br>Jul 20 - Jul 27 | N |
| EMTU* | 39-19.61 | 111- 9.71 | 2932 | Jun 26 - Jul 4<br>Jul 12 - Aug 10 | N |
| ECRU | 39-20.86 | 111- 6.35 | 2725 | Jul 2 - Jul 27 | R |
| FDUU | 39-45.41 | 110-59.40 | 2975 | continuous | ? |

WASATCH PLATEAU STATION DATA

| Station | Lat. (N) | Long. (W) | Elevation (m) | Operating Dates (1984) | Polarity |
|---|---|---|---|---|---|
| FLCU | 39-20.60 | 111-10.32 | 2926 | Jun 23 - Jul 27 | N |
| GASU | 39-35.42 | 111-11.09 | 2627 | Jul 24 - Aug 11 | R |
| HOGU | 39-34.48 | 111-13.69 | 2707 | Jul 27 - Aug 11 | N |
| HUCU | 39-35.51 | 111-11.21 | 2606 | Jul 12 - Jul 23 | R |
| LFHU | 39-30.21 | 111-10.09 | 2365 | Jul 26 - Aug 11 | R |
| NMTU | 39-14.89 | 111- 6.76 | 1897 | Jun 21 - Jul 25 | R |
| NMHU | 39-23.19 | 111- 6.93 | 2173 | Jun 27 - Aug 11 | N |
| NKWU | 39-32.40 | 111- 7.67 | 2588 | Jul 28 - Aug 11 | R |
| OTTU | 39-24.48 | 111- 1.79 | 2219 | Jun 22 - Jul 28 | R |
| RILU | 39-24.28 | 111- 9.58 | 2414 | Jun 21 - Aug 11 | N |
| SNLU | 39-18.51 | 111- 9.21 | 2926 | Jun 26 - Jul 27 | R |
| SNOU | 39-18.86 | 111-32.28 | 2446 | continuous | ? |
| SQNU* | 39-19.64 | 111- 6.95 | 2688 | Jul 6 - Jul 12<br>Jul 13 - Jul 15 | R |
| SPFU | 39-19.83 | 111- 5.00 | 2341 | Jun 22 - Jul 24 | R |
| SPUT | 39-31.35 | 111- 2.60 | 2365 | ?Jun 18 -Aug 31 | ? |
| TI2U | 39-28.34 | 111- 6.85 | 2475 | Jun 20 - Aug 1 | R |
| TOWU | 39-34.83 | 111-18.95 | 3109 | Jul 27 - Aug 11 | N |
| TTUT | 39-19.02 | 111- 5.63 | 2816 | Jun 15 - Aug 31 | ? |
| BRW | 39-27.95 | 111- 2.88 | 2847 | Jul 13 - Aug 24 | ? |
| CAW | 39-29.66 | 111- 4.60 | 2983 | Jul 13 - Jul 15 | ? |
| FGW | 39-28.73 | 111- 4.50 | 2957 | Jul 13 - Aug 24 | ? |
| GEW | 39-29.86 | 111- 6.18 | 2998 | Jul 29 - Aug 24 | ? |
| GRW | 39-29.22 | 111- 6.22 | 2952 | Jul 13 - Jul 25 | ? |

WASATCH PLATEAU STATION DATA

| Station | Lat. (N) | Long. (W) | Elevation (m) | Operating Dates (1984) | Polarity |
|---|---|---|---|---|---|
| GSW | 39-31.03 | 111- 6.28 | 3027 | Jul 28 - Aug 25 | ? |
| HRW | 39-31.37 | 111- 4.93 | 3060 | Aug 15 - Aug 24 | ? |
| HTW | 39-30.22 | 111- 3.69 | 2524 | Jul 14 - Aug 25 | ? |
| (K41W) | 39-29.74 | 111- 4.45 | 2476 | Jul 15 - Aug 25 | ? |
| (K42W) | 39-30.56 | 111- 4.51 | 2521 | Jul 15 - Aug 25 | ? |
| (K43W) | 39-30.86 | 111- 4.53 | 2533 | Aug 20 - Aug 25 | ? |
| (K61W) | 39-28.92 | 111- 3.49 | 2439 | Jul 17 - Aug 25 | ? |
| LFW | 39-27.48 | 111- 4.52 | 2929 | Jul 13 - Aug 15 | ? |
| LPW | 39-32.30 | 111- 5.99 | 2896 | Jul 14 - Aug 25 | ? |
| MHW | 39-27.72 | 111- 5.85 | 2890 | Aug 16 - Aug 24 | ? |
| PSW | 39-29.74 | 111- 4.45 | 2979 | Jul 15 - Aug 14 | ? |
| RFW | 39-30.00 | 111- 1.96 | 2310 | Jul 14 - Jul 26 | ? |
| SPW | 39-31.60 | 111- 3.01 | 2952 | Jul 14 - Aug 10 | ? |
| STW | 39-31.77 | 111- 4.02 | 2969 | Aug 10 - Aug 25 | ? |

[1] Ending of station code indicates operator; U (UT), University of Utah; B, U.S. Bureau of Reclamation; W, Woodward-Clyde Consultants. Parentheses indicate stations operated in subsurface mines. Asterisk identifies station with digital portable seismograph. At other stations, smoked-paper-type portable seismographs were operated--except for stations FDUU, SNOU, SPUT, and TTUT, which operated as telemetry stations of the University of Utah seismic network.

[2] N = Normal, R = Reverse

Appendix C.

CHRONOLOGY OF LARGEST EARTHQUAKES
--1984 EASTERN WASATCH PLATEAU EXPERIMENT--

(Determined from Station TTUT; $t_{5mm} \geq 7$ sec, $t_{F-P} \geq 30$ sec)
JULY 6 - AUGUST 12, 1984

| Date | P | Qual. | Motion | Arrival Time (hr min sec) | F-P | 5mm |
|---|---|---|---|---|---|---|
| 840706 | i | 1 | D | 03 30 29.4<br>30.4 | 33 | 10 |
| 840706 | i | 1 | D | 04 10 59.3<br>11 03.2 | 35 | 7 |
| 840706 | i | 1 | D | 05 35 37.3<br>40.8 | 30 | 7 |
| 840706 | i | 1 | D | 06 06 56.1<br>07 04.2 | 35 | 10 |
| 840706 | i | 1 | D | 09 10 25.6<br>10 29.88 | 31 | 9.5 |
| 840706 | i<br>e | 1 | D | 11 37 15.5<br>24.2 | 30 | 8 |
| 840706 | i<br>e | 1 | D | 15 50 37.2<br>41.7 | 30 | 7 |
| 840706 | i<br>e | 1 | D | 19 00 35.6<br>39.3 | 40 | 10 |
| 840707 | i<br>e | 1 | D | 01 43 03.5<br>07.5 | 32 | 10 |
| 840707 | i | 1 | D | 13 56 52.2<br>55.9 | 30 | 7 |
| 840707 | i | 1 | D | 18 23 18.1<br>22.5 | 40 | 9.5 |
| 840708 | i | 1 | D | 01 50 59.25<br>51 02.4 | 30 | 7.5 |
| 840708 | i | 1 | C | 18 25 25.8<br>27.9 | (35) | 8.5 |
| 840708 | i | 1 | D | 20 01 40.6<br>45.1 | 32 | 7 |
| 840709 | i | 1 | D | 02 29 07.8 | 46 | 11.5 |

| | | | | | | |
|---|---|---|---|---|---|---|
| | | | | 10.6 | | |
| 840711 | i | 1 | D | 22 28 28.5<br>31.5 | 30 | 10 |
| 840711 | i | 1 | D | 22 41 47.1<br>50.0 | 30 | 8 |
| 840712 | i | 1 | D | 13 56 05.0<br>09.3 | 36 | 8 |
| 840712 | i | 1 | D | 15 37 00.5<br>36 58.4 | 50 | 9.5 |
| 840712 | i | 1 | D | 16 57 53.2<br>56.3 | 47 | 14.5 |
| 840712 | i | 1 | D | 18 43 29.8<br>32.7 | 30 | 8 |
| 840712 | i | 1 | D | 22 35 29.7<br>32.7 | 33 | 8 |
| 840713 | i | 1 | D | 14 54 10.2 | 30 | 7.5 |
| 840713 | i | 1 | D | 15 41 40.3<br>44.1 | 40 | 11 |
| 840713 | i | 1 | D | 15 43 23.1<br>27.6 | 40 | 14.5 |
| 840714 | i | 1 | D | 03 10 53.6<br>57.4 | 30 | 7.5 |
| 840714 | i | 1 | D | 03 41 40.7<br>44.5 | 40 | 13 |
| 840714 | i | 1 | D | 09 33 35.8<br>40.3 | 30 | 8.5 |
| 840714 | i | 1 | D | 10 40 25.1<br>29.1 | 55 | 18 |
| 840714 | i | 1 | D | 23 41 36.0<br>40.4 | 32 | 10 |
| 840715 | i | 1 | D | 09 57 48.5<br>52.6 | 49 | 12.5 |

| | | | | | | |
|---|---|---|---|---|---|---|
| | | | | 12.6 | | |
| 840719 | i | 1 | D | 00 41 07.2<br>11.1 | 34 | 7.5 |
| 840719 | i | 1 | D | 02 11 40.1<br>43.8 | 42 | 10 |
| 840719 | i | 1 | D | 06 06 49.9 | 40 | 11.5 |
| 840719 | i | 1 | D | 06 58 22.2<br>25.9 | 85 | 21 |
| 840719 | i | 1 | D | 07 33 13.0 | 47 | 10 |
| 840719 | i | 1 | D | 08 56 37.8 | 35 | 7.5 |
| 840719 | i | 1 | D | 12 28 08.8<br>12.9 | 50 | 11.5 |
| 840719 | i | 1 | D | 13 44 46.4<br>50.5 | 65 | 21 |
| 840719 | i | 1 | D | 19 46 24.0<br>28.1 | 40 | 11.5 |
| 840720 | e | 1 | - | 00 09 12.8 | 42 | 7.5 |
| 840720 | i | 1 | D | 01 25 07.5 | 32 | 8.5 |
| 840720 | i | 1 | D | 05 49 17.1<br>20.7 | 58 | 17.5 |
| 840720 | i | 1 | D | 07 30 45.6<br>49.4 | 33 | 9 |
| 840720 | i | 1 | D | 08 15 15.0<br>18.3 | 35 | 8.5 |
| 840720 | i | 1 | D | 09 23 34.6<br>38.4 | 40 | 9.5 |
| 840720 | i | 1 | D | 13 26 27.6<br>31.6 | 33 | 10 |
| 840720 | i | 1 | D | 13 55 57.5<br>58.2 | 30 | 9.5 |

| | | | | | | |
|---|---|---|---|---|---|---|
| 840720 | i | 1 | D | 16 11 34.9<br>39.8 | 37 | 10 |
| 840720 | i | 1 | D | 16 54 45.6<br>49.9 | 33 | 10.5 |
| 840720 | i | 1 | D | 18 01 06.7 | 70 | 25 |
| 840720 | i | 1 | D | 19 03 21.2<br>24.9 | 35 | 9 |
| 840721 | e | 1 | D | 06 02 07.1<br>08.6 | 30 | 7.5 |
| 840721 | e | 2 | - | 06 58 25.3<br>26.7 | 30 | 8 |
| 840721 | i | 1 | D | 07 26 35.5<br>40.1 | 30 | 7 |
| 840721 | i | 1 | D | 11 21 56.0<br>22 00.2 | 35 | 9.5 |
| 840721 | i | 1 | D | 11 30 24.2<br>31.4 | (45) | 22 |
| 840721 | i | 1 | C | 11 31 12.6<br>18.1 | 34 | 9.5 |
| 840721 | i | 1 | D | 14 46 30.5<br>34.7 | 30 | 8.5 |
| 840721 | i | 1 | D | 18 38 43.1 | 45 | 13 |
| 840721 | i | 1 | D | 23 03 31.6<br>35.5 | 31 | 8 |
| 840721 | i | 1 | D | 23 34 51.0<br>54.4 | 30 | 7.5 |
| 840722 | i | 1 | D | 00 31 40.6<br>44.5 | 30 | 7 |
| 840722 | i | 1 | D | 02 55 05.9<br>09.4 | 31 | 7.5 |
| 840722 | i | 1 | D | 11 58 28.5<br>25.5 | 80 | 24 |

| | | | | | | |
|---|---|---|---|---|---|---|
| 840722 | i | 1 | D | 12 38 37.5 | 50 | 13.5 |
| 840722 | i | 1 | D | 15 44 02.5 | 38 | 8.5 |
| 840722 | i | 1 | D | 19 14 25.0<br>29.2 | 30 | 8 |
| 840722 | i | 1 | D | 20 30 42.4<br>46.2 | 30 | 8 |
| 840722 | i | 1 | D | 22 50 05.0 | 45 | 13 |
| 840723 | i | 1 | D | 00 50 49.0<br>52.9 | 65 | 16 |
| 840723 | i | 1 | D | 05 14 07.0<br>11.1 | (35) | (7) |
| 840723 | i | 1 | D | 06 02 06.6<br>11.6 | 50 | 16 |
| 840723 | i | 1 | D | 07 45 19.3<br>23.4 | 46 | 11.5 |
| 840723 | i | 3 | | 10 12 37.5 | (30) | 9 |

--noise: 14:00 to 15:00--

| | | | | | | |
|---|---|---|---|---|---|---|
| 840723 | i | 1 | D | 15 51 07.0<br>10.8 | 50 | 12.5 |
| 850723 | i | 1 | D | 16 10 51.3<br>55.4 | (35) | 9.5 |
| 840723 | i | 1 | D | 16 49 04.3<br>08.1 | 30 | 9.5 |

--noise: 19:00 to end of day--

| | | | | | | |
|---|---|---|---|---|---|---|
| 840723 | i | 1 | D | 21 20 05.0 | (70) | 23 |

--noise: 00:00 to 01:15--

| | | | | | | |
|---|---|---|---|---|---|---|
| 840724 | i | 1 | D | 02 00 11.0 | 40 | 10 |
| | | | | 14.7 | | |
| 840724 | i | 1 | D | 02 52 10.7 | 35 | 9.5 |
| | | | | 15.2 | | |
| 840724 | i | 1 | D | 03 11 51.9 | 110 | 30 |
| | | | | 50.0 | | |
| 840724 | i | 1 | D | 12 06 46.0 | 70 | 16 |
| | | | | 50.0 | | |

--noise: 12:15 to 16:15--

| | | | | | | |
|---|---|---|---|---|---|---|
| 840724 | ( | | | 13 11 55+ | (35) | ) |
| | | | | 12 02.4 | | |
| 840724 | ( | | | 13 44 40+ | (40) | ) |
| | | | | 49.9 | | |
| 840724 | i | 1 | D | 15 51 15.6 | 60 | 15 |
| | | | | 20.1 | | |
| 840724 | i | 1 | D | 17 23 45.9 | 40 | 10 |
| | | | | 49.5 | | |
| 840724 | i | 1 | D | 18 08 21.4 | (40) | 10 |
| | | | | 25.3 | | |
| 840724 | i | 1 | - | 18 09 02.0 | 30 | 8 |
| | | | | 06.5 | | |
| 840724 | i | 1 | D | 22 39 45.0 | 30 | 7 |
| | | | | 48.7 | | |
| 840724 | i | 1 | D | 23 15 49.9 | 40 | 9.5 |
| | | | | 53.9 | | |
| 840725 | i | 1 | D | 07 37 54.5 | 50 | 15 |

| | | | | | | |
|---|---|---|---|---|---|---|
| 840725 | i | 1 | D | 07 57 16.0<br>19.5 | 40 | 8.5 |
| 840725 | i | 1 | D | 09 11 19.2<br>22.8 | 30 | 10 |
| 840725 | i | 1 | D | 09 56 29.9<br>34.1 | 36 | 10 |

--noise: 15:15 to 20:15--

| | | | | | | |
|---|---|---|---|---|---|---|
| 840725 | i | 1 | D | 17 29 45.9 | 42 | 7 |
| 840725 | i | 1 | D | 18 44 13.6 | 48 | 14 |
| 840725 | (i | 1 | D | 19 15 00.0 | (50) | 15) |
| 840725 | i | 1 | D | 21 55 45.5 | (70) | (25) |
| 840725 | i | 2 | D | 21 20 50.6<br>55.0 | (35) | 9 |

| | | | | | | |
|---|---|---|---|---|---|---|
| 840726 | i | 2 | D | 00 49 52.5<br>56.1 | (50) | 11.5 |
| 840726 | i | 2 | D | 01 17 27.9<br>30.7 | 35 | 9 |
| 840726 | i | 1 | D | 02 27 03.0 | 31 | 8.5 |
| 840726 | i | 1 | D | 02 39 03.1<br>07.3 | (55) | 17.5 |
| 840726 | i | 1 | D | 04 10 38.9 | 36 | 8 |
| 840726 | i | 3 | D | 04 02 11.4<br>15.8 | 40 | 9 |
| 840726 | i | 1 | D | 04 19 28.2<br>32.3 | 40 | 10 |

--noise: 14:30 to 16:30--

| | | | | | | |
|---|---|---|---|---|---|---|
| 840726 | i | 1 | D | 16 47 14.6<br>15.5 | 40 | 7 |

| | | | | | | |
|---|---|---|---|---|---|---|
| 840726 | i | 1 | D | 17 11 52.0 | 54 | 9 |
| | | | | 55.3 | | |
| 840726 | i | 1 | D | 23 59 31.5 | (40) | 11 |
| | | | | 34.7 | | |
| 840727 | i | 1 | D | 02 19 50.8 | (30) | 7 |
| | | | | 55.9 | | |
| 840727 | i | 1 | D | 03 11 26.9 | 35 | 8.5 |
| | | | | 31.2 | | |
| 840727 | i | 1 | D | 05 28 00.0 | 35 | 8.5 |
| 840727 | i | 1 | D | 08 22 42.8 | 30 | 7 |
| | | | | 41.5 | | |
| 840727 | i | 1 | D | 10 44 05.7 | 40 | 8.5 |
| | | | | 09.4 | | |

--noise: 14:00 to 21:00--

| | | | | | | |
|---|---|---|---|---|---|---|
| 840727 | (i | 1 | D | 15 29 24.0 | (40) | 8.5) |
| | | | | 25.3 | | |
| 840727 | (i | 1 | | 16 08 24.0 | (45) | 8) |
| 840727 | (i | 1 | | 16 09 16.3 | (35) | 7.5) |
| 840727 | ( | | | 19 28 49.5 | (40) | (9)) |
| | | | | 51.7 | | |
| 840727 | i | 1 | D | 22 32 06.5 | (50) | 11 |
| | | | | 10.9 | | |
| 840727 | i | 1 | D | 22 41 28.0 | (70) | 12 |
| | | | | 31.4 | | |
| 840727 | i | 1 | D | 23 50 19.0 | 40 | 8 |
| 840728 | i | 1 | D | 00 44 12.4 | 46 | 8 |
| | | | | 16.1 | | |
| 840728 | i | 1 | D | 00 53 28.3 | (50) | 10 |
| | | | | 31.7 | | |
| 840728 | i | 1 | D | 01 13 00.3 | 68 | 17 |
| | | | | 04.7 | | |

| | | | | | | |
|---|---|---|---|---|---|---|
| 840728 | i | 1 | D | 01 51 18.3 | 30 | 7 |
| | | | | 21.2 | | |
| 840728 | i | 1 | D | 03 25 32.8 | (65) | 17 |
| | | | | 36.8 | | |
| 840728 | i | 1 | D | 03 53 58.9 | (50) | 10.5 |
| 840728 | i | 1 | D | 04 04 07.4 | (30) | 7 |
| 840728 | i | 1 | D | 08 15 11.8 | 36 | 9 |
| | | | | 15.7 | | |
| 840728 | i | 1 | D | 13 19 04.6 | 53 | 10.5 |
| | | | | 05.5 | | |
| 840728 | i | 1 | D | 15 12 44.0 | 52 | 10 |
| | | | | 48.7 | | |
| 840729 | i | 1 | D | 00 37 54.8 | 31 | 7 |
| | | | | 58.4 | | |
| 840729 | i | 1 | D | 02 24 29.0 | 59 | 11.5 |
| | | | | 33.1 | | |
| 840729 | i | 1 | D | 05 05 43.3 | 47 | 9 |
| | | | | 47.5 | | |

| | | | | | | |
|---|---|---|---|---|---|---|
| 840729 | i | 1 | D | 11 09 34.7 | 50 | 10.5 |
| | | | | 39.1 | | |
| 840729 | i | 1 | D | 12 27 44.5 | 45 | 9.5 |
| | | | | 48.5 | | |
| 840729 | i | 1 | D | 12 47 50.9 | 36 | 6.5 |
| | | | | 54.6 | | |
| 840729 | i | 1 | D | 14 38 49.1 | 46 | 8 |
| | | | | 53.0 | | |
| 840729 | i | 1 | - | 14 41 46.1 | (40) | 9 |
| | | | | 49.7 | | |
| 840729 | i | 1 | D | 18 00 30.1 | 30 | 7 |
| | | | | 33.9 | | |
| 840730 | i | 1 | | 03 30 30.4 | (35) | 7 |
| 840730 | i | 1 | C | 03 43 07.5 | 30 | 7.5 |
| 840730 | i | 1 | - | 03 49 19.0 | (30) | 7 |
| 840730 | i | 1 | D | 07 13 26.8 | 34 | 7 |
| 840730 | i | 1 | D | 10 12 42.0 | 54 | 10 |
| 840730 | i | 1 | ? | 14 16 50.0 | 65 | 11.5 |
| 840730 | i | 1 | D | 14 20 37.9 | (40) | 8 |
| 840730 | i | 1 | D | 15 50 23.2 | (50) | 9.5 |

| | | | | | | |
|---|---|---|---|---|---|---|
| 840730 | i | 1 | D | 18 12 11.0 | 50 | 9 |
| 840730 | i | 1 | D | 19 27 03.6 | (70) | 13 |
| 840730 | i | 1 | D | 19 48 59.0 | 35 | 7.5 |
| 840730 | i | 1 | D | 20 05 13.6 | (40) | 9 |
| 840730 | i | 1 | D | 21 49 02.8 | (90) | 19.5 |
| 840730 | i | 1 | C | 22 19 55.1 | (30) | 7.5 |
| 840730 | i | 1 | D | 22 20 43.0 | (35) | 7 |
| 840730 | i | 1 | D | 23 41 57.1 | 38 | 7 |
| 840730 | i | 1 | D | 23 54 20.9 | 50 | 10 |

| | | | | | | |
|---|---|---|---|---|---|---|
| 840731 | i | 1 | D | 02 56 46.3 | 30 | 7 |
| 840731 | i | 1 | D | 03 44 30.0 | 35 | 7.5 |
| 840731 | i | 1 | D | 04 50 57.3 | 50 | 10.5 |
| 840731 | i | 1 | D | 04 54 33.3 | 43 | 9 |
| 840731 | i | 1 | D | 05 34 22.5 | 64 | 11 |
| 840731 | i | 1 | D | 05 59 31.4 | 33 | 7.5 |
| 840731 | i | 1 | D | 07 01 27.1 | 35 | 8 |
| 840731 | i | 1 | D | 08 57 17.8 | 36 | 7.5 |
| 840731 | i | 1 | D | 12 14 17.2 | 50 | 8.5 |
| 840731 | i | 1 | D | 13 11 29.1 | 50 | 8.5 |
| 840731 | i | 1 | D | 16 54 05.5 | 30 | 7 |
| 840731 | i | 1 | D | 18 09 37.0 | (40) | 8.0 |
| 840731 | i | 1 | D | 18 42 00.5 | 50 | 9 |
| 840731 | i | 1 | D | 19 54 18.4 | 30 | 7 |
| 840731 | i | 1 | D | 19 55 49.6 | (40) | 8 |
| 840731 | i | 1 | D | 20 50 18.4 | (100) | 27 |

| | | | | | | |
|---|---|---|---|---|---|---|
| 840731 | i | 1 | D | 21 18 26.1 | (70) | 18 |
| 840731 | i | 1 | D | 22 49 33.0 | 33 | 7 |
| | | | | | | |
| 840801 | i | 1 | D | 02 36 27.0 | (30) | 7.5 |
| 840801 | i | 1 | D | 02 36 47.4 | (40) | 8 |
| 840801 | i | 1 | D | 03 11 22.1 | 80 | 14 |
| 840801 | i | 1 | D | 03 58 06.7 | (50) | 9 |
| 840801 | i | 1 | D | 04 52 04.8 | (55) | 12 |
| 840801 | i | 1 | D | 07 24 48.5 | (65) | 17 |
| 840801 | i | 1 | D | 09 09 41.4 | 60 | 9.5 |
| 840801 | i | 1 | D | 13 10 23.0 | 43 | 8 |
| 840801 | i | 1 | D | 13 18 42.7 | 38 | 7 |
| 840801 | i | 1 | D | 14 20 38.6 | (70) | 11 |
| 840801 | i | 3 | D | 16 29 50.0 | (70) | 11 |
| 840801 | i | 1 | D | 17 53 06.8 | (30) | 7 |
| 840801 | i | 1 | D | 17 56 40.6 | (30) | 7 |

--noise: 18:45 to 21:45--

| | | | | | | |
|---|---|---|---|---|---|---|
| 840801 | i | 3 | D | 20 02 58.0 | (60) | 14 |
| 840801 | i | 1 | D | 22 41 52.1 | (60) | 11.5 |
| 840801 | i | 1 | D | 23 15 32.5 | (90) | 14 |
| 840801 | i | 1 | D | 23 57 32.7 | (35) | 7 |
| | | | | | | |
| 840802 | i | 1 | D | 00 36 41.0 | (30) | 7.5 |

| | | | | | | |
|---|---|---|---|---|---|---|
| 840802 | i | 1 | C | 00 48 27.4 | 35 | 6.5 |
| 840802 | i | 1 | D | 00 56 02.5 | (50) | 12 |
| 840802 | i | 1 | D | 01 00 45.0 | 35 | 8 |
| 840802 | i | 1 | D | 03 12 40.1 | (40) | 8.5 |
| 840802 | i | 1 | D | 03 40 13.0 | 45 | 8 |
| 840802 | i | 1 | D | 03 55 22.1 | 30 | 7 |
| 840802 | i | 1 | D | 04 08 08.0 | (30) | 7.5 |
| 840802 | i | 1 | D | 04 18 21.1 | 46 | 8.0 |
| 840802 | i | 1 | D | 05 38 10.2 | (50) | 12.5 |
| 840802 | i | 1 | D | 06 19 27.0 | 30 | 6 |
| 840802 | i | 1 | D | 06 20 12.2 | 55 | 11 |
| 840802 | i | 1 | D | 07 43 01.5 | 60 | 11 |
| 840802 | i | 1 | D | 08 12 31.3 | 40 | 8 |
| 840802 | i | 1 | D | 08 28 03.5 | 40 | 7.5 |
| 840802 | i | 1 | D | 09 49 06.5 | 46 | 9 |
| 840802 | i | 1 | D | 13 46 06.2 | (50) | 10 |
| 840802 | i | 1 | D | 15 26 43.2 | (50) | 10 |
| 840802 | i | 1 | D | 16 37 12.5 | (50) | 9.5 |
| 840802 | i | 1 | - | 16 38 58.0 | (40) | 8 |
| 840802 | i | 1 | D | 21 51 43.6 | (60) | 11 |
| | | | | | | |
| 840803 | i | 1 | D | 01 00 01.4 | (70) | 17 |
| 840803 | i | 1 | D | 01 15 20.5 | 40 | 8 |
| 840803 | i | 1 | D | 01 25 04.4 | (60) | 12 |
| 840803 | i | 1 | D | 02 11 38.0 | 70 | 12.5 |
| 840803 | i | 1 | D | 02 20 18.6 | 33 | 7 |
| 840803 | i | 1 | D | 03 04 47.9 | 38 | 7.5 |

| | | | | | | |
|---|---|---|---|---|---|---|
| 840803 | i | 1 | D | 07 17 31.0 | 38 | 7.5 |
| 840803 | i | 1 | D | 09 14 07.5 | 39 | 8 |
| 840803 | i | 1 | D | 11 40 33.1 | (30) | 7 |

--noise: 14:15 to 20:45--

| | | | | | | |
|---|---|---|---|---|---|---|
| 840803 | i | 1 | D | 15 04 10.8 | (50) | 9.5 |
| 840803 | i | 2 | D | 16 44 09.5 | (40) | 8 |
| 840803 | i | 1 | D | 20 04 04.6 | (100) | 31 |
| 840803 | i | 1 | D | 20 20 14.7 | (70) | 13 |
| 840803 | i | 1 | D | 20 20 44.0 | (50) | 9.5 |
| 840803 | i | 1 | D | 22 58 45.8 | (50) | 9 |
| 840803 | i | 1 | D | 22 59 18.3 | 72 | 12 |
| 840804 | i | 1 | D | 01 00 04.9 | (50) | 9.5 |
| 840804 | i | 1 | D | 01 23 49.1 | 42 | 8 |
| 840804 | i | 1 | D | 02 16 20.5 | 49 | 9.5 |
| 840804 | i | 1 | D | 02 39 30.9 | 56 | 9 |
| 840804 | i | 1 | D | 02 47 58.1 | 54 | 12.5 |
| 840804 | i | 1 | D | 05 03 34.2 | (45) | 8.5 |
| 840804 | i | 1 | D | 06 39 13.2 | 40 | 8.5 |
| 840804 | i | 1 | D | 07 19 00.5 | 59 | 12 |
| 840804 | i | 1 | D | 07 37 20.0 | 114 | 31.5 |
| 840804 | i | 1 | D | 08 20 06.5 | 84 | 20.5 |
| 840804 | i | 1 | D | 08 37 40.5 | 60 | 11.0 |

| | | | | | | |
|---|---|---|---|---|---|---|
| 840804 | i | 1 | D | 09 32 39.0 | 40 | 8.0 |
| 840804 | i | 1 | D | 10 03 35.0 | 61 | 10 |
| 840804 | i | 1 | D | 11 57 34.6 | 70 | 13 |
| 840804 | i | 1 | D | 12 07 49.4 | 50 | 12 |
| 840804 | i | 1 | D | 14 21 06.1 | 55 | 9.5 |
| 840804 | i | 1 | D | 14 23 14.5 | (40) | 8 |
| 840804 | i | 1 | D | 16 17 58.0 | 56 | 11.5 |
| 840804 | i | 1 | D | 16 54 17.0 | 50 | 10 |
| 840804 | i | 1 | D | 17 21 04.0 | 64 | 13.5 |
| 840804 | i | 1 | D | 17 48 30.7 | 33 | 7 |
| 840804 | i | 1 | D | 18 32 19.2 | 44 | 11.5 |
| 840804 | i | 1 | D | 20 16 20.0 | 49 | 7 |
| 840804 | i | 1 | D | 20 53 48.0 | 50 | 10 |
| 840804 | i | 1 | D | 21 03 26.0 | 33 | 7.5 |
| 840805 | i | 1 | D | 01 16 03.0 | 41 | 10 |
| 840805 | i | 1 | C | 02 17 14.5 | 34 | 8.0 |
| 840805 | i | 1 | D | 02 41 54.3 | (40) | 8.5 |
| 840805 | i | 1 | D | 03 54 47.3 | 35 | 9.5 |
| 840805 | i | 1 | D | 04 12 07.0 | 39 | 8 |
| 840805 | i | 1 | D | 05 16 10.1 | 47 | 12 |
| 840805 | i | 1 | D | 08 28 55.9 | 38 | 8 |
| 840805 | i | 1 | D | 09 41 52.3 | 31 | 7 |
| 840805 | i | 1 | D | 09 43 41.1 | 37 | 8.5 |
| 840805 | i | 1 | D | 13 18 54.4 | 32 | 7 |
| 840805 | i | 1 | D | 13 59 12.9 | 43 | 10 |
| 840805 | i | 1 | D | 15 38 11.5 | 30 | 7 |

| | | | | | | |
|---|---|---|---|---|---|---|
| 840805 | i | 1 | D | 17 25 49.0 | 30 | 8 |
| 840805 | i | 1 | D | 21 20 22.3 | 45 | 8 |
| 840805 | i | 1 | D | 21 22 46.3 | 55 | 8.5 |
| 840805 | i | 1 | D | 21 46 26.5 | 58 | 11.5 |
| 840805 | i | 1 | D | 22 09 25.3 | 65 | 12.5 |
| 840805 | i | 1 | D | 23 54 11.0 | 53 | 11 |
| 840806 | i | 1 | D | 00 34 50.0 | 72 | 22 |
| 840806 | i | 1 | D | 02 54 31.3 | 64 | 16 |
| 840806 | i | 1 | D | 06 18 57.6 | 42 | 9 |
| 840806 | i | 1 | D | 06 59 47.5 | 60 | 18 |

--noise: 14:00 to 21:15--

| | | | | | | |
|---|---|---|---|---|---|---|
| 840806 | i | 1 | D | 16 29 02.5 | (50) | 10 |
| 840806 | i | 1 | D | 16 41 10.0 | (40) | 7.5 |
| 840806 | i | 1 | D | 20 44 48.7 | (30) | 7 |
| 840806 | i | 1 | D | 21 29 21.0 | (50) | 13.5 |
| 840806 | i | 1 | D | 23 00 52.5 | 54 | 11 |
| 840807 | i | 1 | D | 01 45 21.3 | 44 | 8 |
| 840807 | i | 1 | D | 03 43 44.3 | 54 | 9.5 |
| 840807 | i | 1 | D | 04 46 24.0 | 38 | 7 |
| 840807 | i | 1 | D | 05 22 43.3 | 4.1 | 8.5 |
| 840807 | i | 1 | D | 07 14 11.4 | 64 | 14.5 |
| 840807 | i | 1 | D | 08 26 02.7 | 82 | 25 |
| 840807 | i | 1 | D | 08 31 20.5 | 41 | 8.5 |

--noise: 09:00 to 10:00--

--noise: 11:00 to 16:40--

| | | | | | | |
|---|---|---|---|---|---|---|
| 840807 | i | 1 | D | 12 02 40.5 | 55 | 11 |
| 840807 | i | 1 | D | 13 14 22.5 | 8 | (40) |
| 840807 | i | 1 | D | 17 08 15.5 | 40 | 7 |
| 840807 | i | 1 | D | 17 42 33.2 | (40) | 8 |
| 840807 | i | 1 | D | 19 19 13.1 | (70) | 20.5 |
| 840807 | i | 1 | D | 22 57 07.0 | (30) | 7.5 |
| 840807 | i | 1 | D | 23 48 54.4 | 46 | 8.5 |
| 840808 | i | 1 | D | 15 41 58.6 | 60 | 13 |
| 840808 | i | 1 | D | 15 43 34.6 | 45 | 8.5 |
| 840808 | i | 1 | D | 22 30 41.4 | 45 | 10 |
| 840809 | i | 1 | D | 02 31 20.0 | 40 | 8.5 |
| 840809 | i | 1 | D | 03 44 48.5 | 30 | 7 |
| 840809 | i | 1 | D | 05 55 09.4 | 42 | 11 |
| 840809 | i | 1 | D | 07 35 17.9 | 35 | 8.5 |

--noise: 11:45 to 14:30--

| | | | | | | |
|---|---|---|---|---|---|---|
| 840809 | i | 1 | D | 17 09 29.0 | 75 | 19.5 |
| 840809 | i | 1 | D | 18 16 12.5 | 60 | 13.5 |
| 840809 | i | 1 | D | 19 14 05.4 | 35 | 7 |

| | | | | | | |
|---|---|---|---|---|---|---|
| 840809 | i | 1 | D | 21 35 04.4 | 37 | 10.5 |
| 840810 | i | 1 | D | 02 12 14.3 | 35 | 7.5 |
| 840810 | i | 1 | D | 02 37 06.1 | 40 | 7.5 |
| 840810 | i | 1 | D | 02 58 54.7 | 45 | 9 |
| 840810 | i | 1 | D | 03 05 41.6 | 50 | 10 |
| 840810 | i | 1 | D | 08 07 25.1 | 40 | 9 |
| 840810 | i | 1 | D | 09 37 06.6 | 80 | 25 |
| 840810 | i | 1 | D | 09 45 21.6 | 45 | 8.5 |
| 840810 | i | 1 | D | 10 01 55.5 | 30 | 7 |
| 840810 | i | 1 | D | 10 39 40.0 | 62 | 14 |
| 840810 | i | 1 | D | 12 41 09.0 | 47 | 8.5 |
| 840810 | i | 1 | D | 14 22 28.5 | 40 | 8 |
| 840810 | i | 1 | D | 16 05 48.0 | (30) | 7 |
| 840810 | i | 1 | D | 16 06 01.5 | 45 | 8 |
| 840810 | i | 1 | D | 18 17 25.7 | 30 | 7 |
| 840810 | i | 1 | D | 18 49 50.8 | 40 | 10 |
| 840810 | i | 1 | D | 20 33 16.4 | (30) | 7 |
| 840810 | i | 1 | D | 23 09 45.0 | 40 | 8.5 |
| 840811 | i | 1 | D | 02 47 33.8 | 30 | 7 |
| 840811 | i | 1 | D | 04 51 17.5 | 35 | 7 |
| 840811 | i | 1 | D | 05 04 04.9 | 52 | 9 |
| 840811 | i | 1 | D | 05 28 05.1 | 60 | 10.5 |
| 840811 | i | 1 | D | 06 08 56.5 | 37 | 8 |
| 840811 | i | 1 | D | 06 33 04.5 | 50 | 8 |

--noise: 06:45 to 08:15--

| | | | | | | |
|---|---|---|---|---|---|---|
| 840811 | i | l | D | 11 44 23.9 | (30) | 7 |
| 840811 | i | l | D | 14 14 15.6 | 50 | 10 |
| 840811 | i | l | D | 17 43 30.7 | 79 | 21 |
| | | | | | | |
| 840812 | i | l | D | 04 16 46.3 | (50) | 10.5 |
| 840812 | i | l | D | 07 48 52.0 | 66 | 12.5 |
| 840812 | i | l | D | 08 31 29.5 | 105 | 30 |
| 840812 | i | l | D | 10 59 12.0 | 38 | 8 |
| 840812 | i | l | D | 11 47 13.3 | 40 | 9.5 |
| 840812 | i | l | D | 14 25 38.5 | 35 | 7 |
| 840812 | i | l | D | 14 49 55.2 | 75 | 18 |
| 840812 | i | l | D | 16 06 48.5 | (60) | 11 |
| 840812 | i | l | D | 16 38 03.5 | 41 | 10 |

## Appendix D.

## SEISMIC EXPLORATION INFORMATION

CGG Land Seismic, ASI
125 E. Pearl Street
Box 2890
Jackson, Wyoming 83001
(307) 733-5079
Wasatch Spec. Line OT-84-301
Contractor's Local Representative Jim Spicer

Poulter (surface) shooting for both reflection and refraction. Permit issued July 15, 1984. On July 26, 1984, Steve Robinson, of the U.S. Forest Service, Ferron Ranger District, flew over line 301 after completion by CGG crew.

Seis-Port Exploration, Inc.
7000 South Potomac
Englewood, Colorado 80112
(303) 790-7347
also:
Suite 2000, 1616 Glenarm
Denver, Colorado 80202
Permit agent- Tom D. Hill

Permit issued June 16, 1984. Both surface and drill-hole lines.
Surface shooting: 50 lb., (10 stakes, 5 lb. each, 4 ft. above the surface) 165 ft. spacing, 32 shot points/mile.
Drill hole: 20 lb. shots in 60 ft. deep holes, 330 ft. spacing.

Northern Geophysics of America (HR)
(contract company for Exxon)
7076 S. Alton Way, Bldg. H
Englewood, Colorado 80112
(303) 741-3700

Permit issued late May, 1984. All surface shooting, 110 ft. length shot points, 48 shot points/mile, 122 miles of shooting.

# Appendix E.

## FOCAL MECHANISM DATA

Hypocentral Information for Fault Plane Solutions Described in Text

| solution | yr | date | orig | time | lat-n | long-w | depth | mag | no | gap | dmn | rms |
|---|---|---|---|---|---|---|---|---|---|---|---|---|
| 1 | 84 | 708 | 1825 | 22.58 | 39-22.50 | 111-14.87 | 3.0 | 0.8 | 20 | 127 | 2 | 0.17 |
| 2 | 84 | 806 | 34 | 46.87 | 39-23.79 | 111-15.12 | 4.3 | 1.5 | 26 | 51 | 3 | 0.17 |
| 3 | 84 | 724 | 1905 | 45.91 | 39-20.37 | 111- 7.55 | 0.7 | 0.9 | 12 | 74 | 1 | 0.12 |
| 4 | 84 | 718 | 819 | 43.03 | 39-19.44 | 111- 9.06 | 0.9 | 0.4 | 11 | 90 | 0 | 0.19 |
| 5 | 84 | 723 | 2036 | 22.40 | 39-19.96 | 111- 9.48 | 1.0 | 0.0 | 10 | 105 | 0 | 0.06 |
| 6 | 84 | 724 | 2027 | 20.69 | 39-19.81 | 111- 7.79 | 1.0 | 0.0 | 13 | 56 | 1 | 0.09 |
| 7 | 84 | 722 | 121 | 49.70 | 39-19.91 | 111- 8.21 | 0.6 | 0.7 | 17 | 54 | 0 | 0.08 |
| | 84 | 723 | 1037 | 15.97 | 39-20.06 | 111- 9.55 | 0.6 | 0.0 | 10 | 103 | 0 | 0.06 |
| | 84 | 723 | 2031 | 4.38 | 39-20.01 | 111- 9.58 | 0.6 | 0.0 | 9 | 112 | 0 | 0.04 |
| | 84 | 724 | 109 | 43.91 | 39-20.02 | 111- 9.65 | 0.7 | 0.4 | 14 | 73 | 0 | 0.06 |
| | 84 | 724 | 950 | 44.35 | 39-20.06 | 111- 9.65 | 0.7 | 0.0 | 11 | 74 | 0 | 0.06 |
| | 84 | 724 | 1147 | 26.56 | 39-20.06 | 111- 9.70 | 0.7 | 0.0 | 12 | 79 | 0 | 0.06 |
| | 84 | 725 | 333 | 49.89 | 39-20.02 | 111- 9.69 | 0.5 | 0.4 | 11 | 76 | 0 | 0.08 |
| 8 | 84 | 724 | 337 | 31.13 | 39-19.38 | 111- 9.12 | 1.4 | 0.0 | 9 | 80 | 0 | 0.22 |
| 9 | 84 | 724 | 2020 | 4.03 | 39-20.03 | 111-10.03 | 1.5 | 0.0 | 6 | 184 | 0 | 0.05 |
| | 84 | 725 | 320 | 57.13 | 39-20.09 | 111-10.12 | 1.6 | 0.4 | 7 | 190 | 1 | 0.06 |
| 10 | 84 | 731 | 1311 | 27.94 | 39-20.89 | 111- 4.71 | 2.3 | 0.8 | 12 | 194 | 3 | 0.31 |
| 11 | 84 | 805 | 828 | 54.86 | 39-20.23 | 111- 4.15 | 2.8 | 0.8 | 16 | 219 | 3 | 0.21 |
| 12 | 84 | 731 | 1954 | 17.33 | 39-20.34 | 111- 4.42 | 2.9 | 0.4 | 13 | 230 | 3 | 0.33 |
| 13 | 84 | 803 | 1140 | 31.82 | 39-19.71 | 111- 2.92 | 3.4 | 0.9 | 14 | 236 | 4 | 0.27 |
| 14 | 84 | 712 | 1657 | 52.10 | 39-20.98 | 111- 6.00 | 0.1 | 0.6 | 21 | 104 | 2 | 0.31 |
| 15 | 84 | 717 | 714 | 31.32 | 39-20.09 | 111- 7.38 | 0.2 | 0.8 | 19 | 52 | 1 | 0.18 |
| 16 | 84 | 721 | 1446 | 29.77 | 39-20.01 | 111- 6.88 | 0.0 | 0.9 | 15 | 111 | 1 | 0.51 |
| 17 | 84 | 723 | 50 | 48.06 | 39-20.42 | 111- 7.37 | 0.0 | 1.0 | 20 | 48 | 1 | 0.17 |
| 18 | 84 | 803 | 2004 | 3.68 | 39-20.60 | 111- 6.80 | 0.0 | 1.8 | 20 | 136 | 3 | 0.16 |
| 19 | 84 | 804 | 837 | 39.47 | 39-20.70 | 111- 7.00 | 0.6 | 1.0 | 17 | 124 | 3 | 0.21 |

# Solution 3

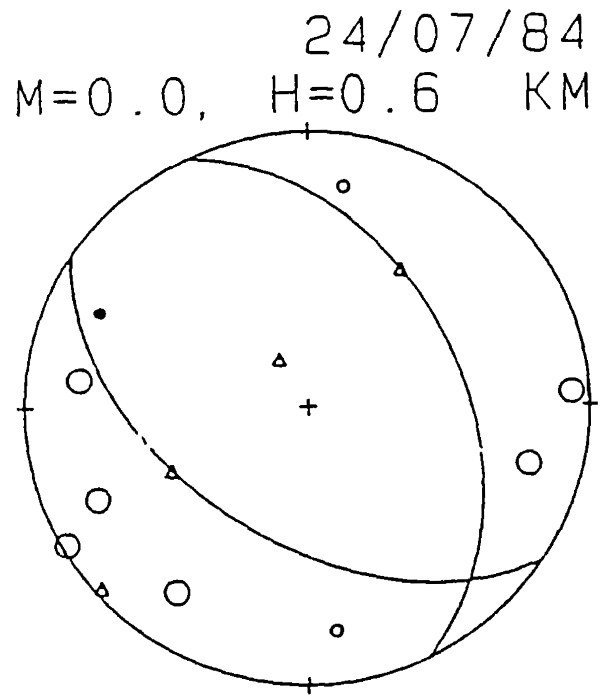

24/07/84
M=0.0, H=0.6 KM


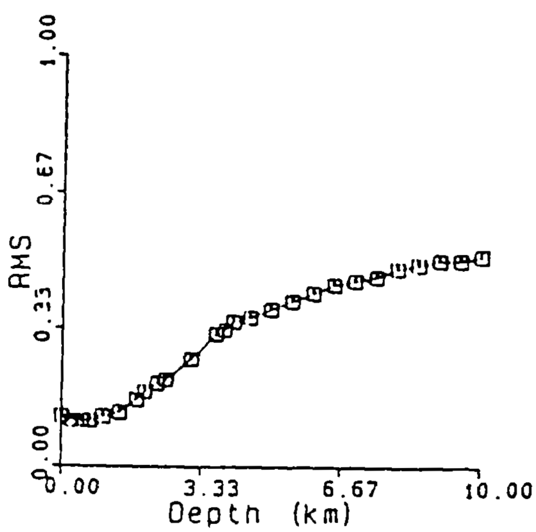

RMS
1.00
0.67
0.33
0.00
0.00
3.33
6.67
10.00
Depth (km)


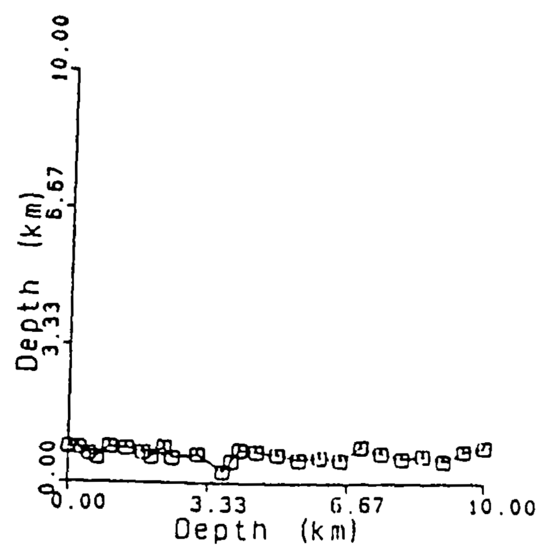

Depth (km)
10.00
6.67
3.33
0.00
0.00
3.33
6.67
10.00
Depth (km)

# Solution 4

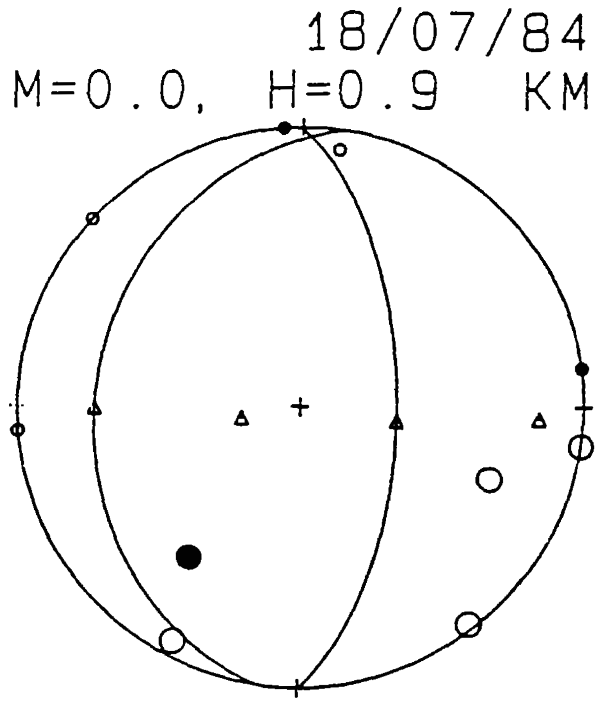
18/07/84
M=0.0, H=0.9 KM

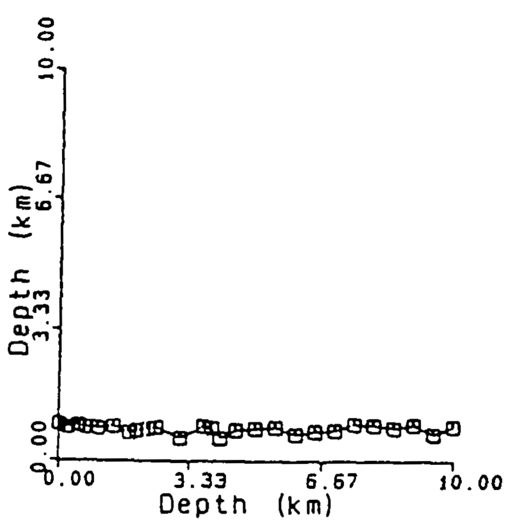
10.00
6.67
3.33
0.00
Depth (km)
0.00
3.33
6.67
10.00
Depth (km)

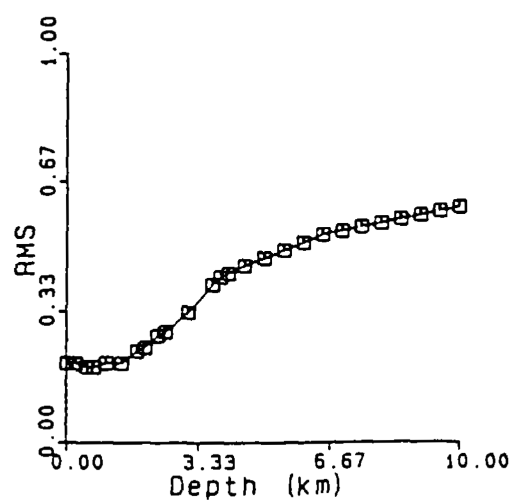
1.00
0.67
0.33
0.00
RMS
0.00
3.33
6.67
10.00
Depth (km)

# Solution 5

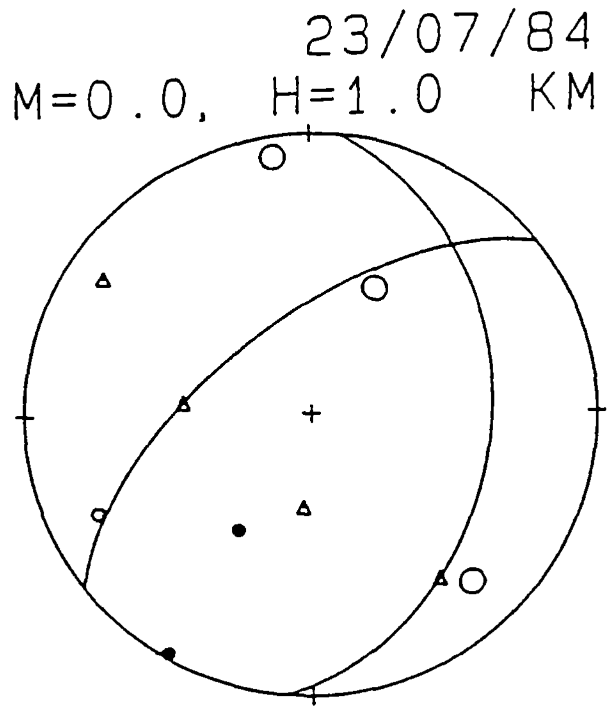
23/07/84
M=0.0, H=1.0 KM

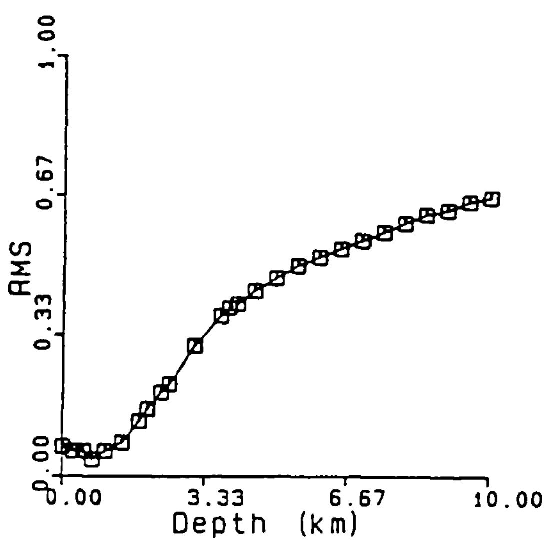
RMS
0.00
0.33
0.67
1.00
0.00
3.33
6.67
10.00
Depth (km)

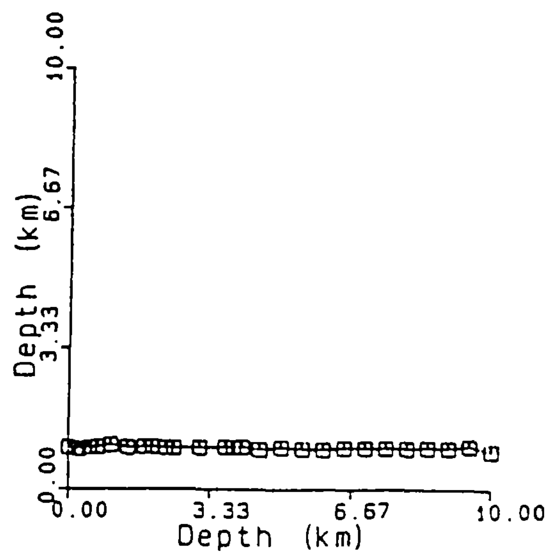
Depth (km)
0.00
3.33
6.67
10.00
0.00
3.33
6.67
10.00
Depth (km)

# Solution 6

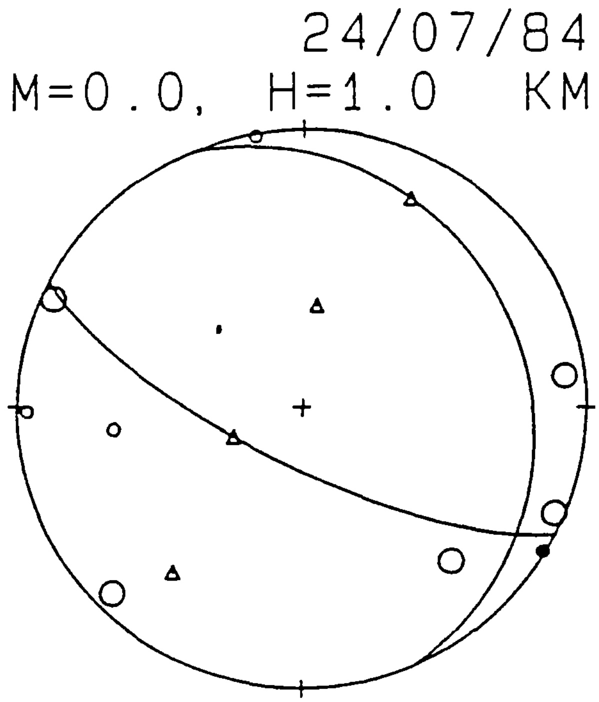
24/07/84
M=0.0, H=1.0 KM

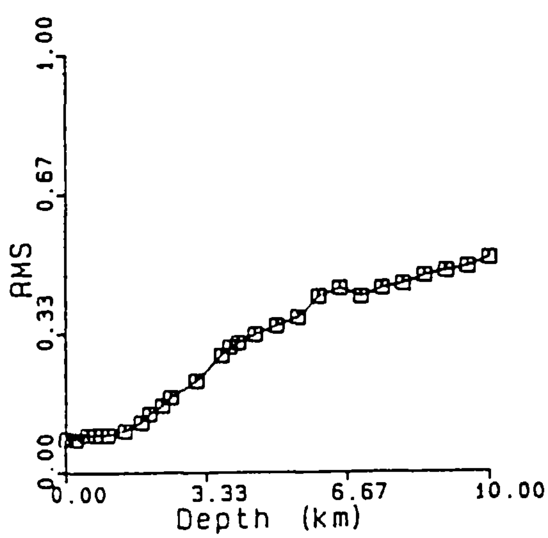
RMS
0.00
0.33
0.67
1.00
0.00
3.33
6.67
10.00
Depth (km)

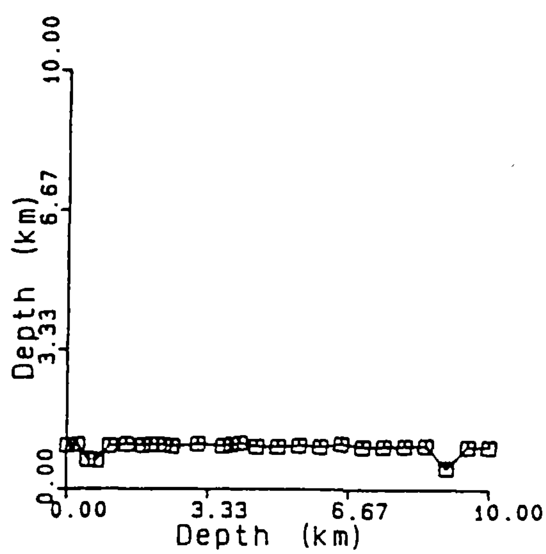
Depth (km)
0.00
3.33
6.67
10.00
0.00
3.33
6.67
10.00
Depth (km)

Solution 7

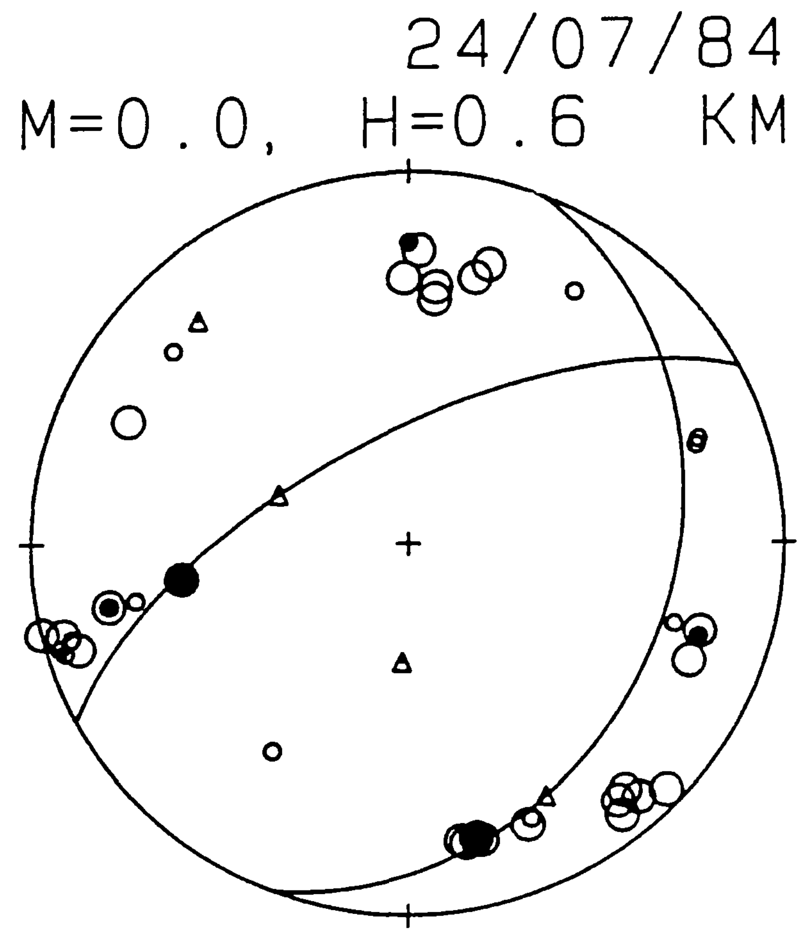

# Solution 8

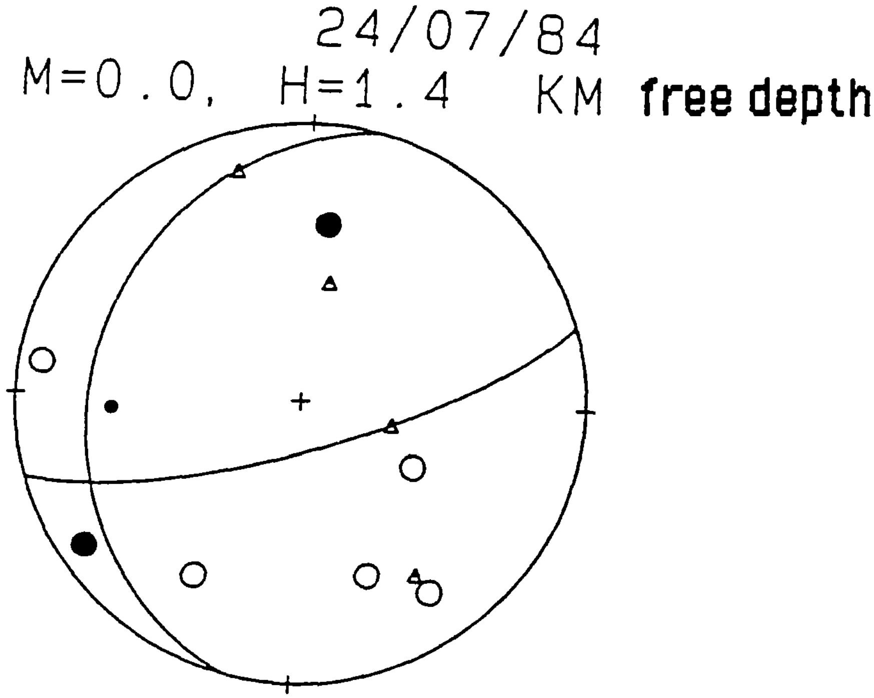
24/07/84
M=0.0, H=1.4 KM free depth

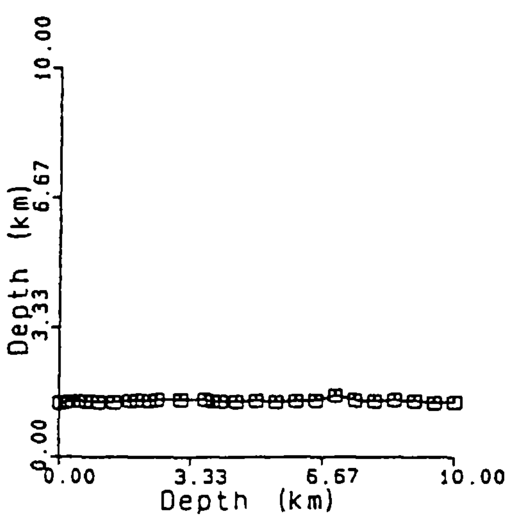
Depth (km)
0.00
3.33
6.67
10.00
Depth (km)
0.00
3.33
6.67
10.00

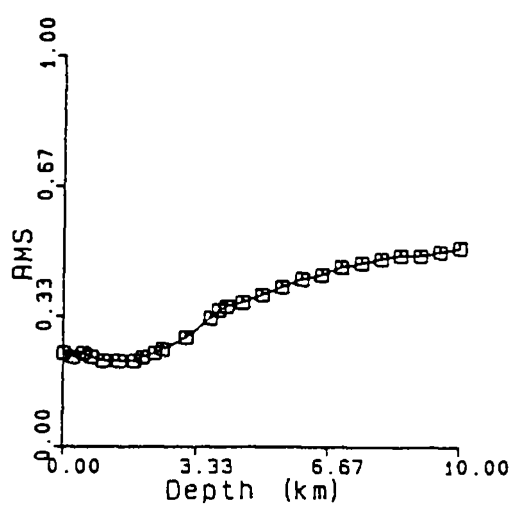
RMS
0.00
0.33
0.67
1.00
Depth (km)
0.00
3.33
6.67
10.00

# Solution 8

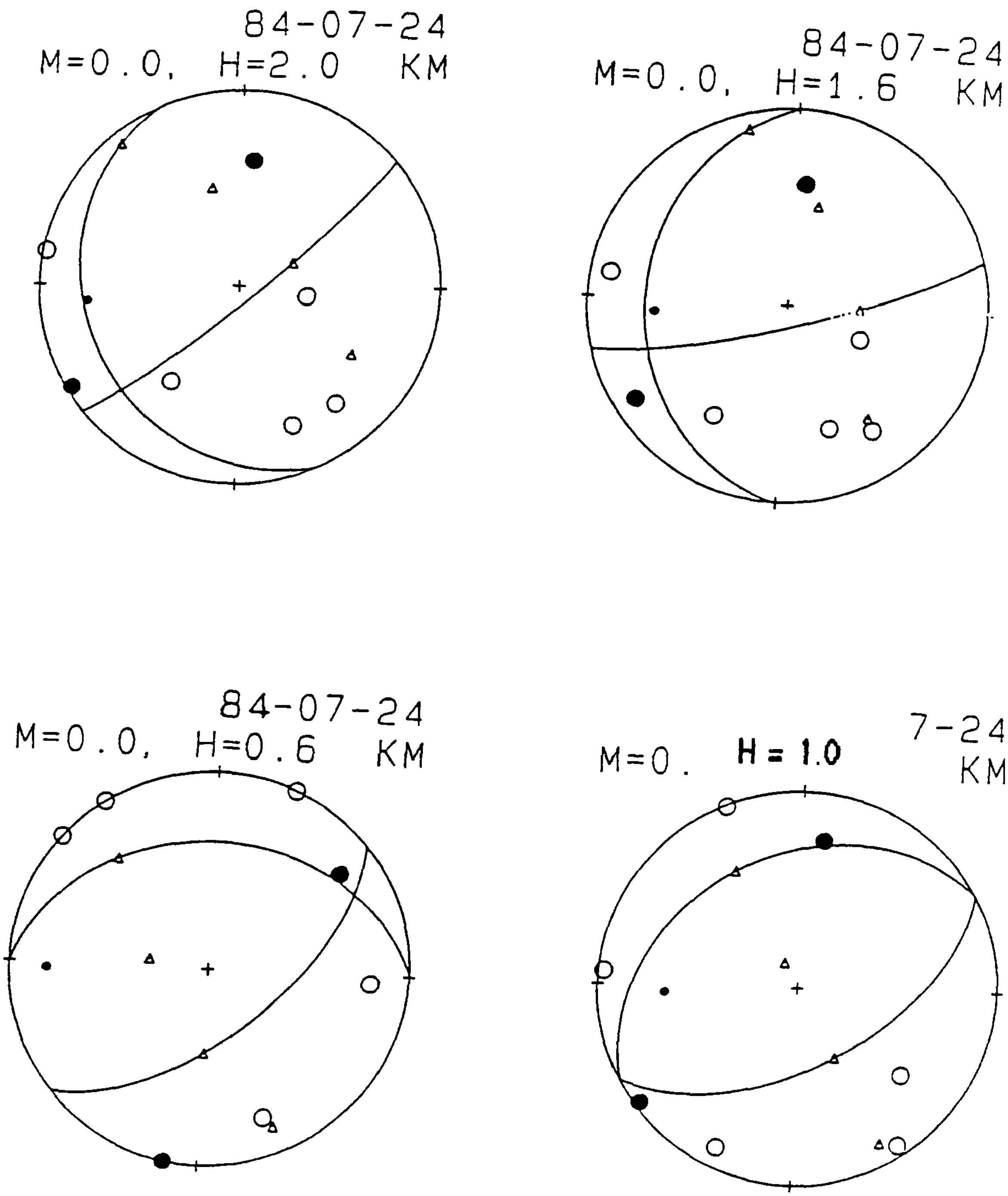
84-07-24
M=0.0, H=2.0 KM
84-07-24
M=0.0, H=1.6 KM
84-07-24
M=0.0, H=0.6 KM
7-24
M=0. H = 1.0
KM

Solution 9

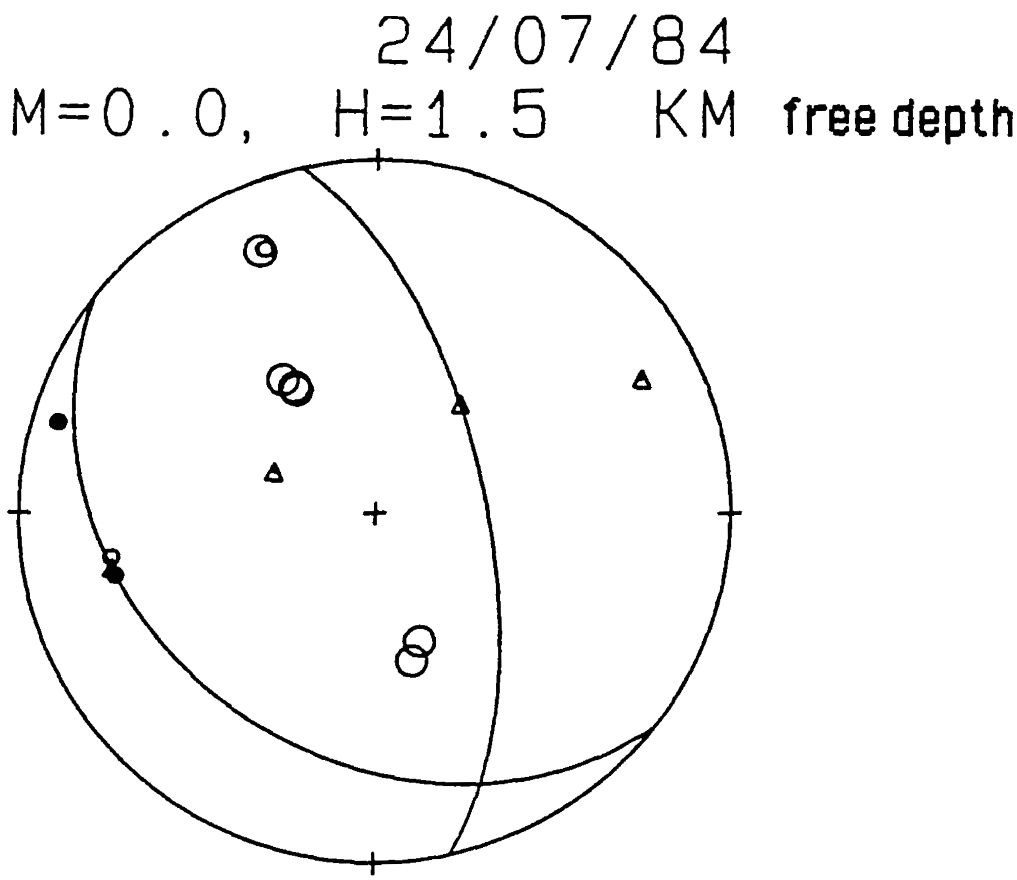

# Solution 9

## 840725 2020

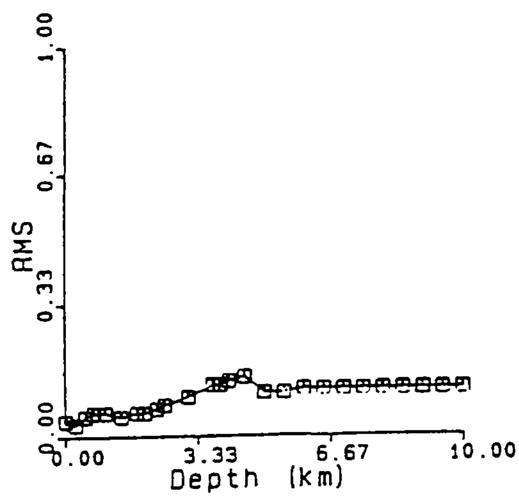


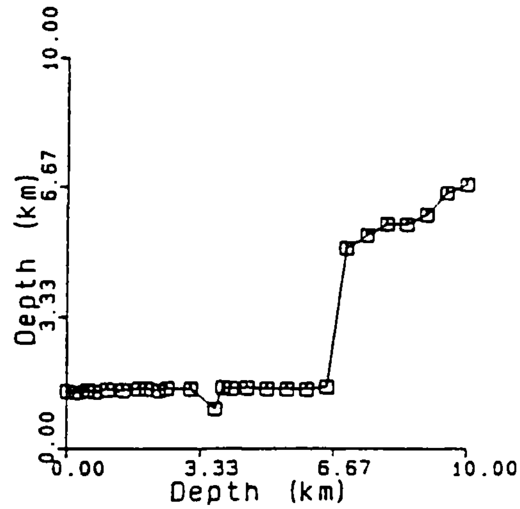


## 840725 0320

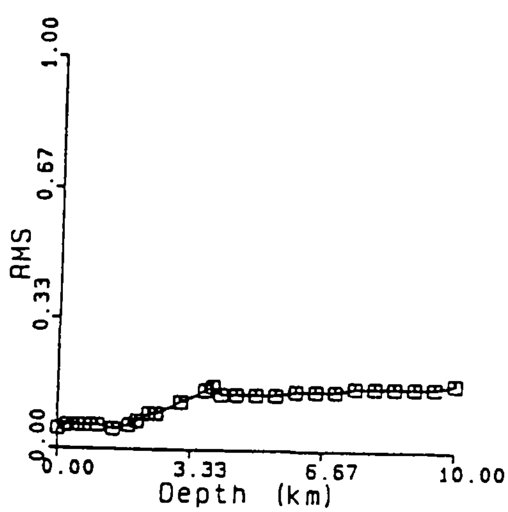


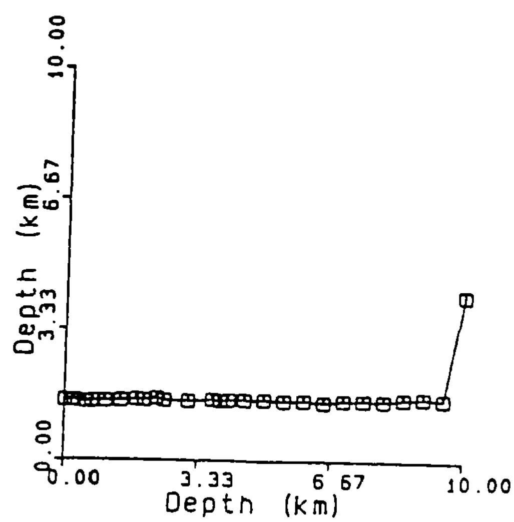

# Solution 9

84-07-24
M=0.0, H=2.0 KM

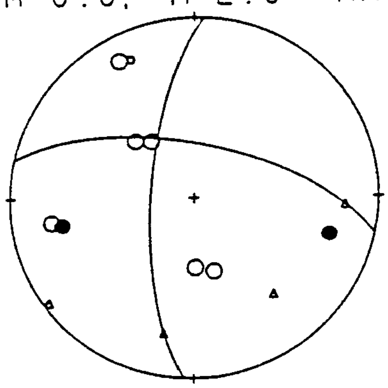

84-07-24
M=0.0, H=1.6 KM

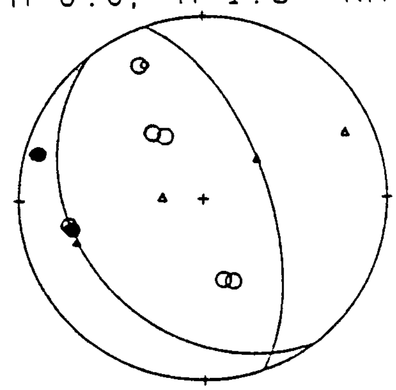

84-07-24
M=0.0, H=1.4 KM

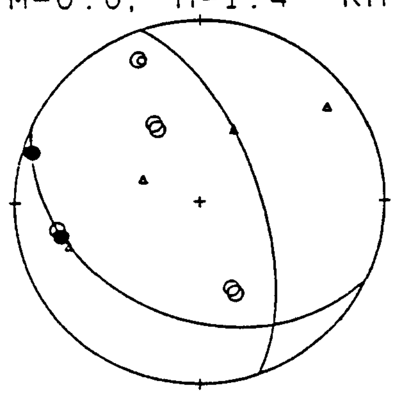

84-07-24
M=0.0, H=0.6 KM

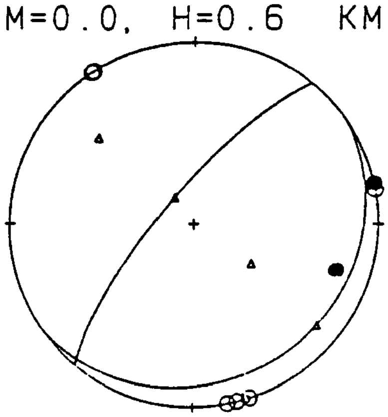

84-07-24
M=0.0, H=1.0 KM

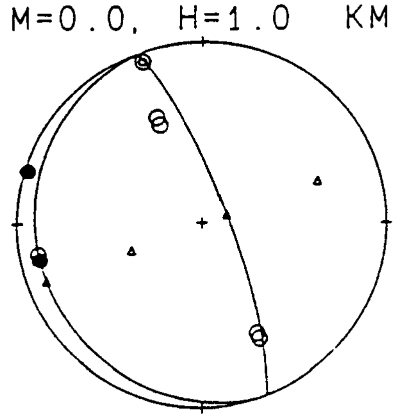

# Solution 10

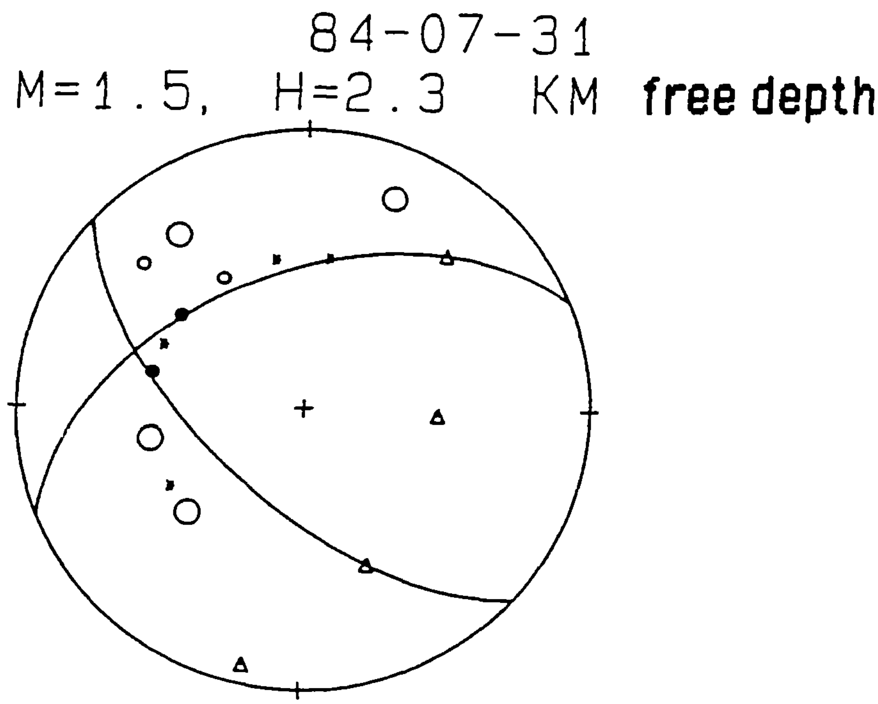
84-07-31
M=1.5, H=2.3 KM free depth

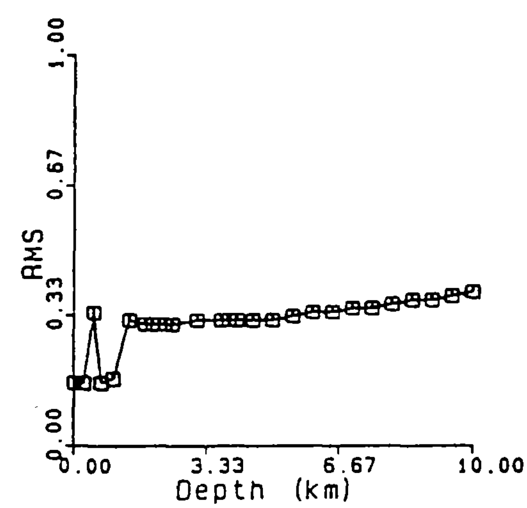
RMS
0.00
0.33
0.67
1.00
0.00
3.33
6.67
10.00
Depth (km)

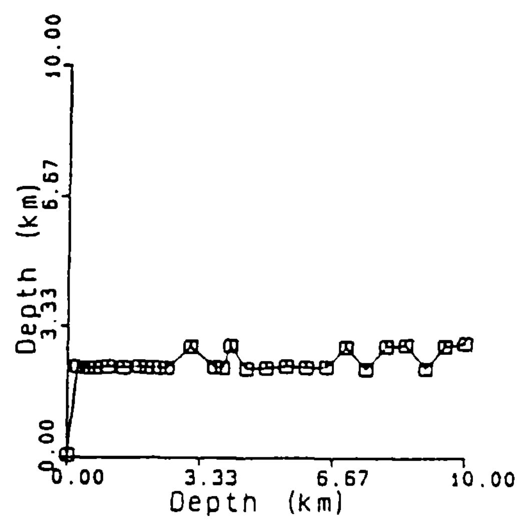
Depth (km)
0.00
3.33
6.67
10.00
0.00
3.33
6.67
10.00
Depth (km)

# Solution 10

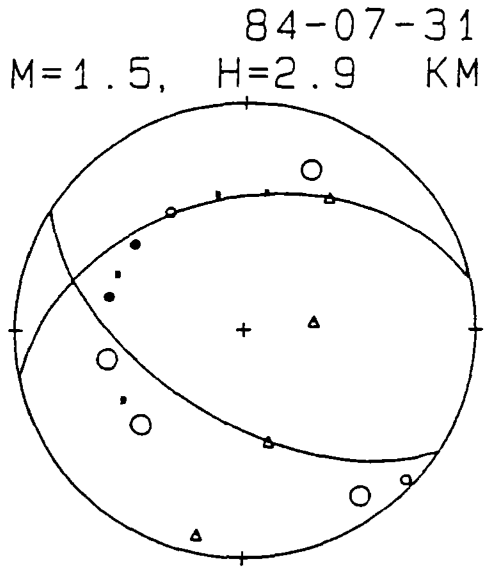
84-07-31
M=1.5, H=2.9 KM

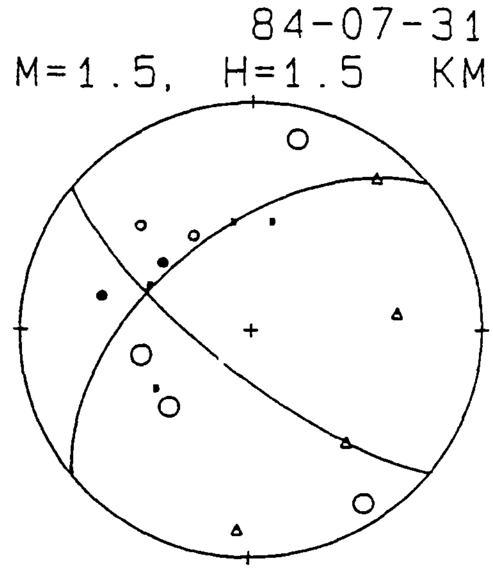
84-07-31
M=1.5, H=1.5 KM

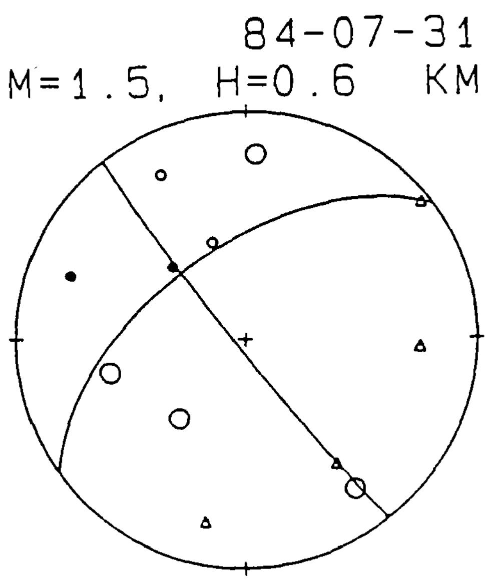
84-07-31
M=1.5, H=0.6 KM

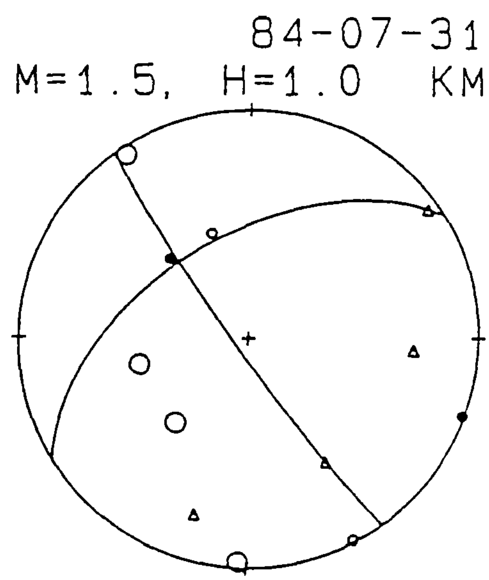
84-07-31
M=1.5, H=1.0 KM

# Solution 11

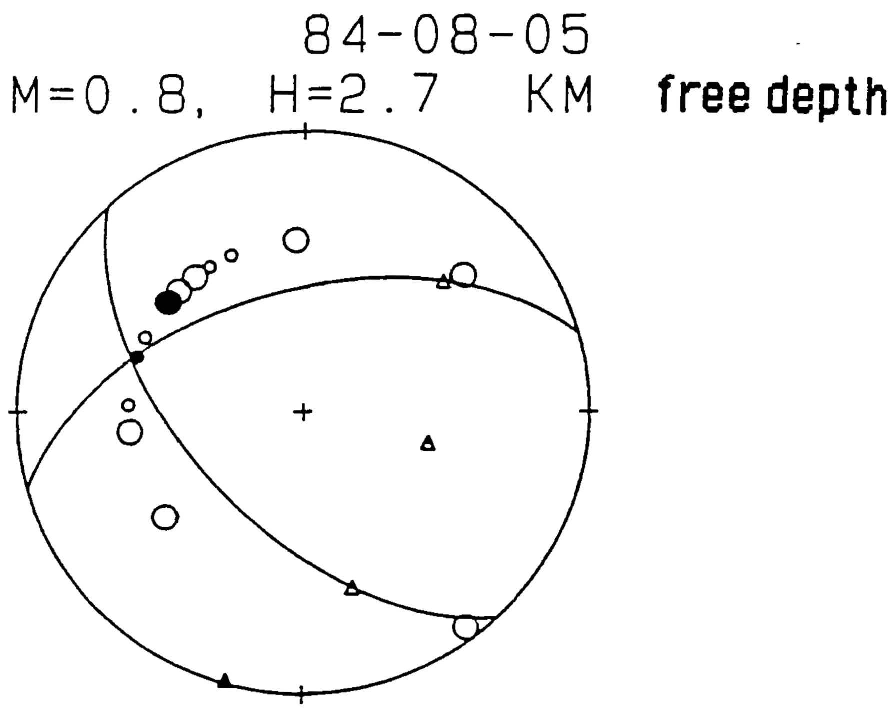

84-08-05
M=0.8, H=2.7 KM free depth


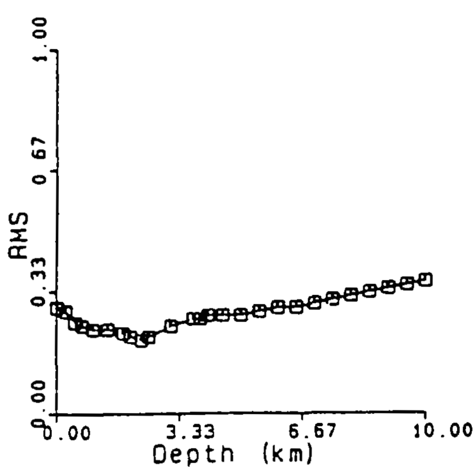

RMS
0.00
0.33
0.67
1.00
0.00
3.33
6.67
10.00
Depth (km)


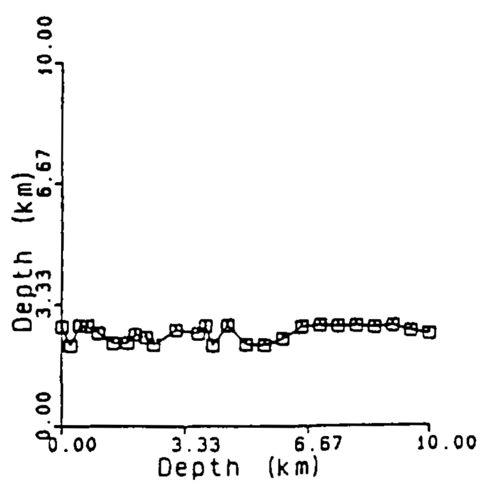

Depth (km)
0.00
3.33
6.67
10.00
0.00
3.33
6.67
10.00
Depth (km)

# Solution 11

84-08-05
M=0.8, H=2.2 KM

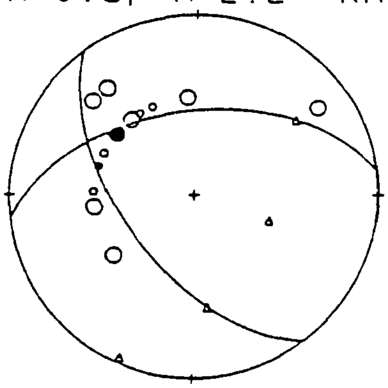

84-08-05
M=0.8, H=2.0 KM

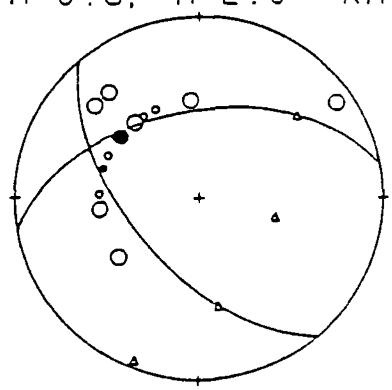

84-08-05
M=0.8, H=0.6 KM

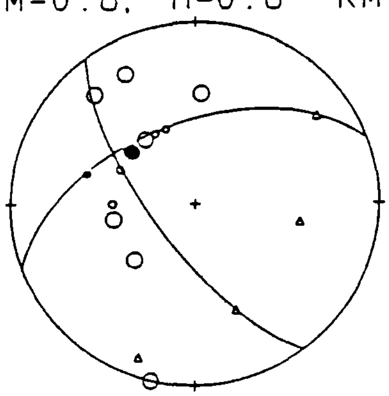

84-08-05
M=0.8, H=1.0 KM

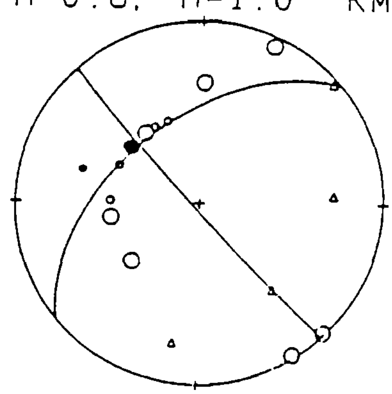

## Solution 12

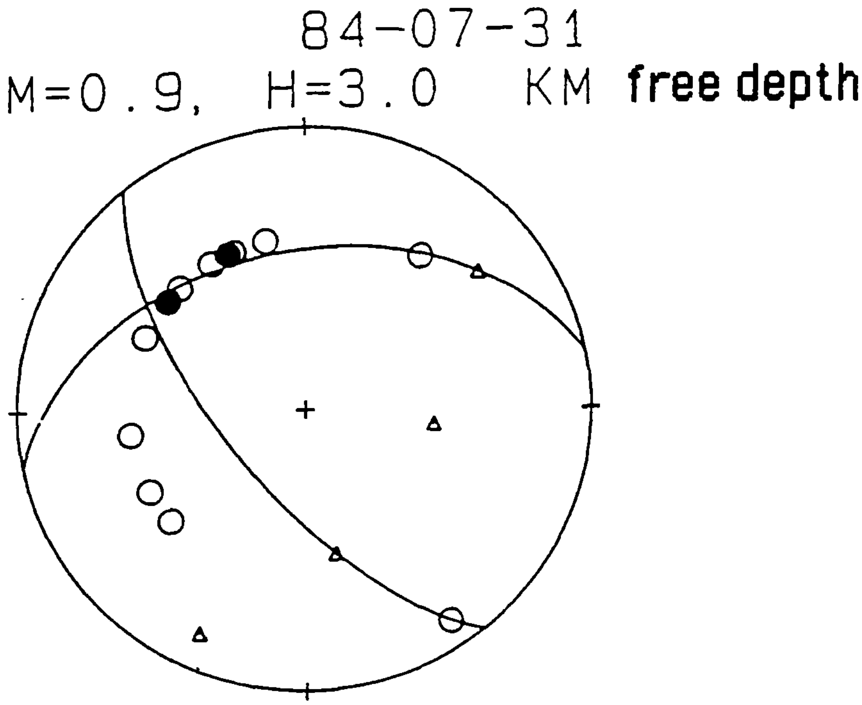
84-07-31
M=0.9, H=3.0 KM free depth

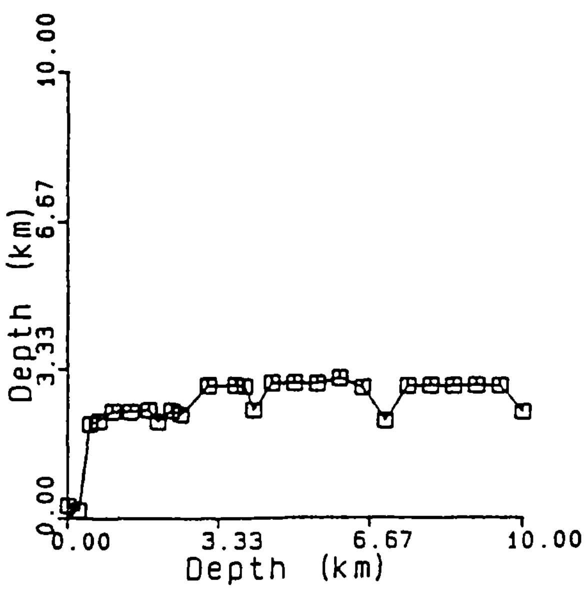
Depth (km)
0.00
3.33
6.67
10.00
Depth (km)

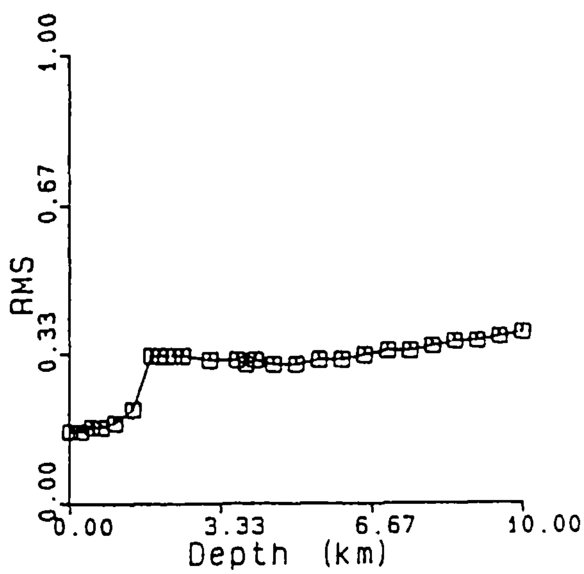
RMS
0.00
0.33
0.67
1.00
0.00
3.33
6.67
10.00
Depth (km)

# Solution 12

84-07-31
M=0.9, H=2.5 KM

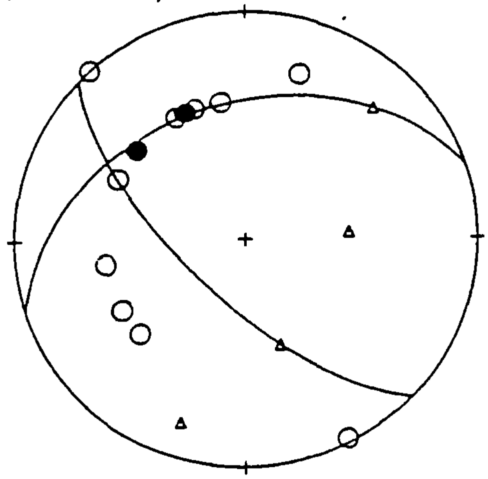

84-07-31
M=0.9, H=2.0 KM

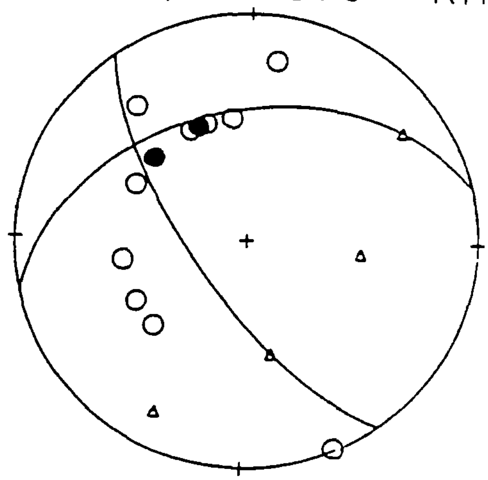

84-07-31
M=0.9, H=0.6 KM

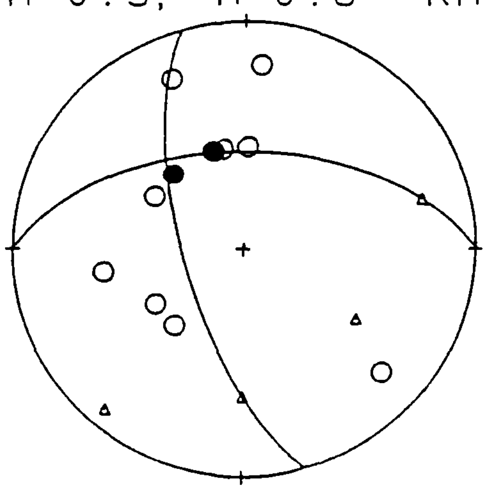

84-07-31
M=0.9, H=1.0 KM

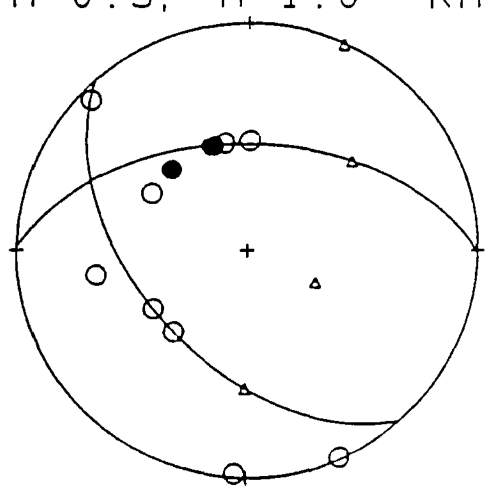

# Solution 13

84-08-03
M=0.9, H=3.4 KM **free depth**

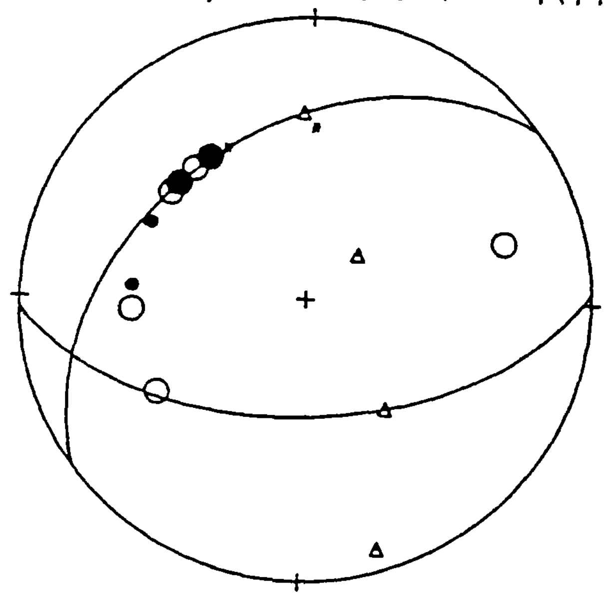

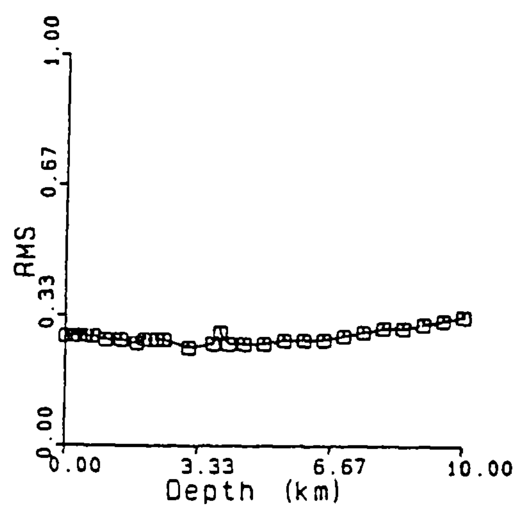


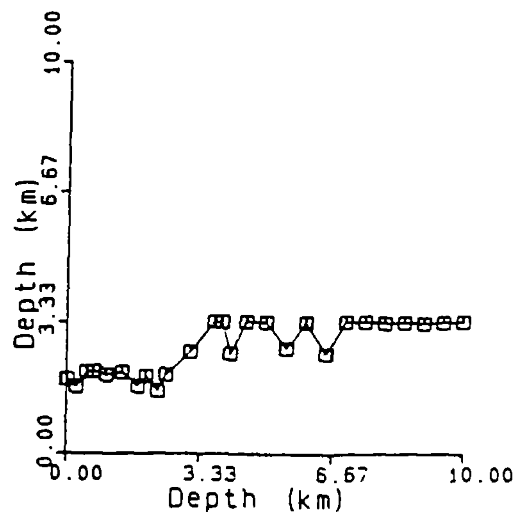

# Solution 13

84-08-03
M=0.9, H=2.5 KM

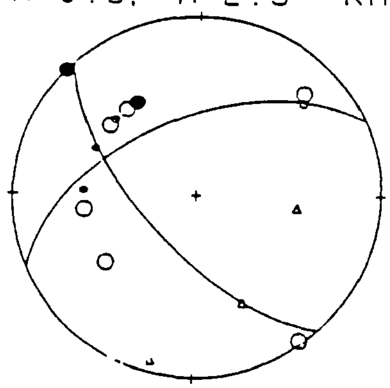

84-08-03
M=0.9, H=2.0 KM

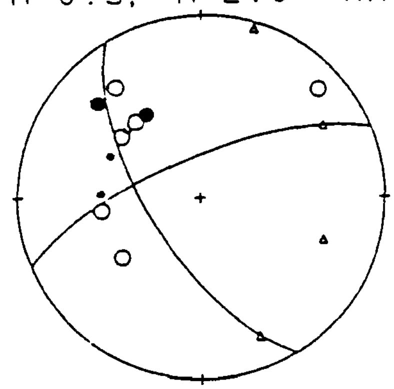

84-08-03
M=0.9, H=1.7 KM

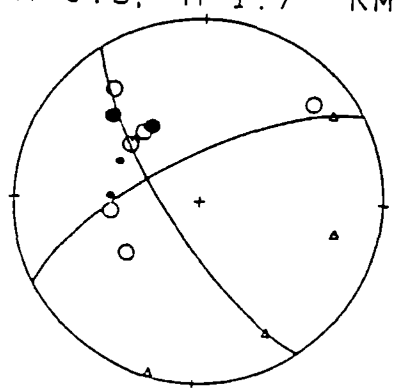

84-08-03
M=0.9, H=0.6 KM

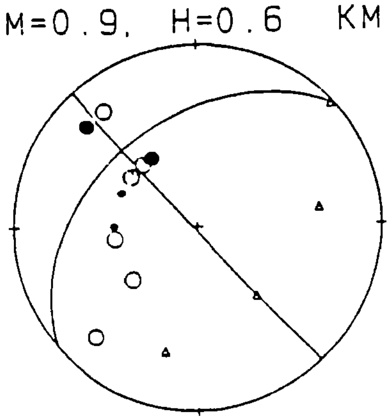

84-08-03
M=0.9, H=1.0 KM

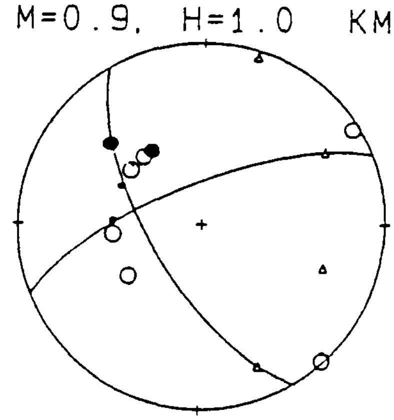

# INTERPRETATION OF INSTRUMENTAL SEISMICITY AND CONTEMPORARY TECTONICS OF THE EASTERN WASATCH PLATEAU RELEVANT TO SEISMIC EXPOSURE OF THE JOES VALLEY AND SCOFIELD DAMS

by

Walter J. Arabasz
Department of Geology and Geophysics
University of Utah
Salt Lake City, Utah 84112

Technical Report to

U.S. Bureau of Reclamation
Seismotectonic Section
Denver, Colorado

Contract Monitor
Richard A. Martin

Contract No.: PO# 4 PG 40 13210
Principal Investigator: Walter J. Arabasz
Award Period: October 15, 1984 - June 30, 1985

November 1985
(Revised August 1986)

CONTENTS



Note from authors: In the interest of space, Attachment No. 1 is not included in this appendix but is available in the literature under the reference "Arabasz and Julander, 1986."

## SUMMARY AND CONCLUSIONS

The purpose of the report is an interpretation of results of a microearthquake field experiment carried out in the eastern Wasatch Plateau of central Utah during June to August 1984. (Data from that experiment, herein referred to as the EWP-84 experiment are presented in a companion report.) Combining results of that experiment with instrumental seismicity recorded by the University of Utah's regional seismic network, interpretations are made with respect to (1) the contemporary tectonics of the eastern Wasatch Plateau, and (2) implications for earthquake hazards relative to Joes Valley and Scofield Dams.

The EWP-84 earthquake field experiment was conceived and carried out for purposes of basic seismological research, rather than as an exercise for engineering application. Nevertheless, two important results that relate to earthquake hazard evaluation for the Joes Valley dam are: (1) the documentation of earthquakes with normal-faulting focal mechanisms 3.0 to 4.4 km deep beneath the Joes Valley graben, and (2) the documentation of a very low level of microseismicity along the Joes Valley fault zone.

Both temporary and continuous regional seismographic monitoring indicate that, with the exception of intense localized seismicity associated with active underground coal mining, the eastern Wasatch Plateau is characterized by a distinctly lower level of background seismicity than that for the western part of the Intermountain seismic belt roughly 50 km to the west. Compelling arguments can be made, however, that background earthquake activity is neither simply associated spatially with major active faults in the region, nor a direct reflection of the potential for future surface-faulting earthquakes on those structures.

Thirteen new fault-plane solutions from the EWP-84 earthquake field experiment add key information for the spatial mapping of changes of stress state in the eastern Wasatch Plateau. Whereas earlier evidence raised questions about whether normal faults of the Joes Valley fault zone might now be situated within a regime of principal horizontal compression, the new data argue for the probable existence of an extensional stress state in the immediate vicinity of Joes Valley—and a change to principal horizontal compression within 10-20 km to the east.

Both Joes Valley and Scofield Dams are located within 20 km of intense seismicity, mostly less than magnitude 3, associated with active underground coal mining. Such seismicity in the Book Cliffs area is reported to have reached magnitudes as large as 4.5 in the 1950's.

Accurately located foci from the EWP-84 study extend at least to 4.4 km depth below a datum 2.9 km above sea level. Foci in the vicinity of the active coal mines predominate above roughly 1.5 km below the surface datum. At least some earthquakes are occurring beneath the Triassic-Jurassic Navajo Sandstone, a marker horizon thought to underlie a regional low-angle detachment. The instrumental seismicity offers no resolution as to the structural relation of such a detachment to Late Tertiary-Recent normal faulting—in particular, faulting associated with the Joes Valley fault zone.

In the absence of compelling evidence to the contrary, current experience and judgment of seismologists and geologists in the Intermountain region would likely lead to adoption of the following positions regarding Pleistocene-Holocene fault scarps, subsurface structure, and seismogenic potential in the Joes Valley area: (1) disbelief that the fault scarps could have been produced aseismically; (2) requirement that observed single-event surface displacements of 1-5 m be associated with earthquakes of about surface-wave magnitude 7.0 0.5; (3) disbelief that surface-faulting earthquakes nucleate and/or be restricted to rupture above 3-4 km depth, that is, be restricted to faulting within upper-plate rocks above an inferred low-angle detachment at shallow depth; and (4) (a corollary of (3)) expectation that the faults of the Joes Valley fault zone penetrate, or somehow be connected by rupture pathway, to a rupture nucleation zone at 10-15 km depth.

# 1. INTRODUCTION

## 1.1 Purpose and Scope

This report is a companion to one prepared for the U.S. Bureau of Reclamation by Arabasz and Williams (1985) entitled, "Analysis and Summary of Seismographic Data Recorded in Vicinity of Joes Valley Dam, Emery County Project, Eastern Wasatch Plateau, Utah." In that report, hereafter referred to as Report 1, a description and summary of results are presented for a multi-institutional, microearthquake field experiment carried out in the eastern Wasatch Plateau of central Utah (fig. 1.1b) during June to August 1984. The purpose of this report is an interpretation of the results of Report 1—together with instrumental seismicity recorded by the University of Utah's regional seismic network—with respect to (1) the contemporary tectonics of the eastern Wasatch Plateau, and (2) implications for earthquake hazards relative to Joes Valley and Scofield Dams.

## 1.2 Related Background

Significant portions of section 2 have been extracted, with modifications, from a 1983 proposal by the author to the National Science Foundation entitled, "Characteristics of Coal-Mining Induced and Tectonic Seismicity, Wasatch Plateau, Utah." That proposal formed the basis for the 1984 earthquake field experiment described in Report 1, and its scientific introduction provides useful background for this report.

During the period of this contract, related research efforts led to completion of a key manuscript by Arabasz and Julander (1986) that summarizes results of observational seismology within the Basin and Range-a

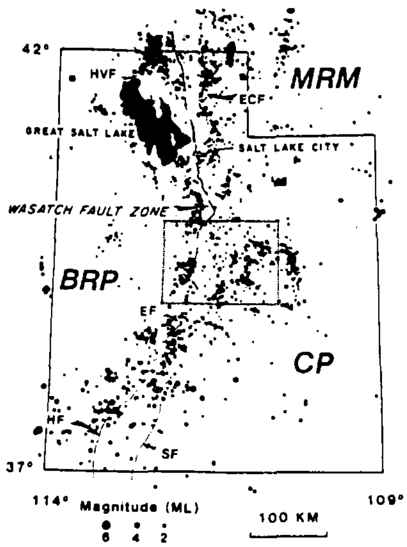


Index map of the Utah region showing the Intermountain seismic belt and the setting of the area of this study (rectangle). Seismicity is for the period July 1962-June 1978, based on University of Utah data (Arabasz et al, 1979). BRP indicates Basin and Range province. CP—Colorado Plateau. MRM—Middle Rocky Mts.. HVF—Hansel Valley fault. ECF—East Cache fault. EF—Elsinore fault. HF—Hurricane fault. SF—Sevier fault.

b

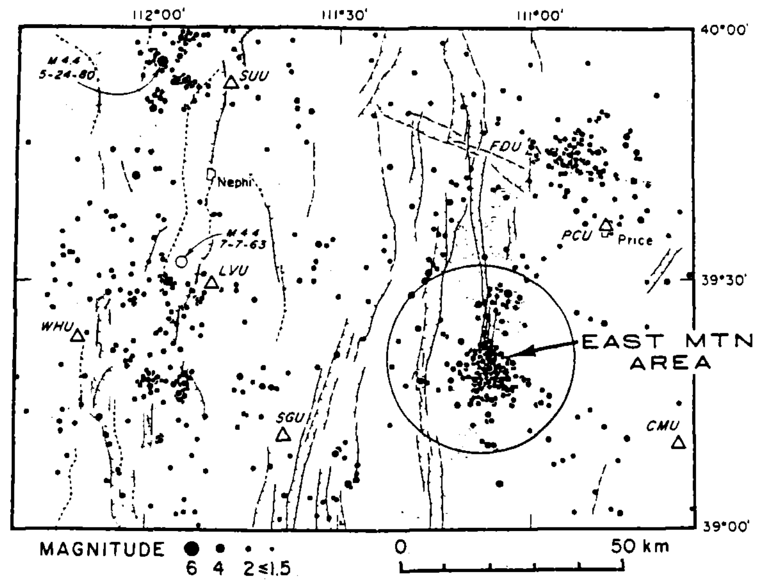


—Seismicity map of study area for the period: October 1, 1974-December 31, 1981, based on network monitoring by the University of Utah.

c

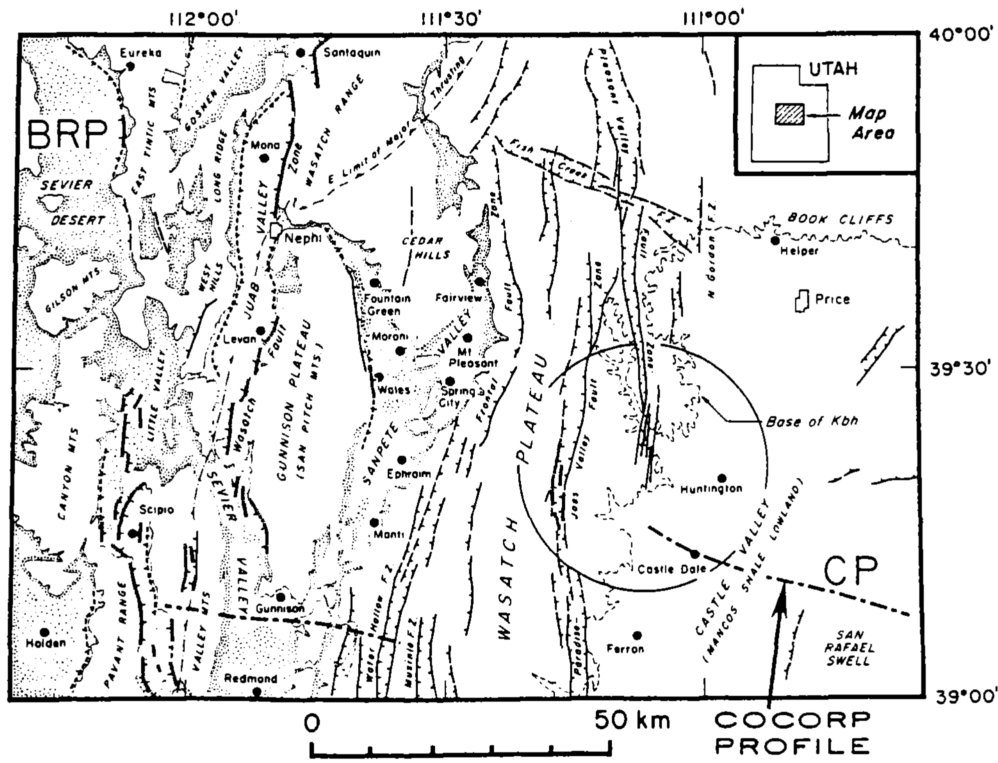


—Geologic sketch map of central Utah study area. Valleys floored with Quarternary alluvium shown by stippled pattern. Cenozoic normal faults shown by heavy lines, hachures on downthrown side; short dashes indicate concealed faults; broad pattern, late Quaternary fault scarps; BRP—Basin and Range province, CP—Colorado Plateau. Outcrop trace of Cretaceous Blackhawk Formation (Kbh) roughly defines erosional eastern boundary of Wasatch Plateau. Geology adapted from Stokes (1963), Witkind et al (1978), Bucknam and Anderson (1979), Doelling (1972), Burchfiel and Hickcox (1972).

Figure 1.1. Index maps showing seismotectonic setting of the study area in the eastern Wasatch Plateau of central Utah (adapted from McKee and Arabasz, 1982).

Colorado Plateau transition in central and southwestern Utah. A preprint of that manuscript accompanies this report as Attachment No. 1. Where appropriate, the reader will be referred to that manuscript for substantial discussion--rather than having the text arbitrarily replicated within the body of this report. Note that the manuscript was completed prior to the availability of results from the 1984 Eastern Wasatch Plateau field experiment.

# 2. SEISMOTECTONIC PROBLEMS, EASTERN WASATCH PLATEAU

## 2.1 Tectonic Setting

The Wasatch Plateau in central Utah (figure 1.1c)—one of the High Plateaus marking the northwestern rim of the Colorado Plateau—is a structural block 30-50 km wide underlain by nearly flat-lying Cretaceous-Tertiary strata and broken by post-Eocene normal faulting. Its steep western margin is formed by the west-dipping Wasatch Monocline; its eastern margin, by an incised erosional escarpment with several hundred meters of relief.

Seismotectonic aspects of the Wasatch Plateau of particular significance to this report (see figure 1.1) are: (1) the occurrence of intense, very shallow seismicity (depth < 4 km) associated with extensive underground coal mining along the plateau's eastern margin (McKee and Arabasz, 1982; Wong, 1985), (2) the occurrence of diffuse natural seismicity (depth < 16 km) throughout the plateau—apparently including mid-crustal earthquakes directly beneath the mining areas (McKee and Arabasz, 1982), (3) the presence of prominent late Pleistocene-Holocene normal fault scarps within Joes Valley less than 20 km west of the mining areas, (4) location of the plateau within a transition zone between the Basin and Range (BR) province and the Colorado Plateau (CP) (with laterally varying crust-mantle structure and upper-crustal stress state), and (5) the inferred presence of a low-angle regional detachment beneath the plateau that is interpreted to have accommodated both Cretaceous-Early Tertiary foreland shortening and Late Tertiary-Recent horizontal extension (Royse, 1983; Standlee, 1982).

The boundary between the BR and CP provinces in central Utah is well known to be a transitional one--not only physiographically (e.g., Stokes, 1977), but also in terms of surficial geology (Burchfiel and Hickcox, 1972; Standlee, 1982), lithospheric thickness (Thompson and Zoback, 1979), crustal velocity structure (Smith et al., 1975), heat flow (Bodell and Chapman, 1982), and other geophysical parameters (see reviews by Thompson and Zoback, 1979; Smith, 1978). Accordingly, the transition zone has become a focus of geodynamic interest. Of seismological interest, the BR-CP transition is seismically active and coincides with a major segment of the Intermountain seismic belt (fig. 1.1a).

## 2.2 Previous Seismological Studies

A program of systematic earthquake field studies focusing on the seismically active BR-CP transition in central and SW Utah was begun by the author, together with graduate students, in 1979. Results from a regional study between 39° and 40°N latitude—including specific studies in the eastern Wasatch Plateau—have been reported by McKee and Arabasz (1982) and by McKee (1982). The results from more detailed target-oriented studies carried out between 38° and 39°N latitude have been summarized by Arabasz (1982) and Julander (1983). (See also Arabasz and Julander, 1986.)

The following subsections give a brief outline of four aspects of the seismotectonics of the eastern Wasatch Plateau that pose fundamental problems for interpretation of earthquake hazards. These relate to (1) the problematic correlation of background seismicity with geologic structure, (2) the interaction of late Cenozoic normal faulting and pre-existing, low-angle detachment faulting, (3) laterally-varying stress state within the BR-CP transition, and (4) implications of mining-related seismicity in the eastern Wasatch Plateau. More complete discussion of these problems—in light of the the instrumental seismicity presented in section 3—is pursued in section 4.

2.3 Correlation of Seismicity with Geologic Structure The problematic correlation of diffuse background seismicity with geologic structure along the BR-CP transition (e.g., Arabasz, 1983; McKee and Arabasz, 1982; Arabasz et al., 1980)—and indeed throughout most of the Intermountain seismic belt (Arabasz and Smith, 1981; Smith, 1978)—represents one of the greatest obstacles for understanding fault behavior and earthquake generation in this region. Subsurface structure is typically more complex than apparent from the surface geology, and commonly there is a discordance between surface fault patterns and seismic fault slip at depth. Precise hypocenters, adequately concentrated seismicity, and abundant reliable single-event focal mechanisms are required to unravel the association of seismicity with structure.

Specifically focusing on central Utah, Arabasz and Julander (1986) pursue lengthy discussion addressing the correlation of diffuse seismicity with geologic structure. Further, they present a working hypothesis (see also Arabasz, 1984) that relates diffuse background seismicity to the influence of low-angle structural discontinuities in the upper crust (see Attachment No. 1 for elaboration).

2.4 Low-Angle Detachment Faulting

According to structural interpretations of Standlee (1982)—based upon extensive industry subsurface data in central Utah—major eastward-directed thrusting in Late Cretaceous to Paleocene time extended eastward beneath the Wasatch Plateau and occurred on a detachment surface within incompetent strata above the Triassic-Jurassic Navajo Sandstone (see figure 2.1, bottom). Backsliding along such a detachment over a west-facing subsurface ramp is inferred to have created the Wasatch Monocline during an episode of "thin-skinned" horizontal extension during Late Tertiary-Recent time (Royse, 1983).

Cenozoic normal faults cutting the Wasatch Plateau (figure 1.1c) have been interpreted not to penetrate the Navajo Sandstone, but interpretations of seismic-reflection data are still not definitive. The Navajo Sandstone lies 4-5 km below surface beneath the western plateau, and about 3 km below surface beneath the eastern plateau. Interpretations of Standlee (1982) suggest that a detachment may lie within incompetent Jurassic strata overlying the Navajo Sandstone. Thus, relationships between surface faulting and seismicity at different crustal levels in the eastern Wasatch Plateau take on fundamental importance. If a shallow low-angle detachment indeed underlies the eastern Wasatch Plateau, it could have a critical bearing on the mechanics and maximum size of shallow earthquakes—as well as on our understanding of crustal faulting and seismogenesis associated with prominent late Quaternary fault scarps along the Joes Valley fault zone.

## 2.5 Laterally-Varying Stress State

Recent focal-mechanism observations by McKee and Arabasz (1982), Wong (1984), and Arabasz and Julander (1986) have provided the first evidence of laterally varying stress state within the BRP-CP transition in central Utah. Such variation is required by the contrast across the transition between WNW-ESE basin-range extension in the BRP and WNW-ESE horizontal

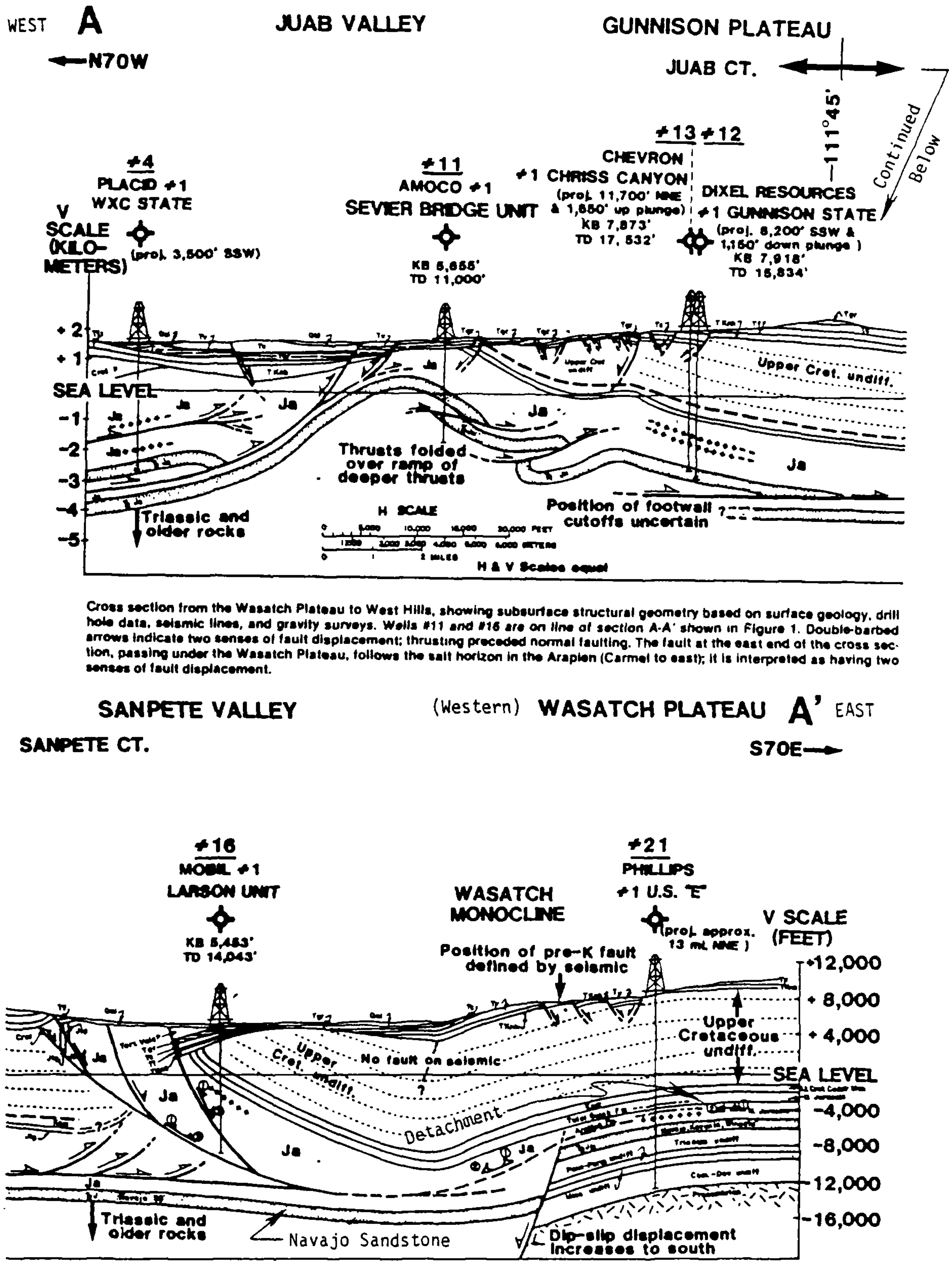


Figure 2.1. Geologic cross section across the western Wasatch Plateau (from Standlee, 1982).

Figure 2.2. (following page). Schematic summary of stress-orientation data for the Basin and Range-Colorado plateau transition (from Arabasz and Julander, 1986). Large arrows indicate regional directions of least (outward-directed) or greatest (inward-directed) principal horizontal compressive stress (from Zoback and Zoback, 1980; Zoback, 1983). Small arrows indicate inferred stress-orientation directions from P and T axes of fault-plane solutions shown in figure 4.1: outward-directed arrows for normal-faulting mechanisms, inward-directed arrows for thrust or reverse-faulting mechanisms, a combination of inward and outward-directed arrows for strike-slip faulting, and outward-directed arrows with perpendicular dashed lines for mixed normal and strike-slip faulting. Small numbers identify data points keyed to figure 4.1; large numbers in parentheses, the total number of other fault-plane solutions combined to produce an average orientation. The heavy patterned line (queried where uncertain) marks the limits of a low-heat-flow thermal interior of the Colorado Plateau surrounded by a high-heat-flow periphery.

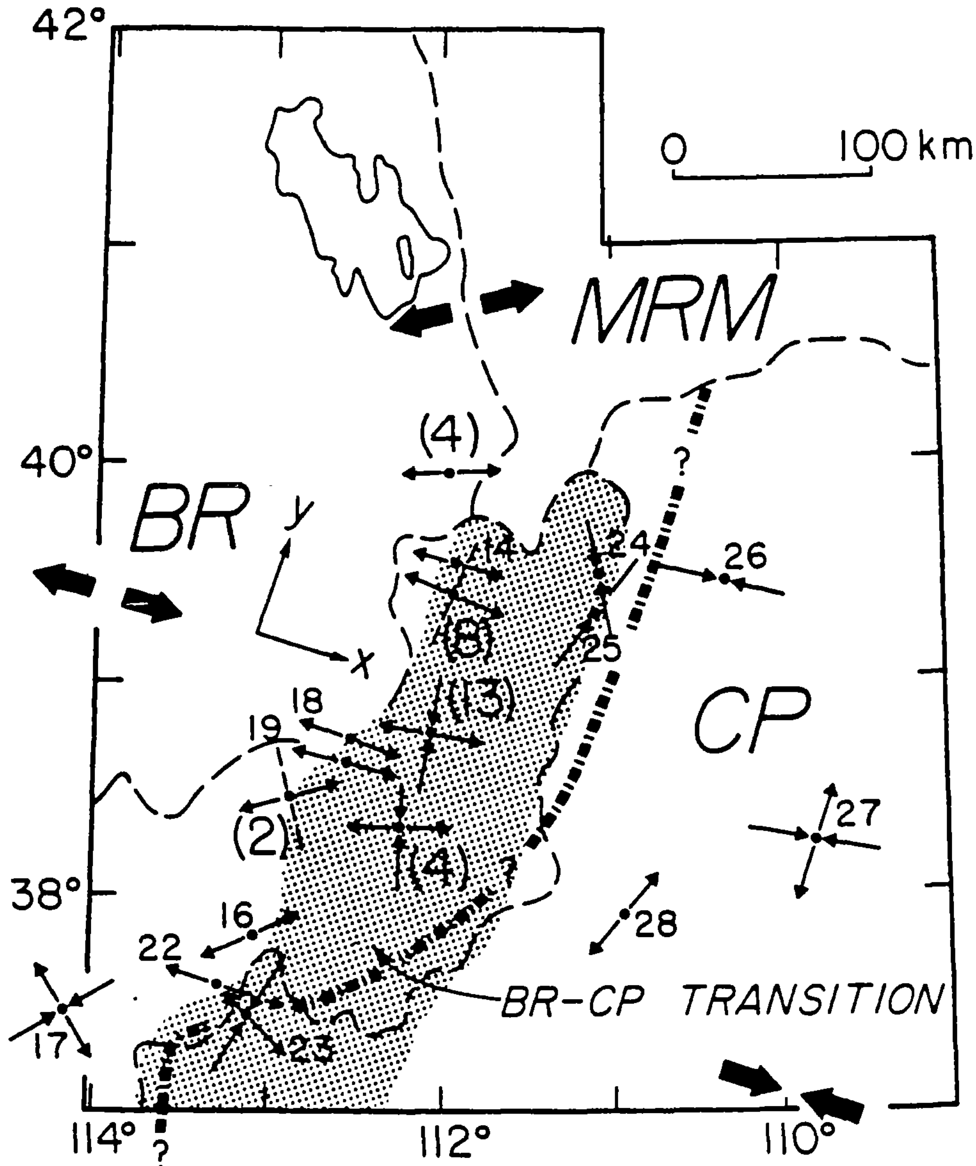
42°
40°
38°
114°
112°
110°
0
100 km
MRM
BR
CP
y
x
(4)
(8)
(13)
(2)
(4)
14
16
17
18
19
22
23
24
25
26
27
28
?
BR-CP TRANSITION

Figure 2.2

compression within the interior of the CP (Zoback and Zoback, 1980). The regional overview of stress orientation sketched in figure 2.2 indicates a predominance of normal-faulting mechanisms in the western part of the transition zone and mixing of strike-slip and reverse-faulting mechanisms eastward. There is a general consistency in the orientation of horizontal principal stress directions within the transition zone: least-compressive horizontal principal stress tends to be perpendicular to the BRP-CP boundary, and maximum compressive horizontal stress tends to be parallel to the boundary.

The appearance of strike-slip and reverse-faulting mechanisms eastward within the transition region can be explained by a systematic change in the relative magnitude of vertical principal stress from a maximum relative value (associated with normal faulting) to intermediate relative value (strike-slip faulting) or minimum relative value (reverse faulting). Such a systematic change in stress magnitude, and the orientation of horizontal principal stresses perpendicular (x-direction) and parallel (y-direction) to the province boundary, qualitatively agree with model predictions of McGarr (1982). The latter assume basal tractions across the BRP-CP boundary resulting from thermally-induced mass transport below the elastic-brittle layer.

The following tasks have been recognized as important to pursue: (a) more rigorous confirmation of stress orientation along the eastern part of the transition, (b) investigation of possible dependence of stress orientation with depth, and (c) spatial mapping of changes--particularly in view of the proximity of Late Pleistocene-Holocene normal fault scarps (along the Joes Valley graben) to the coal-mining areas where McKee and

Arabasz (1982) and Wong (1982) observed consistent reverse faulting mechanisms implying northerly-trending principal horizontal compressive stress.

## 2.6 Mining-Related Seismicity

A prominent feature of the seismicity of east-central Utah is an intense clustering of epicenters in a horseshoe-shaped pattern (figure 1.1a) extending northward along the eastern side of the Wasatch Plateau and then eastward around the Book Cliffs escarpment. The association of seismic events (both rockbursts and earthquakes) as large as $M_L 4.5$ with active underground coal mining in these areas has been evident since the late 1950's. On the scale of figure 1.1b, seismic events appear to concentrate near mining properties where annual coal extraction is of the order of 500,000 tons or greater. The maximum depth of the mine workings is less than 900 m below surface.

On the basis of reconnaissance microearthquake recording in the eastern Wasatch Plateau coal fields during the summer of 1979, McKee and Arabasz (1982) were able to document (see fig. 2.3): (1) intense spatial clustering of seismicity (h <4 km) both at and beneath levels of active underground coal mining, (2) clustering of sub-mine seismicity beneath specific areas of active mining , (3) an average rate of more than 300 microearthquakes per day in the East Mountain coal mining area, (4) the apparent occurrence of microearthquakes 6-16 km deep <u>beneath</u> the shallow mining-related seismicity, and (5) a consistent composite focal mechanism indicating reverse faulting and NW-trending nodal planes--contrasting with N-to-NNE-trending normal faulting mapped at the surface.

Figure 2.3. (following page). Results from reconnaissance earthquake studies in the eastern Wasatch Plateau (adapted from McKee, 1982). Epicenter map (above) is for the period August 8-14, 1979. Cross-section (below) illustrates location of microearthquake foci with respect to level of active mining and position of Tr-J Navajo sandstone.

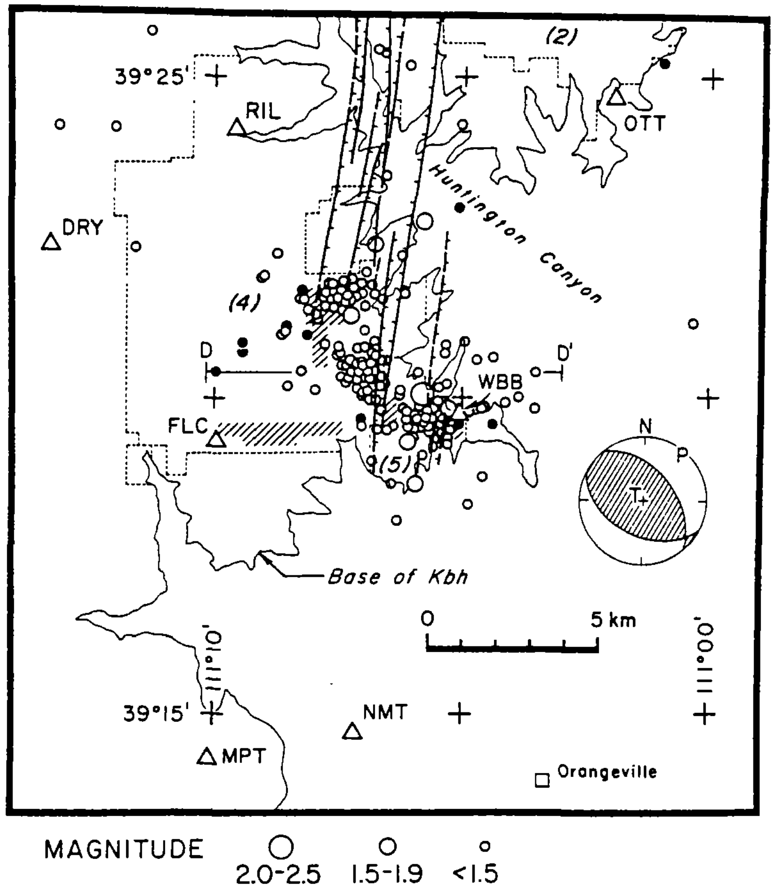
39°25'
RIL
OTT
(2)
DRY
Huntington Canyon
(4)
D
D'
WBB
FLC
(5)
N
P
T
Base of Kbh
0
5 km
111°10'
111°00'
39°15'
NMT
MPT
Orangeville
MAGNITUDE
2.0-2.5
1.5-1.9
<1.5

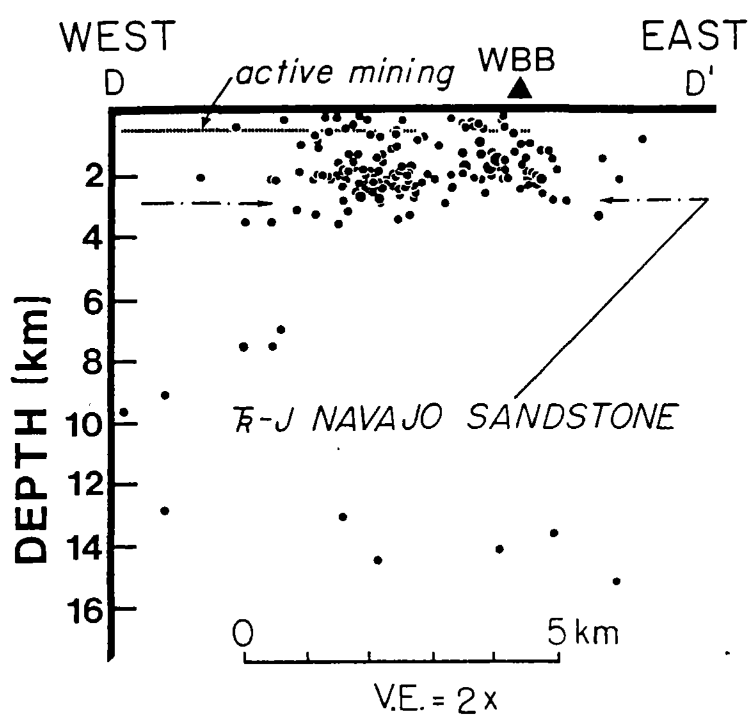
WEST
EAST
D
D'
active mining
WBB
DEPTH (km)
2
4
6
8
10
12
14
16
₸-J NAVAJO SANDSTONE
0
5 km
V.E. = 2x

Apart from seismic strain release in the immediate vicinity (less than a few hundred meters) of mine workings, seismicity at distances of kilometers is unusual, perhaps occurring beneath some coal mines in Poland (Gibowicz and others, 1981). Triggering of tectonic stress is presumed to be a factor.

Wong (1985) has reported the results of two-dimensional finite-element modeling of a typical Wasatch Plateau-Book Cliffs coal mine to evaluate in-situ stress changes induced by mining. In attempting to explain observations made by McKee and Arabasz (1982), Wong (1985) has computed detailed stress changes in a model assuming: an excavation of a 3-m-thick coal seam with pillars, overburden thickness of 610 m, cliff topography and rock properties appropriate for the stratigraphy of the eastern Wasatch Plateau, and an ambient tectonic horizontal stress of 256 bars obtained from an in situ stress measurement in the Sunnyside mine. Important results include: (1) large compressive stress concentration up to 700 bars in and near pillars and mine faces, (2) changes in vertical stress on the order of a few bars or less at depths of 1 to 3 km below mine workings—sufficient to trigger slip on tectonically pre-stressed reverse faults, and (3) prediction that sub-mine seismicity should predominate beneath and toward cliff topography.

# 3. INSTRUMENTAL SEISMICITY

## 3.1 Regional Seismicity

In this section, the setting of Joes Valley and Scofield Dams will be discussed with respect to regional seismicity located by the University of Utah. Large-size epicenter plots have been submitted separately to accompany this report representing summaries of instrumental earthquake locations from the University of Utah catalog for the following: (1) earthquakes of magnitude 2.0 or greater within 100 km, respectively, of Joes Valley and Scofield Dams during the period July 1, 1962-December 31, 1984; and (2) earthquakes of magnitude 0.5 or greater within 25 km, respectively, of Joes Valley and Scofield Dams during the same time period.

For convenience, we will discuss the setting of the two dams in relation to summaries of regional seismicity of the central Utah region recently presented by McKee and Arabasz (1982) and by Arabasz and Julander (1986). Figure 3.1 (an enlargement of fig. 1.1b) shows the setting of the two dams in the eastern Wasatch Plateau, in each case located within 20 km of intense mining-related seismicity (section 2.6) occurring along the erosional topographic escarpment of the eastern Wasatch Plateau and the Book Cliffs. The dams lie 50-60 km east of the Wasatch fault, which lacks prominent associated seismicity, but in the vicinity of which there occur abundant small to moderate-size earthquakes of magnitude 4 or smaller. In discussing figure 3.1, McKee and Arabasz (1982, p. 140) noted that "Throughout most of the intervening area between the Wasatch fault and the eastern Wasatch Plateau, regional earthquake epicenters appear to be randomly scattered, exhibiting no general correlation with faulting...One

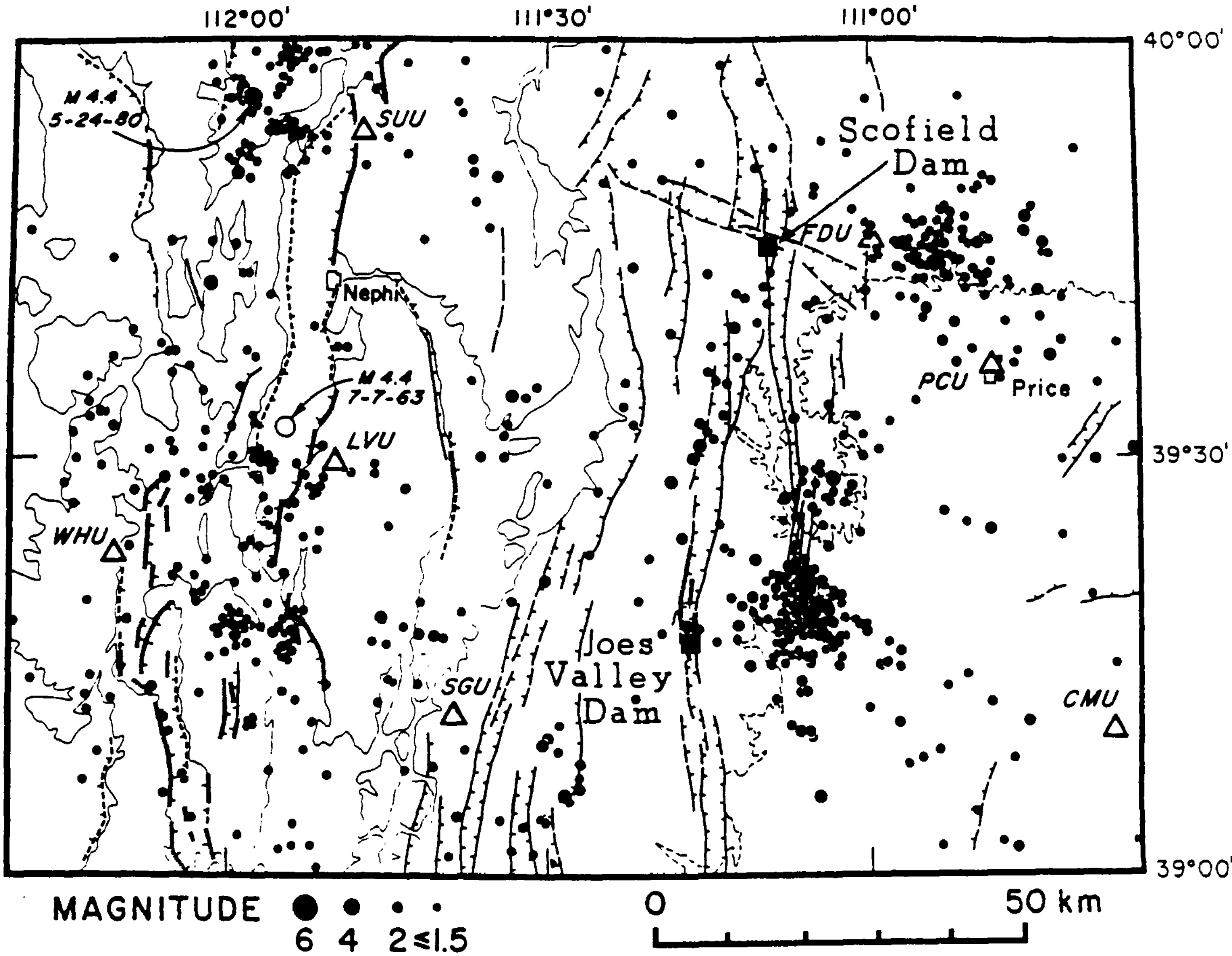


Figure 3.1. Seismicity map of central Utah (location shown in fig. 1.1a), from McKee and Arabasz (1982) showing setting of Joes Valley and Scofield Dams. Earthquake locations are from the University of Utah's regional seismic network for the period: October 1, 1974-December 31, 1981. Epicenters of 1963 Juab Valley earthquake and 1980 Goshen Valley earthquake indicated for reference.

location where there is some suggestive correlation is at the northern end of the Joes Valley graben west of Price."

Figures 3.2 and 3.3 from Arabasz and Julander (1986) give a slighty different perspective on the setting of the Joes Valley and Scofield Dams with respect to the Intermountain seismic belt in central Utah. Figure 3.3 shows the map pattern of approximately 2,000 earthquakes during the period October 1, 1974, to June 30, 1984, based on data from the University of Utah's regional seismic telemetry network. The map includes all earthquakes of magnitude 2.0 or greater (~600) that occurred during the 9.75-year interval. Epicenters for all earthquakes of estimated magnitude 5.0 or greater since 1850 and all earthquakes of magnitude 4.0 since 1962 (see Arabasz and others, 1979; Richins and others, 1981a, 1984) are also included and indicated in figure 3.3.

A first-order feature of figure 3.3 is diffusely scattered seismicity throughout the Basin and Range-Colorado Plateau transition, but with intense local clustering that predominantly reflects cumulative background seismicity rather than isolated temporal sequences. Wechsler (1979) made extensive efforts to refine the precision of regional earthquake epicenters through parts of this map area and verified a scattered regional pattern. Most of the epicenters plotted in figure 3.3 probably have a precision of ±3 km, based on (1) error analysis (Arabasz and others, 1980), (2) comparison of epicenters located independently by the fixed regional network and by local portable arrays, and (3) reasonably good azimuthal station control (see Richins and others, 1984); ±5 km epicentral accuracy would be conservative, but errors as large as ±10 km cannot be ruled out at the fringes of the main seismic belt. At the scale of figure 3.3 the

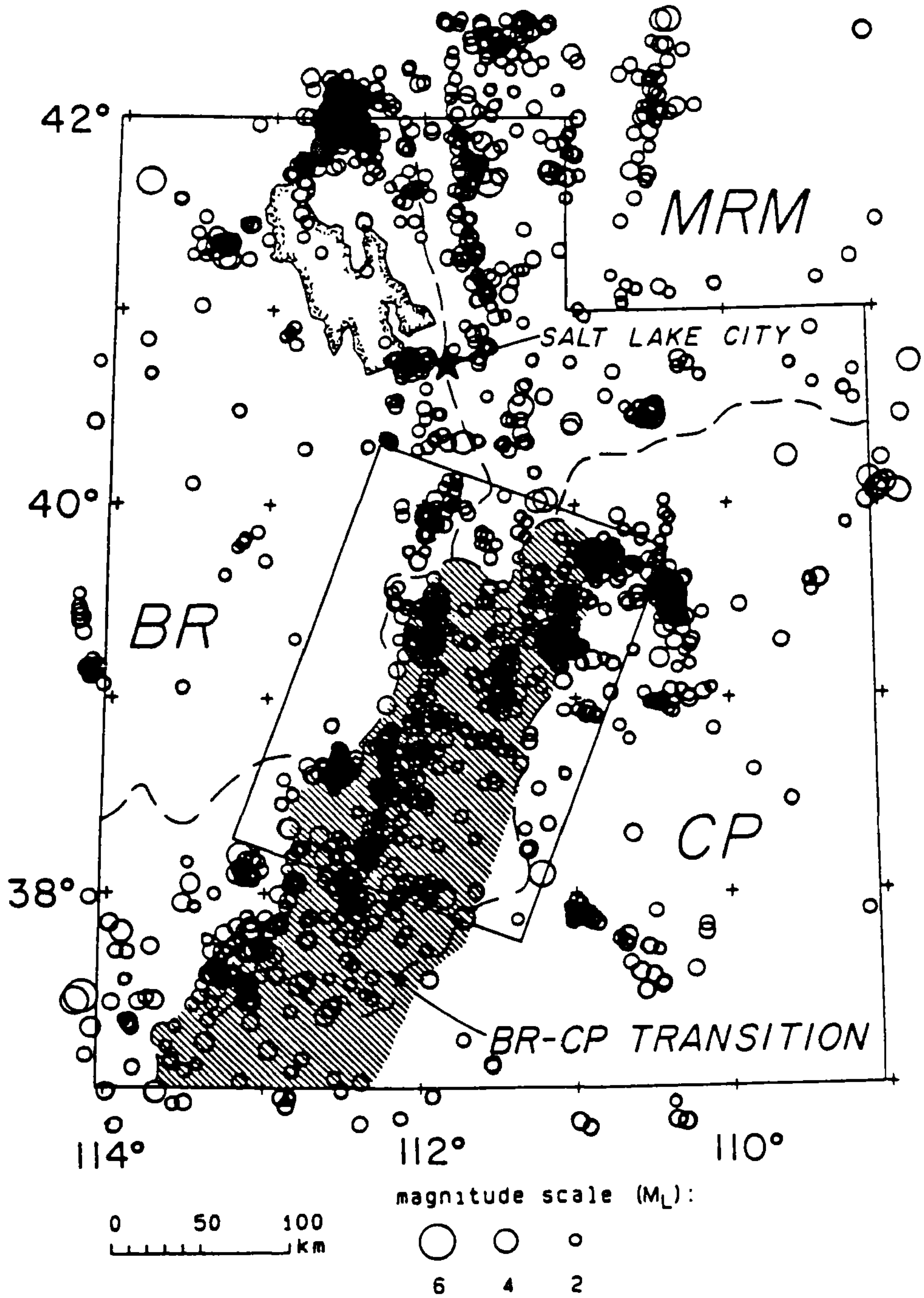


Figure 3.2. Index map of Utah region showing regional seismicity, 1962-1984, located by the University of Utah regional seismic network. Inset rectangle shows location of figure 3.3.

epicenters should provide a reliable depiction of the map projection of earthquake activity—but an inadequate depiction for confident correlation with subsurface geology. Focal-depth control is generally poor, as usual when the distance to a nearest recording station greatly exceeds the earthquake depth. More than three-fourths of the earthquakes in figure 3.3 were located with the distance to the nearest station exceeding 15 km.

Arabasz and Julander (1986) in discussing figure 3.3 noted that in the intervening area between the Wasatch fault and the eastern Wasatch Plateau, "earthquake epicenters appear randomly scattered...(but that) epicentral density increases in the vicinity of the northern Joes Valley fault zone—as it does in the vicinity of fault zones in the southwestern Wasatch Plateau. It remains to be determined whether this seismicity correlates with shallow faulting of post-Jurassic strata or with deep (>4 km) underlying structure."

Figure 3.3 indicates that earthquakes in the magnitude 5 range have occurred historically within 40-50 km of the Joes Valley and Scofield Dams. Since instrumental monitoring by the University of Utah began in July 1962, the largest shocks close to the two dams have been the following. Within 100 km of either dam, the largest earthquake was the magnitude 4.4 Juab Valley earthquake of July 7, 1963 (see fig. 3.1). Within 25 km of Joes Valley Dam, the largest shock was one of magnitude 3.2 on February 9, 1977. Within 25 km of Scofield Dam, the largest shock was one of magnitude 2.6 on March 18, 1977.

## 3.2 Results of EWP-84 Experiment

Figure 3.4 is an epicenter map summarizing the results of

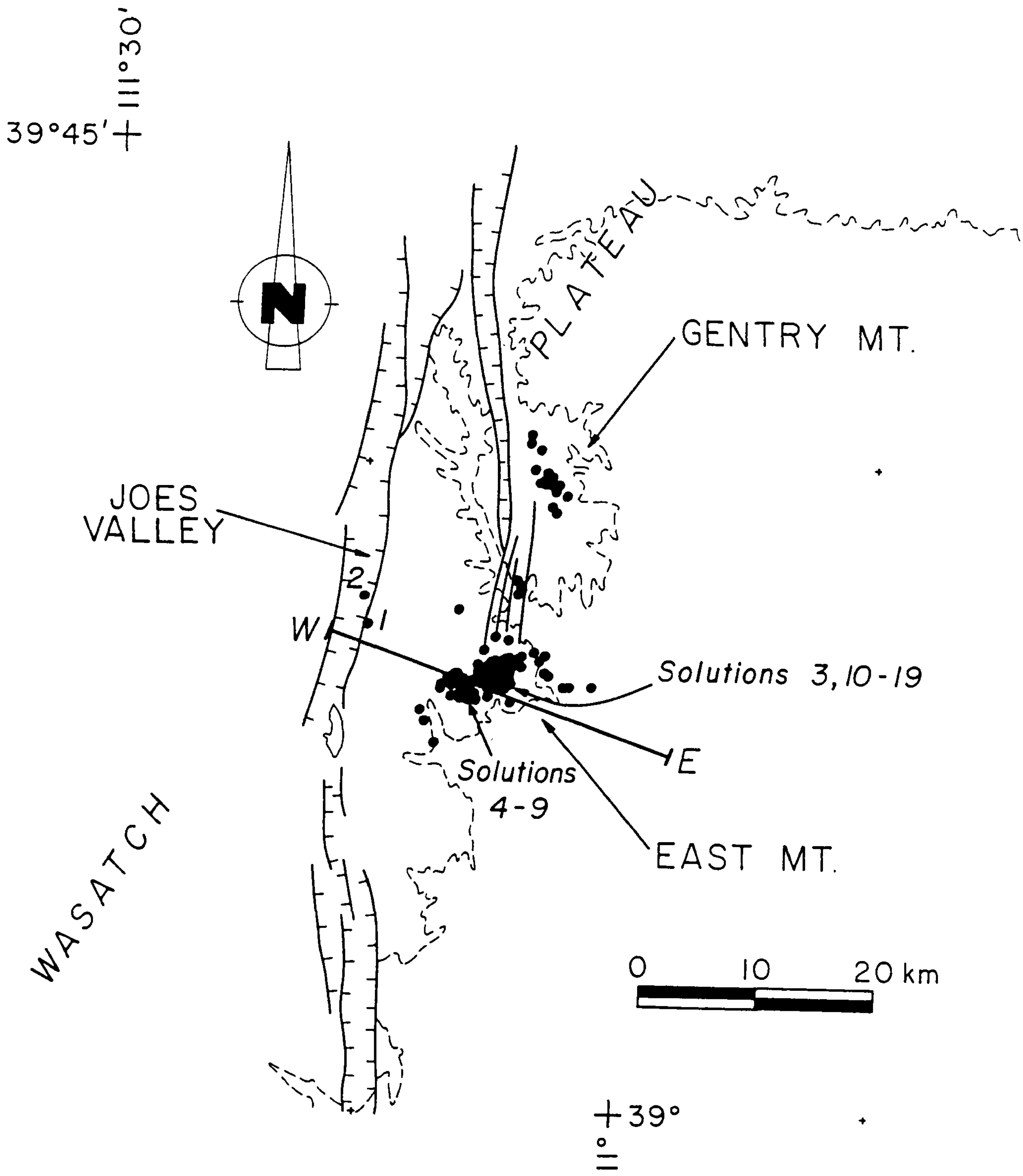


Figure 3.4. Epicenter map of seismic events located as part of EWP-84 experiment (Report 1).

seismographic monitoring in the Joes Valley-eastern Wasatch Plateau area during a 38-day period between July 6 and August 12, 1984 (from Report 1). The map includes epicenters for 475 small earthquakes of magnitude 2.1 or smaller. The description of the locations of the seismic events need not be repeated here (see Report 1, section 5.1), but in general the seismicity is dominated by mining-related seismic events concentrated in the vicinity of active underground coal mining in the East Mountain and Gentry Mountain areas. Minimal earthquake activity was detected and located in the immediate vicinity of the Joes Valley graben. Several kilometers east of the Joes Valley Dam, at least some seismic events judged to be genuine earthquakes were located in the Cottonwood Creek area. A discussion of the implication of these results will be included in section 4.

# 4. IMPLICATIONS OF INSTRUMENTAL SEISMICITY FOR EARTHQUAKE HAZARDS RELATIVE TO JOES VALLEY AND SCOFIELD DAMS

## 4.1 Background Seismicity and Active Faulting

I am consistently led to the thesis that background seismicity of small to moderate size (M5 or smaller) in central Utah—and throughout most of the Intermountain seismic belt—does not simply "illuminate" the major active faults that have the potential of producing the largest earthquakes. Information specific to the central Utah region, together with extended discussion, is presented by Arabasz and Julander (1986, Attachment No. 1 here; see also Arabasz, 1984). Further, there is evidence for disparity in relations of frequency-of-occurrence versus magnitude between background instrumental seismicity and rates of surface faulting earthquakes. This relates to the so-called characteristic earthquake model, developed by Schwartz and Coppersmith (1984) and Wesnousky and others (1983). As described by Schwartz and Coppersmith (1984), this model "postulates that individual faults and fault segments tend to generate essentially same size or chracteristic earthquakes having a relatively narrow range of magnitude near the maximum." Schwartz and Coppersmith (1984) argue for the applicability of the characteristic earthquake model to the Wasatch fault zone on the basis of paleoseismological observations, and they demonstrate that extrapolations of instrumental seismicity underestimate the rate of surface-faulting events on both the Wasatch fault and parts of the San Andreas fault. In sum, there is growing discomfort among seismologists about the applicability of b-value models based on regional data to individual fault zones (see also Davison and Scholz, 1985).

If background seismicity does not simply illuminate the major active faults in the Utah region, and if there is a fundamentally disjoint relationship between rates of occurrence of small to moderate-size earthquakes and large scarp-forming earthquakes, what are the implications for the eastern Wasatch Plateau? Our discussion in section 3 pointed out (1) the historical occurrence of earthquakes only as large as about magnitude 5 in the general region of the Wasatch Plateau, (2) the occurrence of diffusely scattered earthquakes of only small size (M3.2 or smaller) in the vicinity of Joes Valley and Scofield Dams during the past two decades, and (3) the proximity of those dams to areas of intense mining-related seismicity. The results of the EWP-84 experiment (fig. 3.4) emphasize the paucity of background seismicity in the Joes Valley area in contrast to much higher levels of microseismicity in nearby areas of active coal mining. I will address the issue of mining-related seismicity separately, and restrict attention here to natural tectonic earthquakes.

If we disregard for the moment the mining-related seismicity, the data of figures 3.1 and 3.3 show that the eastern Wasatch Plateau is characterized by a distinctly lower level of background seismicity than is the western part of the seismic belt roughly 50 km to the west. The results of the EWP-84 microearthquake monitoring are consistent with this observation—as were the results of regional microearthquake monitoring by McKee and Arabasz (1982, fig. 5). during the summer of 1979

Given the presence of late Pleistocene-Holocene fault scarps along the Joes Valley fault zone, we are forced to evaluate the relative importance of seismicity versus paleoseismology in a hazard evaluation. If our approach is deterministic, it is inescapable that the latter wins out, and experience in the Intermountain seismic belt supports that view. The paucity of contemporary seismicity along the Wasatch fault zone (Arabasz, 1984; Arabasz and others, 1980) is one case in point. The other is the experience of the 1983 M7.3 Borah Peak, Idaho, earthquake—more relevant, perhaps, because of its setting outside a belt of evident, high background seismicity. The Borah Peak mainshock occurred in a part of the Intermountain area that had not been historically active. For at least two decades before the mainshock, no earthquakes of magnitude 3.5 or greater had occurred within 25 km of the mainshock epicenter (Dewey, 1985).

I believe that the consensus of informed seismologists and geologists familiar with the Intermountain seismic belt would be that any prognosis of active faulting is more reliably based on late Quaternary geology than instrumental seismicity. Background seismicity clearly must carry information (albeit not well understood at the present) regarding crustal deformation and the loading of major active faults. And that same seismicity is informative about the rate of occurrence and possible location of small to moderate-size earthquakes below the threshold of surface faulting at about magnitude 6.0. However, in the vicinity of a fault with proven Holocene or late Pleistocene displacement, the absence or paucity of background seismicity can only be considered confusing—and not evidence against imminent surface faulting, unless it can be shown that the fault or fault segment is in the early post-seismic stage of a seismic cycle.

## 4.2 Fault-Plane Solutions and Stress State

With the exception of new fault-plane solution data from the EWP-84 experiment (Report 1), the compilation of figure 4.1 from Attachment No. 1 (Arabasz and Julander, 1986) represents a complete summary of available

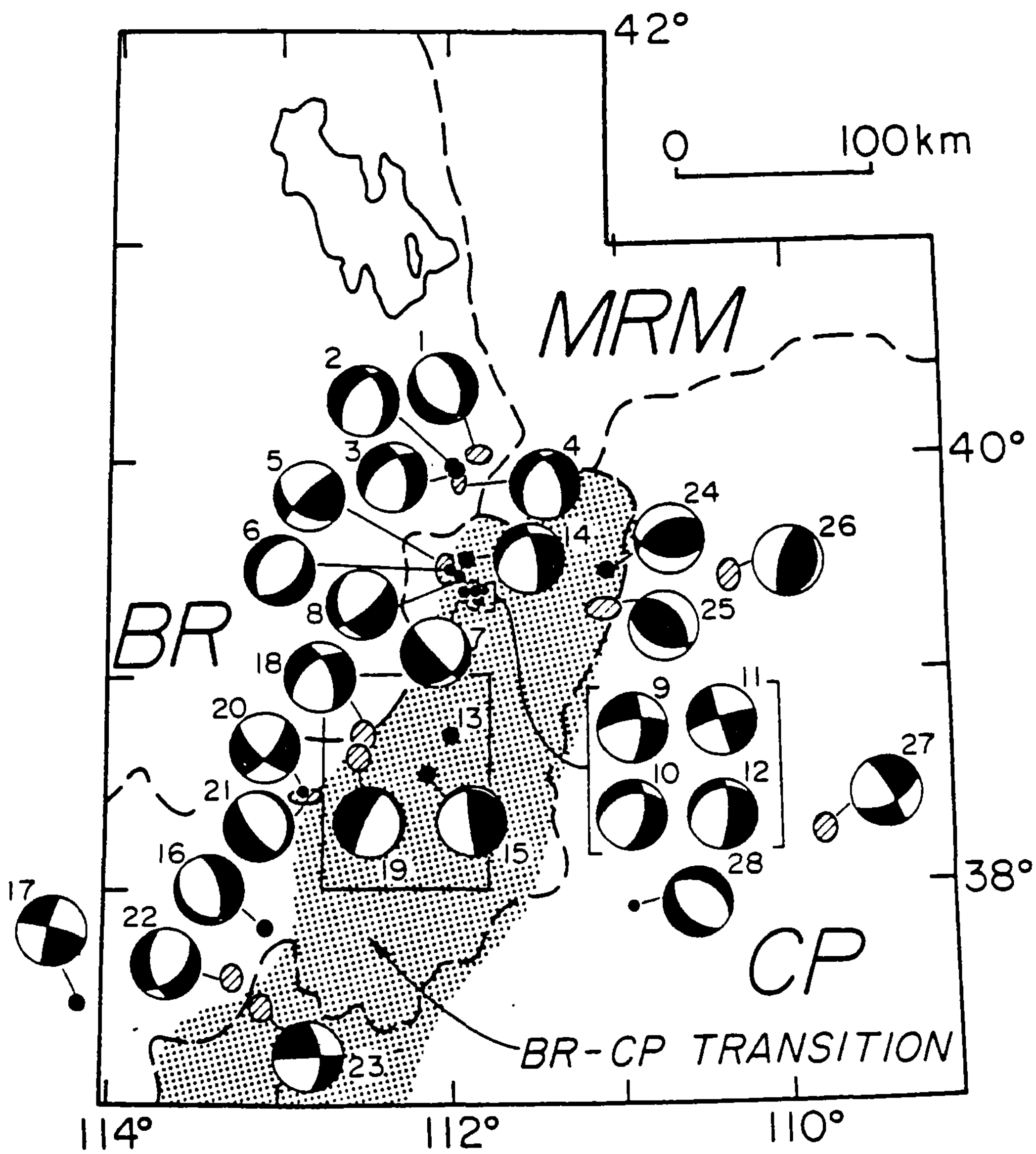


Figure 4.1. Summary of earthquake focal mechanisms (lower-hemisphere, compressional quadrants black) across the Basin and Range-Colorado Plateau transition (from Arabasz and Julander, 1986).

fault-plane solutions for the Wasatch Plateau area and its regional vicinity. An interpretation of the fault-plane solution data in terms of upper-crustal stress state was shown in figure 2.2; it was briefly discussed in section 2.5, and is discussed at length in Attachment No. 1. Outstanding tasks for the eastern Wasatch Plateau included: (1) more rigorous confirmation of stress orientation along the easternmost Wasatch Plateau, (2) investigation of possible dependence of stress orientation with depth, and (3) spatial mapping of changes in stress orientation from principal horizontal extension in the western part of the BR-CP transition to principal horizontal compression implied by mechanisms 24 and 25 (fig. 4.1) in the coal-mining areas of the eastern Wasatch Plateau—especially in view of proximity to normal fault scarps along the Joes Valley graben.

Fault-plane solutions from the EWP-84 experiment schematically shown as lower-hemisphere projections (compressional quadrants shaded) in figure 4.2 represent a significant contribution to addressing tasks (1) and (3) above. (See Report 1 for details and additional discussion relating to the focal-mechanism determinations.) In particular, solutions 1 and 2 for upper-crustal earthquakes within the Joes Valley graben are of considerable importance. They indicate a predominance of normal faulting and argue for the probable existence of an extensional stress state in the immediate vicinity of Joes Valley—removing questions about whether normal faults of the Joes Valley zone might now be situated within a regime of principal horizontal compression. The WNW-ESE orientation of T-axes for those two solutions is consistent with a mean orientation in the $102^{\circ}$-$282^{\circ}$ direction of T-axes for fault-plane solutions in the BR-CP transition region (Attachment No. 1, Arabasz and Julander, 1986).

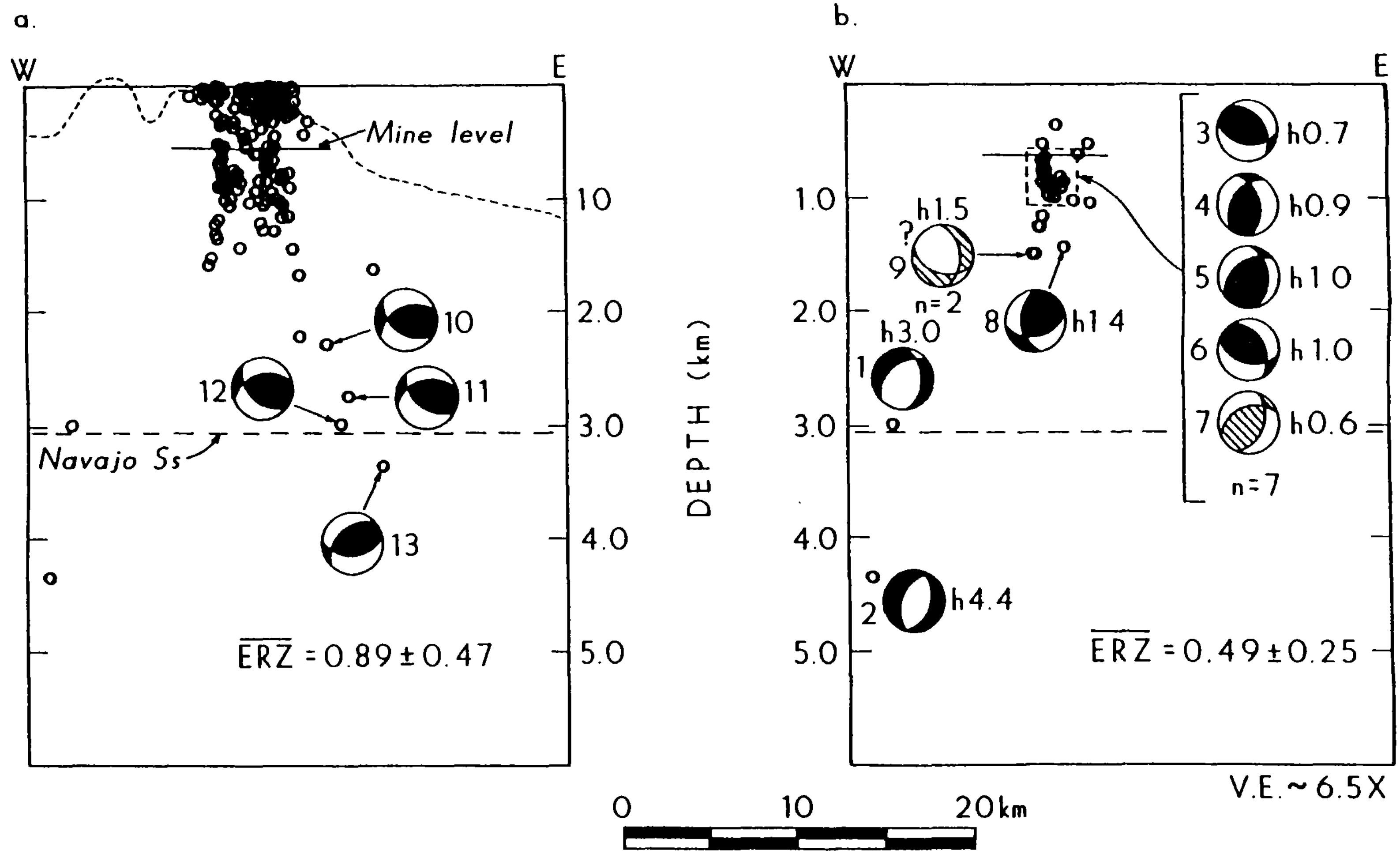


Figure 4.2. Schematic summary of focal-mechanism data from EWP-84 experiment (Report 1). Hypocentral cross section and numbered events keyed to figure 4.3. Beachballs represent stereographic, lower-hemisphere projections onto the equatorial plane. Dilatational quadrants are white and compressional quadrants black (for single events) or hachured (for composite solutions). Dashed line in (a) is an approximation of the topography.

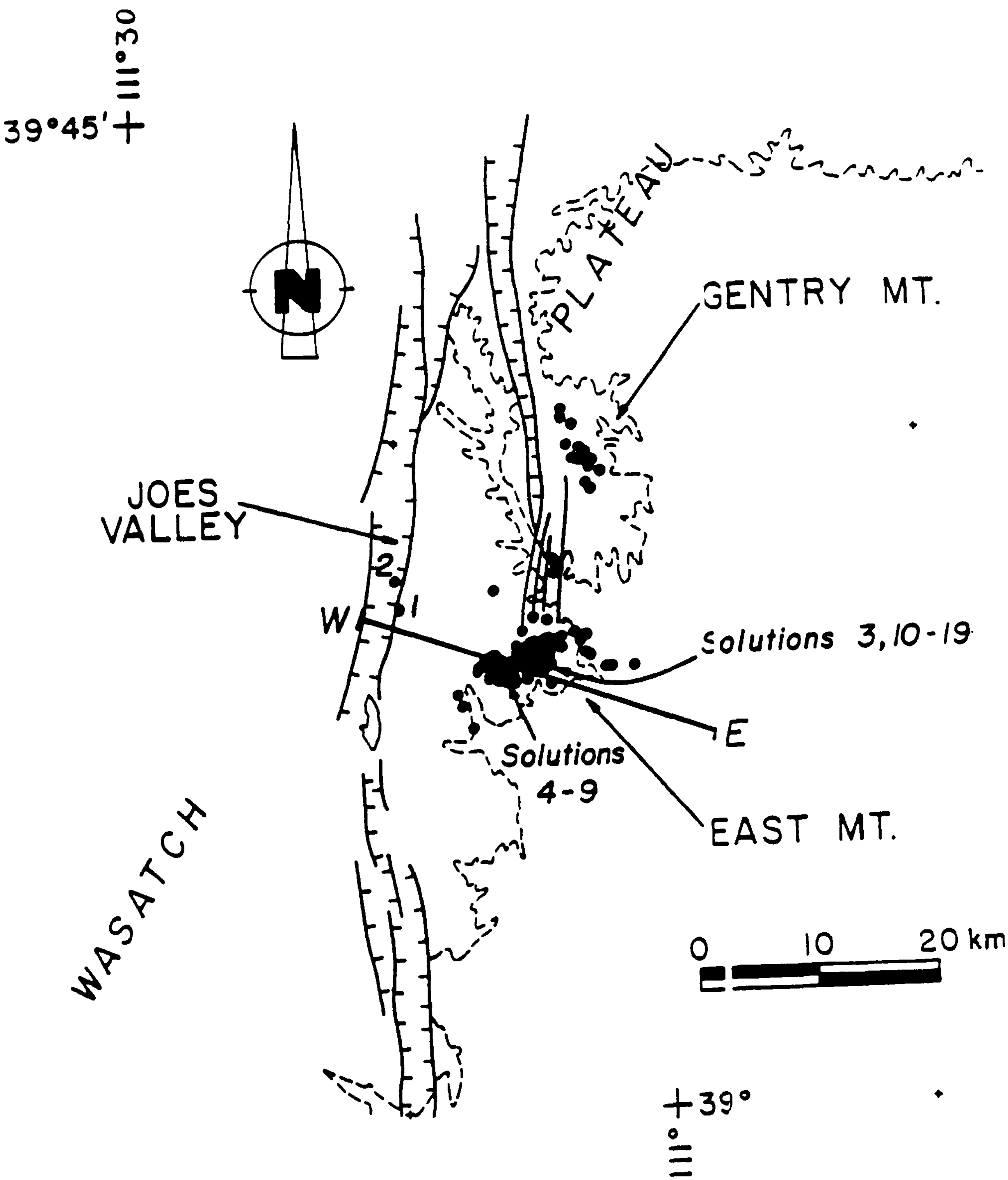


Figure 4.3. Epicenter map (from Report 1) showing locations of well-located seismic events from EWP-84 experiments. Line of section and numbered epicenters identify data shown in figure 4.2.

Figure 4.2 also shows five high-quality fault-plane solutions (solutions 3-7) sampled from the 0.6 km to 1.0 km depth range at or slightly below mine level in the East Mountain area, two solutions (solutions 8 and 9) for events roughly one kilometer below mine level, and from solutions (solutions 10-13) for events having less reliably determined focal depths beneath the mining area at depths between 2.3 and 3.4 km.

In general, solutions 3-6 are consistent in that all are compressional mechanisms with an implied predominance of reverse slip on planes of moderate dip. Solution 7, a composite of seven events at 0.6 ($\pm$0.1) depth is of the same type. Inconsistency of these events is seen in the fact that they have divergent orientations of P-axis, presumably approximating the direction of maximum horizontal compression.

The data of figure 4.2 show convincing evidence for the predominance of compressional-type focal mechanisms at or slightly below mine level. To investigate whether or not there might be a change in stress orientations below mine level, solutions 10-13 were determined for a sample of events located less precisely in terms of focal depths. The results (described more fully in Report 1) suggest the persistence of reverse-type faulting down to 1.5 to 3.0 km below mine level in the East Mountain area.

The combined data of figures 4.1 and 4.2 make it likely that mining-related seismicity along the easternmost margin of the Wasatch Plateau is occurring in a domain of principal horizontal compression. Divergently oriented, near-horizontal P-axes could result if the maximum and intermediate principal stresses in the horizontal plane were close in value, allowing local interchange. The data in hand also suggest that a change in laterally-varying stress state within the BR-CP transition may have been bracketed within the 10-km space between the Joes Valley earthquakes and those in the East Mountain area. An alternative interpretation is that the shallow mechanisms in the East Mountain area may reflect some unusual localized stress field in the immediate vicinity of the active coal mines and not a regional stress field. In either case, the evidence for an extensional stress state beneath Joes Valley appears convincing.

### 4.3 Low-Angle Detachment Faulting

Figure 4.4 schematically illustrates a hypothetical scenario for "thin-skinned" horizontal extension of the Wasatch Plateau, linked to interpretations of Standlee (1982) and Royse (1983) described in section 2.4. Basic elements include: (1) the existence of a near-horizontal detachment surface within incompetent Jurassic strata overlying the Navajo Sandstone, (2) extensional backsliding on the west-sloping detachment originally formed during Mesozoic-early Tertiary thrusting, and (3) non-penetration of the detachment by surficial post-Eocene normal faulting—chiefly a response to the "thin-skinned" extension of upper-plate sedimentary rocks above the detachment. The purpose of this section is to explore implications of observed seismicity and implications for future seismogenesis.

At the outset, it should be noted that the interpretation of extrapolating a detachment from the western Wasatch Plateau to the easternmost Wasatch Plateau is a reasonable one. There exists evidence from subsurface geophysical exploration of the Castle Valley area, along the eastern margin of the Wasatch Plateau, for a system of eastward thrusting that displaces the Ferron Sandstone (above the Navajo Sandstone)

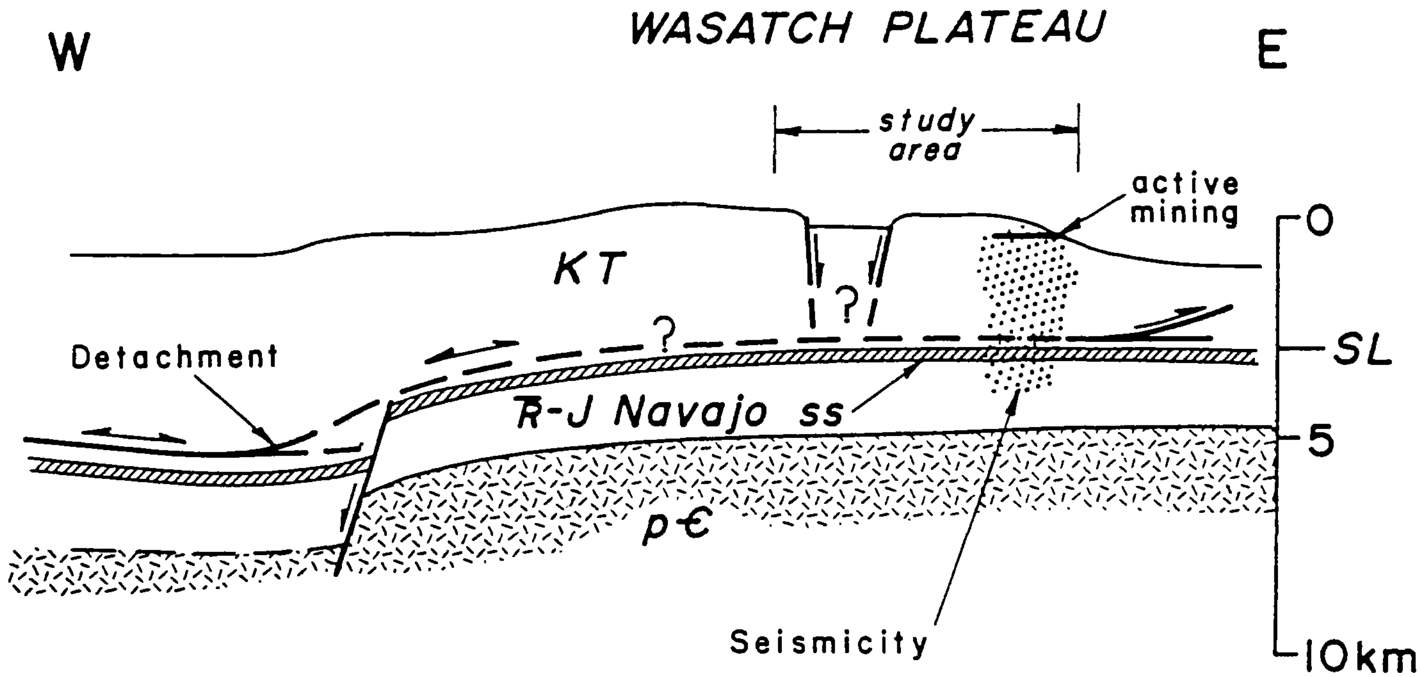


Figure 4.4. Schematic geologic cross-section illustrating hypothetical interpretation of "thin-skinned" horizontal extension in the Wasatch Plateau (compare with fig. 2.1).

and that dies out in the Mancos Shale without breaking to the surface. I have been asked not to cite the source of this proprietary information, which involves multiple pieces of evidence. In schematic form, the situation would resemble that depicting the eastward continuation of detachment structures shown in figure 4.4. A key issue is the structural relation between such detachment faulting and younger normal faulting.

From our discussion in section 3.1, it was apparent that focal-depth resolution for the regional seismicity was inadequate to determine whether diffuse seismicity in the Wasatch Plateau was associated with shallow upper-plate deformation or with deeper buried structures. Only data from special studies such as the EWP-84 experiment have adequate focal-depth resolution even to begin addressing such an issue.

For the data shown in Figure 2.3 (from McKee and Arabasz, 1982), Arabasz and Julander (1986) note that the Navajo Sandstone appears to coincide with a lower bound to the clustered shallow seismicity occurring beneath the area of active mining in the East Mountain area. They present the possibility that a low-angle detachment above the Navajo Sandstone could "conceivably exert an important influence on the depth distribution of sub-mine earthquakes." Alternatively, the depth distribution could relate to in-situ stress changes induced by mining (see section 2.6).

Figure 4.2 presented a cross-section view of hypocenters determined as part of the EWP-84 experiment (Report 1). Note that mine level is at 0.6 km below datum, and the Navajo Sandstone at 3.0 km below datum. The data of figure 4.2 are inadequate to suggest any simple demarcation at the level of the Navajo Sandstone. At least for the earthquake at 4.35 km depth, for which both the focal depth and fault-plane solution 2 are reliably determined (Report 1), we can be confident that the earthquake occurred below the Navajo Sandstone and that the focal-mechanism is of the normal-fault type.

I have made a special effort to test the focal depths of the deeper earthquakes located by McKee and Arabasz (1982) and shown in figure 2.3 in the depth range of 6 to 15 km. After relocating those earthquakes with the velocity model determined for the EWP-84 experiment, and after applying tests for focal-depth stability described in Report 1, I am skeptical about the reliability of those deeper foci. The point becomes a moot one, however, insofar as we are dealing with sparse seismicity away from the active mining areas. Hence the presence or absence of deeper seismicity has uncertain significance. In any case, I feel that foci at least as deep as 4.4 km have been reliably determined and that some earthquakes are occurring below the Navajo Sandstone.

There is a recurrent paradox in the Intermountain seismic belt that either (1) there exist obscure rupture pathways between surface scarps and deep nucleation points at about 10-15 km depth, or (2) shallow upper-crustal detachments can be engaged seismically to produce large scarp-forming earthquakes, or (3) surface fault scarps with 1-5 m displacement can be produced without magnitude 7+ earthquakes. I believe that the collective wisdom of seismologists and geologists working in the Intermountain seismic belt would lead to the assignment of subjective probabilities to these alternatives such that $P(1) > P(2) >> P(3)$. This is particularly true in the aftermath of the 1983 Borah Peak earthquake, whose experience will likely for some time remain a yardstick for evaluating future scenarios for surface-faulting earthquakes elsewhere in the

Intermountain seismic belt. Issues relating to the nucleation depth of large surface-faulting earthquakes in the Intermountain seismic belt, whether low-angle faults can be seismogenic in an extensional regime, and the apparent influence of horizontal detachments on the depth distribution of background seismicity in the central Utah region are discussed in detail in Attachment No. 1.

It would take extraordinary data to establish that the bounding faults of the Joes Valley graben were truncated by a horizontal detachment and hence not adequately penetrative into the crust to generate a large earthquake. Even if it can be shown by seismic-reflection data that such detachment faulting truncates surficial normal faults elsewhere in the Wasatch Plateau, we cannot conclude that such a detachment is everywhere coherent and undisturbed by younger normal faulting. The question simply is, What are the subsurface relations beneath Joes Valley? Existing seismicity data are equivocal and cannot be relied upon to support any hypothesis that would preclude future surface-faulting earthquakes of large size (say, magnitude 6-1/2 to 7-1/2) along the Joes Valley fault zone.

## 4.4 Mining Related Seismicity

Figure 3.4 shows that small-magnitude earthquake activity occurs within 10 km of the Joes Valley Dam, and there is abundant seismicity (mostly smaller than magnitude 3) within 15-20 km of the dam. We have observed that the largest seismic event in the East Mountain mining area since 1962 was a shock of magnitude 3.2 in 1977. Since the mid-1970's amounts of coal extraction in the East Mountain area have been as high or higher than anywhere in the Wasatch Plateau-Book Cliffs coal fields (see Report 1). Historically, seismic events as large as $M_L$4.5 have occurred in the vicinity of coal mines in the Book Cliffs area (Cook and Smith, 1967).

The conclusion to be drawn here is that both the Joes Valley and Scofield Dams lie close to areas of active coal mining. In principle, their exposure to mining-related seismic events as large as magnitude 4.5 should be accepted. (To my knowledge, the size estimation of magnitude 4.5 for shocks that occurred in the 1950's in the Book Cliffs area has not been critically checked.)

## ACKNOWLEDGMENTS

Numerous individuals made contributions relating to various aspects of the acquisition, analysis, and interpretation of data presented in this report. R.A. Martin, of the U.S. Bureau of Reclamation (USBR), I.G. Wong of Woodward-Clyde Consultants (WCC), and J.C. Pechmann of the University of Utah (U of U) were primary co-investigators (together with W.J. Arabasz) in the 1984 Eastern Wasatch Plateau field experiment. Their help and useful discussions through all stages leading to this report are gratefully acknowledged. I am particularly indebted to D.J. Williams of the U of U, who completed much of the data analysis from the 1984 field experiment, and who provided significant assistance in preparing this report.

The cooperation of officials of Utah Power & Light Company was crucial to the 1984 field experiment—notably in connection with investigations of mining-related seismic activity in the East Mountain area; I especially thank R.C. Fry for key assistance and for helpful discussions. I also thank G.L. Hunt of Cyprus Mining Company, and J. Mercier and M. Adkins of Getty Mining Company, for helpful discussions on the general geology of the eastern Wasatch Plateau.

Preparation of this report was supported by U.S. Bureau of Reclamation Contract No. 4PG 40 13210. Companion research at the University of Utah was supported by the National Science Foundation, Grant No. EAR-8319661.

# REFERENCES


Arabasz, W.J., 1982, Seismological studies across the Basin and Range-Colorado Plateau transition in Utah: Final Report to National Science Foundation, Grant No. EAR-8008799.

Arabasz, W.J., 1983, Geometry of active faults and seismic deformation within the Basin and Range-Colorado Plateau transition, central and SW Utah: Earthquake Notes, v. 54, no. 1, p. 48.

Arabasz, W.J., 1984, Earthquake behavior in the Wasatch Front area: association with geologic structure, space-time occurrence, and stress state: in U.S. Geological Survey Open-File Report 84-763, p. 310-339.

Arabasz, W.J., and Julander, D.R., 1986, Geometry of seismically active faults and crustal deformation within the Basin and Range-Colorado Plateau transition in Utah in Mayer, L. ed., Extensional tectonics of the southwestern United States: A perspective on processes and kinematics: Geological Society of America Special Paper 208, in press.

Arabasz, W.J., Smith, R. B., and Richins, W. D., eds., 1979, Earthquake studies in Utah, 1850 to 1978: Salt Lake City, Utah, University of Utah Seismograph Stations Special Publication, 552 p.

______, 1980, Earthquake studies along the Wasatch Front, Utah: Network monitoring, seismicity and seismic hazards: Seismological Society of America Bulletin, v. 70, p. 1479-1499.

Arabasz, W.J. and Smith, R.B., 1981, Earthquake prediction in the Intermountain seismic belt—An intraplate extensional regime, in Simpson, D.W., and Richards, P.G., eds., Earthquake prediction—An international review: American Geophysical Union, Maurice Ewing Series, v. 4, p. 238-258.

Arabasz, W.J., and Williams, D.J., 1985, Analysis and summary of seismographic data recorded in vicinity of Joes Valley Dam, Emery County Project, eastern Wasatch Plateau, Utah: Technical Report to U.S. Bureau of Reclamation, Seismotectonic Section, Denver, Colorado.

Bodell, J.M., and Chapman, D.S., 1982, Heat flow in the north-central Colorado Plateau: Journal of Geophysical Research, v. 87, p. 2869-2884.

Burchfiel, B.C., and C.W., Hickcox, 1972, Structural development of central Utah, in Baer, J.L., and Callaghan, E., eds., Plateau-Basin and Range transition zone, central Utah, 1972: Salt Lake City, Utah, Utah Geological Association Publication 2, p. 55-66.

Davison, F.C., and Scholz, C.H., 1985, Frequency-moment distribution of earthquakes in the Aleutian arc: A test of the characteristic earthquake model: Bulletin of the Seismological Society of America, v. 75, p. 1349-1362.

Dewey, J. W., 1985, Instrumental seismicity of central Idaho, in Proceedings of Workshop XXVIII on the Borah Peak, Idaho, Earthquake: U. S. Geological Survey Open-file Report 85-290, v. A, p. 264-284.

Gibowicz, S.J., Droste, Z., Guterch, B., and Hordejuk, J., 1981, The Belchatow, Poland, earthquakes of 1979 and 1980 induced by surface mining: Engineering Geology, v. 17, p. 257-271.

Julander, D.R., 1983, Seismicity and correlation with fine structure in the Sevier Valley area of the Basin and Range-Colorado Plateau transition, south-central Utah: Salt Lake City, Utah, University of Utah, M.S. thesis, 143 p.

McGarr, A., 1982, Analysis of states of stress between provinces of constant stress: Journal of Geophysical Research, v. 87, p. 9279-9288.

McKee, M.E., 1982, Microearthquake studies across the Basin and Range-Colorado Plateau transition zone in central Utah: Salt Lake City, Utah, University of Utah, M.S. thesis, 118 p.

McKee, M.E., and Arabasz, W.J., 1982, Microearthquake studies across the Basin and Range-Colorado Plateau transition in central Utah, in Nielson, D.L., ed., Overthrust belt of Utah: Salt Lake City, Utah, Utah Geological Association Publication 10, p. 137-149.

Richins, W.D., Arabasz, W.J., Hathaway, G.M., McPherson, E., Oehmich, P.J., and Sells, L.L., 1984, Earthquake data for the Utah region: January 1, 1981 to December 31, 1983: Salt Lake City, Utah, University of Utah Seismograph Stations Special Publication, 111 p.

Richins, W.D., Arabasz, W.J., Hathaway, G.M., Oehmich, P.J., Sells, L. L., and Zandt, G., 1981a, Earthquake data for the Utah Region: July 1, 1978 to December 31, 1980: Salt Lake City, Utah, University of Utah Seismograph Stations Special Publication, 125 p.

Royse, F., 1983, Extensional faults and folds in the foreland thrust belt, Utah, Wyoming, Idaho: Geological Society of America Abstracts with Programs, v. 15, no. 5, p. 295.

Schwartz, D.P., and Coppersmith, K J., 1984, Fault behavior and characteristic earthquakes: Examples from the Wasatch and San Andreas fault zones: Journal of Geophysical Research, v. 89, p. 5681-5698.

Smith, R.B., Braile, L., and Keller, G.R., 1975, Crustal low velocity layers: Possible implications of high temperature at the Basin Range-Colorado Plateau transition: Earth and Planetary Science Letters, v. 28, p. 197-204.

Smith, R.B., 1978, Seismicity, crustal structure, and intraplate tectonics of the interior of the western Cordillera, in Smith, R.B., and Eaton, G., eds., Cenozoic tectonics and regional geophysics of the western cordillera: Geological Society of America Memoir 152, p. 111-144.

Standlee, L.A., 1982, Structure and stratigraphy of Jurassic rocks in central Utah: Their influence on tectonic development of the Cordilleran foreland and thrust belt: in Powers, R.B., ed., Geologic studies of the Cordilleran thrust belt: Denver, Colorado, Rocky Mountain Association of Geologists, v. 1, p. 357-382.

Stokes, W.L., 1977, Subdivisions of the major physiographic provinces in Utah: Utah Geology, v. 4, no. 1, p. 1-17.

Thompson, G.A., and Zoback, M.L., 1979, Regional geophysics of the Colorado Plateau: Tectonophysics, v. 61, p. 149-181.

Wechsler, D.J., 1979, An evaluation of hypocenter location techniques with applications to southern Utah: Regional earthquake distributions and seismicity of geothermal areas: Salt Lake City, Utah, University of Utah, M.S. thesis, 225 p.

Wesnousky, S., Scholz, C.H., Shimazaki, K., and Matsuda, T., 1983, Earthquake frequency distribution and the mechanics of faulting: Journal of Geophysical Research, v. 88, p. 9331-9340.

Wong, I.G., 1984, Mining-induced seismicity in the Colorado Plateau, western United States, and its implications for the siting of an underground high level nuclear waste repository, in Gay, N.C., and Wainwright, E.H., eds., Proceedings of the 1st International Congress on Rockbursts and Seismicity in Mines: Johannesburg, South African Institute of Mining and Metallurgy, p. 147-152.

Wong, I.G., 1985, Mining-induced earthquakes in the Book Cliffs and eastern Wasatch Plateau, Utah, U.S.A.: International Journal of Rock Mechanics & Geomechanical Abstracts, v. 22, no. 4, p. 263-270.

Zoback, M.L., and Zoback, M.D., 1980, State of stress in the conterminous United States: Journal of Geophysical Research, v. 85, p. 6113-6156.

Zoback, M.L., 1983, Structure and Cenozoic tectonism along the Wasatch fault zone, Utah: Geological Society of America Memoir 157, p. 3-27.


EXPLANATION
Late Cenozoic normal fault, ball on downthrown side, dashed where approximately located.
Fault scarp in late Quaternary deposits.
Photolineament in late Quaternary deposits.
SCALE OF KILOMETERS
NOTE: Base map is from U.S.G.S. Price and Salina 1° X 2° sheets.
SANPETE VALLEY
SNOW LAKE GRABEN
AREA OF PLATE 2
GOOSEBERRY GRABEN
AREA OF PLATE 3
Seely Segment
Straight Canyon Segment
Ferron Segment
Huntington Segment
Miller Flat Segment
JOES VALLEY DAM
SCOFIELD DAM
HUNTINGTON NORTH DAM
SEELY CANYON
BLACK CANYON
SEISMOTECTONIC STUDY FOR JOES VALLEY, SCOFIELD AND HUNTINGTON NORTH DAMS
LATE CENOZOIC FAULTS ON THE EASTERN WASATCH PLATEAU
PLATE 1


## EXPLANATION

| | |
|---|---|
| Qu | Quaternary deposits, undifferentiated, includes colluvium and alluvium |
| Qaf | Alluvial fan |
| Qt | Alluvial terrace |
| Qdf | Debris flow |
| Qls | Landslide |
| $Qm_3$ | Inner terminal moraine |
| $Qm_2$ | Intermediate terminal moraine |
| $Qm_1$ | Outermost terminal moraine |
| KTu | Cretaceous and Tertiary sedimentary rocks, undifferentiated |
| ▲ | Soil pit |
| ⑤ | Scarp height, meters |
| | Late Quaternary normal fault, ball on downthrown side, dashed where approximately located, dotted where concealed by younger deposits |
| | Fault scarp in late Quaternary deposit, hachures on downthrown side |
| | Photolineament in late Quaternary deposit |
| | Normal fault inferred to be late Quaternary, hachures on downthrown side |
| | Late Cenozoic normal fault, hachure on downthrown side |

2 1 0 2 4

SCALE OF KILOMETERS

## NOTES

Base maps are the following U.S. Geological Survey 7.5 minute quadrangles: Ferron Canyon, The Cap, Joes Valley Reservoir, Mahogany Point, South Tent Mountain, Rilda Canyon, Huntington Reservoir, and Candland Mountain.

Southern ¼ of map is a generalized compilation of geology and faults from Ellis (1981a, 1981b).

SEISMOTECTONIC STUDY FOR JOES VALLEY, SCOFIELD AND HUNTINGTON NORTH DAMS

QUATERNARY GEOLOGY AND LATE CENOZOIC FAULTS IN THE NORTHERN JOES VALLEY GRABEN

PLATE 2

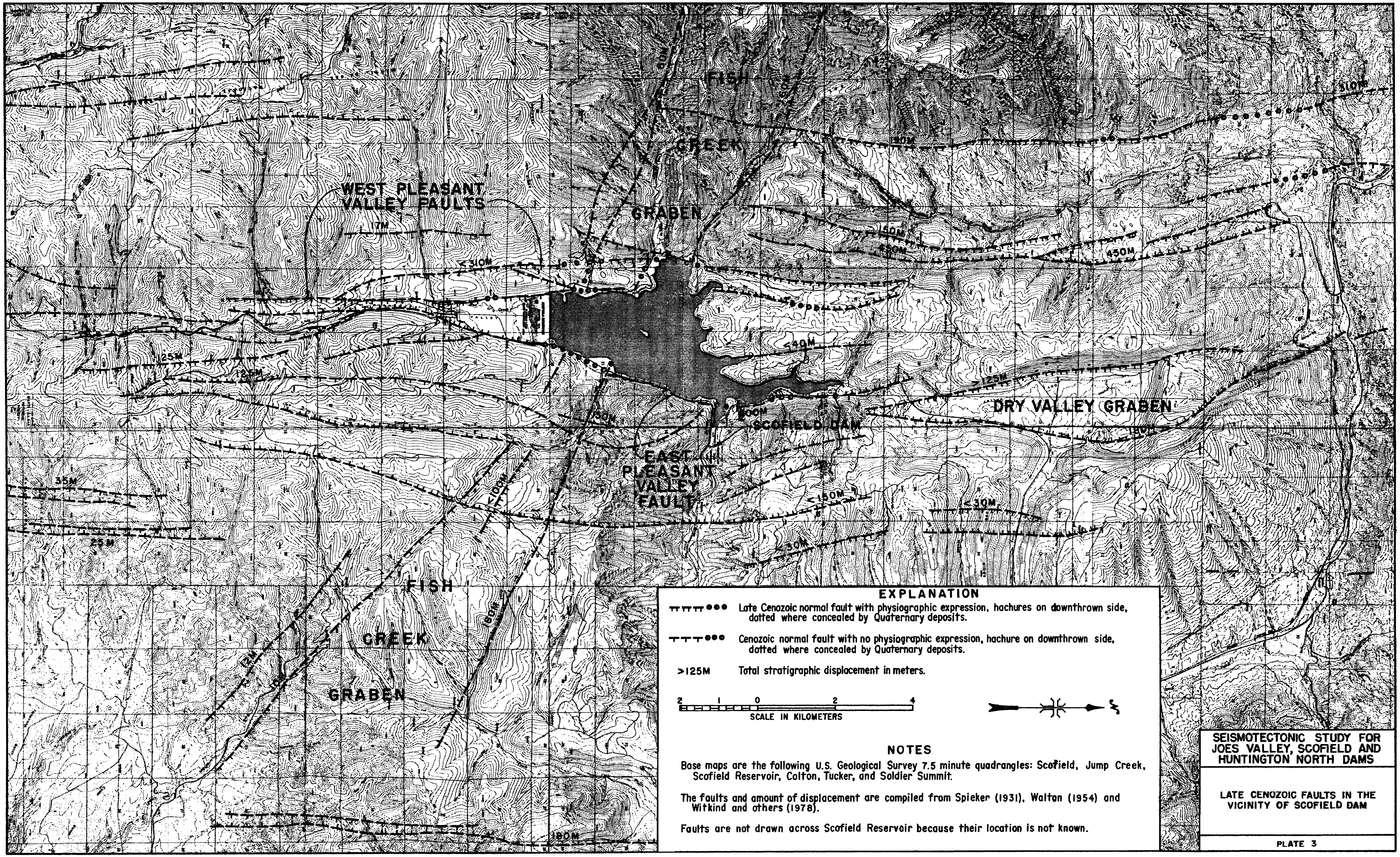


## EXPLANATION

Late Cenozoic normal fault with physiographic expression, hachures on downthrown side, dotted where concealed by Quaternary deposits.

Cenozoic normal fault with no physiographic expression, hachure on downthrown side, dotted where concealed by Quaternary deposits.

>125M Total stratigraphic displacement in meters.

2 1 0 2 4
SCALE IN KILOMETERS

## NOTES

Base maps are the following U.S. Geological Survey 7.5 minute quadrangles: Scofield, Jump Creek, Scofield Reservoir, Colton, Tucker, and Soldier Summit.

The faults and amount of displacement are compiled from Spieker (1931), Walton (1954) and Witkind and others (1978).

Faults are not drawn across Scofield Reservoir because their location is not known.

SEISMOTECTONIC STUDY FOR JOES VALLEY, SCOFIELD AND HUNTINGTON NORTH DAMS

LATE CENOZOIC FAULTS IN THE VICINITY OF SCOFIELD DAM

PLATE 3